

**PREDICTING THE RELATIVE IMPACTS OF URBAN DEVELOPMENT
POLICIES AND ON-ROAD VEHICLE TECHNOLOGIES ON AIR QUALITY IN
THE UNITED STATES:**

MODELING AND ANALYSIS OF A CASE STUDY IN AUSTIN, TEXAS

Final Report

Project Period: 12/20/2004-12/19/2008

Submitted to

The United States Environmental Protection Agency
Bryan Bloomer (Project Officer)
USEPA/ORD/NCER/ASD (8723F)
1200 Pennsylvania Ave NW
Washington, DC 20460-0001

By

Alba Webb, Jihee Song, David Allen,
and Elena McDonald-Buller (Principal Investigator)
The University of Texas at Austin
Center for Energy and Environmental Resources
10100 Burnet Rd., M.S. R7100
Austin, TX 78758

Brenda Zhou, Shashank Gadda, Jason Lemp, Sumala Tirumalachetty
and Kara Kockelman (Co-Principal Investigator)
Department of Civil, Architectural, and Environmental Engineering
Cockrell School of Engineering
1 University Station, C1700
Austin, TX 78712

Barbara Parmenter
Department of Urban and Environmental Policy
97 Talbot Ave.
Tufts University
Medford, MA 02155

December 2008

Table of Contents

	Page
1.0 Introduction	1
2.0 Envision Central Texas Scenarios	3
2.1 Background	3
2.2 Emissions Inventory Development	5
2.2.1 Biogenic Emissions and Dry Deposition	5
2.2.2 Anthropogenic Emissions	9
2.2.3 Emissions Inventory Summary	14
2.3 Air Quality Modeling Predictions	15
2.3.1 Daily Maximum 1-hour Ozone Concentrations	16
2.3.2 Hourly Episodic Ozone Concentrations	18
2.3.2 Hourly Episodic Ozone Concentrations	22
2.4 Comparison of ECT Results with U.S. EPA’s post-Clean Air Act Amendment Emission Scenario Projections	25
2.5 Comparison of ECT Results with changes in On-road Mobile Source Controls	25
3.0 Integrated Transportation Land Use Model (ITLUM) Scenarios	28
3.1 Introduction	28
3.2 Existing Land Use Models	28
3.3 Gravity Land Use Model	30
3.3.1 G-LUM Specification	31
3.3.2 Data Sets Used in the G-LUM	32
3.3.3 G-LUM Calibration	33
3.3.4 G-LUM Application	34
3.3.5 G-LUM Application Results	39
3.3.6 Findings	44
3.4 A Hybrid Land Use Model System	45
3.4.1 Model System	45
3.4.2 Data Sets Used in the LUC-LUI Model System	47
3.4.3 Calibration of the LUC Model	50
3.4.4 Calibration of the LUI Model	53
3.4.5 LUC-LUI Application and Results	55
3.4.6 Findings and Lessons Learned	62
3.5 Emissions Inventory Development	64
3.5.1 Biogenic Emissions and Dry Deposition	64
3.5.2 Anthropogenic Emissions	66
3.5.3 Emissions Inventory Summary	66
3.6 Air Quality Modeling Predictions	67
4.0 Conclusions	71
5.0 Publications/Presentations	74
6.0 Description of Expenditures for FY2007-2008	78
7.0 References	79
Appendix A	91
Appendix B	93

Appendix C	101
Appendix D	109
Appendix E	110
Appendix F	126
Appendix G	145
Appendix H	153

1.0 Introduction

Urban development results in changes to land use and land cover and, consequently, to biogenic and anthropogenic emissions, meteorological processes, and processes such as dry deposition that influence future predictions of air quality. This study examines the impacts of alternative regional development patterns using Austin, Texas as a case study.

The Austin – Round Rock Metropolitan Statistical Area (MSA), shown in Figure 1.1, is located in Central Texas and includes Travis, Williamson, Hays, Bastrop and Caldwell Counties. The Austin MSA is among the most rapidly growing urban areas in the United States with a current population of approximately 1.7 million concentrated in Travis County. Williamson (5th), Hays (26th), Bastrop (30th), and Caldwell (51st) Counties were among the 100 fastest growing counties by percent change in the country, while Travis (32nd) County was one of 100 fastest growing counties by numeric change in the country between 2000 and 2001.

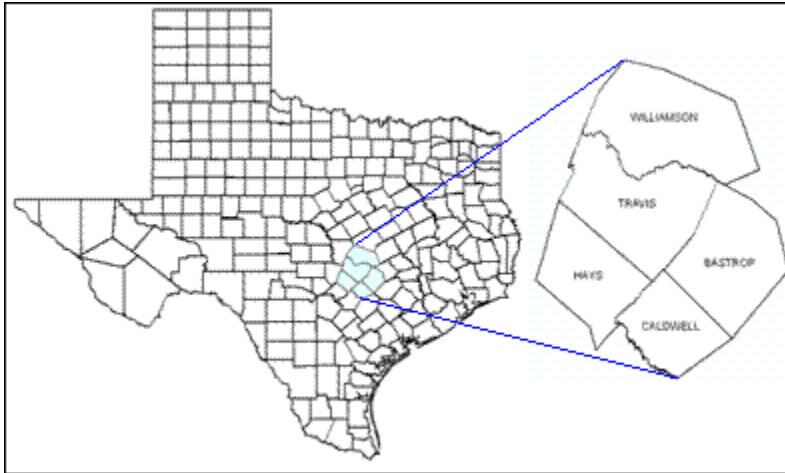


Figure 1.1. The five-county Austin MSA with an enlarged view of Williamson, Travis, Bastrop, Hays, and Caldwell Counties.

The objectives of this study included:

1. Applying an integrated transportation-land use model (ITLUM) to investigate the impacts of regional development scenarios on the magnitude and spatial distribution of emissions of ozone precursors. ITLUM-based forecasts were contrasted with four pre-determined urban growth scenarios developed through a regional visioning initiative known as Envision Central Texas (ECT).
2. Comparing the air quality impacts of regional development scenarios on predicted ozone concentrations and human exposure patterns using a photochemical grid model.
3. Testing the hypothesis that predicted human exposure patterns based on ITLUM emission forecasts will differ from those based on the U.S. EPA's post-Clean Air Act Amendment emission scenario projections.
4. Testing the hypothesis that changes in land use and dry deposition patterns have at least as significant an impact on future air quality as changes in on-road vehicle emission control technologies.

Urban growth scenarios evaluated in this study were developed using two distinct approaches: visioning and mathematical modeling. Visioning is a highly community-oriented planning technique used to create regional land use and transportation goals (FHWA 1996). It is typically performed as a cooperative, inclusive process among business owners, community residents, interest groups, and local officials and results in broad goals and principles which can guide future policies and plans. In contrast, land use models are based on historical trends and attempt to forecast or predict what future land use patterns will look like based on those trends (along with changes in any policy, land use, travel cost or other variable that the analyst has incorporated into the model). They are typically driven by technical experts, relying on data for calibration and model specification, and result in a set of probable future trends and indicators which can guide the implementation of growth management strategies. Consequently, direct comparisons of results for the two methods are not really relevant. However, it is important to understand both approaches offer their own relative advantages from a planning perspective and the visioning and modeling processes appear quite complementary (Lemp *et al.* 2008).

Both regional visioning and land use modeling approaches can provide key inputs to models of travel demand, emissions, and air quality. Air quality modeling in this study was performed using the Comprehensive Air Quality Model with extensions (CAMx), which is currently the photochemical model used by the State of Texas for attainment demonstrations. Austin was among the first areas to prepare an Early Action Compact (EAC) or voluntary State Implementation Plan (SIP) under the National Ambient Air Quality Standard (NAAQS) for ozone concentrations averaged over 8-hours. As part of the EAC, the September 13 – 20, 1999 multi-day high ozone episode with projected 2007 emissions was developed for use in CAMx (CAPCOG 2004a, 2004b). For this study, projected emission inventories were developed for the year 2030 for each urban growth scenario and used with the identical meteorological data and CAMx configuration developed for the 2007 EAC case (referred to in this report as the Base Case) in order to evaluate impacts on future air quality.

2.0 Envision Central Texas Scenarios

2.1 Background

Four urban growth scenarios were developed through a community-driven regional visioning initiative known as Envision Central Texas (ECT 2004). The ECT process engaged state and local government, business, environmental, and community development organizations, and elected leaders from the five counties. Based on information discussed in public workshops, the ECT process projected a set of four possible growth scenarios. All of the scenarios are based on a doubling of population in 20 to 40 years from 2001, but assume different types of growth. ECT Scenario A assumes low-density, segregated-use development based on extensive highway provision; ECT Scenario B assumes concentrated, contiguous regional growth within 1-mile of transportation corridors; ECT Scenario C concentrates growth in existing and new communities with distinct boundaries; ECT Scenario D assumes high-density development in existing towns and cities with balanced-use zoning. Figure 2.1 shows land use development patterns for each of the four scenarios.

As part of the visioning process, Fregonese Calthorpe estimated households and average household size by county for each ECT scenario as shown in Table 2.1. Because direct estimates of human population by county were not available, the households and average household size data developed by Fregonese Calthorpe were obtained from Smart Mobility Inc. and used to estimate population for each ECT scenario for this study. Human population estimates among the ECT scenarios, shown in Table 2.2, differed by 0.3 - 1%.

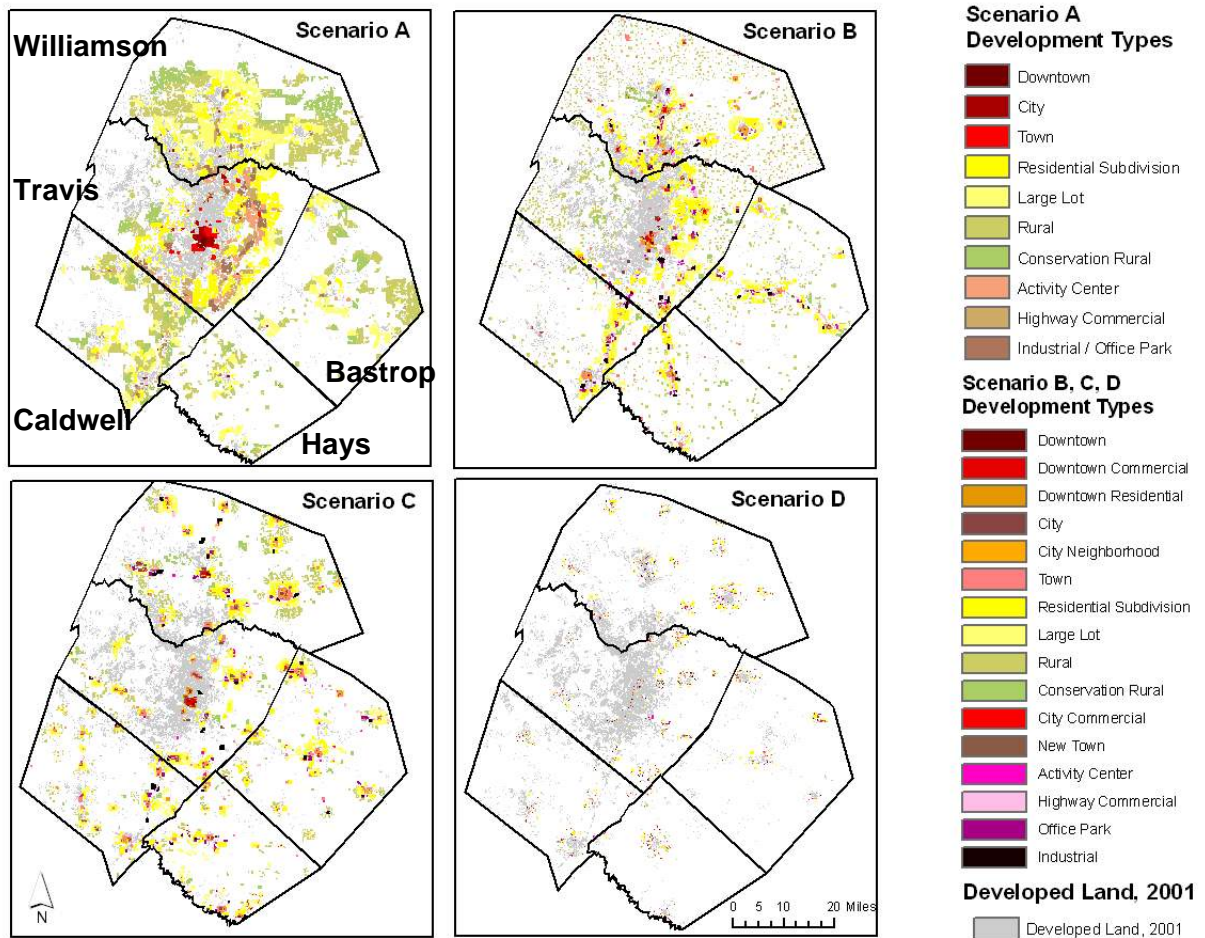


Figure 2.1. ECT Scenarios: maps indicating land use changes that will occur for each of the growth scenarios. 2001 developed land and counties within the Austin-Round Rock MSA are identified for reference (Song *et al.* 2008)

Table 2.1. 2001 housing units and projected households for each ECT scenario by county

Households	2001 (U.S. Census Housing Unit)	ECT A	ECT B	ECT C	ECT D	<i>Average Household Size</i>
Bastrop	22,723	52,621	72,309	92,180	72,108	2.87
Caldwell	12,188	24,171	41,742	59,652	41,698	2.98
Hays	37,946	81,690	84,607	90,271	85,005	2.92
Travis	353,272	556,367	507,621	447,476	494,382	2.53
Williamson	98,120	215,637	222,604	235,980	226,335	2.88
Total	524,249	930,486	928,883	925,559	919,528	-

Table 2.2. 2001 human population and projected human population for each ECT scenario by county

Population	2001 (U.S. Census)	ECT A	ECT B	ECT C	ECT D
Bastrop	61,480	151,023	207,527	264,555	206,950
Caldwell	33,808	72,029	124,390	177,762	124,261
Hays	104,514	238,536	247,051	263,590	248,215
Travis	842,638	1,407,609	1,284,282	1,132,114	1,250,786
Williamson	276,749	621,035	641,099	679,622	651,846
Total	1,319,189	2,490,231	2,504,349	2,517,644	2,482,059

2.2 Emissions Inventory Development

Future air quality is most often assessed using photochemical models with projected anthropogenic emissions, but land cover is typically presumed to remain constant. However, previous analyses (Vizuite *et al.* 2002; McDonald-Buller *et al.* 2001; Wiedinmyer *et al.* 2001) have shown that changes in land cover can have substantial impacts on biogenic emissions, deposition velocities, surface albedo, soil moisture and other physical parameters. Biogenic and anthropogenic emission inventories, along with land cover estimates for estimation of dry deposition velocities, were developed for each of the four ECT scenarios.

2.2.1 Biogenic Emissions and Dry Deposition

Biogenic Emissions Model

The Global Biogenic Emissions and Interactions System (GloBEIS) version 3.1 (Yarwood *et al.*, 1999, 2003) was used to develop biogenic emissions inventories for the ECT scenarios. GloBEIS requires data on temperature, photosynthetically active radiation (PAR), wind speed, humidity, and land use/land cover (LULC).

Hourly ambient surface temperatures were developed by spatially interpolating temperatures measured by National Weather Service (NWS) and other weather stations throughout eastern Texas (Vizuite *et al.* 2002). Estimates of PAR flux were based on calculations done by the University of Maryland and the National Oceanic and Atmospheric Administration (NOAA) for the Global Energy and Water Cycle Experiment (GEWEX) Continent Scale International Project (GCIP). NOAA uses a modified version of the GEWEX (2005) surface radiation budget (SRB) algorithm (version 1.1) to calculate radiation flux fields from Geostationary Operational Environmental Satellite (GOES-8) data. Wind speed and humidity estimates were derived from simulations using the fifth generation NCAR/Penn State Mesoscale Model (MM5).

The LULC input data required by GloBEIS were derived from a number of databases. It is important to distinguish between land use and land cover data and their relative roles in emissions and air quality modeling. Land use categories describe how humans use or intend to use the land, e.g., high or low density, rural or urban. Land cover describes the physical features that occur on the land surface, such as water, vegetation, bare soil, rock and built features, or more specifically vegetation species. The first LULC database, shown in Figure 2.2, was developed by Wiedinmyer *et al.* (2000, 2001) in order to improve the characterization of land cover in Texas. These data contain emission factors for 156 different vegetation types; 41 types are identified at the species level (e.g. *Quercus alba*), 80 types are identified according to genera (e.g. *Quercus*), and 35 are defined as broad land cover types (e.g., Pecan Elm forest). The 1-km data were aggregated to the 4-km resolution used in the photochemical modeling for the purposes of this study. The other LULC databases were derived from each of the ECT scenarios and contain various land use classes (10 land use types for Scenario A and 16 for the other scenarios).

In contrast to the Wiedinmyer *et al.* database, the ECT land use classifications include assumptions concerning impervious ground cover but no information on vegetation types. Therefore, the ECT land use scenarios were overlaid on the original land cover data from Wiedinmyer *et al.* and used to modify the original vegetation density. ECT planners estimated the fraction of impervious cover for each ECT land use type, which was used in this study to adjust the fraction of original vegetation expected to exist in that land use category. For example, areas which are designated to develop as “Downtown” are assumed to have 95.4% impervious cover, leaving 4.6% pervious cover remaining. It was estimated that half of that cover would remain, leaving 2.3% of the original vegetation types, the rest being converted to ornamental or other uses. These assumptions were based on visual studies of development impacts on tree cover using orthophotography from 1995 and 2002, and on local knowledge of development practices. Table 2.3 shows the assumed fraction of original vegetation remaining for each land use type for the ECT scenarios. The biogenic emissions modeling was a collaborative effort with EPA Project RD83145201, *Impacts of Climate Change and Land Cover Change on Biogenic Volatile Organic Compounds (BVOCs) Emissions in Texas*, which was also conducted by the University of Texas at Austin.

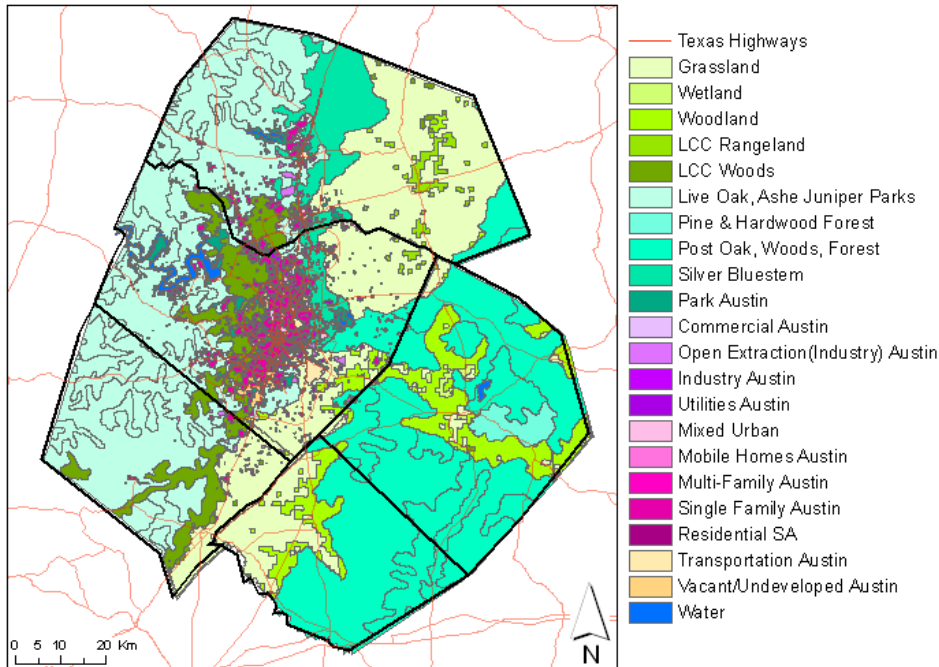


Figure 2.2. Base case land cover types for the Austin MSA described by Wiedinmyer *et al.* (2001)

Table 2.3. Assumed fraction of vegetative cover remaining for each development type used to estimate biogenic emissions for the four ECT scenarios

Development Type	Assumed Fraction of Vegetative Cover Remaining	
	ECT Scenario A	ECT Scenarios B,C, and D
1 Downtown	0.023	0.023
2 Downtown Commercial		0
3 Downtown Residential		0.055
4 City	0.146	0.146
5 City Neighborhood		0.193
6 Town	0.171	0.171
7 Residential Subdivision	0.363	0.363
8 Large Lot	0.493	0.492
9 Rural Housing	0.763	0.763
10 Conservation Rural	0.827	0.827
11 City Commercial		0.011
12 New Town		0.148
13 Activity Center	0.042	0.041
14 Highway Commercial	0.023	0.023
16 Office Park	0.144	0.144
17 Industrial		0.025

Dry Deposition Model

Dry deposition, which is the dominant physical loss mechanism for air pollutants in central Texas, is a strong function of land use/land cover type. The dry deposition model used in most air quality simulations was developed using algorithms based on the work of Wesely (1989) and Walmsley and Wesely (1996). Deposition rates are estimated as a series of mass transfer resistances to deposition. These resistances are due to aerodynamic transport, diffusion across a quasi-laminar sub-layer, and surface uptake. The dry deposition flux is calculated as:

$$F_c = V_d \cdot C_z \quad (2.1)$$

where F_c is the dry deposition flux of the gas of interest, V_d is the dry deposition velocity, and C_z is the concentration or mixing ratio at the mid-point of first vertical layer height in CAMx. For gases, the dry deposition velocity is calculated as:

$$V_d = \frac{1}{r_a + r_d + r_s} \quad (2.2)$$

where r_a is the aerodynamic resistance above the surface, r_d is the deposition layer (or quasi-laminar sub-layer) resistance and r_s is the bulk surface (or canopy) resistance (Wesely 1989).

When the land cover is classified as urban or barren, the rate of deposition is controlled by aerodynamic transport and diffusion across the quasi-laminar sub-layer. Deposition rates for other land cover categories are dominated by the resistances due to surface uptake. Because different resistances can dominate, deposition rates for different land cover types can have different magnitudes and diurnal patterns. For example, dry deposition velocities for forest land covers are a factor of 2-2.5 higher than those of urban and barren land during the daytime. Eleven land use/land cover categories are used in CAMx which are urban land, agricultural land, range land, deciduous forest, coniferous forest, mixed forest including wetland, water, barren land, non-forested wetland, mixed agricultural/range land, and rocky open areas with low-growing shrubs. To estimate deposition rates, CAMx land use files assign the areal fractional distribution (0 to 1) of eleven land use categories in each individual grid cell. In this study, the land cover data from Wiedinmyer *et al.* (2001) were mapped to one of the eleven land use/land cover categories used by the dry deposition module in CAMx (McDonald-Buller *et al.*, 2001). For the ECT scenarios, the remaining vegetation for each development type was classified as the original land cover, and the area fraction of newly developed land was classified as urban. Table 2.4 shows the fraction of each of the eleven land use/land cover categories for the Base Case and the ECT scenarios as well as the percent of vegetative cover converted to urban land use. ECT A, which continues the current pattern of low-density development, had the largest reduction in vegetative cover as compared to the Base Case.

Table 2.4. Area fraction of eleven land use categories for the Base Case and ECT scenarios (Song *et al.* 2008)

Land Use Category	Area Fraction of Land Use Category across the five-county area				
	Base Case	ECT A	ECT B	ECT C	ECT D
Urban	0.07	0.23	0.14	0.13	0.10
Agricultural	0	0	0	0	0
Rangeland	0.06	0.04	0.05	0.05	0.05
Deciduous Forest	0.26	0.24	0.25	0.25	0.26
Coniferous Forest	0	0	0	0	0
Mixed Forest	0.34	0.28	0.32	0.32	0.33
Water	0.01	0.01	0.01	0.01	0.01
Barren Land	0	0	0	0	0
Non-forested Wetlands	0	0	0	0	0
Mixed Agricultural/Range	0.27	0.20	0.23	0.24	0.25
Rocky, with Low Shrubs	0	0	0	0	0
Percentage of reduced vegetation (%)		17	7	6	4

2.2.2 Anthropogenic Emissions

Changes in population, demographic, employment and land use patterns have complex influences on emission forecasts. Anthropogenic emissions are typically classified into four sectors: (a) on-road mobile sources, (b) non-road mobile sources, (c) area sources and (d) point sources. Projections of emissions from mobile sources are based on engine technology, fleet turnover and activity. Projections of emissions from area and point sources are typically developed through the application of socioeconomic growth factors and models of economic activity dynamics, in the absence of factors generated from local economic and demographic activity data.

With the exception of emissions from non-road mobile sources that are described below, the 2007 future year anthropogenic emission inventories developed for Austin’s Early Action Compact served as the Base Case for this study (CAPCOG 2004a, 2004b). Emissions from stationary point sources for 2007 were developed by the Texas Commission on Environmental Quality (TCEQ) for the Houston-Galveston area Mid-Course Review and were supplemented with local activity projections from the Capital Area Council of Governments (CAPCOG). Because forecasts of growth of point source emissions have been small relative to changes in mobile source emissions and because the assessment of future energy needs in Texas is on-going, point source emissions remained constant between the 2007 Base Case and ECT future development scenarios. The methodology used to develop emission estimates for mobile and area sources for the ECT scenarios is described below.

On-road Mobile Source Emissions

On-road mobile source emission inventories were developed for each of the ECT scenarios by combining travel demand model output from the Envision Central Texas Transportation Model (ECTTM) for the 5-county Austin area link network with emission factors from the EPA’s MOBILE6.2 model (EPA 2003a). The ECTTM was developed

by Smart Mobility Inc. (2003), with support from the Capital Area Metropolitan Planning Organization (CAMPO). The ECTTM follows the general four-step modeling framework used by CAMPO and most other Metropolitan Planning Organizations in the United States, consisting of trip generation, trip distribution, mode choice, and trip assignment, but includes a number of enhancements that make it sensitive to transportation infrastructure and land use. These include: (a) an auto availability model that is sensitive to residential density and transit service, (b) a walk/bike trip model that is sensitive to residential density, employment density, and the balance between jobs and housing, (c) a mode choice model that is sensitive to land use and (d) feedback of congested travel times to affect traveler behavior. Transportation characteristics for each of the ECT scenarios are summarized in Table 2.5 (ECT 2004, CAMPO 2005).

Table 2.5. Transportation characteristics for the ECT scenarios

Scenario	Daily VMT per capita	Auto trips (%)	Transit trips (%)	Bike and walk trips (%)	Commuter rail and toll roads	Light rail	Bus rapid transit
2000	26.4	94	3	3	No	No	No
ECT A	34.3	92	4	4	Yes	No	Yes
ECT B	30.1	90	6	4	Yes	Yes	No
ECT C	29.0	88	4	8	Yes	No	Yes
ECT D	27.4	85	6	9	Yes	Yes	No

For each ECT scenario, output of the ECTTM includes vehicle miles traveled (VMT) and congested travel speeds by link direction for each of four time periods: Morning Peak (6:30am – 9:00am), Afternoon Peak (3:00pm – 7:00pm), Off-peak (9:00am – 3:00pm and 7:00pm -9:00pm), and Overnight (9:00pm – 6:30am). VMT was apportioned by hour for each of four day-types: Weekday (average Monday through Thursday), Friday, Saturday, and Sunday. Day-type and hourly VMT adjustment factors were based on Austin area automatic traffic recorder (ATR) data collected by the Texas Department of Transportation (TxDOT) and used by the Texas Transportation Institute (TTI 2003) to develop the on-road mobile source emission inventories in support of the Austin area Early Action Compact. The hourly VMT on each roadway type link was disaggregated into each of the 28 MOBILE6.2 vehicle types by using VMT mix factors developed from TxDOT vehicle classification count data, vehicle registration data, and MOBILE6.2 default gasoline/diesel fractions (TTI 2003).

MOBILE6.2 was used to calculate emission factors (grams mile⁻¹) for volatile organic compounds (VOC), carbon monoxide (CO), and nitrogen oxides (NO_x) by hour of day, by vehicle type, and by road type (or drive cycle). Local input values for parameters such as ambient temperature and humidity, fuel characteristics and fleet characteristics were used when available. For each ECT scenario, disaggregated link VMT was matched with corresponding pollutant-specific MOBILE6.2 emission type factors tabulated by speed, hour, vehicle type, and roadway type in order to obtain link-level emission estimates. Since the ECT scenarios are based on a projected doubling of population within 20 to 40 years from 2001, emission factors which include default federal motor vehicle control programs (FMVCP) were developed for the year 2030. The EPA’s FMVCP rules regulate fuel characteristics and require increasingly lower exhaust and evaporative

standards for new vehicles. The most recently adopted FMVCP rules modeled in MOBILE6.2 include the Tier 2 and the heavy-duty 2007 rules (EPA 2001). As a consequence of fleet turnover which occurs over the span of decades, the number of older vehicles with less effective pollution controls which are still on the road will decrease resulting in an overall cleaner fleet for the ECT scenarios as compared to the Base Case.

On-road mobile source emissions were then processed through the Emissions Preprocessor System 2 software (EPA 1992) to provide emissions in the appropriate format for CAMx. Chemical speciation profiles developed for the Carbon Bond IV mechanism (CB-IV) were assumed not to change for the ECT scenarios relative to the Base Case. Spatial and temporal allocation of on-road mobile source emissions using EPS2 was not necessary since the on-road mobile source emissions were specified by link and hour.

Non-road Mobile Source Emissions

The 2007 non-road mobile source emission inventory that was developed for Austin's Early Action Compact analysis was not used for this study. Instead, population and households from 2001 that served as the base year for the visioning process by Envision Central Texas and land use and parcels data, that had become available from the City of Austin and CAPCOG since the development of the original 2007 non-road inventory, were used in conjunction with the EPA's NONROAD Model version 2005 (NONROAD 2005) to project a new 2007 non-road inventory. Emissions from aircraft, military service operations, locomotives, and residential and commercial gas cans were estimated separately outside of the framework of the NONROAD model using local survey data (CAPCOG 2004a, 2004b).

Austin currently has one major airport, Austin-Bergstrom International Airport, and military base, Camp Mabry, which is the headquarters of the Texas State Military Forces. Although airport and military operations may experience future growth, it is highly uncertain, and consequently, no additional growth was assumed between 2007 and 2030. Although no additional growth was also assumed for locomotives, required federal NOx emission reductions of 40% were included in the projections (ERG 2004, CAPCOG 2004c). Residential and commercial gas can emissions for 2030 were projected from 2007 emissions using household trends data with assumptions based on a survey done by NuStats, Inc. (ERG 2002). A control factor of 62.4% with a 100% compliance rate was applied for projected VOC emissions from gas cans for 2007 and 2030 to address controls that are under consideration for adoption in the Austin area (EPA 2007a). Due to the absence of Source Classification Codes (SCC) for gas cans, their estimated emissions were added to those from the lawn and garden equipment category obtained from the NONROAD model.

Non-road mobile source emission inventories for agricultural, commercial, construction, industrial, lawn and garden, and recreational equipment were developed for each of the ECT scenarios using the NONROAD2005 model (EPA 2005). NONROAD 2005 estimates total VOC, CO, and NOx emissions by county, and by day. In the model, exhaust emissions are estimated as:

$$E_{\text{Exhaust}} = EF_{\text{Exhaust}} \cdot A \cdot L \cdot P \cdot N \quad (2.3)$$

where E_{exhaust} is the exhaust emission inventory (tons day⁻¹), EF_{exhaust} is the emission factor (tons hp⁻¹ hr⁻¹ vehicle or equipment type⁻¹), A is the equipment activity (operating hr yr⁻¹), L is the loading factor which is described as average proportion of rated power used during operation (%), P is the average rated power (hp), and N is the equipment population (number of vehicles or equipment type). In order to estimate and spatially allocate emissions, the NONROAD model requires data on fuel specification, ambient temperature conditions, deterioration factors, emissions factors, equipment population and county-level spatial allocation, equipment activity, average lifetime, growth factors, and technology types.

Fuel specification, ambient temperature data, equipment population, and activity data were developed by the TCEQ and CAPCOG. National to county-level spatial allocation factors in the model were adjusted with local data and demographic projections for the ECT scenarios. For most other modeling parameters, default values derived from national averages were used. Given the uncertainty involved in estimating future equipment populations for each ECT scenario, it was assumed that the non-road equipment population follows the national growth rate and emissions standards included in the EPA's NONROAD model (EPA 2004). The spatial allocations of emissions for each ECT scenario differ, for example according to population and number of households, but equipment population growth rates for each ECT scenario are the same, which may not be representative of future conditions. Changes in equipment populations would be expected to be affected by local changes in land use; for example, differences in the population and activity of road construction equipment between urban sprawl versus high-density mixed-use development. However, quantifying these differences is complex and further study is needed to address the scaling of equipment populations and activity to reflect future land use patterns within the framework of the NONROAD model. Unanticipated future federal or state emission controls may also result in additional emission reductions.

Two levels of spatial allocation needed to be considered: first, spatial allocation factors incorporated within the NONROAD model used to allocate state-level equipment populations to county-level equipment populations, and second, spatial surrogates for allocating county-level emissions to each grid cell in the CAMx modeling domain for the five-county Austin area. A variety of spatial allocation factors are used to allocate state-level equipment populations to county-level equipment populations in NONROAD2005. For example, state-level emissions from residential lawn and garden equipment are allocated by the number of single- and double-family households; whereas state-level emissions from commercial lawn and garden equipment are allocated by the number of employees in landscaping services. Among the most important spatial allocation factors are human population and numbers of single- and multi-family households. Housing unit and population estimates for 2001, the base year for the ECT visioning process, were obtained from the U.S. Census Bureau and used in the NONROAD model with national growth factors (EPA 2004) to obtain projections of emissions in 2007. Households and

population data for the ECT scenarios are summarized in Table 2.1 and Table 2.2, respectively.

Non-road mobile source emissions were then processed through the EPS2 software to provide emissions in the appropriate format for CAMx. Chemical speciation and temporal allocation profiles were assumed not to change for the ECT scenarios relative to the Base Case. County-level non-road mobile source emissions for the 2007 Base Case and the four ECT scenarios were allocated to each model grid cell using spatial surrogates. EPS2 includes fifteen surrogate categories: 1-County Area; 2- Population; 3- Households; 4-Urban; 5-Agriculture; 6-Range; 7-Deciduous Forest; 8- Coniferous Forest; 9-Mixed Forest; 10-Water; 11-Barren; 12-Non-forested Wetlands; 13-Mixed Agriculture/Range; 14-Rocky with Lichens; 15- Rural. The fraction of each category within the county (i.e., area of specific grid cell / county area total) is used to allocate the county-level emissions to grid cells in the modeling domain. For the 2007 Base Case, population and household distributions (categories 2 and 3) were based on demographic data from the U.S. Census Bureau's 2000 TIGER/Line® files. These population and household data were combined with the grid domain definition using Geographic Information Systems (GIS) software, and redistributed using an area weighting to obtain the total population and number of households for each grid cell in the modeling domain. For the remaining EPS2 surrogate codes (i.e., categories 4 through 15), a composite LULC database, shown in Figure 2.3, was developed for the 2007 Base Case by merging the following: (a) a 2003 land use dataset from the City of Austin (2003); (b) a parcels dataset developed by CAPCOG (2005); and (c) the USGS 1992 National Land Cover Dataset (1992). With the use of GIS, the composite dataset was overlaid with county boundary files and the gridded 4-km × 4-km modeling domain. The area for each polygon in each grid was calculated, and the gridded dataset was exported for use as surrogates in EPS2. LULC codes from the exported dataset were assigned to the surrogates recognized by EPS2 as shown in Appendix A.

For each of the 2030 ECT scenarios, county-level households in Table 2.1 were allocated to grid cells based on the development pattern from Smart Mobility Inc. Human population in Table 2.2 was assumed to follow the spatial allocation of households. Spatial surrogates for the remaining categories were developed by overlaying the composite LULC database developed for the Base Case on the ECT land use development patterns using an approach similar to that used for the biogenic emissions estimation in which newly developed areas were classified as urban; the remaining land use/land cover was classified as the original category. Emissions estimates for the four ECT scenarios were processed to obtain chemically speciated, spatially and temporally allocated, gridded emissions suitable for input into CAMx.

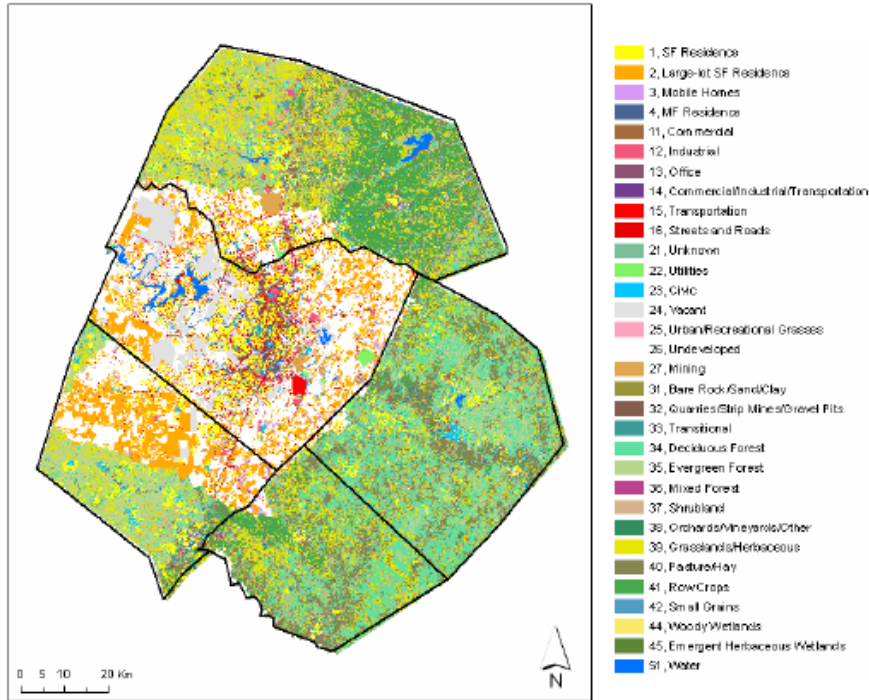


Figure 2.3. Composite LULC database used to develop spatial surrogates for Austin area

Area Source Emissions

Area sources include stationary point sources that are too small or numerous to be surveyed and characterized individually. Emissions from these sources are estimated collectively and spatially allocated according to surrogates such as population or income. Area source emission inventories for each ECT scenario were developed by projecting 2007 base year area emissions using human population growth. Federal and state emission standards for architectural coating operations, auto-body refinishing, degreasing operations, and Stage I and Stage II controls were included (CAPCOG 2004a, 2004c). Uncertainties with the projection exist, and other growth factors, such as gasoline/oil consumption, may show different growth patterns relative to human population. Unanticipated future federal or state emission controls may also result in additional reductions. Area sources were processed through the EPS2 software using the same approach as for the non-road emissions, including the use of spatial surrogates.

2.2.3 Emissions Inventory Summary

A summary of NO_x and VOC emissions from biogenic and anthropogenic sources for the 2007 Base Case and each ECT scenario is presented in Table 2.6. Disaggregation of these estimates by individual source categories as well as plots showing differences in the spatial distribution of emissions are included in Appendix B (Song *et al.* 2008).

Table 2.6. Emissions of VOC and NO_x (tpd) for the 2007 Base Case and each ECT scenario

Categories	2007 Base Case VMT = 44.5*		ECT A VMT = 82.4*		ECT B VMT = 72.2*		ECT C VMT = 69.5*		ECT D VMT = 65.9*	
	VOC	NO _x	VOC	NO _x	VOC	NO _x	VOC	NO _x	VOC	NO _x
On-road mobile	33.8	62.1	22.0	18.4	19.2	16.0	18.8	15.6	17.0	14.3
Non-road mobile	22.2	21.7	23.2	9.5	24.0	9.6	24.0	9.6	23.2	9.5
Area	110.7	10.2	214.3	20.6	237.7	22.1	261.6	23.6	236.2	22.1
Point	3.0	2.8	3.0	2.8	3.0	2.8	3.0	2.8	3.0	2.8
Biogenic	211.2	20.2	198.8	20.2	205.2	20.2	205.3	20.2	207.6	20.2

Note: ECT scenario emissions are calculated for a future year of 2030.

*VMT is given in units of 10⁶ miles per day in the 5-county Austin area.

Biogenic sources and, because they have been projected using human population, area sources are predicted to remain the most significant sources of VOC emissions in the five-county area. Emissions from most on-road and non-road mobile source categories, with the exception of those from lawn and garden equipment, decreased for the ECT scenarios relative to the Base Case due to more stringent federal motor vehicle emission control programs, including the EPA's Tier 2 and heavy-duty 2007 rules and Tier 4 engine standards (EPA 2003b). Emission reductions are concentrated in the urban core and along major transportation corridors, while emissions increase relative to the Base Case in newly developed areas. Differences between ECT D and ECT A were smaller than the differences between these two scenarios and the Base Case. In general, ECT D resulted in lower anthropogenic emissions than ECT A.

2.3 Air Quality Modeling Predictions

Air quality modeling in this study was performed using the Comprehensive Air Quality Model with extensions (CAMx), a publicly available Eulerian photochemical grid model developed by ENVIRON (2004). Photochemical modeling was conducted using the September 13-20, 1999 CAMx modeling episode that was developed for Austin's Early Action Compact. As shown in Figure 2.4, nested regional and urban scale domains were used: a 36-km regional domain, a 12-km East Texas subdomain, and a 4-km Central Texas subdomain. CAMx was used to predict the spatial and temporal patterns of ozone

concentrations for each ECT scenario, and the results were contrasted with the 2007 Base Case to evaluate impacts on future air quality.

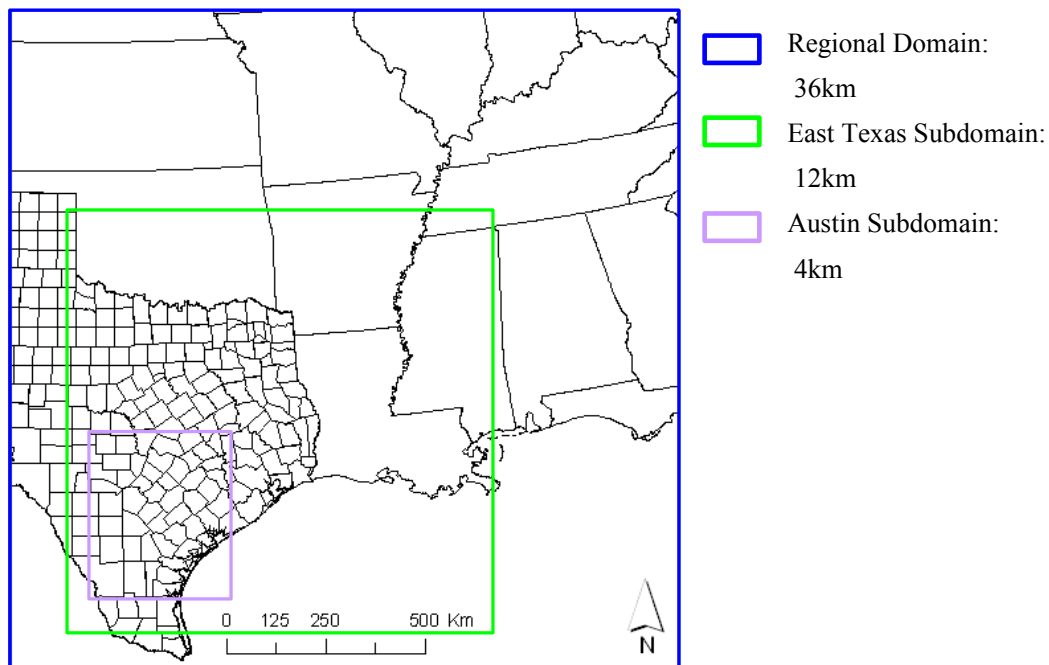


Figure 2.4. Air quality modeling domain

The focus of the work with the ECT scenarios was to examine the response of biogenic emissions, air pollutant deposition velocities, and overall regional air quality, as represented by ozone concentrations, to land use development. The ECT scenarios were compared based on their impact to daily maximum 1-hour ozone concentrations, hourly episodic ozone concentrations, and population exposure. The influences of changes in biogenic emissions and deposition velocities from each of the four ECT scenarios on daily maximum 1-hour ozone concentrations and hourly episodic ozone concentrations were considered both separately, and in tandem for the five-county Austin area. The influences of changes in anthropogenic emissions from area and non-road mobile sources and on-road mobile sources were also considered separately and in tandem.

2.3.1 Daily Maximum 1-hour Ozone Concentrations

Predicted 1-hour averaged daily maximum ozone concentrations for the 2007 Base Case ranged from 72 ppb to 90 ppb across the episode. Differences in daily maximum 1-hour ozone concentrations due to the combined changes in dry deposition, biogenic emissions, and anthropogenic emissions from on-road mobile, non-road mobile and area sources ranged from -11 ppb to -2 ppb with typical values of -6 ppb as shown in Table 2.7.

Table 2.7. Daily maximum 1-hour ozone concentrations for the Base Case and differences in the daily maximum ozone concentrations relative to the Base Case

Episode Day	Base Case Daily Max. O ₃ Conc. (ppb)	ECT A	ECT B	ECT C	ECT D
9/15	80.5	-4.7	-4.9	-5.3	-5.3
9/16	72.0	-1.8	-2.0	-2.0	-2.1
9/17	85.8	-6.9	-6.9	-6.9	-6.9
9/18	86.2	-4.1	-4.1	-4.1	-4.1
9/19	90.4	-5.8	-6.0	-6.6	-6.7
9/20	90.5	-9.7	-9.9	-10.3	-10.8

For ECT scenarios A and D which represent the two most extreme development scenarios, Table 2.8 shows results segregated by changes due to the impacts of urbanization on biogenic emissions and dry deposition only, on anthropogenic emissions only, and on the combined effects of biogenic emissions, dry deposition, and anthropogenic emissions.

Table 2.8. Daily maximum 1-hour ozone concentrations for the Base Case and differences in the daily maximum ozone concentrations relative to the Base Case for ECT A and ECT D.

Episode Day	Base Case Daily Max. O ₃ Conc. (ppb)	ECT A: Difference in Daily Max O ₃ Conc. from Base Case (ppb)			ECT D: Difference in Daily Max O ₃ Conc. from Base Case (ppb)		
		Bio	Anthro	Combined	Bio	Anthro	Combined
9/15	80.5	0.0	-4.6	-4.7	0.0	-5.3	-5.3
9/16	72.0	0.1	-2.1	-1.8	0.1	-2.2	-2.1
9/17	85.8	-0.1	-7.0	-6.9	0.0	-6.9	-6.9
9/18	86.2	-0.4	-4.1	-4.1	-0.2	-4.1	-4.1
9/19	90.4	-0.6	-5.5	-5.8	-0.1	-6.7	-6.7
9/20	90.5	-0.9	-9.2	-9.7	-0.1	-10.7	-10.8

Note that: (1) 'Bio' indicates impacts of urbanization due to changes in biogenic emissions and dry deposition only; (2) 'Anthro' indicates impacts of urbanization due to changes in on-road, non-road, and area source emissions only (point source emissions did not change); and (3) 'Combined' indicates impacts due to changes in both 'Bio' and 'Anthro'.

Changes in daily maximum 1-hour ozone concentrations relative to the Base Case due to decreases in biogenic emissions alone ranged from -0.02 ppb to -1 ppb among all four ECT scenarios, with a typical value of -0.3 ppb for the Austin area. The decreases in ozone concentrations were consistent with the loss of vegetative cover in developing areas and reductions in biogenic emissions. Changes in daily maximum 1-hour ozone concentrations relative to the Base Case due to differences in dry deposition velocities alone ranged from 0 ppb to 0.3 ppb. In Wesely's model, dry deposition velocities for mixed agricultural/range land or forests are higher than for urban areas during the

daytime, but lower at night during mid-summer conditions (Song 2007). Consequently, loss of vegetative cover due to urbanization leads to less removal of ozone during the afternoon and higher maximum daily ozone concentrations, but decreases in ozone concentrations during the night. Changes in daily maximum 1-hour ozone concentrations relative to the Base Case due to the combined impacts of changes in biogenic emissions and dry deposition ranged from -0.9 ppb to 0.1 ppb among all four ECT scenarios, with typical values of -0.2 ppb for the Austin area. Although these impacts appear small, they are comparable in magnitude to some commonly employed air pollution control measures that were adopted as part of Austin's Early Action Compact.

Changes in daily maximum 1-hour ozone concentrations relative to the Base Case due to changes in area and non-road mobile source emissions only ranged from -0.1 ppb to 0.8 ppb among all four ECT scenarios, with typical values of 0.2 ppb for the Austin area. Changes in daily maximum 1-hour ozone concentrations relative to the Base Case due to changes in on-road mobile source emissions only were substantially larger. Reductions in on-road mobile source emissions, resulting from implementation of federal motor vehicle control programs, led to changes in area-wide daily maximum hourly ozone concentrations for the ECT scenarios of up to -10 ppb.

2.3.2 Hourly Episodic Ozone Concentrations

In addition to differences in area-wide daily maximum 1-hour ozone concentrations between the ECT scenarios and the Base Case, maximum and minimum differences in 1-hour ozone concentrations that occurred across the region regardless of time of day or magnitude were investigated. Figure 2.5 shows the range of changes in 1-hour ozone concentrations between the ECT scenarios and the Base Case due to changes in (a) biogenic emissions and dry deposition, (b) non-road mobile and area source emissions, (c) on-road mobile source emissions, (d) anthropogenic emissions, and (e) biogenic emissions, dry deposition, and anthropogenic emissions. Changes in ozone concentrations due only to changes in biogenic emissions and dry deposition are relatively smaller than the changes due to anthropogenic emissions. Both significant increases and decreases in ozone concentrations were associated with changes in anthropogenic emissions, and the spatial patterns of ozone changes with urbanization were heterogeneous. Maximum differences in hourly ozone concentrations were predicted between ECT A and the Base Case for the changes due to biogenic emissions and dry deposition alone (+0.7 ppb to -1.4 ppb), anthropogenic emissions alone (+22 ppb to -14 ppb), and both in tandem (+22 ppb to -14 ppb). As shown in Figure 2.6, decreases occurred in the afternoon in eastern Travis County and western Bastrop County, while increases were primarily due to reductions in on-road mobile source emissions along transportation corridors in the Austin urban core which resulted in less titration of ozone by NO_x emissions during the early morning hours. The range of differences in hourly ozone concentrations between the other ECT scenarios and the Base Case were generally within 1-2 ppb of the range of differences between ECT A and the Base Case.

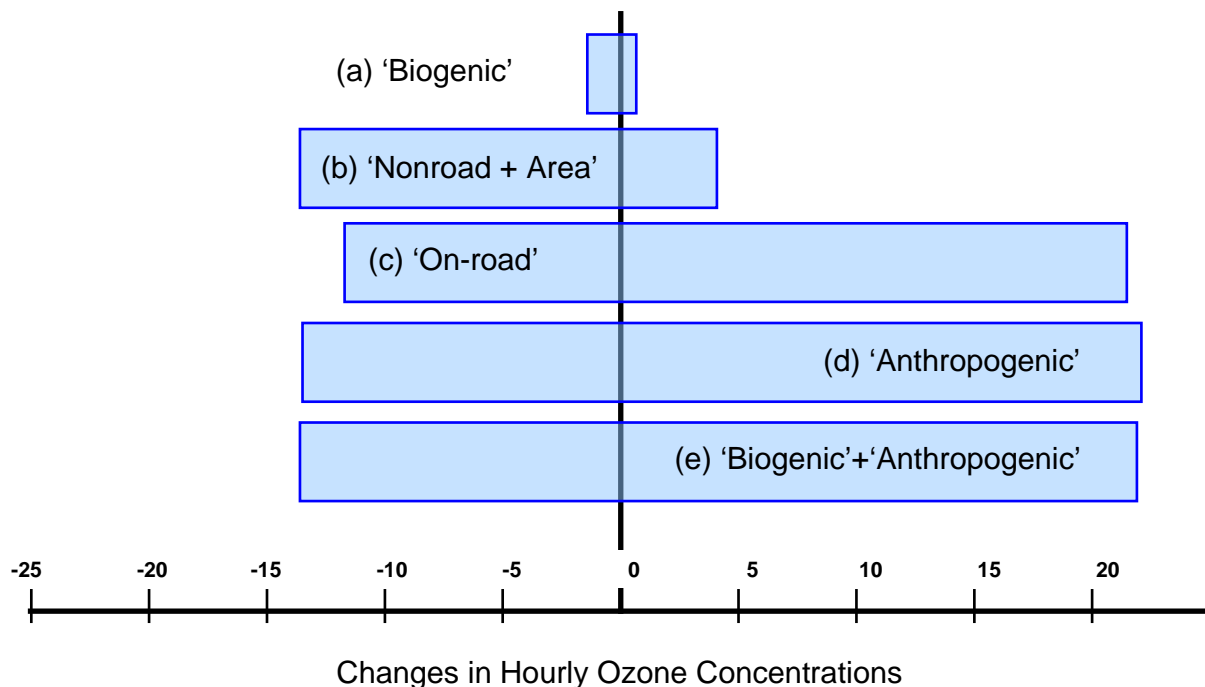


Figure 2.5. Range of changes in hourly ozone concentrations (ppb) between the ECT Scenarios and the Base Case across the 5-county Austin area due to changes in (a) biogenic emissions and dry deposition only, (b) non-road mobile and area source emissions only, (c) on-road mobile source emissions only, (d) anthropogenic emissions only, and (e) biogenic emissions, dry deposition and anthropogenic emissions. (Song *et al.* 2008)

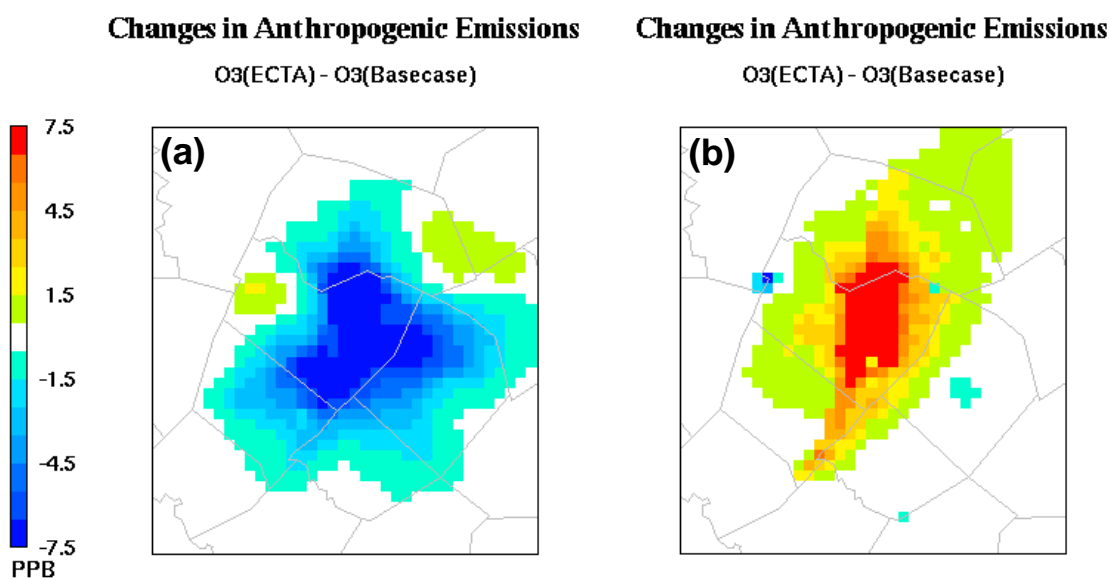


Figure 2.6. Differences in hourly ozone concentrations on one episode day (September 20) between ECT A and the Base Case due to changes in anthropogenic emissions at (a) 1400 and (b) 0600

These results are consistent with previous studies that have shown that ozone formation in the Austin area is generally NO_x-limited with VOC-limited conditions near the I-35 corridor in central Travis County (CAPCOG 2004b). Consequently, as part of its Early Action Compact, the Austin area has pursued NO_x control strategies as more effective than VOC strategies for reducing ozone levels. The responsiveness of hourly peak ozone concentrations to anthropogenic NO_x reductions in the Austin area is predicted to continue with future patterns of urbanization. Figure 2.7 shows the differences in hourly ozone concentrations between ECT A and the Base Case versus the Base Case across all grid cells and episode days due to the combined changes in biogenic emissions, dry deposition, and anthropogenic emissions. Figure 2.7 indicates that decreases in ozone concentrations are primarily associated with high ozone concentrations. Plots for the other ECT Scenarios showed similar trends. Both reductions in high ozone concentrations and increases in lower ozone concentrations were due primarily to reductions of emissions from on-road mobile sources in the future scenarios.

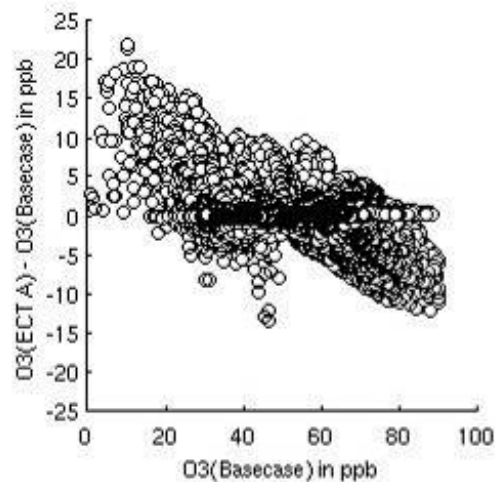


Figure 2.7. Difference in hourly ozone concentrations between ECT A and the Base Case versus hourly ozone concentrations for the Base Case across all episode days and grid cells in the five-county Austin area due to changes in biogenic emissions, dry deposition, and anthropogenic emissions.

Differences in hourly ozone concentrations between the ECT scenarios and the Base Case were much greater than differences between the ECT scenarios due to the large changes in emissions between the Base Case and future year projections. For all of the ECT scenarios, changes due to biogenic emissions and dry deposition were relatively smaller than changes due to anthropogenic emissions. Maximum differences in hourly ozone concentrations between ECT D and ECT A, shown in Figure 2.8, ranged from -3.0 ppb to 4.5 ppb. Figure 2.9 shows an example of the spatial differences in predicted ozone concentrations between ECT D and ECT A. Overall the doubling of population and implementation of new federal mobile source standards produced greater changes in

emissions and air quality than differences in spatial patterns due to different types of regional development implying that controlling the environmental impacts of urbanization involves multi-faceted strategies.

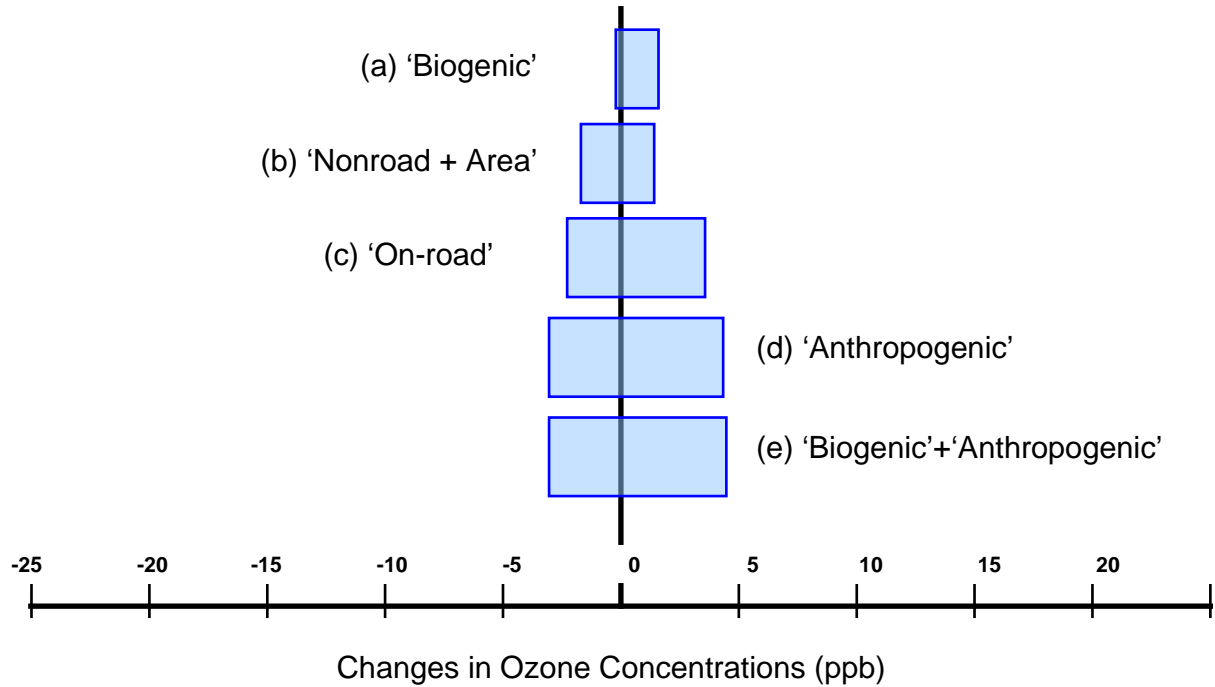


Figure 2.8. Range of changes in hourly ozone concentrations (ppb) between ECT D and ECT A across the 5-county Austin area due to changes in (a) biogenic emissions and dry deposition only, (b) non-road mobile and area source emissions only, (c) on-road mobile source emissions only, (d) anthropogenic emissions only, and (e) biogenic emissions, dry deposition and anthropogenic emissions. (Song *et al.* 2008)

Changes in Development Pattern

O3(ECTD) - O3(ECTA)

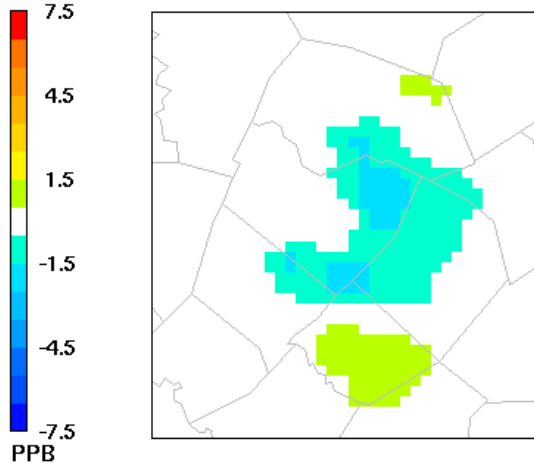


Figure 2.9. Differences in hourly ozone concentrations between ECT D and ECT A at 1400 on one episode day (September 20)

2.3.3 Population Exposure

In addition to changes in hourly ozone concentrations, a characterization of air pollutant exposure was examined. Total daily population-weighted exposure above a threshold ozone concentration (ppb) (Wang 2006) was characterized using the following metric:

$$M_{pop} = \sum_h \sum_g \frac{p_g}{p_t} s_{g,h} \quad (2.4)$$

where p_t is the total population in the five-county Austin area for the scenario, p_g is population in each grid cell g and $s_{g,h}$ is the ozone concentration (ppb) over the threshold

$$c_{thresh} \text{ for each grid cell } g \text{ at hour } h, s_{g,h} = \begin{cases} 0, c_{g,h} \leq c_{thresh} \\ c_{g,h} - c_{thresh}, c_{g,h} > c_{thresh} \end{cases}.$$

Note that the population doubles from approximately 1,250,000 people in the Base Case to 2,500,000 people in the ECT scenarios. This metric was evaluated for various threshold values and estimated for each grid cell, summed over the Austin area modeling domain, and over all hours of the day.

Evaluating daily population exposure, in addition to differences in hourly ozone concentrations, provides additional information about the magnitude and spatial distribution of changes due to urban development and can be particularly relevant in the context of environmental equity. Total daily population-weighted exposure, described above, was estimated for the Base Case and the two ECT scenarios that represent the most extreme differences in development patterns: (1) ECTA, which is consistent with Austin's historical pattern of low-density, segregated-use development based on

extensive highway provision, and (2) ECT D, which is high-density development and balanced-use zoning. Figure 2.10 shows the total daily population-weighted exposure for the Base Case and ECT Scenarios A and D using threshold values of 40 ppb, which is a value typical of clean background conditions, 60 ppb, and 80 ppb, respectively. For a threshold value of 40 ppb, all ECT scenarios show greater exposure than the Base Case due to additional increases in ozone and population in newly developed areas. For higher threshold values, Figure 2.10 shows the variation in exposure over the episode with typically lower exposure values for ECT Scenario D and higher values for the Base Case. For example, for a threshold value of 80 ppb, the Base Case shows greater exposure than the ECT scenarios since daily maximum ozone concentrations were lower for the ECT scenarios.

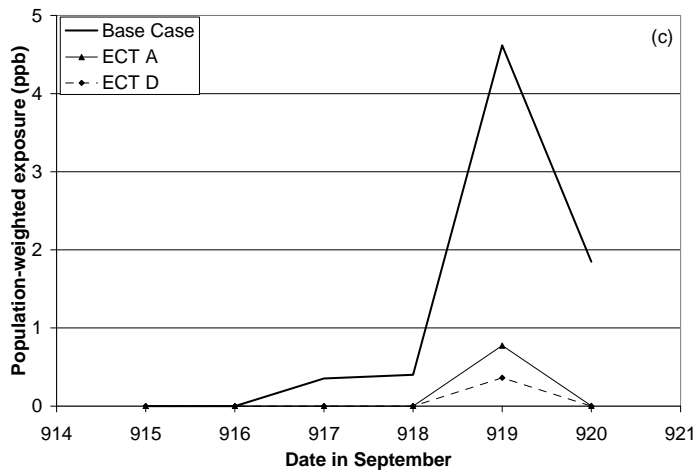
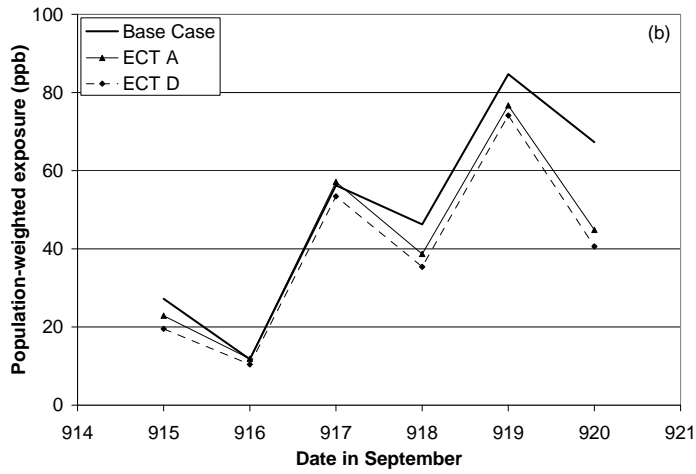
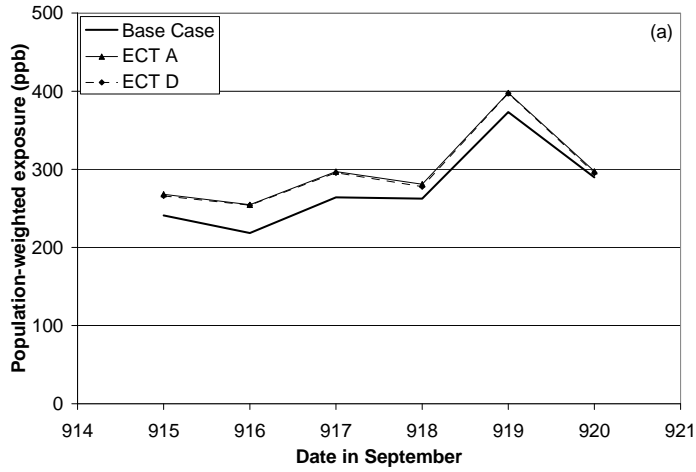


Figure 2.10. Total daily population-weighted exposure using a (a) 40 ppb, (b) 60 ppb, and (c) 80 ppb threshold for ECTA, ECTD and the Base Case.

2.4 Comparison of ECT Results with U.S. EPA's post-Clean Air Act Amendment Emission Scenario Projections

A goal of this study was to test the hypothesis that predicted human exposure patterns based on ECT and ITLUM emission forecasts would differ from those based on the U.S. EPA's post-Clean Air Act Amendment emission scenario projections, however the county-level data required for this comparison was not publicly available from EPA in time to include in this study.

2.5 Comparison of ECT Results with changes in On-road Mobile Source Controls

A goal of this study was to test the hypothesis that changes in land use and dry deposition patterns have at least as significant an impact on future air quality as changes in on-road vehicle emission control technologies. The Energy Independence and Security Act of 2007, which focuses on improving vehicle fuel economy and reducing U.S. dependence on foreign oil, includes a mandatory Renewable Fuel Standard which requires significant increases in the use of biofuels through 2022. For at least the next few years, it is expected that the majority of this mandate will be met by corn ethanol. E85 is a blend of 85% denatured fuel ethanol and 15% gasoline that can be used in flex fuel vehicles (FFVs).

A photochemical modeling run was performed in which on-road mobile source emissions for ECT A were modified to simulate use of E85 by 30% of the gasoline fleet. Total VOC, CO, and NO_x emissions were adjusted using factors from Jacobson (2007) Relative to gasoline-fueled vehicles, E85-fueled vehicles were assumed to emit 30% less NO_x, 5% greater CO, and 19.6% greater VOC (non-methane hydrocarbons). Additionally, the data presented by Jacobson were used to develop a VOC chemical speciation profile for E85 using the Carbon Bond IV mechanism (CB-IV) (Gery *et al.* 1989). The CB-IV mechanism speciates organic compounds into a set of eleven components based on their structure; OLE (Olefin), PAR (Paraffin), TOL (Toluene), XYL (Xylene), FORM (Formaldehyde), ALD2 (Higher aldehyde), ETH (Ethene), MEOH (Methanol), ETOH (Ethanol), ISOP (Isoprene), and UNR (Unreactive Species). The gasoline exhaust VOC profile used in EPS2 was developed from exhaust composition measurements in the Washburn Tunnel in Houston during the Texas Air Quality Study (TexAQS) in 2000 (McGaughey *et al.* 2004). A hybrid approach was used to develop an E85 VOC speciation profile based on the original gasoline exhaust profile. For species listed explicitly by Jacobson, the compounds in the original gasoline profile were multiplied by the corresponding adjustment factors and supplied to Carter's speciation database (2008). The remaining species in the original gasoline profile (except MTBE which was replaced with ethanol) were supplied to Carter's database and speciated into lumped bond groups. Adjustment factors for corresponding bond groups from Jacobson were then applied to the speciated mixture. The explicit and lumped profiles were combined using a mass-weighted approach into a single profile for E85: ETOH 64%, ETH 3.7%, FORM 2.3%, TOL 1.3%, XYL 1.8%, ISOP 0.1%, ALD2 8.1%, OLE 1.4%, PAR 8.3%, MEOH 0% and UNR 9.2%. Thus for the composite E85 profile that was developed based on available data, approximately 64% of VOC emissions by

mass are speciated as ethanol. In contrast, the original gasoline profile was speciated as ETOH 0.2%, ETH 6.0%, FORM 1.8%, TOL 7.7%, XYL 10.4%, ISOP 0.3%, ALD2 3.9%, OLE 3.1%, PAR 51.9%, MEOH 0.2%, and UNR 14.5%.

It should be noted that the method used to develop the E85 profile for this study is indirect, and while generally consistent with emission summaries provided by Jacobson, it is only an approximation. Additionally, as with gasoline emissions, exhaust and evaporative VOC profiles for E85 are likely to vary.

Total on-road mobile source VOC emissions for the ECT A scenario assuming 30% conversion to E85 increased from 22.0 tons per day (tpd) in the unmodified ECT A scenario to 23.2 tpd. Total on-road mobile source NOx emissions in the E85 scenario decreased from 18.4 tpd to 16.8 tpd. Figure 2.11 shows reductions in daily maximum 1-hour ozone concentrations for the E85 scenario and ECT scenarios B, C, and D relative to ECT A. Changes in daily maximum 1-hour ozone concentrations relative to ECT A due to the introduction of E85 ranged from -0.4 to 0.0 ppb, with typical values of -0.2 ppb for the Austin area. Although these impacts appear small, they are comparable in magnitude to some commonly employed air pollution control measures that were adopted as part of Austin’s Early Action Compact. Figure 2.12 shows the maximum and minimum differences in 1-hour ozone concentrations relative to ECT A that occurred across the region regardless of time of day or magnitude. Differences in hourly ozone concentrations due to the introduction of E85 are relatively smaller than changes due to development patterns. Maximum differences in hourly ozone concentrations between the E85 scenario and ECT A ranged from -0.6 ppb to 0.8 ppb. Use of E85 fuel will also impact emissions and exposure to air toxics, particulate matter, and greenhouse gases, however evaluation of these impacts was beyond the scope of this study.

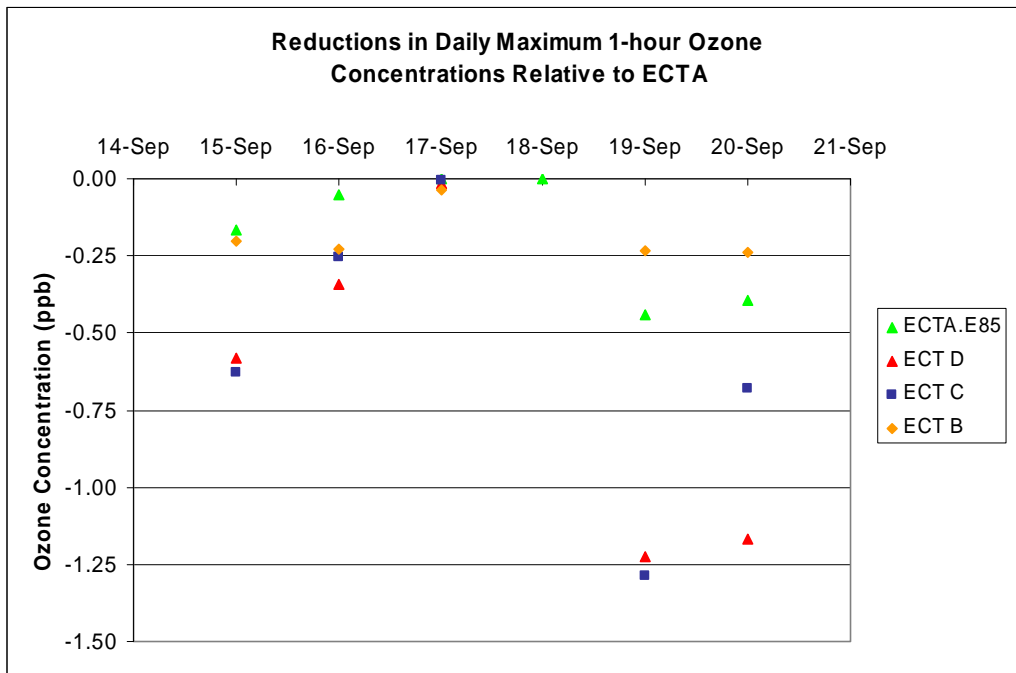


Figure 2.11. Reductions in daily maximum 1-hour ozone concentrations relative to ECTA

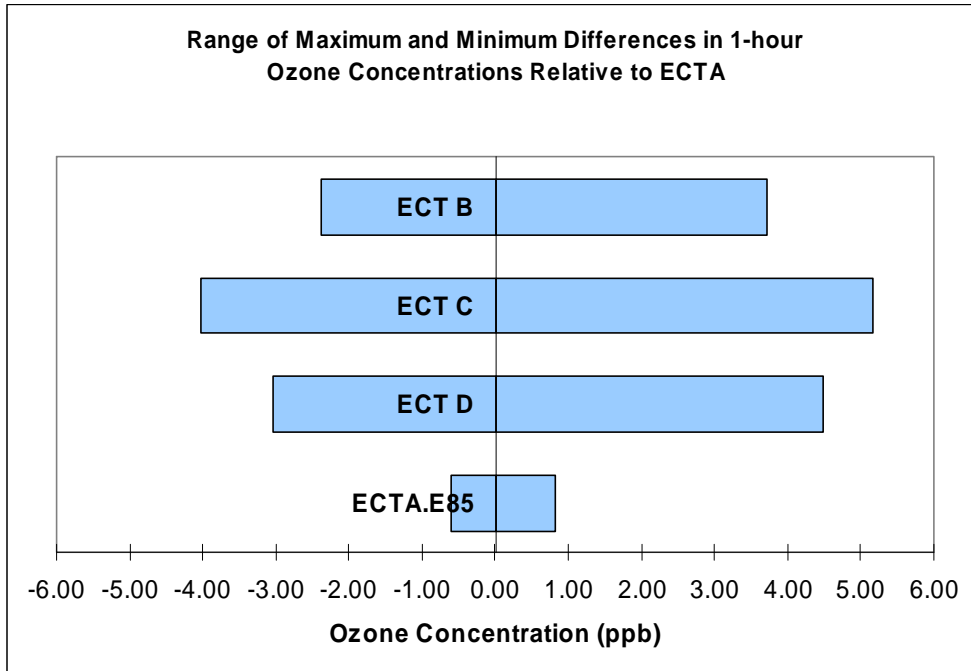


Figure 2.12. Range of changes in hourly ozone concentrations (ppb) relative to ECT A

3.0 Integrated Transportation Land Use Model (ITLUM) Scenarios

3.1 Introduction

Urban land use models (LUMs) seek to predict a region's future spatial distribution of households and employment, and provide key inputs to models of travel demand, emissions, and air quality. Integrated transport-land use models (ITLUMs) allow analysts to anticipate system response to new policies, preference functions, economic conditions and other scenarios. With increasing computational power and theoretical advances, many operational LUMs have been developed, and several studies have summarized and compared existing models (e.g., Miller *et al.* 1998, PBQ&D 1999, US EPA 2000, and Dowling *et al.* 2005). The general consensus is that many limitations remain. However, innovative research in this area is still emerging due to the complexity of transport-land use systems.

The year 2030 travel conditions and household and employment distributions for the Austin-Round Rock Metropolitan Statistical Area (MSA) of Texas were predicted using two ITLUMs. The first utilizes a variation of Steven Putman's Integrated Transportation-Land Use Package (ITLUP), and the second involves a new style of land LUM developed to examine land use change at the parcel level and apply systems of equations for land use intensity (household and employment counts by type) at the level of travel analysis zones (TAZs). Both ITLUMs include a travel demand model (TDM) that is largely based on Smart Mobility's specification. However, this model was modified in order to consider travel costs in the distribution and network assignment of personal trip-making, as described in Appendix C. In addition, Appendix D provides more technical details related to commercial travel (or truck flows), as deduced from the GIS-DK code developed by Smart Mobility. Appendix H presents models for decisions in different stages of the passenger vehicle cycle of ownership and use, capturing the effects of household demographics and location on fleet evolution across the Austin region.

3.2 Existing Land Use Models

To date, many operational LUMs have been developed based on different theoretical framework. The appropriateness and usefulness of any tool varies by context. Lemp *et al.* (2008) summarized four major theoretical constructs underlying the majority of LUMs: gravity allocation, cellular automata, input-output, and discrete response simulation. This summary is a bit simplistic and is based on models' primary features; some advanced models attempt to combine advantages of two or more approaches, but their key attributes determine where they stand in the family of land use models.

In *gravity models*, regional transportation accessibility is core to the spatial allocation of jobs (by type) and households (by category). Zone-based specifications generally include lagged jobs and households, as well as some measure of land availability and land use conditions. Other influential factors, such as price adjustments, presence of built space, zoning restrictions, and topographic conditions are overlooked. Gravity models tend to use regional totals to adjust forecasts across all zones, and have been found to perform

less well with disaggregate zone systems and/or sparse zone activity levels (PBQ&D 1999).

A representative gravity model is the Federal Highway Administration-sponsored Transportation Economic and Land Use Model (TELUM), which enjoys a user-friendly graphical user interface and is freely downloadable at <http://www.telus-national.org/index.htm>. However, its code is not shared, zone count is limited, and some key documentation is missing in its User Manual (2006) (e.g., parameter calibration, objective functions and land consumption variable definitions). A more flexible, open-source version of this model has been written in MATLAB and applied in this study¹.

Cellular automata (CA) models are a class of artificial intelligence (AI) methods. Other AI methods include neural networks and generic algorithms, which also have been used to simulate and/or optimize land use change (Raju *et al.* 1998, Balling *et al.* 1999), but the CA-based SLEUTH model (Slope, Land use, Exclusion, Urban extent, Transportation and Hill shade) is the most widely applied (Clarke *et al.* 1997, Silva and Clarke 2002, Syphard *et al.* 2005). It represents a dynamic system in which discrete cellular states are updated according to a cell's own state, as well as that of its neighbors. However, SLEUTH relies on just five coefficients, and is calibrated in a rather ad hoc fashion². While CA models may mimic many aspects of the dynamic and complex land use systems, they generally lack behavioral foundations to explain the process. Moreover, they emphasize land-cover type, not land use intensity, so post-processing is needed to generate employment and household count patterns (which are, of course, critical to travel demand modeling).

Spatial **input-output models** are used to anticipate the spatial and economic interactions of employment and household sectors across zones, using discrete choice models for mode and input-origin choices. Production and demand functions consider transport disutility between zones, and people (and generally freight) move from one location to another in order to equilibrate supply and demand. Representative models include TRANUS (see, e.g., Johnston and de la Barra 2000), PECAS (e.g. Hunt and Abraham 2003), and RUBMRIO (e.g., Kockelman *et al.* 2004). PECAS has introduced a disaggregate version of space development submodel, which models the actions of developers at either the level of land parcels or grid cells (e.g., PECAS 2007, Hunt *et al.* 2008). This advance made PECAS a hybrid of spatial input-output (on its activity allocation submodel) and random utility maximization techniques, but PECAS is still classified into this category because its key component, activity allocation module, is based on market clearing at zonal level. Trade-based spatial input-output models are most suitable for larger spatial units (e.g., countries, regions, states and/or nations), so spatial resolution can be poor. Good trade and production data are also difficult to come by.

¹ The open source code is available at http://www.ce.utexas.edu/prof/kockelman/G-LUM_Website/homepage.htm

² The model is calibrated by minimizing a variety of discrepancy measures, using historical data to initialize the runs and current data for comparison.

Random utility maximization for *discrete choices* (McFadden 1978) is the basis of most microsimulation models. Waddell's UrbanSim (Waddell 2002, Waddell *et al.* 2003, Waddell and Ulfarsson 2004, Borning *et al.* 2007) simulates location choices of individual households and jobs, while anticipating new development on the basis of such models. In some contrast, Gregor's LUSDR (Land Use Scenario DevelopeR) emphasizes fast model runs and the stochastic nature of results, seeking a balance between model completeness and practicality (Gregor 2007). Allocating groups of residential and business development on the basis of mostly multinomial logit (MNL) equations, LUSDR does not model price adjustments. The rationale behind utility maximization is defensible, but these choice-based models tend to require extensive data and composed of several submodels. The interactions among these model components make it hard to discern effects of a policy-decision variable, and uncertainties of one submodel could be easily passed to other parts of the model system. In addition, numerous factors affect decisions of individual households and firms, and these factors interact in an intrinsic way; therefore, improvement opportunities always exist. For example, UrbanSim does not recognize the effects of travel distance, time or cost on location decisions for individual households. Many studies (Van Ommeren *et al.* 1999, Rouwendal and Meijer 2001, Clark *et al.* 2003, and Tillema *et al.* 2006) have suggested significant impacts of commute time (or cost) on residential and/or job site location decisions.

3.3 Gravity Land Use Model

Putman's ITLUP has three components: a *Disaggregated Residential Allocation Model* (DRAM^{®3}), an *EMPloyment Allocation model* (EMPAL[®]) and *LANd CONsumption model* (LANCON). While specification of our gravity-LUM (G-LUM)'s three components was designed to mimic Putman's ITLUP and to follow Putman's published materials as closely as possible (e.g. Putman 1983, TELUM 2007), actual model equations are no doubt slightly different from the trademarked, proprietary software. Therefore, these coded components are referred to as RESLOC, EMPLOC, and LUDENSITY. A reasonably standard sequential TDM was linked externally to the LUM system in order to update travel conditions and provide a well-defined, series of related steps to all future household and employment forecasts (at five-year intervals).

In this integrated modeling framework, the EMPLOC model runs before the RESLOC, followed by LUDENSITY and the TDM. The EMPLOC model output (employment by category by zone) serves as an input to the RESLOC. Predicted household and employment levels (by category/type) are LUDENSITY's primary inputs. A TDM was applied right after allocating households and jobs (and estimating land consumption levels), in order to update travel times between zones and the relative attractiveness of each zone. Figure 3.1 shows the interactions between these components.

³ DRAM and EMPAL are trademarks of S.H. Putman Associates, Inc.

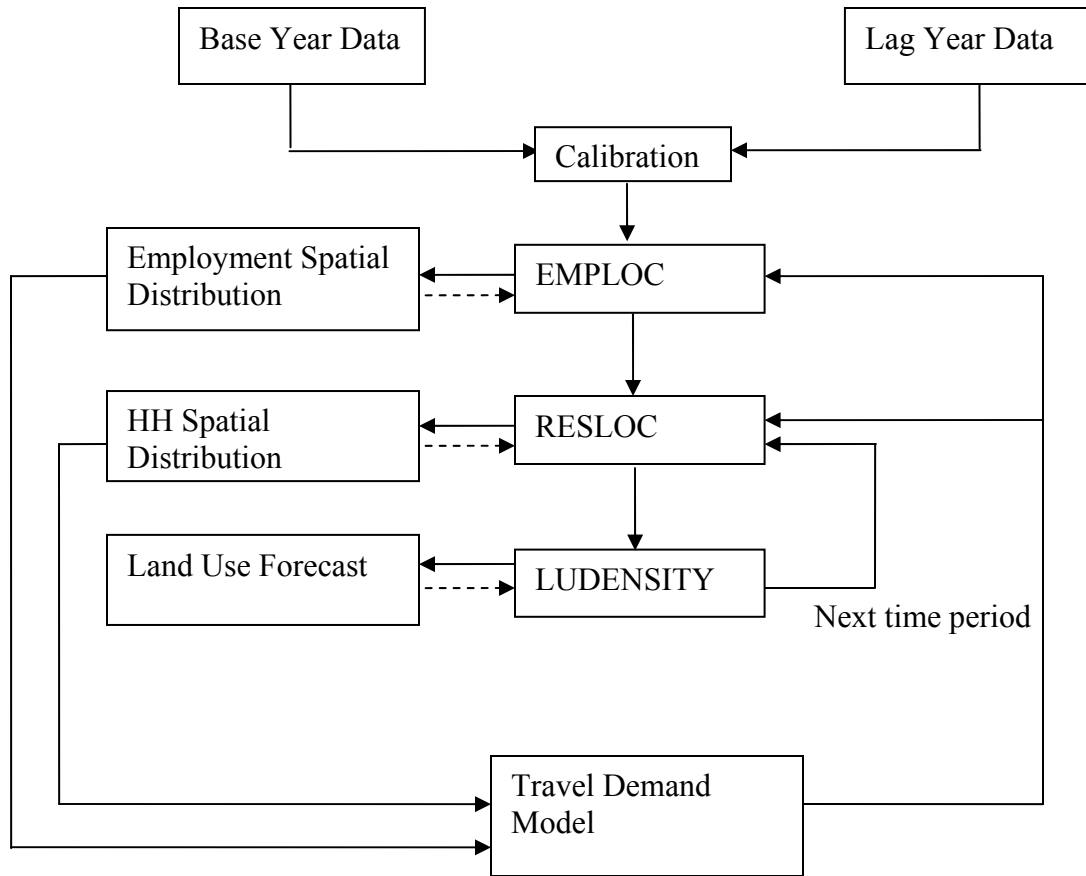


Figure 3.1. Model Logic of the Gravity Land Use Model

3.3.1 G-LUM Specification

RESLOC presumes that current household distribution is determined by current employment locations (jobs), land availability (helping avoid excessive assignment of new households to small and well-developed zones), travel impedances between all zones (as a function of travel cost and time), and prior-year distribution of households. Future-year household allocation/assignment is guided by the residential attractiveness of each zone, measured as a function of (a) each zone's presently vacant yet developable land, (b) the proportion of developable land that already has been developed, (c) residentially developed land, and (d) current numbers of residents by type. The importance of these variables is determined by model calibration, using least squares, maximum likelihood estimation (MLE), maximum entropy (ME) or other methods. The specification is largely non-linear in nature, and calibration requires two time points of data on household and employment distribution, with associated land use maps.

Similarly, the EMPLOC model forecasts the spatial distribution of jobs by category (basic, retail and service). Employment allocation is based on zonal attractiveness, as measured by prior-year employment and zone size. Prior-year population and travel impedances (to all zones) also impact employment distribution.

Finally, the LUDENSITY model uses three log-linear multivariate equations to estimate land consumption by type (residential, basic and commercial) in each zone. Variables determining land consumption include the forecasted spatial distributions of households and employment, and prior-year land use conditions. Key equations for all three models are detailed in Appendix E.

Essentially, the G-LUM model formulation follows FHWA’s freely available Transportation Economic and Land Use Model (TELUM) in its TELUM-RES and TELUM-EMP components, and Caliper’s land use module in its land consumption component. Both TELUM’s and Caliper’s programs are representative applications of Steven Putman’s ITLUP, as it is documented in available publications. TELUM has several restrictions that cannot be overcome due to its “black box” nature. First, the model is limited in the geographies it can consider by restrictions on the average population per zone, which must lie above 3,000 persons (and is recommended to lie below 10,000 persons). Second, the documentation is incomplete, neglecting to cover details of the LANCON model and the parameter calibration process. Caliper’s land use module does not (yet) allow users to estimate model parameters, so this must be done outside the model. To overcome such restrictions, complete Matlab code was developed for model calibration and application in this study.

Of course, there are countless ways that the base ITLUP models can be modified. For example, Krishnamurthy and Kockelman (2003) calibrated and applied a variation for Austin. In addition to slight differences in the specifications of household and employment allocation models, they enforced strict land use constraints by using maximum density values as caps on job and household allocations (to each zone). They were not aware of the LANCON model at the time, and so did not include such equations. In fact, LANCON represents a relatively recent innovation, and many others, such as North Central Texas Council of Governments (NCTCOG), do not use it.

3.3.2 Data Sets Used in the G-LUM

To be consistent with the Envision Central Texas (ECT) scenarios, the model system predicts the spatial distributions of six household types (categorized by number of workers (0, 1 and 2+) and presence of children) and three employment categories (basic, retail and service jobs). Table 3.1 provides the household and employment classifications. Three other employment types (namely Airport, K-12 Education and Higher Education) were assumed to follow ECT’s trend scenario (Scenario A, as generated by the Fregonese Calthorpe Associates)⁴, because these three employment types vary significantly over space yet are relatively stable over time (at least for all zones that have non-zero employment counts).

Table 3.1. Employment and Household Classification

Category	Definition
Type I Household	0-worker household, with at least one child under 18 years of age

⁴ These three types of employment account for 4.7% of total jobs in ECT’s trend scenario.

Type II Household	1-worker household, with at least one child under 18 years of age
Type III Household	2 or more-worker household, with at least one child under 18 years of age
Type IV Household	0-worker household, with no children
Type V Household	1-worker household, with no children
Type VI Household	2 or more-worker household, with no children
Basic Employment	Division A (agriculture, forestry, and fishing) Division B (mining) Division C (construction) Division D (manufacturing) Division E (transportation, communications, electric, gas, and sanitary services) Division F (wholesale trade)
Retail Employment	Division G (retail trade)
Service Employment	Division H (finance, insurance and real estate) Division I (services) Division J (public administration)

Here, the RESLOC, EMPLOC, and LUDENSITY models were calibrated using 2000 and 2005 demographic data (jobs and households, by type) and 2005 land use data (development type) for Austin’s five-county MSA. The Capital Area Metropolitan Planning Organization (CAMPO) provided the 2000 household counts and 2007 projections at the level of traffic analysis zones (TAZs). Total zonal household counts for year 2005 were interpolated using the 2000 and 2007 data, and households by type were calculated using the household type proportions evident in ECT’s trend scenario.

High-quality land use data for the entire MSA is quite limited, and only one set of land use data (in year 2005) could be obtained (via the Capital Area Council of Governments [CAPCOG]). The data was refined using the City of Austin’s (CoA’s) relatively accurate 2003 land use data base, along with year 2004 orthophotos (to fill in over 3,000 parcels that lacked a land use code). Overlapping parcels were eliminated, and missing parcels were added manually. Obtaining a second historical land use data to calibrate the models presently is highly impractical. Therefore, land use conditions for the year 2000 were backcast in each travel analysis zone (TAZ), using 2000 and 2005 household and employment counts (along with the 2005 land use data).

3.3.3 G-LUM Calibration

Two common goodness-of-fit measures can serve as the objective function (to be maximized or minimized) as part of model calibration. These are the R^2 and the data set’s likelihood. Due to the nonlinearities embedded in the model specification, non-linear least squares (NLLS) techniques are needed here (as described in Greene [2000]). Putman (1983) explained that least-squares techniques tend to seek the optimum over a relatively flat surface, while the likelihood tends to enjoy a steeper surface. However, comparisons of results from applications of our Matlab code and TELUM for Austin and Waco, Texas case studies reveal that the optimization surface for such gravity-based land

use models is highly irregular and non-convex (Valsaraj *et al.* 2007), which compromises the alleged advantage of maximum likelihood estimation methods (or their equivalent, entropy maximization). NLLS techniques are easier to understand and implement. For these reasons, NLLS techniques were used for parameter calibration in this study. Tables E.1 through E.3 in Appendix E provide the estimated parameter values and their corresponding t-statistics.

The model calibration results reveal that past counts of households and jobs ($\Delta t = 5$ years) are strong predictors of current counts of all household types, as well as basic and retail employment, because the estimated η 's and λ 's are close to zero; so the estimated coefficients of (and reliance on) the historical counts are close to one. In general, rising travel times reduce a zone's relative attractiveness for new residential development, as shown by the negative signs of α 's and β 's. However, for job distributions, the role of travel time appears mixed. Moreover, many coefficients in the attractiveness function (Function 4) for household allocations are statistically insignificant, especially the ones in the following multiplicative function:

$$\prod_{n'} \left[\left(1 + \frac{N_{i,t-1}^{n'}}{\sum_n N_{i,t-1}^n} \right)^{b_n^{n'}} \right] \quad (3.1)$$

This suggests the possibility of over-specification of the household attractiveness function. However, in order to maintain the model specification of the Gravity-LUM, statistically insignificant coefficients were retained in final model specification.

In terms of land consumption, the amount of developable land in each zone is a valuable predictor of residential, basic and commercial development, with a high level of statistical significance. The ratios of developed, basic and commercial uses to developable land are more statistically significant, as compared to the ratios of households by type to the total household counts in predicting residential uses. The ratio of residential use to developable land is statistically insignificant in basic and commercial developments.

3.3.4 G-LUM Application

The models were applied every five years (partly because the data required for parameter calibration were available in five year intervals). The year 2030 regional households were assumed to be 931,000 (rather than 476,000 in year 2000) and employment (including basic, retail and service) was assumed to be 1,348,000 jobs (rather than 614,000 in 2000). Each household type and employment category was assumed to follow an exponential growth pattern, and the intermediate region-wide totals controlled the LUM behavior. The control totals are necessary in order to predict a level of households and employment in year 2030 that is comparable to the visioning approaches.

Technical Details in the Land Use Model

If some household types or employment categories in a TAZ have zero values in the base year, they will remain so because of the multiplicative nature of the RESLOC and EMPLOC model specifications. However, it is often desired that these household types or employment categories can move to such a zone in the future. Therefore, small values (e.g., 1) were added to TAZ counts of households or jobs in each category, to serve as “seeds”. When the initial counts of households or jobs were smaller than the pre-specified seed value, the seed value was added before applying the models (Equations E.1 through E.7 in Appendix E). After applying the models, the seed value was deducted from the corresponding results (before the systematic adjustment using regional control totals). If any forecasted counts of households or jobs became negative due to the seed value deduction, a zero value was used.

Residuals from model calibration represent some unobserved factors that influence the spatial distributions of households and employment. In order to take these unobserved factors into account, residuals should be added to the model applications (or forecasts of household and employment distributions). It is argued that the influence of unobserved factors should diminish over time (TELUM 2007). So, a linear deduction of residuals was applied in this study, with zero impacts in year 2030 (e.g., 1.0, 0.75, 0.5, 0.25, and 0).

In order to ensure reasonable population and jobs forecasts, certain rules were implemented in the model application. First, households and jobs in one TAZ were not allowed to decrease by more than 5% in any one five-year time interval. Second, increases in household and job counts were limited by land availability. For each household type, the maximum increase in the ratio of counts between two periods in any given zone was assumed to be the ratio of developable land to residentially developed land. For each job category, the maximum increase was set as the ratio of developable land to the sum of basic and commercially developed land. Third, in fully developed TAZs, households and jobs were not allowed to increase by more than 5% per time interval⁵. TAZs that violated the first rule were marked, and then the corresponding type of households or jobs was “drawn” from the un-marked TAZs, in proportion to their original, forecasted counts. Similarly, TAZs that violated the second rule were marked, and then the “extra” households or jobs were re-allocated to the un-marked TAZs, in proportion to their original counts. This re-allocation process was run interactively until all TAZs satisfied the two rules.

The multiplicative nature of LUDENSITY model requires positive values for the numbers of households (by type and total) or jobs (by category and total) and the amounts of developed, residential, basic, commercial and developable land. Therefore, zero or extremely small values were adjusted to 0.0001 (for counts of households and employment) or 1E-10 (for acres of land). Like household and employment forecasts, the residential, basic and commercial land were not allowed to fall by more than 5% in any 5-year interval; and in fully developed TAZs, residential, basic, and commercial lands

⁵ This decision-rule relaxes the second decision-rule for fully developed zones in order to allow for infill in those zones.

were not allowed to increase by more than 5% in one time interval. In addition, the minimum land per job or household depended on two additional factors: land consumptions in the previous period, and a pre-specified minimum land required per household, basic job or commercial job. These were assumed to be 500, 250, and 1000 square feet (per person or job), respectively. When projected new development needed more than the available land, the forecasted sizes of residential, basic and commercial development were proportionally reduced.

Transportation and Land Use Policies

The land use and transportation effects of four distinctive policies were investigated here. These include a business-as-usual (BAU or base) scenario, a road pricing scenario (congestion pricing plus a per-mile-traveled carbon tax, CPCT), a density floor scenario (no new low-density development), and an urban growth boundary (UGB) scenario (prohibiting new development in presently peripheral, largely undeveloped zones).

The **Road-Pricing scenario** (congestion pricing plus a carbon tax) required modifications to the model system's TDM component. A congestion charge was set to equal the difference between the marginal cost and average cost of using each link in the network. The social marginal cost (MC) and average private cost (AC) of using a link, in terms of travel time, are defined as follows:

$$MC = VOTT \times t(ff) \times \left(1 + \mu(\varphi + 1) \left(\frac{v}{c} \right)^\varphi \right) \quad (3.2)$$

$$AC = VOTT \times t(ff) \times \left(1 + \mu \left(\frac{v}{c} \right)^\varphi \right) \quad (3.3)$$

where $VOTT$ is the value of travel time (assumed to be \$6.75/hour⁶, as suggested by Appendix C, $t(ff)$ is the free-flow travel time for the link, v is demand volume for the link (in vehicles per hour), c is the link's capacity (also in vehicles per hour), and μ and φ (assumed to be 0.83 and 5.5) are the coefficients in the well-known Bureau of Public Roads (BPR) formula, which are used to calculate link speeds and thus link performance under a given demand. When another vehicle enters the roadway, it raises v by 1 unit, causing both MC and AC to rise. The added cost endured by others, and thus not perceived by the new traveler, is the different between these. When converted to dollars, via $VOTT$, one has the recommend link-specific congestion toll, as follows:

$$CP = VOTT \times t(ff) \times \mu \varphi \left(\frac{v}{c} \right)^\varphi \quad (3.4)$$

⁶ VOTTs are \$9/hour for work and airport trips and \$4.5/hour for non-work trips in destination and mode choice. The average of the two was used in trip assignment.

The carbon tax is assumed to be 4.55 cents per mile on all links in the network, and this number was calculated as follows:

$$CT = \frac{26 \text{ lbs/gal}}{20 \text{ mile/gal}} \times \frac{70 \text{ \$/ton}}{2000 \text{ lbs/ton}} \quad (3.5)$$

Here, it was assumed that every gallon of gasoline emits 26 pounds of carbon dioxide (EPA 2007b), the removal cost of carbon is 70 dollars per ton⁷, and the average fuel efficiency is 20 mile per gallon of gasoline.

Since tolling technology (overhead gantries, variable message signs, and communications equipment for link use and customer accounts) is pricey (see, e.g., Gulipalli and Kockelman [2008]), only links that are classified as freeway (by CAMPO) were assessed a congestion toll. Two networks were used in this study: one represents the network configuration and capacities until year 2015, while the other represents a somewhat expanded network, after 2015. Figures 3.2 and 3.3 depict these two networks and their freeways (which are tolled in the road pricing scenario).

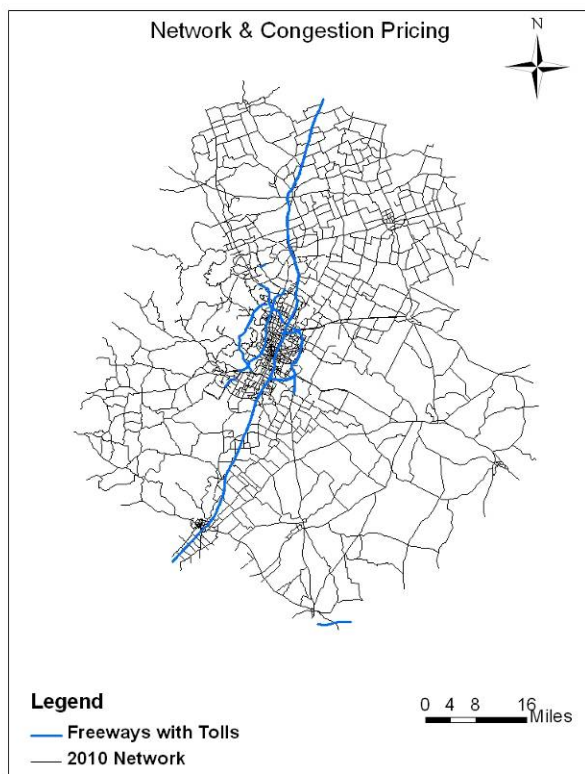


Figure 3.2. Austin Network with Toll Roads Highlighted for Years 2010 & 2015

⁷ Using different discount rates, risk values and distributions of carbon savings, Tol (1999) estimated a wide range of possible carbon emissions – from just \$1 or \$2/ton to over \$300/ton. \$70 per ton corresponds to Tol's (1999) median cost estimate with a discount rate of 3%. Based on recent trends, estimates lie closer to \$50 per ton (see e.g., Fischer *et al.* 2007, U.S. Environmental Protection Agency 2008, CRAI 2008).

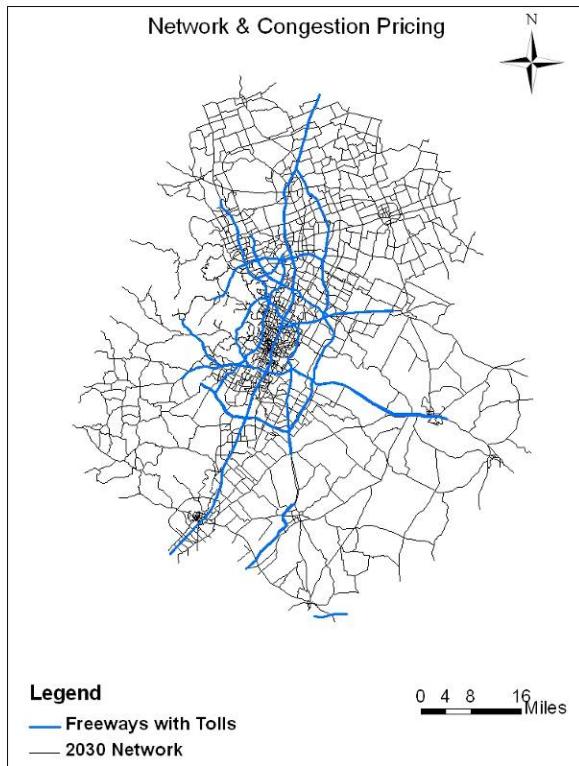


Figure 3.3. Austin Network with Toll Roads Highlighted for Years 2020, 2025 & 2030

The *Density-Floor Scenario* required minimum densities for new development in each zone to be 2 households per added, residentially developed acre or 5 jobs per new commercially/industrially developed acre; otherwise, such development was not permitted. This policy was implemented in the model’s LUDENSITY component. Since LUDENSITY only provides direct feedback to the RESLOC, EMPLOC employment allocation was not directly affected by this policy.

The *Urban Growth Boundary (UGB) scenario* restricted all types of new development to a pre-defined set of largely contiguous zones, centered on existing population centers. Lands outside of this “boundary” were not permitted any new residential, basic or commercial development. Developable zones were defined as TAZs who have 2 or more job-equivalents⁸ per acre, and any TAZs touching their boundaries (essentially to ensure adequate lands for 25 more years of Austin’s development). Figure 3.4 shows the set of zones lying within and outside the UGB used in this study.

⁸ One household is counted as 1.4 jobs, because the regional employment rate is 1.4 jobs per household.

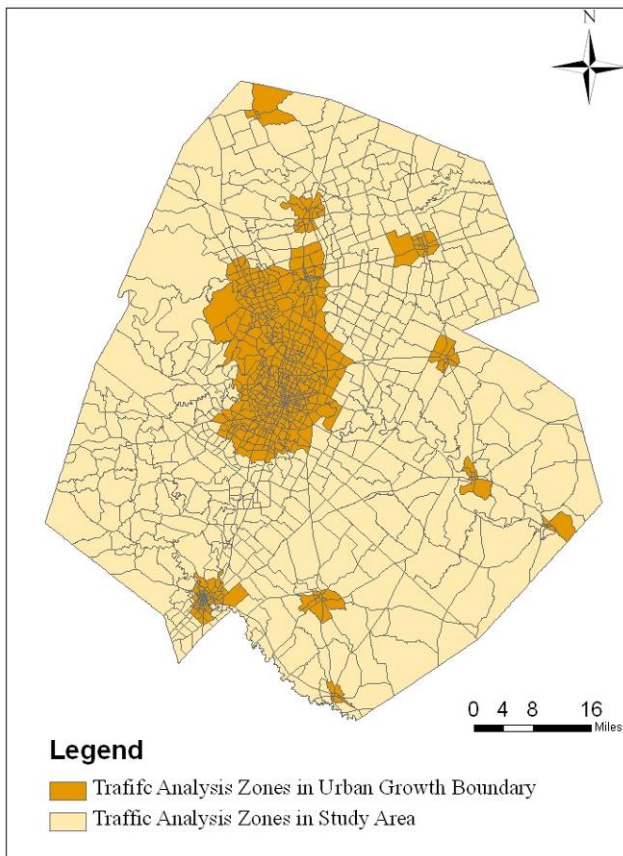


Figure 3.4. Urban Growth Boundary

3.3.5 G-LUM Application Results

This section emphasizes the results of model application for the business-as-usual (BAU), road pricing, and urban growth boundary (UGB) scenarios in detail. Variables like vehicle-miles traveled (VMT), traffic flows, volume-to-capacity ratios, speed, land use densities, and downtown accessibility of households and employment are summarized.

The density-floor scenario is not discussed at length here because it, surprisingly, did *not* promote denser development patterns than the BAU scenario. Instead, it generated a more “sprawling” residential development pattern and a relatively similar spatial distribution of jobs (as compared to the BAU scenario). Several reasons contribute to these unexpected results. First, as explained earlier, in the Model Application section, this policy was implemented in the LUDENSITY component that has only limited influence on the spatial distribution of households and jobs. Implementation in the RESLOC and EMPLOC components may generate more concentrated development patterns. Second, thanks to the positive signs of the q^n parameters (which are specific to the vacant developable land in each zone), zones with more vacant developable land are modeled as more attractive to households. High household densities in residentially

preferred zones preserve more vacant developable land, so more households prefer such zones, often on the City's periphery. Third, as evident in the model logic, LUDENSITY does not provide direct feedback to the EMPLOC module. As a result, this policy generated a similar job distribution to the BAU scenario. The results are not felt to be reasonable for the density floor set-up, so only the other three scenarios' results are detailed here.

Household and Employment Distributions

Figures E.1 and E.2 in Appendix E present the forecasted distribution of households and jobs at the TAZ level in year 2030, assuming *business as usual*. As shown by the maps, households and employment tended to remain concentrated in the urban areas and along regional freeways.

The households and employment density forecasts when implementing *road pricing* (congestion pricing plus a carbon tax) are shown in Figures E.3 and E.4 in Appendix E. The distribution patterns are similar to the results of business as usual, using the selected grouping thresholds in the map legend. This suggests that the combined policy of congestion pricing and a carbon tax did not alter the location choices of households and firms in a significant way, but did affect how far people travel (as discussed in the following subsection, such policies significantly reduced overall VMT).

Such lack of responsiveness is suspected to come from two important sources: First, added travel costs (4.55¢/mile for added fuel costs and another 1.5 to 3.2¢/mile for average congestion tolls during peak hours) are just 10 percent of underlying car ownership and use costs (FHWA 2001), except in highly congested corridors at peak times of day when demand-based tolls sometimes reach \$1/mile. Thus, locators may consider such cost changes to be rather negligible. Second, and more critical for future scenario testing: the gravity model formulation is relatively insensitive to constant shifts in travel costs (Equations E.1 and E.5's c_{ij}). This seems fundamentally unrealistic, since a lack of good regional access (e.g., all trips suddenly incur a fixed toll of \$10) should result in more clustering at central and other nodal locations. Of course, if speeds are all reduced on the network or new tolls apply per mile traveled, there will be more of a scaled (rather than constant) shift in travel costs and thus more centrally located zones will enjoy improvements in their *relative* attractiveness, but such relative movements may be insufficient to generate new preference patterns accompanying such network conditions. A new paradigm/LUM specification is needed, to allow for more appropriate response opportunities. A third reason for such insensitivity is that over 90 percent of next-period ($\Delta t = 5$ years) predictions are simply the lagged count value in each zone (except for basic employment), resulting in much "friction" in the system. While not unreasonable for many scenarios, more dramatic scenarios (e.g., those with strong incentives for household-move decisions) may not keep pace with actual location changes, at least not in the short term.

Figures E.5 and E.6 in Appendix E show household and employment density forecasts for the *UGB* scenario. As required by the policy, all the new development (households, basic, retail and service employment) happens within the pre-defined zones; any

households and basic, retail and service jobs outside of the boundary already existed in year 2005.

The G-LUM forecasted some extremely high values of household and employment densities, even with all the constraints discussed in the Model Application section. For example, two TAZs close to the CoA’s downtown and three TAZs in San Marcos’s downtown were predicted to have more than 10,000 households/mile² (or 15.6 households per acre) in year 2030, assuming business as usual. The same five TAZs were forecasted to have high densities under road pricing as well. In the UGB scenario, the number of TAZs having such high household densities rose to 20 (most are in the region’s core and San Marcos’s downtown). In terms of jobs, the BAU scenario predicted 4 TAZs in Austin’s downtown to have more than 100,000 jobs/mile² (or 156 jobs per acre) in year 2030. When implementing road pricing, the same four TAZs were forecasted to have high employment densities, but with slightly different values. In the UGB scenario, one additional downtown Austin TAZ, another in the northern part of the City, and another in San Marcos’s downtown were predicted to have more than 100,000 jobs/ mile². These extreme values suggest that G-LUM, even with a series of constraints, may have problems running without any local knowledge and expert opinion.

In order to quantify the differences between the three scenarios with a single index, an **accessibility index (AI)** for the region’s central business district (CBD) was developed as follows:

$$AI = \sum_i \frac{Count_i}{DistToCBD_i} \tag{3.6}$$

where $Count_i$ is the count of households or jobs in zone i , and $dist_i$ is the inter-centroid distance (in miles) from TAZ i to one of Austin’s core TAZs (housing Texas’s capitol). This simple AI was calculated for both households and employment for each scenario, and the results are shown in Table 3.2. The spatial distributions of households and employment under the UGB policy exhibit the highest AI value, indicating that the UGB policy generated the highest level of clustered development. The AI values for the BAU scenario and the road pricing policy scenario are close, as expected. It seems that road pricing may not affect locational accessibilities enough to prompt regional centralization of land uses, but, as discussed below, it is expected to have a strong impact on travel.

Table 3.2. Accessibility Index for Households and Employment for Each Policy Scenario

	Households (x 10 ⁶)	Employment (x 10 ⁷)
Base Scenario	1.81	6.29
Congestion Pricing & Carbon Tax	1.53	6.32
Urban Growth Boundary Policy	3.74	6.93

Note: The accessibility index is computed with respect to Austin’s downtown.

In terms of *density* outcomes, the count-weighted⁹ average densities of households and employment were calculated, and are shown in Table 3.3. Again, the BAU and road pricing scenarios constitute the most similar scenario pair. As expected, the UGB policy generates the highest weighted densities. Within the UGBs, the simple average (without using weights) densities reach 4,132 households/mile² (or 6.5 households/acre) and 6,630 jobs/mile² (or 10.4 jobs/miles).

Table 3.3. Count-Weighted Average Densities for Each Policy Scenario (counts/mile²)

	Households	Employment
Base Scenario	1,483	7,995
Congestion Pricing & Carbon Tax	1,477	8,047
Urban Growth Boundary Policy	29,696	22,581

Note: The count-weighted average densities for UGB policy were calculated for the entire study area.

As a further demonstration of the *changes* in households and employment distributions over time, the model results were compared to the conditions in year 2005 (when the forecasting starts). Figures E.7 and E.8 in Appendix E present the household and employment density changes from year 2005 to year 2030, assuming the business as usual scenarios. Some TAZs in the CoA core were predicted to lose households over the next 25 years, while some TAZs at the City’s periphery, especially in the northern part of the CoA, were predicted to gain households during that time period. Most TAZs were predicted to gain jobs between 2005 and 2030, with a few exceptions for downtown TAZs and TAZs in the northern part of the CoA.

The change patterns for the road pricing scenario (Figures E.9 and E.10 in Appendix E) look very similar to the base scenario, relying on the maps’ legends. Figures E.11 and E.12 in Appendix E show household and employment density changes when implementing the UGB policy. As expected, household growth was predicted to concentrate within the predefined boundaries, though a few TAZs within the UGB were forecasted to lose households. The change pattern for employment is less clear because three employment types (Airport, K-12 Education and Higher Education) were not modeled in this study; thus, they were allowed to grow outside of the UGB. Other than that, the employment change pattern is similar to households in the sense that most TAZs within the UGB were predicted to gain jobs while a few zones within the boundary were predicted to lose jobs.

Results of the Travel Demand Models

Of course, the TDM results are of great interest as well. VMT estimates, link flows, and mode splits for all scenarios closely relate to congestion levels as well as mobile-source emissions. Table 3.4 summarizes projected VMT values for the year 2030 (by time-of-day) across the three policy scenarios. The results suggest that the road pricing and UGB policies are very effective, in terms of reducing VMT. These two policy scenarios were estimated to reduce regional VMT relative to the BAU case, by 16.0% and 17.2%,

⁹ The number of households or jobs by type was used as weight in calculating the count-weighted averages.

respectively, resulting in reductions of 13.54 million and 14.58 million VMT per day (or 14.5 or 15.7 VMT per household per day), respectively.

Table 3.4. Vehicle Miles Traveled (VMT) in Year 2030 for Each Policy Scenario

	Time-of-Day				Total
	AM	OP	PM	MID	
Base Scenario	17,010	6,463	27,176	34,146	84,795
Congestion Pricing & Carbon Tax	14,636	5,468	22,821	28,326	71,252
Urban Growth Boundary Policy	14,205	5,336	22,488	28,187	70,216

Note: Values are in thousands of daily VMT.

The total intra-regional personal and commercial trips in year 2030 are given in Table 3.5. The BAU and road pricing policies generated similar numbers of personal and commercial trips, while the UGB policy generated fewer of both types. In contrast, the UGB policy was estimated to reduce total tripmaking by 4.8%, or 0.57 million trips per weekday. Comparisons of the VMT and trip numbers across scenarios suggest that VMT reductions under the road pricing policy basically come from shorter trips, while VMT reduction under the UGB policy comes both from shorter trips and fewer trips. The external-local and external-through personal trips are assumed constant, at 185,660 and 73,461 trips per day for the three policy scenarios in each model year because we do not have a model for trip production and attraction outside the study area. (Readers may refer to Appendix H for estimates of passenger-vehicle fleet composition over similar scenarios.)

Table 3.5. Intra-Regional Personal and Commercial Trips in Year 2030 for Each Policy Scenario

	Total Person Trips (x10 ⁶)	Total Commercial Trips (x10 ⁶)	Sum (x10 ⁶)
Base Scenario	11.25	0.642	11.89
Congestion Pricing & Carbon Tax	11.25	0.642	11.89
Urban Growth Boundary Policy	10.70	0.622	11.32

Table 3.6 provides the numbers of personal trips by mode (walk/bike, transit and auto), and Table 3.7 shows mode shares. The road pricing and UGB policies are effective in promoting transit usage while reducing the number of automobile trips; however, the overall differences are quite slight, suggesting that not even policies as strict as these can shift Austinites' reliance on the automobile. The UGB policy enjoys the highest number of walk/bike trips, bettering the other two policies by 27 percent.

Table 3.6. Number of Personal Trips by Mode per Day in Year 2030 for Each Policy Scenario

	Walk/Bike (x10 ⁶)	Transit (x10 ⁶)	Auto (x10 ⁶)	Sum (x10 ⁶)
Base Scenario	0.37	0.90	9.97	11.25
Congestion Pricing & Carbon Tax	0.37	1.03	9.85	11.25

Urban Growth Boundary Policy	0.47	0.97	9.27	10.70
------------------------------	------	------	------	-------

Table 3.7. Personal Trip Mode Shares in a Weekday in Year 2030 for Each Policy Scenario

	Walk/Bike	Transit	Auto
Base Scenario	3.3%	8.0%	88.6%
Congestion Pricing & Carbon Tax	3.3%	9.1%	87.5%
Urban Growth Boundary Policy	4.4%	9.0%	86.6%

Table 3.8 provides the VMT-weighted average speeds for each of the three policy scenarios. It seems that the road pricing policy is the most effective in increasing average speed across the region's network.

Table 3.8. VMT-Weighted Average Speed for Each Policy Scenario

	VMT-Weighted Average Speed (miles/hour)	
	AM	PM
Base Scenario	47.3	52.2
Congestion Pricing & Carbon Tax	52.0	55.1
Urban Growth Boundary Policy	49.3	52.8

Table 3.9 gives the VMT-weighted average v/c ratios for the three policy scenarios. It suggests that the road pricing policy is the most effective for reducing the region's overall v/c ratio (or traffic congestion level in the region).

Table 3.9. VMT-Weighted Average Volume-to-Capacity Ratio for Each Policy Scenario

	VMT-Weighted Average Volume-to-Capacity Ratio	
	AM	PM
Base Scenario	0.692	0.592
Congestion Pricing & Carbon Tax	0.576	0.475
Urban Growth Boundary Policy	0.656	0.577

3.3.6 Findings

The estimated parameters generally have the expected signs, but some variables are not statistically significant. However, in order to provide maximum consistency with a gravity-style model, applications described here use all publicly available formulations and explanatory variables (as published in Putman 1983, TELUM 2007).

In addition to the base forecast scenario (assuming business-as-usual), three other policies were investigated using the gravity-based LUM and a standard TDM. These are a road pricing policy, a density floor policy, and an urban growth boundary (UGB) policy. The model results suggest that the base-case and road-pricing scenarios will result in similar household and employment distributions. As required by the policy, the UGB policy will

allocate all the new development (households, basic, retail and service employment) within the pre-defined zones. Households and employment opportunities remain heavily concentrated in the region's core under each policy scenario. An accessibility index (AI) for the region's core zone was developed to quantify the differences between the three scenarios, for both households and employment. The UGB policy ends up offering the highest AI values in 2030, generating the highest level of clustered development. Interestingly, the business as usual and road pricing scenarios have similar AI values.

In terms of travel behavior impacts, the road pricing and UGB policies appear to be powerful tools for VMT reductions. As compared to the base-case, these two policy scenarios were estimated to reduce regional VMT relative to the BAU case, by 16.0% and 17.2%, respectively. The base-case and road pricing scenarios generate similar levels of personal and commercial trips, while the UGB policy generates fewer of both types. This suggests that the VMT reduction of the road pricing policy basically comes from shorter trips, while VMT reductions under the UGB policy come both from shorter trips as well as fewer trips. VMT-weighted averages for speed and volume-to-capacity ratio provide single-value measures for the entire study area. The road pricing policy was estimated to reduce link-level and regional congestion the most.

The G-LUM forecasted extremely high population and job densities in downtown Austin and San Marcos zones under the UGB scenario, even subject to various growth/development constraints included in the model. This suggests that local knowledge and expert opinion may be needed to manually adjust gravity-based model forecasts. In addition, the LUDENSITY component should be improved by adding a lagged density term to pivot off of current/past land use densities in each zone, rather than reflecting model averages (thus ignoring each zone's current densities). Nevertheless, the restricted version of G-LUM appears to highlight interesting directions for land use patterns while facilitating traffic forecasts into the far future, when fast-growing regions may head in any number of directions, depending on local land use and transportation policies. Such models are another tool for anticipating the general direction and potential magnitude of policy and investment impacts.

3.4 A Hybrid Land Use Model System

In addition to the rather straightforward G-LUM, a hybrid land use model system was constructed and applied to the 5-county region. It consists of two model components, operated on individual parcel and zonal levels. The model system emphasizes parcel-level applications, which offer more behavioral realism and enjoy significant potential in the land use modeling domain. Parcel-level data is becoming widely available, thanks to the advances in geographic information system (GIS) technologies. It also relies on recent advances in spatial econometrics which recognize spatial autocorrelation across TAZs via both spatial lag and spatial error processes.

3.4.1 Model System

Figure 3.5 shows the model components and their relationship. The *Land Use Change Model (LUC Model)* determines how individual parcels evolve: whether an undeveloped parcel will subdivide into several smaller parcels during a specified time interval (e.g., 5 years in this study) (the *Subdivision Model*), how big these subdivided parcels are (the *Parcel Size Model*), and what land use types will emerge on each individual parcel (the *Land Development Model*). Land use change is generally associated with increases (or decreases) of land use intensity levels (household and employment counts), and the effect is aggregated at the level of TAZs to provide key inputs to a standard TDM.

Tobler’s first law of geography states “everything is related to everything else, but near things are more related than distant things.” (1970, p. 236) Therefore, changes in land use intensity at one TAZ correlate with the changes of its neighbors. In addition, many studies have detected correlations between population and employment (e.g., Carruthers and Vias 2005, Boarnet *et al.* 2005). A *Land Use Intensity Model (LUI Model)* allocates households and employment by type, using a seemingly unrelated regression (SUR) with two spatial processes. The specifications are highly statistical in nature, and described in detail in Zhou and Kockelman (2006 and 2008).

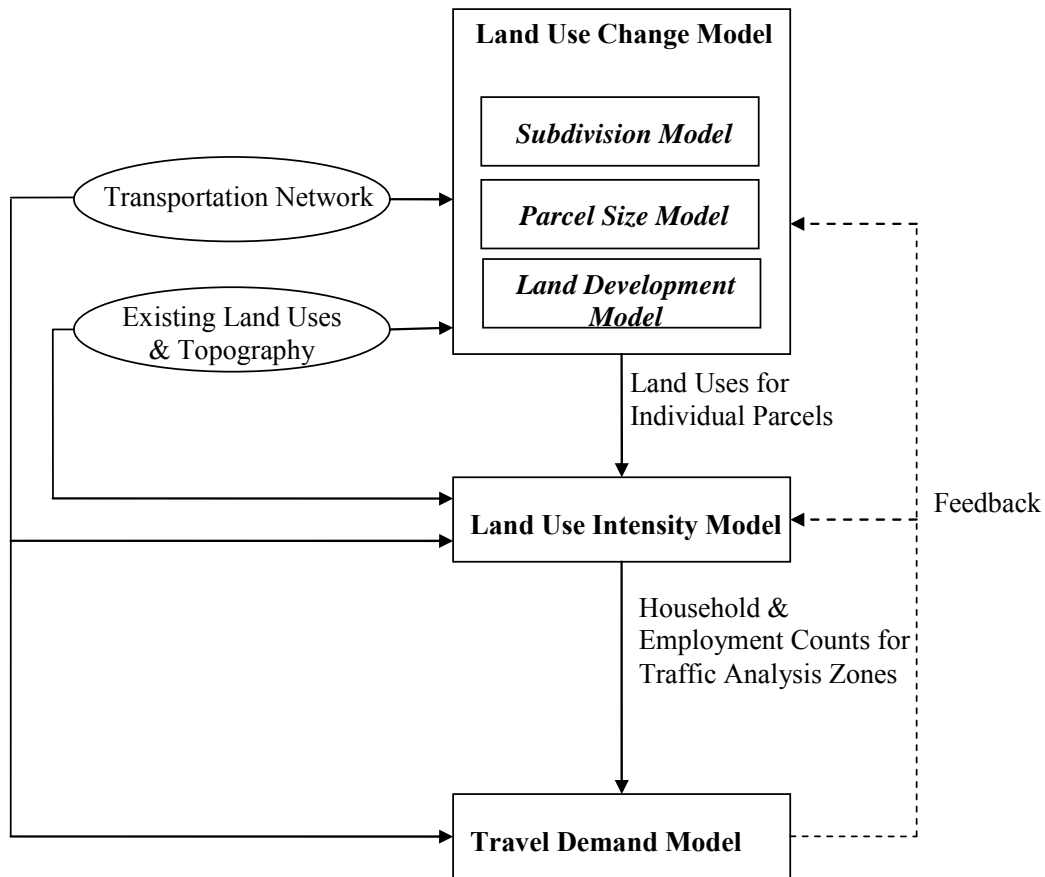


Figure 3.5. Model Logic of the LUC-LUI Model System

3.4.2 Data Sets Used in the LUC-LUI Model System

Data sets used in this LUC-LUI model system include land use parcel maps, current and past household counts (by category) and employment counts (by type) at the level of TAZs, transportation network details, and topographic data. The following sub-sections discuss all data sets used in model calibration and application, as well as data challenges encountered and their solutions.

Land Use Data

The City of Austin’s Neighborhood Planning and Zoning Department (NPZD) provided land use parcel maps for years 1995 and 2000. Parcels located in the overlay of the two maps were used in calibrating the LUC model, resulting in a 420-square mile study area centered of the City of Austin. The parcels were classified into 14 distinct land use categories. Considering ease of interpretation and data set limitations for the larger, 5-county application, these 14 categories were grouped into 10, as listed in Table 3.10.

Table 3.10. Land Use Categories

Original Land Use Classification	Description	Final Classification
Large-lot single-family	Single-family detached, two-family attached with lot size bigger than 10 acres	Large-lot single-family
Single-family	Single-family detached, two-family attached	Single-family
Mobile homes	Mobile homes	Multiple-family
Multi-family	Three/fourplex, apartment/condo, group quarters, retirement	
Commercial	Retail and general merchandise, apparel and accessories, furniture and home furnishings, grocery and food sales, eating and drinking, auto related, entertainment, personal services, lodgings, building services	Commercial or Office
Office	Administrative offices, financial services (banks), medical offices, research and development	
Industrial	Manufacturing, warehousing, equipment sales and service, recycling and scrap, animal handling	Industrial
Mining	Resource extraction	
Civic	Semi-institutional housing, hospital, government services, educational meeting and assembly, cemetery	Civic
Undeveloped/Rural	Rural uses, vacant land, land under construction	Undeveloped
Open Space	Parks/greenbelts, golf courses, camp grounds and open spaces set aside for preservation or protection.	Excluded
Water	Water	
Utilities	Utility services	Utility

Transportation	Railroad facilities, transportation terminal, aviation facilities, marina parking facilities	Transportation
----------------	--	----------------

Source: Land Use Survey Project Description, City of Austin

611 parcels labeled as “unknown” were checked against 1995 and 2002 orthophotos¹⁰, and appropriate land use codes were determined. In addition, a GIS shape file for existing protected lands, future protected lands and the region’s 100-year floodplain was assembled by Dr. Barbara Parmenter. As with open space and water categories in the City’s dataset, the protected lands and 100-year floodplains are excluded from future development.

Only one set of land use data (in year 2005) is available for the entire 5-county region, and this came from the Capital Area Council of Governments (CAPCOG). This parcel map was refined using the City of Austin’s relatively accurate 2003 land use data, along with year 2004 orthophotos (to fill in over 3,000 parcels that lacked a land use code). This data set has a classification scheme similar to the City of Austin’s parcel maps. However, it does not separate commercial and office uses, thus requiring the combination of these two types in LUC model calibration. This data set was also used to calibrate the LUI model and kick off the land use projections for the entire region.

The nature and extent of each undeveloped parcel’s surrounding “neighborhood” were quantified using land use area totals and land use balance in a series of concentric neighborhoods (e.g. circular or ring geometries). The defining radii ranged from 0.5 mile to 2.0 miles, in increments of 0.5 mile. A measure of local land use balance was constructed based on deviations in local land use percentages, relative to a “perfect” (equal-proportions) land use balance (Kockelman 1997). This explanatory variable was defined as follows:

$$Entropy = -\frac{1}{\ln(J)} \sum_j^J P_j \ln(P_j) \quad (3.7)$$

where J is the number of land use types under consideration and P_j is the fraction of the neighborhood that is of land use type j (for large-lot single-family, single-family, multi-family, commercial or office, industrial, and civic uses). In this model system, the entropy index helps reveal the preference of land development for neighborhoods offering more balanced land use patterns.

Transportation and Topographic Data

Variables emerging from TDM outputs (e.g. travel time or cost across zones) should be considered for use in land use model specifications in order to integrate the two model systems and allow land use patterns to respond to changes in transportation conditions. Central business district (CBD) and regional accessibility indices were considered here. CBD accessibility was measured as each parcel’s network travel time to the nearest CBD

¹⁰ The 1995 orthophotos provide images with a 1m x 1 m resolution, and were obtained from the Texas Natural Resource Information System (TNRIS) website. The 2000 orthophotos have 2 ft x 2 ft resolution, and were downloaded from the Capital Area Council of Governments (CAPCOG) webpage.

under peak-hour conditions, while regional accessibility was calculated using the destination choice model.

In model calibration, only Austin’s CBD was considered, but in model application, another 12 urban clusters (defined by Caliper in its geographic data distributed with TransCAD 4.7) were treated as CBDs in order to capture the effects of more local business. These urban clusters include Georgetown and Taylor in Williamson County, Lakeway and Lago Vista in Travis County, San Marcos, Woodcreek and Green Pastures in Hays County, Smithville, Bastrop and Elgin in Bastrop County, and Lockhart and Luling in Caldwell County.

Regional accessibility represents zone access to all activity opportunities in a region, and was calculated as follows:

$$AI_i = \log \left(\sum_j \exp(-0.831 \times GC_{ij} + 0.0000259 \times Attraction_i) \right) \quad (3.8)$$

where, GC_{ij} is the generalized cost between zone i and j , $Attraction_i$ is the total number of trips attracted to zone i . Appendix C shows how to obtain the Equation 3.8’s estimated parameters. This regional accessibility is the log-sum in a TDM, which equals the expectation of maximum utilities in the *Destination Choice Model* (a sub-model of the TDM) (Ben-Akiva and Lerman, 1985). In addition, Euclidean distances to the nearest freeway were computed from parcel centroids using ArcGIS’s spatial analyst (as a Euclidean distance), and transit access was defined as the number of transit stops within a 0.5 mile radius of each undeveloped parcel’s centroid. The Capital Area Metropolitan Planning Organization’s (CAMPO) highway and transit networks were used to calculate these two explanatory variables.

The U.S. Geological Survey’s national elevation dataset (NED) offers the best-available elevation data for the Austin region, at approximately 10-meter resolution. Slopes were computed as the maximum (percentage) change in elevation over the distance between each cell’s centroid and those of its 8 neighbors. Slopes of multiple pixels having centroids within a single parcel then were averaged.

Household and Employment Data

CAMPO provided household and employment count estimates by type at the TAZ level for the years of 2000 and 2005. The same employment and household classification in Table 3.1 was used here. The year-2030 regional household total is assumed to be 931,000 (versus 476,000 in year 2000) and total 2030 employment (including basic, retail and service) 1,285,000 jobs (rather than 613,000 in 2000), in order to be consistent with Envision Central Texas (ECT) forecasts (Envision Central Texas 2003). The models were applied every five years (in large part because the data required for parameter calibration were available in five year intervals). Household and employment counts (by type) were assumed to follow an exponential growth pattern, and these intermediate region-wide totals thus constrain the ITLUM’s results.

Challenges of Data Availability

In order to track the dynamics of parcel evolution, the LUC model requires parcel maps at two (or more) points in time. Only one for the entire 5-county region (for the year 2005) could be obtained from CAPCOG. Thus, the LUC model was estimated only for the City of Austin and its two-mile extraterritorial jurisdiction (ETJ) using 1995 and 2000 parcel maps. This model was then applied to the entire region's set of year-2005 undeveloped parcels. The alternative specific constants in the *Land Development Model* were iteratively adjusted because the calibration and application data sets differ. Parameters in the other two models (the *Subdivision Model* and the *Parcel Size Model*) are less obvious for adjustment, given that we only observe the final results of the three models that are sequentially applied.

Since the only set of parcel data available for the entire MSA is for the year 2005, a “target” set of land use conditions in year 2010 was forecasted, using the available data and year 2010 expectations of regional household and employment counts. Basically, the region-wide total large-lot single-family, single-family and multi-family residential land acreages were inflated by the ratio of household counts in year 2010 and 2005. Similarly, industrial, commercial or office, and civic land acreages were calculated using the ratios of basic, retail and service jobs in years 2010 and 2005, respectively.

The LUI model allocates the *changes* in household and job counts between two points of time. This model involves sophisticated spatial processes, so it cannot be easily applied to spatial configurations that differ from that used in model calibration. So the parameter adjustment technique used in the LUC model does not apply here. Instead, year 2000 land use conditions were backcasted in each TAZ, using 2005 parcel map and household and employment counts in years 2000 and 2005. More specifically, total residential land (including large-lot single-family, single-family and multi-family) in year 2000 was scaled down using the ratio of household counts in 2000 and 2005. Since developed lands rarely change their use types, the backcasted residential land in year 2000 was not allowed to be more than that in year 2005 for each TAZ. Using this same method, land for industrial, commercial or office, and civic uses were backcasted using 2005 parcel map and basic, retail and service employment, respectively.

3.4.3 Calibration of the LUC Model

As functionally distinct observational units, parcels lend themselves to disaggregate analysis with discrete responses for use type and subdivision. This work models the processes of parcel subdivision, size determination and land development using three models. First, the likelihood of subdivision was modeled using a binomial logit model (Greene 2000). Second, if a parcel is predicted to subdivide in the model year, newly generated parcels sizes were determined using a linear regression (with a log-transformed dependent variable to ensure non-negativity). And finally, land development on such previously undeveloped parcels was modeled using a multinomial logit model (MNL) for

various use alternatives (e.g., large-lot single-family, single-family, multi-family, commercial/office, industrial, civic, and undeveloped).

Subdivision Model

The *Subdivision Model* anticipates the likelihood of parcel subdivision, using a binomial logit. Table F.1 in Appendix F provides summary statistics of all explanatory variables used in the final model specification (where $y = 1$ if the undeveloped parcel subdivided between 1995 and 2000), and the parameter estimates are shown in Table F.2.

Not surprising, bigger, regularly-shaped (i.e., with lower value for the perimeter-to-area-ratio variable), and flatter parcels are more likely to subdivide. Peak-hour travel time to the CBD was estimated to have a positive impact on subdivision: the further away from the CBD an undeveloped parcel, the more likely it will subdivide, everything else constant. In contrast, the distance to the nearest freeway was estimated to exert a negative impact on subdivision likelihood, indicating that undeveloped parcels that enjoy easy access to freeways are more likely to subdivide (and then be developed). The proximity of more undeveloped parcels within a parcel's 1.0-mile neighborhood dampens the likelihood of subdivision, as expected.

Parcel Size Model

The linear regression model determines the size of each new sub-parcel. Table F.3 in Appendix F shows summary statistics for all explanatory variables, and the parameter estimates are given in Table F.4.

As Table D.3 shows, the maximum size of original, un-divided parcels is 0.35 square mile, and the maximum distance to the nearest freeway is 1.20 miles. These two maximum values were “capped” on parcels having larger size or longer distance. Visual inspection reveals that parcels bigger than 0.35 square mile share similar subdivision pattern: an undeveloped parcel was subdivided into multiple small parcels (likely to be developed into single-family residential uses later) plus a relatively large, irregular-shaped remainder (between years of 1995 and 2000). This indicates that the effects of original sizes on new sub-parcels do not change after original sizes exceed this threshold value (i.e., 0.35 square mile). Therefore, parcels bigger than 0.35 square mile were treated as if their sizes were 0.35 square mile. In addition, Euclidean distances to the nearest freeway were capped at 1.2 miles, because the longest distance is 1.22 miles for City of Austin parcels (used for model calibration), while this value jumps to as high as 40.3 miles in the Austin-Round Rock MSA (used for model application). Applying the same model to parcels with values outside the range used in model calibration is questionable. In addition, model application results show that the pattern of multiple small parcels plus a large remainder too rarely emerges if the original parcel size or the actual distance to the nearest freeway is used.

As expected, undeveloped parcels with irregular shape and higher regional accessibility tend to subdivide into smaller parcels (and then further develop). The model indicates a concave relationship between original parcel size and the resulting subdivided parcels sizes: the bigger the original parcel, the bigger its subdivided parcels, when the original

parcel is smaller than 0.21 square mile. This positive relationship is predicted to reverse as the original parcel size exceeds this threshold. Similarly, a convex relationship between freeway access and new parcels sizes was revealed by the model: distance to the nearest freeway has a negative impact on the new subdivided parcels size, when the original parcel is less than 0.50 mile away from the nearest freeway, and a positive impact if the distance exceeds this threshold. The amounts of industrial land within the 1.0-mile neighborhood and undeveloped land in the 0.5-mile neighborhood were estimated to increase the subdivided parcels sizes, while civic uses have a mixed impact, depending on the neighborhood range.

Land Development Model

The *Land Development Model* decides future land uses of individual undeveloped parcels (un-divided and newly generated through subdivision). Table F.5 in Appendix F provides summary statistics of all explanatory variables used in the final model specification (where the undeveloped use type is the base), and the parameter estimates are shown in Table F.6.

The magnitudes and signs of estimated parameters for variables like parcel size, distance to the nearest freeway and slope are as expected. Small parcels are more likely to develop into single-family use. Distance-to-freeway was estimated to decrease likelihood of all development types, except industrial use where the effect is neutral (the parameter is statistically close to zero). Parcel slope has a negative effect on single-family, commercial/office, industrial and civic development types, most likely due to higher costs of construction and access issues.

The positive signs for travel time-to-CBD parameters for residential and commercial/office development indicate that such uses are more likely to appear on undeveloped parcels near the city fringe. This is consistent with the process of urban sprawl, as well as Ota and Fujita's (1993) economic models for multi-unit firms in suburban areas.

It may seem counterintuitive that the negative transit access parameter suggests single-family residential development is less likely in neighborhoods better served by transit. However, transit stops are clustered in the most developed areas of the City, where land development is rare and non-residential uses are relatively common. Thus, this transit variable may be picking up many effects of centrality and commercial development, rather than noting purely access considerations.

The entropy measure of neighborhood land use balance was estimated to have a negative impact on single-family development likelihood, suggesting that single-family residences favor neighborhoods with less diverse land use pattern. This clustering of like land uses is also found in the estimates of surrounding-neighborhood land conditions. For example, the amount of land developed in single-family uses within a 0.5-mile radius was estimated to increase the likelihood of such development, while more commercial/office and industrial uses decrease this likelihood. Interestingly, greater land use balance is estimated to have a positive impact on industrial development likelihoods, indicating that

industrial uses are more likely to emerge in neighborhoods with diverse uses. This finding is also supported by the negative sign of industrial-use parameter within a 0.5-mile radius on industrial development.

Generally speaking, land that is undeveloped or excluded from development was estimated to have negative impacts on commercial/office, and industrial uses, as one would expect. Some neighborhood attributes have mixed effects. For example, the presence of undeveloped lands within a 0.5-mile neighborhood was estimated to have a positive impact on single-family conversion, revealing a general preference for living near undeveloped, and possibly more scenic and less polluted areas. However, undeveloped areas in a wider, 0.5 to 1-mile ring around an undeveloped parcel do not inspire to attract residential development, possibly because other, closer undeveloped parcels provide more development opportunities. The same result is also found for excluded land impacts.

3.4.4 Calibration of the LUI Model

The processes of parcel subdivision, size determination and land use are covered by the LUC model, and the associated allocation of households and jobs is modeled using a SUR with both spatial lag and spatial error processes. This SUR is composed of four equations, each representing changes in households or employment counts (by type) at the TAZ level between 2000 and 2005.

Anselin (1988) noted that dependence is often present in cross-sectional data obtained using arbitrary delineation of spatial units (e.g., TAZs). Thus, zone-based household and employment counts (and changes over time) are likely to exhibit such correlation, even after controlling for observable factors. Models without explicit treatment of these spatial dependencies can result in inappropriate inferences and conclusions. The LUI model recognizes dependencies emerging from three sources. First, response variables depend on neighboring unit responses, via a spatial lag component. Second, error terms are spatially correlated across observational units, via a weight matrix-based spatial error component. Third, these same error terms are correlated across equations, implying a SUR structure. The estimation procedure follows Kelejian and Prucha's (2004) approach in a simultaneous equations model (SEM), adjusted to fit a SUR framework. Their three-stage least-squares (3SLS) estimation approach derives from their earlier work, using a generalized method of moments (Kelejian and Prucha 1999) and spatial two-stage least-squares procedures for single-equation models (Kelejian and Prucha 1998; Das, Kelejian and Prucha 2003).

The SUR model specification, with both spatial lag and spatial error processes, is specified as follows:

$$\begin{aligned} \mathbf{y}_m &= \rho_m \mathbf{W}\mathbf{y}_m + \mathbf{X}_m \boldsymbol{\beta}_m + \boldsymbol{\varepsilon}_m = (\mathbf{W}\mathbf{y}_m, \mathbf{X}_m)(\rho_m, \boldsymbol{\beta}'_m)' + \boldsymbol{\varepsilon}_m = \mathbf{Z}_m \boldsymbol{\delta}_m + \boldsymbol{\varepsilon}_m \\ \boldsymbol{\varepsilon}_m &= \lambda_m \mathbf{W}\boldsymbol{\varepsilon}_m + \boldsymbol{\xi}_m \end{aligned} \quad (3.9)$$

where $m = 1:M$ ($M = 9$ in this study), $\xi = (\xi_1', \xi_2', \dots, \xi_M')$, $E[\xi | X_1, X_2, \dots, X_M] = \mathbf{0}$, and $E[\xi\xi' | X_1, X_2, \dots, X_M] = \mathbf{\Omega}$. In addition, y_m is an n by 1 vector of response variables for equation m , X_m is an n by k_m matrix of explanatory variables for equation m (β_m is a k by 1 vector of parameters to be estimated, ρ_m and λ_m are two scalars describing the strength of spatial dependencies).

In this study, four distinct sparse weight matrices were examined, in order to discern the most relevant one.¹¹ A first-order contiguity matrix (using the queen criterion¹²) considered is sparse when the number of observations is large. This first sparse matrix was generated using GEODA software (Anselin 2005). The second weight matrix relies on the inverse of Euclidean distances between zone centroids, in order to reflect the decay of relationships with distance. A 7-mile “threshold distance” was chosen to ensure sparseness of this weight matrix¹³. The third and fourth matrices also use this threshold distance, but the inverse of inter-centroid distances are raised to powers of 1.5 and 2.0, respectively. These four relatively sparse weight matrices are labeled W_{con} , $W_{\text{dist1.0}}$, $W_{\text{dist1.5}}$ and $W_{\text{dist2.0}}$, respectively. All are row-standardized (so that row elements sum to one), in order to facilitate interpretation (Anselin 1988). More specifically, a right-hand-side weight matrix represents a weighted average of the variable under consideration in neighboring units.

The estimation procedure was applied using each of four weight matrices. Equation 3.10’s goodness-of-fit measure for SUR models (McElroy 1977) was calculated for each case:

$$R^2 = 1 - \frac{\hat{\xi}' \hat{\Omega}^{-1} \hat{\xi}}{\sum_{i=1}^M \sum_{j=1}^M \hat{\sigma}^{ij} \left(\sum_{t=1}^n (y_{it}^* - \bar{y}_i^*) (y_{jt}^* - \bar{y}_j^*) \right)} \quad (3.10)$$

where $\hat{\sigma}^{ij}$ is the ij th element in matrix $\hat{\Omega}^{-1}$, \bar{y}_i^* is the mean of response values for equation i , and other terms are as previously defined. The case with W_{con} yielded the highest goodness-of-fit value (0.325, as compared to 0.239, 0.231 and 0.303 for $W_{\text{dist1.0}}$, $W_{\text{dist1.5}}$ and $W_{\text{dist2.0}}$ matrices). Therefore, this weight matrix was used in the final specification. Table F.7 in Appendix F provides summary statistics of all explanatory variables used in the model, and the results are shown in Table F.8.

As expected, single- and multi-family land in a TAZ were estimated to increase its household count, while industrial, commercial/office, and civic land values were estimated to increase the numbers of basic, retail, and service jobs, respectively. In addition to these “direct” impacts that may come from the backcasting procedure used with Austin’s 2000 land use parcel map (described in the Challenges of Data Availability

¹¹ Please refer to Zhou and Kockelman (2006) for a discussion regarding the use of sparse weight matrices, as compared to full matrices.

¹² Queen criterion defines neighbors as those that have either common boundaries or common corners.

¹³ The maximum and minimum numbers of neighbors for one observation are 2 and 304 in this study.

sub-section), “indirect” influences were found among less related categories of land type and land use intensity type. For example, multi-family land in a TAZ was estimated to have a positive impact on the changes in a zone’s basic and retail job counts, and commercial or office land is estimated to have a positive impact on household counts, indicating that correlations among households and jobs exist at the level of TAZs.

While development of parcels in a TAZ generally increases the zone’s land use intensity, prior year land use intensities are more likely to dampen such activity in that zone. For example, prior year basic, retail and service jobs were estimated to negatively impact the changes in basic, retail and service jobs, indicating a repelling effect among the same employment category. However, this effect was not found among households: prior year household counts seem to attract new households. In addition, prior year job counts are estimated to attract different job types. For example, basic jobs are estimated to increase retail and service jobs, retail jobs increase basic and service jobs, and service job counts increase retail jobs. These suggest that the degree of job mixing is likely to increase over time.

Rising household counts are more likely to appear in TAZs with lower land use balance (or less diverse uses), indicating a clustering pattern for households. Regional accessibility was estimated to increase household and service job growth, as one would expect.

Finally, the spatial lag coefficients are all statistically significant. The spatial lag and spatial error coefficients are estimated to both be positive in the household count equation, but have opposite signs for each of the three job types. It is expected that households tend to cluster, as revealed by the two positive spatial autocorrelation coefficients. It is hard to explain the exact reasons for the opposite signs of the two spatial autocorrelation coefficients for employment. As Anselin (2001, pp. 316) explains, a spatial lag is designed to reveal the “existence and strength of spatial interaction” while a spatial error seeks to correct for “potentially biasing influences of the spatial autocorrelation”. The final spatial distribution of employment is determined by combining the effects of these two spatial processes.

3.4.5 LUC-LUI Application and Results

The LUC model, the LUI model, and a TDM constitute the new integrated model used here. This ITLUM was applied to investigate the spatial distribution of households and jobs, along with travel conditions in 2030 across the Austin-Round Rock MSA of Texas, under two policy scenarios: business-as-usual (BAU or base case) and a road pricing scenario (congestion pricing plus a mileage-based carbon tax, CPCT). An interesting land use policy, urban growth boundary, cannot be applied here because the sophisticated SUR model is not easily adapted to zone exclusions (where certain zones are “excluded” from model prediction), such as zoning constraints or prior knowledge of development.

Application of the LUC Model

Land use development in each 5-year step was generated using one *random simulation*. More specifically, a series of random variables that are uniformly distributed on the [0,1] range were generated to determine whether an undeveloped parcel will subdivide and what development type an undeveloped parcel will be (after its size is simulated by the *Parcel Size Model*). If the random value is less than the subdivision probability (determined by the systematic utility in the binomial logit model), the undeveloped parcel subdivides; otherwise, the parcel remains whole. Similarly, probabilities of all the possible land use types form a type of histogram¹⁴, and the “position” of a random variable among the cumulative distribution function determines the parcel’s future land development type.

In contrast, an extreme value distribution was used in the *Parcel Size Model*. Its location and scale parameters were estimated to be 0.523 and 0.987, using maximum likelihood estimation (MLE) on the residuals in calibrating the *Parcel Size Model*. There are two reasons for using an extreme value distribution. First, the histogram of residuals shows a skewed distribution. Second, the commonly used normal distribution failed to generate the observed pattern of multiple small subdivided parcels plus a large remainder for large undeveloped parcels.

An undeveloped parcel subdivided according to simulated sizes of the new parcels, and its size was continuously reduced until the remainder is smaller than the next simulated size. In the last step, the remainder was treated as the last piece of new parcels, and the number of new parcels was simultaneously determined. The *Parcel Size Model* only determines the sizes of subdivided parcels, but not the shapes. The shape of a two-dimensional object is difficult to measure and define. This study took an approach that is easy to implement and replicate, using ArcGIS and MATLAB software. The original parcel map was rasterized into 240-foot grid cells (using the field of parcel IDs), and the raster map was converted into ASCII files for use (as a matrix) in MATLAB software. This matrix represents the shape (approximated by the rasterizing process) and location of the original parcels. A MATLAB code scanned all the elements of the matrix, and updated the values of the elements that were selected to generate a new, subdivided parcel. The updated matrix was converted back into a raster file and then a shape file, and the shape and location of all the parcels (newly-generated, subdivided parcels together with the remaining, whole parcels) were generated and displayed in ArcGIS. It is worth mentioning that this approach only determined the shape of new, subdivided parcels, while original shapes of undivided parcels were kept as they are. MATLAB assembled 240 ft cells from left to right in each subdividing parcel, and then up to down, in order to hit predicted new-parcel sizes. This arbitrary approach resulted in new parcels with a strong west-east orientation, rather than more natural patterns of parcel formation. For example, subdivided parcels bigger than one and half times the grid cell size have a rectangular shape, and some parcels “wrapped” from the east to the west edge of the original parcel. Figure 3.6 shows a snap shot of a few subdivided parcels. The west-east orientation is clear for the new parcels subdivided from an originally large, undeveloped

¹⁴ These probabilities are determined by systematic utilities for each land use type in the multinomial logit model, and they sum to 1.

parcel (located in the center of the map), and many new parcels are forecasted to have square or rectangular shapes.



Figure 3.6. Examples of Subdivided Parcels

The *Subdivision Model* and *Parcel Size Model* were directly implemented without any modifications, but the *Land Development Model*'s alternative specific constants were adjusted because the data sets for model calibration and application differ. As described in the Challenges of Data Availability sub-section, “targeted” land use conditions in year 2010 were forecasted. A series of simulations were run and alternative specific constants were adjusted until forecasts of regional land use totals matched the corresponding target values. Table 3.11 provides the adjustment results and their precision.

Table 3.11. Adjusted Alternative Specific Constants in the Land Development Model

	LLSF	SF	MF	Commercial or Office	Industrial	Civic	Undeveloped
Original constants	-20.8	0.593	-4.63	-2.09	0.175	-4.26	0.00
Adjusted constants	-23.3	0.660	-5.79	-5.24	-6.12	-7.20	0.00
Target area (mile ²)	29.6	34.5	2.12	3.10	21.3	10.1	2682
Projected area (mile ²)	30.4	33.6	2.17	3.50	21.2	10.2	2681
Difference (mile ²)	0.810	-0.843	0.053	0.490	-0.126	0.197	-0.581
Ratio of projected	1.03	0.98	1.03	1.16	0.99	1.02	1.00

to target							
-----------	--	--	--	--	--	--	--

Application of the LUI Model

The LUI model allocates forecasted growth of households and jobs by type to TAZs, considering the correlations among neighboring TAZs and across households and job counts. This model is a SUR with two spatial processes, and each equation represents the change in households or jobs by type. Changes in land use at the level of individual parcels were predicted by the LUC model, and the results served as primary inputs to the LUI model, together with prior-year household and employment counts and transportation conditions.

Again, simulation was utilized to forecast changes in household and job counts at the zonal level. The residuals in calibrating the LUI model were used to generate the variance-covariance matrix, which is shown in Table 3.12. A series of random numbers, correlated according to this covariance matrix, were generated using normal distributions and Cholesky decomposition (Greene 2001).

Table 3.12. Covariance Matrix of Residuals in the Land Use Intensity Model

	Households	Basic Jobs	Retail Jobs	Service Jobs
Households	22,461	2,214	-251	824
Basic Jobs	2,214	170,054	346	-9,115
Retail Jobs	-251	346	23,968	7,013
Service Jobs	824	-9,115	7,013	135,772

Note: The independent variables for this model are changes in household and employment counts; number of observation is 1245.

As shown in Table 3.12, variances are relatively high, which can produce some extreme values in individual simulations. When adding these extreme values to the systematic component of the LUI model (determined by the explanatory variables and the estimated parameters), forecast values could be unreasonably high or low. For example, two TAZs in downtown San Marcos were forecasted to have very high household densities, as shown by the 3D- maps in the Application Results sub-section. These two TAZs are only 0.013 square mile in area, but were forecasted to accommodate 562 and 301 households in the business-as-usual scenario, resulting in household densities as high as 56.2 and 30.1 thousand per square mile¹⁵.

Three facts contribute to the relatively high variances. First, the inconsistencies in data used for model calibration take a toll on model performance. In this study, although the land use intensity data in years 2000 and 2005 were provided by the same planning agency (CAMPO), there exist unrealistic shifts in household and job counts during the 5-year interval (after taking TAZ shape changes into account). For example, four TAZs

¹⁵ These two TAZs are forecasted to accommodate 546 and 293 households (equivalent to 54.6 and 29.3 thousand per square mile) when implementing road pricing policy. Note that the same series of random numbers were used for the two policies in order to ensure a fair comparison.

lost more than 500 households (the biggest loss is 1645) and six gained more than 1000 households (the biggest being 2338); seven TAZs lost more than 2000 basic jobs (the biggest being 8062) and five gained more than 2000 basic jobs (the biggest being 9118); six TAZs gained more than 1000 retail jobs (with a high of 2133); six TAZs lost more than 2000 service jobs (with a high of 4413) and four gained more than 2000 service jobs (with a high of 6277). Gaining thousands of households or jobs over a five-year period is questionable, and losing thousands is generally unrealistic during a period when the region is growing. The second factor is closely related to the first one: the relatively low value of goodness-of-fit in the LUI model. This model is sophisticated enough to consider spatial and across-equation correlations, and was found to generate the highest R^2 , as compared to other existing model specifications (Zhou and Kockelman 2006). However, there is still a large portion of variation that could not be explained by the model. Last, heteroskedasticity in job and household counts (across zones) was unaccounted for in the LUI model specification. This indicates that TAZs were treated equally in model application regardless of their significant differences in size.

The forecasted household and job changes were adjusted to match control totals for each model year in two steps. In the first step, the relative values across TAZs and equations were kept, because they were produced by a SUR model that had already considered the impacts of neighboring TAZs. Therefore, households or jobs were added or removed in proportion to predicted totals to match control totals. In the second step, unreasonable forecasts were simply removed. For example, if a TAZ was forecasted to lose more than it had available to lose, a zero value was assigned.

While the growth is higher in the model years than in the forecast years (i.e., household and employment totals increased 23.0% and 17.3% between 2000 and 2005, respectively; but the 5-year growth rates for households and employment are only about 11.0% and 14.0% from 2010 to 2030), the original forecasted household and employment totals were lower than the control totals in virtually all cases, except for retail jobs in year 2030. This indicates a mismatch in over-all development between the model years (in the early 2000's) and the forecast years (2010-2030). It also raises a question: what is the regional development limit? If targets are not embedded naturally into the model, post-processing is generally used, requiring heroic and unsatisfying assumptions (such as proportional adjustment of all zones' values) in order to hit regional control totals. In the case of the proposed model system with LUC and LUI models, parcel subdivision and land use change could be undertaken until a certain target of total land in each use is met. But this does not guarantee that application of the subsequent LUI model will then result in reasonable household and job counts for each model year. In this study, control totals were used to modify the forecast results of LUI model, to be consistent with the regional totals forecasted by a visioning process (e.g. ECT).

Application Results

Figures F.1 (a to e) in Appendix F depict forecasted land use changes in each model year (2010, 2015, 2020, 2025 and 2030), assuming *business as usual*. Land that has already been developed is shown as blank in the maps. The City was forecasted to lose undeveloped land quickly, as compared to other parts of the region. Many of the smaller,

undeveloped parcels were forecasted to convert to single-family residential or commercial/office uses¹⁶. Many large lot single-family uses are predicted to emerge in Williamson and Caldwell Counties, while Bastrop and Caldwell Counties are expected to experience relatively high levels of industrial development over the coming 20 years. Commercial or office uses tend to emerge in places close to the urban clusters and regional highways (e.g., I-35). As expected, civic uses were forecasted to spread over the entire region. This may relate to the nature of civic uses, which seek broad distribution in order to provide reasonable access to schools, post offices and hospitals.

Figures F.2 (a to d) in Appendix F show forecasted land use changes in years 2015, 2020, 2025, and 2030 after implementing **road pricing** (congestion pricing plus a carbon tax). The overall development pattern is similar to the business-as-usual result. However, land close to regional highways seems to be more likely to be developed, and Caldwell County appears to have less development opportunities when implementing the road pricing policy. Table 3.13 provides comparisons between the two policies, in terms of land consumption by type by 2030. Road pricing reduces land consumption by large-lot single-family, single-family and civic uses, and promotes denser development patterns (e.g., more multi-family uses), resulting in a 20.6-square mile land savings (or 0.86%) across the entire region, as compared to the BAU scenario.

Table 3.13. Land Consumption between the Two Policies

Land Consumption (mile ²)	Business-as-usual	Congestion Pricing & Carbon Tax
Large lot single family	419	410
Single family	485	472
Multi-family	41.4	42.5
Commercial or Office	77.8	78.3
Industrial	110	114
Civic	154	151
Undeveloped	2,394	2,414

Two-dimensional maps of development densities classify values into bins (as shown in map legends), and mask fluctuations of values within bins. Therefore, three-dimensional maps are also presented. Figures F.3 and F.4 in Appendix F show forecasted household and employment densities at the TAZ level in year 2030 for the **business as usual** scenario. As shown, households and employment tend to remain concentrated in the urban areas and along regional freeways.

Figures F.5 and F.6 in Appendix F present household and employment density forecasts when implementing **road pricing**. The distribution patterns are very similar to the results of business-as-usual, suggesting that such policy will not significantly alter household and firm location. This finding is consistent with gravity-based LUMs predictions.

¹⁶ This phenomenon is hard to see in the figures, but could be easily detected using zoom-in function of ArcGIS.

However, the road pricing policy does have noticeable impacts on travel behavior, as discussed below.

This simple *accessibility index* (as defined by Equation 3.6) was calculated for both households and employment in each scenario, and the results are shown in Table 3.14. The BAU scenario generated a slightly higher level of clustered residential development, with a 6.39% higher household AI value.

Table 3.14. Accessibility Index for Households and Employment for Each Policy Scenario

	Households (x 10 ⁶)	Employment (x 10 ⁷)
Business-as-usual	2.58	6.369
Congestion Pricing & Carbon Tax	2.42	6.368

Note: This accessibility index is computed with respect to Austin’s downtown.

In terms of *density* outcomes, the count-weighted¹⁷ average densities of households and employment were calculated, and are shown in Table 3.15. The BAU scenario generates a slightly denser residential use intensity pattern, as compared to the road pricing scenario (household density was 2.38% higher than under the road pricing scenario).

Table 3.15. Count-Weighted Average Densities for Each Policy Scenario (counts/mile²)

	Households	Employment
Business-as-usual	1,568	6,391
Congestion Pricing & Carbon Tax	1,532	6,375

The TDM results are of great interest because they relate to congestion levels and mobile-source emissions. Table 3.16 summarizes projected VMT values for the year 2030 (by time-of-day) for the two policy scenarios. The results suggest that road pricing can be quite effective in reducing VMT: reducing regional VMT by 12.7 million (or 15.2%), as compared to the business-as-usual scenario. When compared to the base year 2005, the BAU anticipates a 96.2% increase in regional VMT, which is higher than household and job growths (59.0% and 87.1%, respectively). The road pricing scenario is forecasted to control VMT growth, with only a 66.3% increase in regional VMT.

Table 3.16. Vehicle Miles Traveled (VMT) in Year 2030

	Time-of-Day				Total
	AM	OP	PM	MID	
Business-as-usual	16,767	6,386	26,839	33,741	83,733
Congestion Pricing & Carbon Tax	14,558	5,452	22,737	28,238	70,985

Note: Values are in thousands of daily VMT.

Table 3.17 provides VMT-weighted average speeds for the two policy scenarios, and Table 3.18 gives the VMT-weighted average volume-to-capacity (v/c) ratios. The road pricing policy is forecasted to increase average speeds during peak hours by 9.16% and

¹⁷ The number of households or jobs by type was used as weight in calculating the count-weighted averages.

4.95% during the AM and PM peak period, respectively), and is effective in reducing the region’s overall v/c ratio: by 16.2% and 19.1%, respectively.

Table 3.17. VMT-Weighted Average Speed for Each Policy Scenario

	VMT-Weighted Average Speed (miles/hour)	
	AM Peak	PM Peak
Business-as-usual	47.7	52.5
Congestion Pricing & Carbon Tax	52.0	55.1

Table 3.18. VMT-Weighted Average Volume-to-Capacity Ratio for Each Policy Scenario

	VMT-Weighted Average Volume-to-Capacity Ratio	
	AM Peak	PM Peak
Business-as-usual	0.684	0.584
Congestion Pricing & Carbon Tax	0.573	0.472

3.4.6 Findings and Lessons Learned

The estimation results appear reasonable and are generally supported by the prevailing development trends and others’ findings. In some cases, multiple rounds of model estimation are needed when expected land use and travel patterns fail to emerge. For example, when using the original values of the un-divided parcel size and distance to the nearest freeway variables, a common pattern of multiple small parcels plus a large remainder was hard to generate in model application. As a result, the two variables were capped during model calibration, ensuring more typical subdivision tendencies.

In addition to the base forecast scenario (assuming business as usual), a combined policy of road pricing and a flat-rate carbon-based tax was investigated using this novel LUM and a standard TDM. The model results suggest that the road pricing policy results in less region-wide land consumption, and land close to regional freeway seems more likely to develop. These two policies were estimated to generate similar household and employment distribution patterns: households tend to remain concentrated in the urban areas and along regional freeways, and employment has a higher level of concentration in the urban areas (especially in the City of Austin’s CBD area). The road pricing policy appears to be effective in reducing regional VMT, as well as increasing average speed and reducing overall traffic congestion during peak hours. These findings are consistent with G-LUM predictions.

The model application results relied on only one random simulation. The same series of random numbers were generated for the two policies in order to ensure a fair comparison between them, but different seeds were used in each model year. The five model years may average out some elements of randomness over the 25-year span. Ideally, LUMs relying on simulation should run multiple times for each forecast. However, long run

times prevented multiple runs here. Thus we could not easily deduce the range and average of behavioral tendencies over time and across scenarios.

The data sets used here come from multiple sources; and creative solutions to data availability challenges may be critical to application success. Most decisions need to be made before model formulation. For example, the *Land Development Model* considered only six land use types because the data for model application does not separate commercial and office uses. Some decisions had to be made during model application. For example, the LUC model generated unreasonable forecasts when directly applied to the entire MSA (ten times bigger than the area used for model calibration). As a result, alternative specific constants in the *Land Development Model* were adjusted according to simple region-wide land use forecasts. Other data issues also impacted model performance. Unrealistic shifts in household and employment count data provided by the MPO resulted in a relatively low R^2 value (even though the sophisticated LUI model specification outperformed others) and high covariance values (which can cause extreme random numbers in a single run).

In addition to data challenges in developing a LUM, several key lessons were learned: (1) there may be no limit on development, (2) the LUI model may not accommodate zone exclusion, and (3) it is not easy to gauge what magnitudes of adjustments are needed in the systematic “utilities” of the MNL specification.

Past trends in land use change can lead to over-development or under-development in the future. If targets are not embedded naturally into the model, post-processing is generally used. Meeting control totals is a tricky issue that deserves great care. In order to match regional control total expectations for Austin, the LUI model results were post-processed. Adjustment of zone-level LUC model results (by scaling land acreages up or down, according to use type) could have been pursued as well. But this does not guarantee that application of the subsequent LUI model will then result in reasonable household and job counts for each model year. Either way, both post-processing techniques are unsatisfying.

The second lesson learned refers to the idea that a clever model of counts, using a spatial system of equations that share information in their error terms is not easily adapted to cases where certain zones are not allowed to experience growth in certain land use intensity values (due to zoning or other constraints) or some subset of values are otherwise pre-determined (due to prior knowledge of near-term development, for example). Spatial econometric tools are still emerging, and this challenge may one day be resolved, but in the meantime it represents a hurdle here that was unforeseen.

The third lesson learned simply refers to the fact that various explanatory factors are not controlled for in the specification. If modelers want to incentivize certain types of development in certain zones (e.g., high-density mixed use), they will have to guess how such incentives compare to the effects of included variables (such as nearby acreage of retail land or distance to the nearest freeway). Such decisions are not at all transparent. Ideally, more meaningful factors impacting land development decisions should be

included, to enhance model flexibility in application. Of course, this brings us back to the very fundamental issue of data availability: someone will first need to assemble such variables for all zones/locations, trusting that these vary a fair bit across zones (which is unlikely with many variables of interest, like construction costs), and then hope that they emerge as statistically significant and with intuitive signs in the estimated parameter set. There are simply no guarantees that the data acquisition efforts will pay off. And it generally is enough work to acquire more basic information (like parcel location, current and past land uses, network and demographic variables, neighborhood land use conditions for each parcel, and so forth); expending constrained resources to acquire variables that may or may not offer much to the model is a real risk.

In general, the LUM developed and applied here utilizes advances in spatial parcel data and GIS techniques, as well as cutting-edge spatial econometric theories and estimation techniques. Parameter estimates and model results appear reasonable. A mathematical model for the shapes of subdivided parcels could serve as a worthwhile extension of this work. Such effort will rely heavily on ArcGIS software capabilities, a deeper understanding and possibly fracture analysis of parcel subdivision mechanisms.

3.5 Emissions Inventory Development

Biogenic and anthropogenic emission inventories, along with land cover estimates for estimation of dry deposition velocities, were developed for each of the five ITLUM scenarios. These scenarios included three gravity-based land use model (G-LUM) forecasts for a business-as-usual (BAU) scenario, a road pricing scenario consisting of congestion pricing plus a mileage-based carbon tax (CPCT), and an urban growth boundary (UGB) scenario, and two land use change land use intensity model (LUC-LUI) forecasts for a business-as-usual (BAU) scenario and a road pricing (CPCT) scenario.

3.5.1 Biogenic Emissions and Dry Deposition

Biogenic emission estimates were developed for the ITLUM scenarios using the methodology described in Section 2.2.1. In contrast to the ECT LULC databases which included estimates of impervious cover for each land use type, the classifications used in the G-LUM and LUC-LUI models did not directly provide information that could be used to estimate the fraction of original vegetation remaining. Instead, the classifications used in the models were mapped to one of the ECT development types as shown in Tables 3.19 and 3.20. Each TAZ polygon was classified as central business district (CBD), urban, suburban or rural as follows:

$$DF_{TAZ} = P_{TAZ} + B\left(\frac{E_{TAZ}}{A_{TAZ}}\right) \quad (3.11)$$

- CBD: $DF_{TAZ} \geq 50$
- Urban: $50 > DF_{TAZ} \geq 10$
- Suburban: $10 > DF_{TAZ} \geq 1$
- Rural: $1 > DF_{TAZ} \geq 0$

where DF is a density factor, P is the population in the TAZ, E is the employment in the TAZ, A is the acreage of the TAZ, and B is the ratio of the study area population to the study area employment (Alliance 2003). The reclassified ITLUM scenarios were then overlaid on the original land cover data from Wiedinmyer *et al.* and used to modify the original vegetation density. Land cover estimates for estimation of dry deposition were developed using the reclassified ITLUM scenarios and the methodology described in Section 2.2.1.

Table 3.19. Assumed fraction of vegetative cover remaining for each G-LUM classification

G-LUM classification	ECT classification	Assumed Fraction of Vegetative Cover Remaining
CBD Residential	Downtown	0.023
CBD Basic Employment	Downtown	0.023
CBD Commercial Employ.	Downtown	0.023
Urban Residential	Town	0.171
Urban Basic Employment	Activity Center	0.042
Urban Commercial Employ.	Activity Center	0.042
Suburban Residential	Residential Subdivision	0.363
Suburban Basic Employment	Industrial/Office Park	0.144
Suburban Commercial Employ.	Industrial/Office Park	0.144
Rural Residential	Rural Housing	0.763
Rural Basic Employment	Industrial/Office Park	0.144
Rural Commercial Employ.	Industrial/Office Park	0.144

Table 3.20. Assumed fraction of vegetative cover remaining for each LUC-LUI classification

LUC-LUI classification	ECT classification	Assumed Fraction of Vegetative Cover Remaining
CBD LLSF	Downtown	0.023
CBD SF	Downtown	0.023
CBD MF	Downtown	0.023
CBD Commercial/Office	Downtown	0.023
CBD Industrial	Downtown	0.023
CBD Civic	Downtown	0.023
Urban LLSF	Large Lot	0.493
Urban SF	Residential Subdivision	0.363
Urban MF	Town	0.171
Urban Commercial/Office	Activity Center	0.042
Urban Industrial	Activity Center	0.042
Urban Civic	Activity Center	0.042
Suburban LLSF	Large Lot	0.493
Suburban SF	Residential Subdivision	0.363
Suburban MF	Town	0.171
Suburban Commercial/Office	Industrial/Office Park	0.144
Suburban Industrial	Industrial/Office Park	0.144
Suburban Civic	Industrial/Office Park	0.144
Rural LLSF	Rural Housing	0.763
Rural SF	Rural Housing	0.763

Rural MF	Town	0.171
Rural Commercial/Office	Industrial/Office Park	0.144
Rural Industrial	Industrial/Office Park	0.144
Rural Civic	Industrial/Office Park	0.144

3.5.2 Anthropogenic Emissions

Anthropogenic emission estimates for on-road mobile, non-road mobile, and area sources were developed for the ITLUM scenarios using the methodology described in Section 2.2.2. Housing and population values used in the projection and spatial allocation of anthropogenic emissions for the ITLUM scenarios are summarized in Tables 3.21 and 3.22, respectively.

Table 3.21. 2001 housing units and projected households for each ITLUM scenario by county

Households	2001 (U.S. Census Housing Unit)	G-LUM BAU	G-LUM CPCT	G-LUM UGB	LUC-LUI BAU	LUC-LUI CPCT	<i>Average Household Size</i>
Bastrop	22,723	64,422	65,468	49,425	65,170	62,571	2.87
Caldwell	12,188	30,405	31,446	25,962	55,729	54,996	2.98
Hays	37,946	87,024	86,998	73,279	94,249	93,727	2.92
Travis	353,272	512,209	510,626	582,458	495,316	496,735	2.53
Williamson	98,120	236,610	236,133	199,549	220,208	222,641	2.88
Total	524,249	930,671	930,671	930,671	930,671	930,671	-

Table 3.22. 2001 human population and projected human population for each ITLUM scenario by county

Population	2001 (U.S. Census)	G-LUM BAU	G-LUM CPCT	G-LUM UGB	LUC-LUI BAU	LUC-LUI CPCT
Bastrop	61,480	184,891	187,893	141,850	187,038	179,579
Caldwell	33,808	90,607	93,709	77,367	166,072	163,888
Hays	104,514	254,110	254,034	213,975	275,207	273,683
Travis	842,638	1,295,889	1,291,884	1,473,619	1,253,149	1,256,740
Williamson	276,749	681,437	680,063	574,701	634,199	641,206
Total	1,319,189	2,506,934	2,507,583	2,481,511	2,515,666	2,515,095

3.5.3 Emissions Inventory Summary

A summary of NO_x and VOC emissions from biogenic and anthropogenic sources for the 2007 Base Case and each ITLUM scenario is presented in Table 3.23.

Table 3.23. Emissions of VOC and NO_x (tpd) for the 2007 Base Case and each ITLUM scenario

Categories	2007 Base Case VMT = 44.5*		G-LUM BAU VMT = 84.8*		G-LUM CPCT VMT = 71.3*		G-LUM UGB VMT = 70.2*		LUC-LUI BAU VMT = 83.7*		LUC-LUI CPCT VMT = 71.0*	
	VOC	NO _x	VOC	NO _x	VOC	NO _x	VOC	NO _x	VOC	NO _x	VOC	NO _x
On-road mobile	33.8	62.1	22.6	24.1	19.0	20.3	18.7	20.1	22.4	23.8	19.0	20.2
Non-road mobile	22.2	21.7	22.7	9.4	22.7	9.4	22.6	9.4	22.7	9.4	22.7	9.4
Area	110.7	10.2	224.4	21.7	225.5	21.8	215.1	20.0	254.3	22.5	253.7	22.5
Point	3.0	2.8	3.0	2.8	3.0	2.8	3.0	2.8	3.0	2.8	3.0	2.8
Biogenic	211.2	20.2	149.7	20.2	151.1	20.2	206.4	20.2	201.3	20.2	201.7	20.2

Note: ITLUM scenario emissions are calculated for a future year of 2030.

*VMT is given in units of 10⁶ miles per day in the 5-county Austin area.

Biogenic sources and, because they have been projected using human population, area sources are predicted to remain the most significant sources of VOC emissions in the five-county area. Biogenic emission estimates for the G-LUM BAU and G-LUM CPCT scenarios are considerably lower than for other scenarios. These scenarios forecast large changes in undeveloped land, particularly in rural zones, resulting in large reductions in vegetative cover as compared to the Base Case. The increased development rates, due to model limitations and no constraints on maximum developable land, result in unrealistic predictions of vegetative cover loss and over-predictions of urbanization in those zones. Emissions from most on-road and non-road mobile source categories decreased for the ITLUM scenarios relative to the Base Case due to more stringent federal emission controls. Differences in spatially allocated emissions for each ITLUM scenario relative to the Base Case are shown in plots included in Appendix G.

3.6 Air Quality Modeling Predictions

The ITLUM scenarios were compared based on their impact to daily maximum 1-hour ozone concentrations, hourly episodic ozone concentrations, and population exposure.

Predicted 1-hour averaged daily maximum ozone concentrations for the 2007 Base Case ranged from 72 ppb to 90 ppb across the episode. Differences in daily maximum 1-hour ozone concentrations due to the combined changes in dry deposition, biogenic emissions, and anthropogenic emissions from on-road mobile, non-road mobile and area sources ranged from -10 to -2 with typical values of -5 as shown in Table 3.24.

Table 3.24. Daily maximum 1-hour ozone concentrations for the Base Case and differences in the daily maximum ozone concentrations relative to the Base Case

Episode Day	Base Case Daily Max. O ₃ Conc. (ppb)	G-LUM	G-LUM	G-LUM	LUC-LUI	LUC-LUI
		BAU	CPCT	UGB	BAU	CPCT
9/15	80.5	-4.1	-4.9	-4.4	-4.9	-5.6
9/16	72.0	-1.5	-1.6	-2.2	-2.1	-2.2
9/17	85.8	-6.5	-6.5	-6.4	-6.9	-6.9
9/18	86.2	-3.9	-3.9	-4.1	-4.1	-4.1
9/19	90.4	-6.0	-7.3	-5.5	-6.1	-7.5
9/20	90.5	-8.3	-9.7	-8.0	-8.6	-10.1

Maximum and minimum differences in 1-hour ozone concentrations that occurred across the region regardless of time of day or magnitude were also evaluated. Figure 3.7 shows the range of changes in 1-hour ozone concentrations between the ITLUM scenarios and the Base Case due to changes in biogenic emissions, dry deposition, and anthropogenic emissions. Maximum decreases of up to 16 ppb were predicted in the LUC-LUI scenarios. The G-LUM UGB scenario resulted in decreases of up to 14 ppb as compared to 9.5 ppb in the G-LUM BAU scenario.

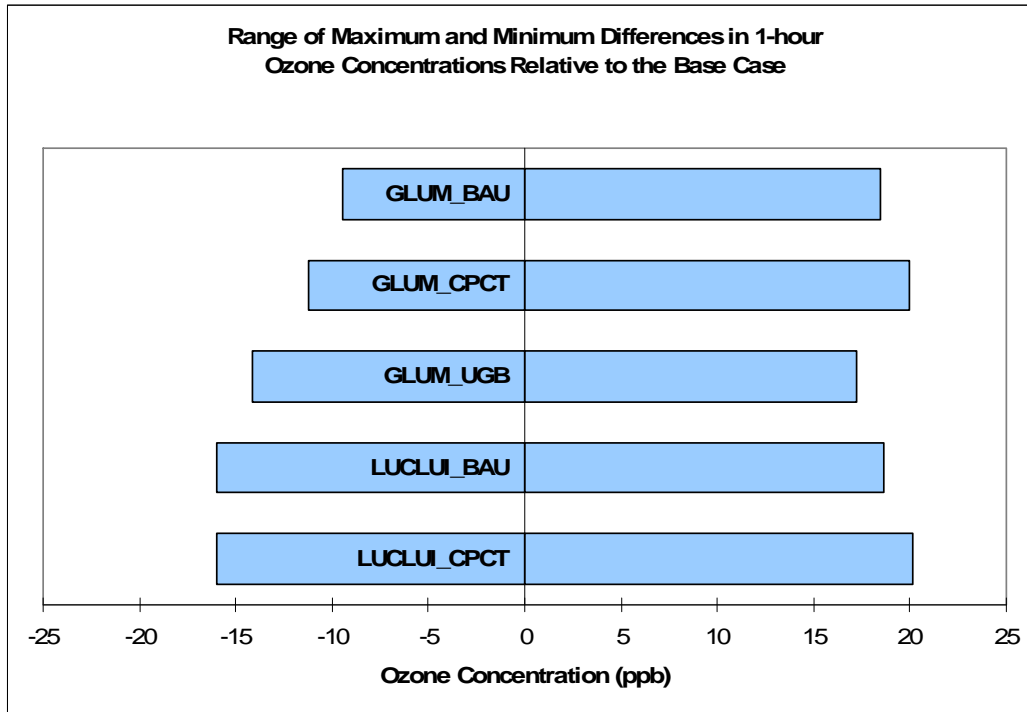


Figure 3.7. Range of changes in hourly ozone concentrations (ppb) between the ITLUM scenarios and the Base Case across the 5-county Austin area

Total daily population-weighted exposure was estimated for the Base Case and the ITLUM scenarios as shown in Figure 3.8.

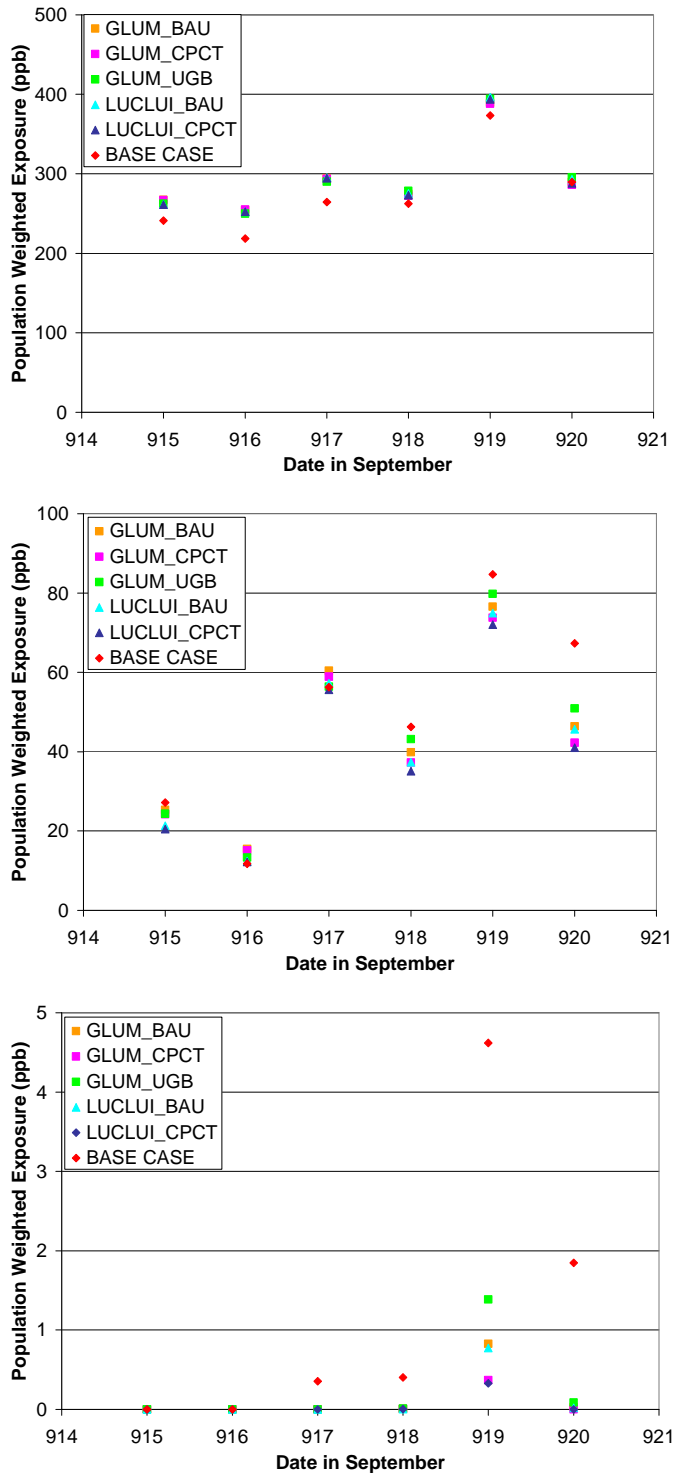


Figure 3.8 Total daily population-weighted exposure using a (a) 40 ppb, (b) 60 ppb, and (c) 80 ppb threshold for the ITLUM scenarios and the Base Case

For a threshold value of 40 ppb, all ITLUM scenarios show greater exposure than the Base Case due to additional increases in ozone and population in newly developed areas. For higher threshold values, Figure 3.8 shows the variation in exposure over the episode with typically lower exposure predicted for the road pricing scenarios and higher values for the urban growth boundary scenario where population is more concentrated.

4.0 Conclusions

This study presents the results of an integrated modeling effort that provides the structure needed for comprehensive modeling of regional land use, transportation, and air quality futures. The impacts of alternative regional development patterns on land use/land cover, emissions, dry deposition, and air quality, were examined using Austin, Texas as a case study. Although the case study focuses on the Austin area, Austin is typical of many urban areas that are or could be facing designation as non-attainment under the 8-hour NAAQS for ozone, and the modeling framework is applicable to other urban areas.

Four regional visioning scenarios and five land use modeling scenarios were developed and used in a photochemical grid model, CAMx, to predict changes in the magnitude and spatial distribution of hourly ozone concentrations due to regional development trends. Key findings are summarized below:

- While fundamentally different, both the community-oriented visioning and land use modeling processes carry benefits and appear complementary.
- Three distinctive transportation and land use scenarios were investigated using the gravity-based LUM and a standard TDM. In addition to the business-as-usual (BAU) scenario, these include a road pricing policy which entails a flat-rate carbon-based tax and congestion pricing (CPCT) of all Austin area freeways, and an urban growth boundary (UGB) policy. In terms of travel behavior impacts, the CPCT and UGB policies appear to be powerful tools for VMT reduction. The BAU and CPCT policies generate similar amounts of personal and commercial trips, while the UGB policy generates fewer trips of both types. This suggests that the CPCT policy's VMT reduction basically comes from shorter trips, while the VMT reduction of the UGB policy comes from both shorter trips and fewer trips. In terms of personal trips by mode, the CPCT and UGB policies are most effective in promoting transit usage and decreasing auto trips, and the UGB policy enjoys the highest number of walk/bike trips.
- Two distinctive transportation and land use scenarios were investigated using a novel LUM based on land use change and land use intensity (LUC-LUI) at the parcel level and a standard TDM. In addition to the business-as-usual (BAU) scenario, a road pricing policy (CPCT) was investigated. The model results suggest that the CPCT policy results in less region-wide land consumption, and land close to regional freeway seems more likely to develop. These two policies were estimated to generate similar household and employment distribution patterns: households tend to remain concentrated in the urban areas and along regional freeways, and employment has a higher level of concentration in the urban areas (especially in the City of Austin's CBD area). The CPCT policy appears to be effective in reducing regional VMT, as well as increasing average speed and reducing overall traffic congestion during peak hours. These findings are consistent with G-LUM predictions.

- Although VMT is predicted to continue increasing, emissions of NO_x and VOCs from on-road mobile sources are predicted to decrease through approximately 2025 due to the phase-in of new emission standards. Similarly, NO_x emissions from non-road mobile sources in the Austin area are also predicted to decrease due to the phase-in of new emission standards, while VOC emissions are predicted to increase by 5-9%.
- Future changes in daily maximum 1-hour ozone concentrations due to the combined changes in dry deposition, biogenic emissions, and anthropogenic emissions in the ECT scenarios ranged from -11 ppb to -2 ppb, with typical values of -6 ppb. Differences due to changes in biogenic emissions and dry deposition only between ECT A (continuation of current development patterns) and the Base Case ranged from -0.9 ppb to +0.1 ppb. Differences due to changes in anthropogenic emissions only between ECT A and the Base Case were far more significant, ranging from -9 ppb to -2 ppb.
- Maximum differences in hourly ozone concentrations due to changes in biogenic emissions and dry deposition only between the ECT scenarios and the Base Case ranged from -1.4 ppb to +0.7 ppb. Maximum differences in hourly ozone concentrations due to changes in anthropogenic emissions only between the ECT scenarios and the Base Case were far more significant, ranging from -14 ppb to +22 ppb.
- Differences in ozone concentrations between the ECT scenarios (-3 ppb to +5 ppb) were smaller than the differences between the ECT scenarios and the Base Case. Doubling of population and implementation of new federal mobile source standards produced greater changes in emissions and air quality than differences in spatial patterns due to different types of regional development. These results imply that the pattern of urban development is not as significant as reductions in emissions per capita, but the effects of urbanization patterns are non-negligible.
- Future changes in daily maximum 1-hour ozone concentrations due to the introduction of E85 relative to ECT A ranged from -0.4 to 0.0 ppb, with typical values of -0.2 ppb for the Austin area. Although these impacts appear small, they are comparable in magnitude to some commonly employed air pollution control measures that were adopted as part of Austin's Early Action Compact. Differences in hourly ozone concentrations due to the introduction of E85 are relatively smaller than changes due to development patterns.
- Future changes in daily maximum 1-hour ozone concentrations due to the combined changes in dry deposition, biogenic emissions, and anthropogenic emissions in the ITLUM scenarios ranged from -10 ppb to -2 ppb, with typical values of -5 ppb. Maximum decreases in hourly ozone concentrations of up to -16 ppb were predicted in the LUC-LUI scenarios. The G-LUM UGB scenario resulted in maximum decreases of up to -14 ppb as compared to -9.5 ppb in the G-LUM BAU scenario.

- For the ECT scenarios, concentrated high-density development in existing towns with balanced-use zoning produced lower exposure to high ozone concentrations than a more typical pattern of urban sprawl. For the ITLUM scenarios, lower exposure was typically predicted for the road pricing scenarios and with relatively higher values predicted for the urban growth boundary. Evaluating daily population exposure can provide additional information about the magnitude and spatial distributions of changes in ozone due to urban development.

These results imply that controlling the environmental impacts of urbanization involves multi-faceted strategies. Integrated modeling efforts, such as the ones described in this study, have the potential to facilitate policy decisions that support balanced growth for U.S. communities.

5.0 Publications/Presentations

Duthie, J., Kockelman, K., Valsaraj, V. and Zhou, B. “Applications of Integrated Models of Land Use and Transport: A Comparison of ITLUP and UrbanSim Land Use Models”, presented at the 54th Annual North American Meetings of the Regional Science Association International, Savannah, Georgia, November 2007.

Lemp, J., L. McWethy, and K. Kockelman, “From Aggregate Methods to Microsimulation: Assessing the Benefits of Microscopic Activity-Based Models of Travel Demand”, *Transportation Research Record No. 1994*, pp. 80-88, 2007. Proceedings of the 86th Annual Meeting of the Transportation Research Board, Washington D.C., January 2007 and presented at the 11th World Conference on Transport Research Society, Berkeley, USA, June 2007.

Lemp, J., Zhou, B., Kockelman, K. and Parmenter, B. “Visioning Vs. Modeling: Analyzing the Land Use-Transportation Futures of Urban Regions”, *Journal of Urban Planning and Development*, 134 (3). Proceedings of the 86th Annual Meeting of the Transportation Research Board, Washington D.C., January 2007, and presented at the 53rd Annual North American Meetings of the Regional Science Association International, Toronto, Canada, November 2006, and the 11th World Conference on Transport Research Society, Berkeley, USA, June 2007.

Lemp, Jason and Kara Kockelman. “Travel Demand Forecasting Models: Development, Application, and Comparison of Aggregate and Activity-Based Approaches for the Austin, Texas Region.” Under consideration for publication in *Transportation Research Record*, October 2008.

McDonald-Buller, E. and K Kockelman, “Regional Development, Population Trend, and Technology Change Impacts on Future Air Quality: A Case Study in Austin, Texas”, presented at the Envision Central Texas Liveable City - Capital Air Metropolitan Planning Organization meeting, Austin, TX, November 3, 2005.

McDonald-Buller, E., J. Song, A. Webb, G. McGaughey, B. Zhou, K. Kockelman, J. Lemp, B. Parmenter, and D. Allen “The Impacts of Urban Development on Anthropogenic and Biogenic Emissions and Air Quality: A Case Study in Austin, Texas,” Transportation, Land Use Planning, and Air Quality 2007 Conference, Orlando, FL, July 2007.

McDonald-Buller, E. “Urban Development Policies & Air Quality”, Invited Presentation, Air Quality 2006: Energy Leadership & Emissions Reduction, Houston, TX, October 11-12, 2006.

McDonald-Buller, E., A. Webb, J. Song, S. Gadda, B. Parmenter, K. Kockelman, D. Allen. Predicting the Relative Impacts of Urban Development on Air Quality: A Comparative Study of the Impacts of Land Cover and Transportation. presented at the EPA Science Forum 2006 "Your Health, Your Environment, Your Future", Ronald

Reagan Building and International Trade Center, Washington, DC. 16-18 May, 2006. 2nd prize winner in the Built Environment Category.

McDonald-Buller, E., J. Song, A. Webb, and D. Allen. "Regional Visions of Urbanization in Austin, Texas and the Impacts on Air Quality and Population Exposure Metrics", Proceedings of the Air & Waste Management Association Annual Meeting, Portland, OR, June 2008.

McDonald-Buller, E., J. Song, A. Webb, and D. Allen, The Impacts of Land Use/Land Cover Change on Future Emissions and Air Quality: A Case Study in Austin, Texas, Texas Commission on Environmental Quality, Austin, TX, August 2008.

McDonald-Buller, E., K. Kockelman, J. Song, A. Webb, B. Zhou, S. Gadda, B. Parmenter, and D. Allen, The Impacts of Land Use/Land Cover Change on Future Emissions and Air Quality: A Case Study in Austin Texas, Future Air Quality with Projected Global Changes: A Progress Review Meeting Presented by EPA Global Change STAR Grantees Research Triangle Park, North Carolina October 27-28, 2008.

Song, J., B. Parmenter, D. Allen, and E. McDonald-Buller. Impacts of Urbanization on Biogenic Emissions and Air Pollutant Deposition, presented at the 99th Annual Conference & Exhibition of the Air & Waste Management Association, New Orleans, LA, 2006.

Song, J., B. Parmenter, A. Webb, D. Allen, and E. McDonald-Buller, Impacts of Urbanization on Emissions and Air Quality: Comparison of Four Visions of Austin, Texas, *Environmental Science & Technology*, 42 (19), 7294-7300, 2008.

Tirumalachetty, Sumala, Kara Kockelman and Saurabh Kumar. "Microsimulation Models of Urban Regions: Anticipating Greenhouse Gas Emissions from Transport and Housing in Austin, Texas." To be presented at and included in the Meeting Compendium of the Transportation Research Board's 88th Annual Meeting, Washington, DC, January 2009.

Wang, X. and K. Kockelman. Tracking Land Cover Change in a Mixed Logit Model: Recognizing Temporal and Spatial Effects. *Transportation Research Record* No.1977, pp 112-120, and presented at the 85th Annual Meeting of the Transportation Research Board, Washington DC, 2006 and at the 52nd Annual North American Meetings of the Regional Science Association International, Las Vegas, Nevada, 2005.

Wang, Xiaokun and Kara Kockelman. "Specification and Estimation of a Spatially and Temporally Autocorrelated Seemingly Unrelated Regression Model: Application to Crash Rates in China". *Transportation* (3), pp. 281-300. Proceedings of the Transportation Research Board's 86th Annual Meeting, Washington, DC, January 2007 and presented at the 53rd Annual North American Meeting of the Regional Science Association International, Toronto, Canada, November 2006 and the 11th World Conference on Transport Research Society, Berkeley, USA, June 2007.

Wang, Xiaokun and Kara Kockelman. "Maximum Simulated Likelihood Estimation with Correlated Observations: A Comparison of Simulation Techniques." Forthcoming in *Monograph on Transportation Statistics*. Presented at the 53rd Annual North American Meeting of the Regional Science Association International, Toronto, Canada, November 2005 and the the 11th World Conference on Transport Research Society, Berkeley, USA, June 2007.

Webb, A, S. Gadda, B. Parmenter, D. Allen, K. Kockelman, and E. McDonald-Buller. Predicting the Relative Impacts of Regional Development Trends on Air Quality. presented at the 99th Annual Conference & Exhibition of the Air & Waste Management Association, New Orleans, LA, 2006.

Zhou, B. and Kockelman, K. "Microsimulation of Residential Land Use for Market Equilibrium", presented at the Transportation Research Board Specialty Conference: Innovations in Travel Modeling, Austin, Texas, May 2006 and at the 53rd Annual North American Meetings of the Regional Science Association International, Toronto, Canada, November 2006, and to be presented at the 11th World Conference on Transport Research Society, Berkeley, USA, June 2007.

Zhou, B. and Kockelman, K. "Predicting the Distribution of Households and Employment: A Seemingly Unrelated Regression Model with Two Spatial Processes", forthcoming in the *Journal of Transport Geography*. Presented at the 53rd Annual North American Meetings of the Regional Science Association International, Toronto, Canada, November 2006, the 86th Annual Meeting of the Transportation Research Board (TRB), Washington D.C., January 2007, and the 11th World Conference on Transport Research Society, Berkeley, USA, June 2007.

Zhou, B. and K. Kockelman. "Neighborhood Impacts on Land Use Change: a Multinomial Logit Model of Spatial Relationships", published in the *Annals of Regional Science*, 42 (2), pp. 321-340, and presented at the 52nd Annual North American Meeting of the Regional Science Association International, Las Vegas, Nevada, November 2005.

Zhou, B. and Kockelman, K. "Self-selection in Home Choice: Use of Treatment Effects in Evaluating the Relationship between the Built Environment and Travel Behavior", forthcoming in *Transportation Research Record*, and presented at the 87th Annual Meeting of the Transportation Research Board, Washington D.C., January 2008 and at the 54th Annual North American Meetings of the Regional Science Association International, Savannah, Georgia, November 2007.

Zhou, Brenda and Kara Kockelman. "Microsimulation of Residential Land Development and Household Location Choices: Bidding for Land in Austin, Texas." Forthcoming in *Transportation Research Record*, Journal of the Transportation Research Board, 2008.

Zhou, Brenda, Kara Kockelman and Jason Lemp. "Transportation and Land Use Policy Analysis using Integrated Transport and Gravity-based Land Use Models." Under review

for publication in *Transportation Research Record*, October 2008. To be presented at and included in the Meeting Compendium of the Transportation Research Board's 88th Annual Meeting, Washington, DC, January 2009.

Zhou, Brenda and Kara Kockelman. "Lessons Learned in Developing and Applying Land Use Model Systems: A Parcel-based Example." Under review for publication in *Transportation Research Record*, and to be presented at and included in the Meeting Compendium of the Transportation Research Board's 88th Annual Meeting, Washington, DC, January 2009.

6.0 Description of Expenditures

FY 2004-2005

Dr. McDonald-Buller (the PI) received partial support from September of 2005-December of 2005. Dr. David Allen received partial support in June 2005. Alba Webb, a Research Associate in Dr. McDonald-Buller's group at the Center for Energy and Environmental Resources, received partial support from July 2005-December 2005. Three graduate research assistants in Dr. Kockelman's (Co-PI) group also received partial support (i.e., 50% time with tuition): Jason Lemp- 9/1/2005-12/31/2005; Xiaokun Wang- 1/1/05 -12/31/05; Bin Zhou -1/1/05 -12/31/05; and Shashank Gadda-1/1/5-8/31/05. Expenditures for travel expenses for Dr. McDonald-Buller and Dr. Kockelman were also incurred in November 2005 in order to attend the annual PI meeting in Washington D.C.

FY 2005-2006

Ms. Alba Webb, a Research Engineer/Scientist Associate III in Dr McDonald-Buller's group received support from 1/1/06-2/28/06 at 37.50% time; 10/01-11/30 at 100% time; 12/01-12/31/06 at 50% time; and 3/01-4/30/07 at 100% time. Mr. Gary McGaughey, a Research Engineer/Scientist Associate IV also in Dr. McDonald-Buller's group received support from 12/08-12/31/06 at 50% time. Dr McDonald-Buller, a Research Associate Professor, received support from 1/01-5/31/06 at 35% time; 7/01-7/31/06 at 29.51% time; 10/01-10/31/06 at 100% time; 11/01-11/30/06 at 50.63% time; 12/01/06-4/30/07 at 100% time. Funds were spent on a portable hard drive; 4 ArcGIS Licenses and travel to a conference in Houston for Dr McDonald-Buller.

Four graduate research assistants in Dr. Kockelman's (Co-PI) group received partial support (i.e., 50% time and tuition for B. Zhou & X. Wang only): Mr. Jason Lemp (1/1/06 - 5/31/06 and 9/1/06 -12/31/06); Ms. Bin (Brenda) Zhou (1/1/06 - 5/31/06 and 9/1/06 -12/31/06); Mr. Jianming Ma (3/17/06 - 3/31/06) and Ms. Xiaokun Wang (1/1/06-1/15/06). Please note that while Ms. Wang conducted research on the EPA project for the entire 12 months of 2006, her salary was provided by the Stevens Fellowship for 11.5 months of the year. One undergraduate workstudy assistant, Ms. Laura Narat also received partial support (i.e, approx. 20% hourly time from 1/15/06-5/15/06).

FY 2006-2007

Ms. Alba Webb, a Research Engineer/Scientist Associate III in Dr McDonald-Buller's group received support from 12/01-12/31/06 at 50% time; 3/01/07-5/31/07 at 50% time; 10/01-10/31/07 at 100% time; and 11/01-11/30/07 at 50% time. Mr. Gary McGaughey, a Research Engineer/Scientist Associate IV also in Dr. McDonald-Buller's group received support from 12/01-12/31/06 at 50% time. Dr McDonald-Buller, a Research Associate Professor, received support from 12/01/06-3/31/07 at 100% time; 4/01-4/30/07 at 18% time; 8/01-8/31/07 at 39.17% time; 10/01-10/31/07 at 100% time; and 11/01-11/30/07 at 50% time. Funds were spent on a printer, a portable hard drive, and conference registration for Dr McDonald-Buller.

Two graduate research assistants in Dr. Kockelman's (Co-PI) group received support on this project. Mr. Jason Lemp, from 12/20/06 -8/31/07 salary at 100% time, from 9/1/07-10/31/07 salary at 50% time, with Jason's tuition for the reporting period paid by the Advanced Institute Fellowship. Ms. Bin (Brenda) Zhou, from 12/20/06-8/31/07 salary at 100% time, from 10/1/07-10/31/07 and 12/1/07-12/19/07 salary at 100% time, with Spring '07 and Fall '07 tuition also paid by this project.

FY 2007-2008

In the past year, Dr Elena McDonald-Buller received support on this project as did Alba Webb, Research Engineer. Dr McDonald-Buller received salary support from 10/01/07-10/31/07 at 100% time, 11/01/07-11/30/07 at 50% time, 12/01/07-12/31/07 at 100% time, 02/01/08-02/29/08 at 75% time, and 03/01/08-03/31/08 at 19.25% time. Ms. Alba Webb received salary support from 10/01/07-10/31/07 at 100% time, 11/01/07-11/30/07 at 50% time, 02/01/08-03/31/08 at 100% time, 07/14/08-08/31/08 at 50% time, and 09/01/08-10/15/08 at 50% time.

Dr Elena McDonald-Buller incurred travel expenses for two meetings. She attended the AWMA Annual Meeting in Portland, OR during 06/22/08-06/27/08 and incurred expenses in the amount of \$2,806.29 in addition to the conference registration fee in the amount of \$560. She also attended the STAR Grantees Progress Review Meeting at the U.S. EPA in Raleigh, North Carolina during 10/26/08–10/29/08 and incurred expenses in the amount of \$871.31.

Two graduate research assistants in Dr. Kockelman's (Co-PI) group received support on this project and some summer support was received by Dr. Kockelman as well. Ms. Bin (Brenda) Zhou received salary support from 12/01/07-01/31/08 at 100% time, 02/01/08-05/31/08 at 50% time, 11/01/08-11/30/08 at 41% time and Spring '08 tuition also paid by this project. Ms. Sumala Tirumalachetty received salary support from 07/01/08-11/30/08 at 100% time, 12/01/08-12/31/08 at 50% time and Summer '08 & Fall '08 tuition also paid by this project. Dr. Kockelman received salary support from 06/01/08-06/30/08 at 22% time and from 08/01/08-8/31/08 at 39% time.

7.0 References

Alliance-Texas Engineering Group. (2003) *City of Pflugerville Refined Transportation Model Development Report*, November 2003.

Anselin, L. (1988). *Spatial Econometrics: Methods and Models*. Kluwer Academic, Dordrecht.

Anselin, L. (2001). Rao's score test in spatial econometrics. *Journal of Statistical Planning and Inference* 97, 113–139.

Anselin, L. (2005). Exploring Spatial Data with GeoDa: a Workbook. Retrieved June, 2006 from <https://geoda.uiuc.edu/pdf/geodaworkbook.pdf>.

Balling, R.J., J.T. Taber, M.R. Brown, and K. Day. (1999) Multi-objective Urban Planning Using Genetic Algorithm. *Journal of Urban Planning and Development* 125 (2), 86-99.

Ben-Akiva, M, and Lerman, S.R. (1985). *Discrete Choice Analysis*. MIT Press, Cambridge, MA.

Borning, A., P. Waddell, and R. Förster. (2007) UrbanSim: Using Simulation to Inform Public Deliberation and Decision-Making. *Digital Government: Advanced Research and Case Studies*, R. Traunmueller, *et al.* (eds.), Springer-Verlag, New York.

Capital Metropolitan Planning Organization (CAMPO 2005) *Mobility 2030 Plan*. June 2005. <http://www.campotexas.org/pdfs/AdoptedMobility2030Plan.pdf>

CAPCOG (2004a) *Austin-Round Rock MSA 2007 Future Year Ozone Precursor Modeling Emissions Inventory*, March 2004. <http://www.tceq.state.tx.us/implementation/air/sip/nov2004eac.html>

CAPCOG (2004b) *Photochemical Modeling for Austin's Early Action Compact: Development of the September 13-20, 1999 Photochemical Model with 2007 Projected Emissions and Analysis of Future 8-hour Ozone Design Values*, March 2004. <http://www.tceq.state.tx.us/implementation/air/sip/nov2004eac.html>

CAPCOG (2004c) *Austin/Round Rock MSA Emissions Reductions Strategies*, March 2004. <http://www.tceq.state.tx.us/implementation/air/sip/nov2004eac.html>

CAPCOG (2005) *Parcels – 2005*. http://www.capco.org/Information_Clearinghouse/geospatial_main.asp (accessed November 2006).

Carter, W. "Development of an Improved Chemical Speciation Database for Processing Emissions of Volatile Organic Compounds for Air Quality Models".

<http://www.engr.ucr.edu/~carter/emitdb/>

City of Austin. (2003) Land Use. ftp://coageoid01.ci.austin.tx.us/GIS-Data/Regional/coa_gis.html (accessed November 2006).

Clarke, K.C., S. Hoppen, and L. Gaydos. (1997) A self-modifying cellular automaton model of historical urbanization in the San Francisco Bay area. *Environment and Planning B: Planning and Design* 24, 247-261.

Clark, W.A.V., Huang, Y., and Withers, S. (2003) Does commuting distance matter? commuting tolerance and residential change. *Regional Science and Urban Economics* 33(2), 199-221.

CRAI. Economic Modeling of the Lieberman-Warner Bill: S.2191 as Reported by Senate EPW. Charles River Associates, International, January, 2008.

Das, D., Kelejian, H., and Prucha, I. (2003). Finite sample properties of estimators of spatial autoregressive models with autoregressive disturbances. *Papers in Regional Science* 82, 1-26.

Dowling, R., R. Ireson, A. Skabardonis, D. Gillen, and P. Stopher. (2005) *National Cooperative Highway Research Program (NCHRP) Report 535: Predicting Air Quality Effects of Traffic-Flow Improvements: Final Report and User's Guide*. Transportation Research Board, Washington, D.C.

Eastern Research Group. (2002) emissions from Portable Gasoline Containers in Texas: Final Report.

<http://www.tceq.state.tx.us/assets/public/implementation/air/sip/sipdocs/2004-10-DAL/Appendix%20H.pdf> (accessed February 2007).

Eastern Research Group. (2004) ProjectH018.2003: Locomotive emissions.

<http://www.harc.edu/Projects/AirQuality/Projects/Projects/H018.2003> (accessed March 2007).

Envision Central Texas (2003). *Scenario Briefing Packet*, 2003.

Envision Central Texas (2004). *A Vision for Central Texas*, May 2004.

<http://www.envisioncentraltexas.org>

ENVIRON International Corporation (2004). *Users Guide to the Comprehensive Air Quality Model with Extensions (CAMx) version 4.03*. (<http://www.camx.com>), 101 Rowland Way, Suite 220, Novato, California.

Federal Highway Administration (1996). *Public Involvement Techniques for Transportation Decision-Making*. U.S. Department of Transportation, Federal Highway

Administration and Federal Transit Administration. Publication NO. FHWA-PD-96-031 HEP-30/9-96/(4M)QE.

Federal Highway Administration. (2001) Our Nation's Highways, 2000. Retrieved July, 2008 from http://www.fhwa.dot.gov/ohim/onh00/our_ntns_hwys.pdf.

Fischer, C., Harrington, W. and Parry, I.W.H. (2007) Should Automobile Fuel Economy Standards be Tightened? *The Energy Journal* 28 (4), 1-29.

Gery, M., Whitten, G., Killus, J., Dodge, M. (1989) A Photochemical Kinetics Mechanism for Urban and Regional Scale Computer Modeling. *J. Geophys. Res.*, 1989, 94(D10), 12,925-12,956.

GEWEX Continental Scale International Project (GCIIP) and GEWEX Americas Prediction Project (GAPP). Surface Radiation Budget (SRB) Data. Surface Downward Photosynthetically Active Radiation (PAR). Available at <http://www.atmos.umd.edu/~srb/gcip/cgi-bin/historic.cgi> (accessed June 2005).

Greene, W. (2000). *Econometric Analysis*. Upper Saddle River: Prentice-Hall.

Gregor, B. (2007) The Land Use Scenario Developer (LUSDR): A Practical Land Use Model Using a Stochastic Microsimulation Framework. *Transportation Research Record*, 07-0438, 93-102.

Gulipalli, P. and Kockelman, K. (2008) Credit-Based Congestion Pricing: A Dallas-Fort Worth Application. *Transport Policy* 15 (1): 23-32.

Hunt J.D., and J.E. Abraham. (2003) Design and application of the PECAS land use modelling system. The 8th Computers in Urban Planning and Urban Management Conference, Sendai, Japan.
<http://www.ucalgary.ca/~jabraham/Papers/pecas/summary.html>.

Hunt J.D., J.E. Abraham, D. De Silva, M. Zhong, J. Bridges, and J. Mysko. (2008) Developing and Applying a Parcel-Level Simulation of Developer Actions in Baltimore. Proceeding of the 87th Annual Meeting of the Transportation Research Board, Washington D.C., January 2008.

ITLUP (Integrated Transportation-Land Use Package) (2007) ITLUP Models Documentation, the Caliper Corporation.

Jacobson, M. (2007) Effects of Ethanol (E85) versus Gasoline Vehicles on Cancer and Mortality in the United States. *Environ. Sci. Technol.* 2007, 41(11), 4150-4157.

Johnston, R.A., and T. de la Barra. (2000) Comprehensive Regional Modeling for Long-Range Planning: Linking Integrated Urban Models and Geographic Information Systems. *Transportation Research Part A: Policy and Practice* 34(2), 125-136.

Kelejian, H.H. and Prucha, I. (1998). A generalized spatial two stage least squares procedure for estimating a spatial autoregressive model with autoregressive disturbances. *Journal of Real Estate Finance and Economics* 17, 99–121.

Kelejian, H.H. and Prucha, I.R. (1999). A Generalized Moments Estimator for the Autoregressive Parameter in a Spatial Model. *International Economic Review* 40, 509–533.

Kelejian, H.H. and Prucha, I.R. (2004). Estimation of simultaneous systems of spatially interrelated cross sectional equations. *Journal of Economics* 118, 27–50.

Kockelman, K.M. (1997). Travel behavior as a function of accessibility, land use mixing, and land use balance: evidence from the San Francisco Bay Area. *Transportation Research Record* 1607, 117–125.

Kockelman, K.M. (2000). To LDT or Not to LDT. *Transportation Research Record*. No. 1738, 3-10.

Kockelman, K. M., L. Jin, Y. Zhao, and N. Ruiz-Juri (2004) Tracking Land Use, Transport, and Industrial Production using Random-Utility-Based Multizonal Input-Output Models: Applications for Texas Trade. *Journal of Transport Geography* 13(3), 275-286.

Krishnamurthy, S. and Kockelman, K. (2003) Propagation of Uncertainty in Transportation-Land Use Models: An Investigation of DRAM-EMPAL and UTPP Predictions in Austin, Texas. *Transportation Research Record* No. 1831: 219-229.

Lemp, J., Zhou, B., Kockelman, K. and Parmenter, B. (2008) “Visioning Vs. Modeling: Analyzing the Land Use-Transportation Futures of Urban Regions”, *Journal of Urban Planning and Development*, 2008, 134(3), 97-109.

McDonald-Buller, E., Wiedinmyer, C., Kimura, Y., Allen, D. (2001) Effects of land use data on dry deposition in a regional photochemical model for eastern Texas. *J. Air Waste Manage.* 2001, 51(8), 1211-1218.

McGaughey, G., Desai, N., Allen, D., Seila, R., Lonneman, W., Fraser, M., Harley, R., Pollack, A., Ivy, J., Price, J. (2004) Analysis of motor vehicle emissions in a Houston tunnel during the Texas Air Quality Study 2000. *Atmos. Environ.* 2004, 38, 3363-3372.

Miller, E.J., Kriger, D.S. and Hunt, J.D. (1998) *Integrated Urban Models for Simulation of Transit and Land-Use Policies: Final Report*. Transit Cooperative Research Project, National Academy of Sciences.

Nordhaus, W.D. (1991). The Cost of Slowing Climate Change: A Survey. *The Energy Journal*, 19 (1), 37-65.

Ota M, Fujita M (1993) Communication technologies and spatial organization of multi-unit firms in metropolitan areas. *Regional Science and Urban Economics* 23: 695-729

PBQ&D. (1999) *NCHRP Report 423A: Land-Use Impacts of Transportation*. A Guidebook. Parsons Brinckerhoff Quade and Douglas, for the National Cooperative Highway Research Program of the Transportation Research Board, Washington, D.C.

PECAS (2007) Theoretical Formulation: System Documentation Technical Memorandum 1. October 2007. (Received from John Abraham in March 2008)

Putman, S. (1983) *Integrated Urban Models: Policy Analysis of Transportation and Land Use*, Pion, London.

Raju, K.A., P.K. Sikdar, and S.L. Dhingra. (1998) Micro-simulation of residential location choice and its variation. *Computers, Environment and Urban Systems* 22 (3), 203-218.

Rouwendal, J., and Meijer, E. (2001) Preferences for housing, jobs, and commuting: a mixed logit analysis. *Journal of Regional Science* 41(3), 475-505.

Silva, E.A., and K.C. Clarke. (2002) Calibration of the SLEUTH urban growth model for Lisbon and Porto, Portugal. *Computers, Environment and Urban System* 26, 525-552.

Smart Mobility, Inc. (2003) *Envision Central Texas Transportation Model: Technical Documentation*. 16 Beaver Meadow Road #3, Norwich, Vermont 05055.

Song, J. (2007) Land Use Forecasting in Regional Air Quality Models, Ph.D. Dissertation. The University of Texas at Austin. May 2007.

Song, J., Webb, A., Parmenter, B., Allen, D. T., McDonald-Buller, E. (2008) The Impacts of Urbanization on Emissions and Air Quality: Comparison of Four Visions of Austin, Texas. *Environ. Sci. Technol.* 2008, 42(19), 7294-7300.

Syphard, A.D., K.C. Clarke, and J. Franklin. (2005) Using a cellular automaton model to forecast the effects of urban growth on habitat pattern in southern California. *Ecological Complexity* 2, 185-203.

TELUM (Transportation Economic and Land Use Model) (2007) TELUM User Manual, retrieved February 2007 from <http://www.telus-national.org/index.htm>.

Tol, R.S.J. (1999) The Marginal Costs of Greenhouse Gas Emissions. *The Energy Journal* 20 (1), 61-81.

Texas Transportation Institute. (2003) *Austin/San Marcos Metropolitan Statistical Area On-Road Mobile Source Emissions Inventories: 1995, 1999, 2002, 2005, 2007, and 2012*. August 2003.

Tillema, T., Ettema, D., and Van Wee, B. (2006) Road pricing and (re)location decisions of households. Proceeding of the *85th Annual Meeting of the Transportation Research Board*, Washington D.C.

U.S. Environmental Protection Agency. (1992) *User's guide for the Urban Airshed Model, Volume IV: User's Manual for the Emissions Preprocessor System 2.0*. EPA-450/4-90-007D. June 1992.

U.S. Environmental Protection Agency. (2000) *Projecting Land-Use Change: A Summary of Models for Assessing the Effects of Community Growth and Change on Land-Use Patterns*. EPA 600-R-00-098, Washington D.C.

U.S. Environmental Protection Agency. (2001) *Accounting for the Tier 2 and Heavy-Duty 2005/2007 Requirements in MOBILE6*. EPA420-R-01-057. November 2001.

U.S. Environmental Protection Agency. (2003a) *User's guide to MOBILE6.1 and MOBILE6.2: Mobile Source Emission Factor Model*. EPA420-R-03-010. August 2003.

U.S. Environmental Protection Agency. (2003b) *Program Update: Reducing Air Pollution from Nonroad Engines*. EPA420-F-03-011. April 2003.

U.S. Environmental Protection Agency. (2004). *Nonroad Engine Growth Estimates*. EPA420-P-04-008. April 2004.

U.S. Environmental Protection Agency. (2005) *User's Guide for the Final NONROAD2005 Model*. EPA420-R-05-013. December 2005.

U.S. Environmental Protection Agency. (2007a) Control of Hazardous Air Pollutants From Mobile Sources: Final Rule. Regulatory Documentation published February 2007. <http://www.epa.gov/otaq/toxics.htm#mobile>

U.S. Environmental Protection Agency. (2007b) Lifecycle Impacts on Fossil Energy and Greenhouse Gases. Chapter 6 of *Regulatory Impact Analysis: Renewable Fuel Standard Program*, Report EPA420-R-07-004, Washington, D.C.

U.S. Environmental Protection Agency. (2008) EPA Analysis of the Lieberman-Warner Climate Security Act of 2008, S. 2191 in 110th Congress, Washington, D.C.

U.S. Geological Survey. (1992) National Land Cover Dataset 1992. <http://landcover.usgs.gov/natl/landcover.php> (accessed November 2006).

Valsaraj, V., Kockelman, K. Duthie, J. and Zhou, B. (2007) Forecasting Employment & Population in Texas: An Investigation on TELUM Requirements, Assumptions, and Results, including a Study of Zone Size Effects, for the Austin and Waco Regions.

Van Ommeren, J., Rietveld, P., and Nijkamp, P. (1999) Job moving, residential moving, and commuting: a search perspective. *Journal of Urban Economics* 46(2), 230-253.

Vizuete, W., Junquera, V., McDonald-Buller, E., McGaughey, G., Yarwood, G., Allen, D.T. (2002) Effects of temperature and land use on predictions of biogenic emissions in eastern Texas. *Atmos. Environ.* 2002, 36(20), 3321-3337.

Waddell, P. (2002) UrbanSim: Modeling Urban Development for Land Use, Transportation and Environmental Planning. *Journal of the American Planning Association* 68(3), 297-314.

Waddell, P., A., Borning, M. Noth, N. Freier, M. Becke, and G. Ulfarsson. (2003) Microsimulation of Urban Development and Location Choices: Design and Implementation of UrbanSim. *Networks and Spatial Economics* 3(1), 43 – 67.

Waddell, P., and G.F. Ulfarsson. (2004) Introduction to Urban Simulation: Design and Development of Operational Models. In *Handbook in Transport, Volume 5: Transport Geography and Spatial Systems*, Stopher, Button, Kingsley, Hensher eds. Pergamon Press.

Walmsley, J.L., Wesely, M.L. (1996) Modification of coded parametrizations of surface resistances to gaseous dry deposition. *Atmos. Environ.* 1996, 30(7), 1181-1188.

Wang, L. (2006) Inter-pollutant and reactivity-weighted air pollutant emission trading in Texas, Ph.D. Dissertation. The University of Texas at Austin. 2006.

Wesely, M.L. (1986) Parametrization of surface resistances to gaseous dry deposition in regional-scale numerical models. *Atmos. Environ.* 1989, 23(6), 1293-1304.

Wiedinmyer C., Strange I., Estes M., Yarwood, G., Allen D. (2000) Biogenic hydrocarbon emission estimates for north central Texas. *Atmos. Environ.* 2000, 34(20), 3419-3435.

Wiedinmyer C., Guenther, A., Estes, M., Strange, I., Yarwood, G., Allen, D. (2001) A land use database and examples of biogenic isoprene emission estimates for the state of Texas, USA. *Atmos. Environ.* 2001, 35(36), 6465-6477.

Yarwood, G., Wilson, G., Emery, C., Guenther, A. (1999). *Development of the GloBEIS – a state of the science biogenics emissions modeling system: Final Report to the Texas Natural Resource Conservation Commission*; 12100 Park 35 Circle, Austin, Texas 78753.

Yarwood, G., Wilson, G., Shepard, S., Guenther, A. (2003). *User's Guide to the Global Biosphere Emissions and Interactions System – Version 3.1.* (<http://www.globeis.com>), 101 Rowland Way, Suite 220, Novato, California.

Zhou, B. and Kockelman, K. M. (2006). Predicting the Distribution of Employment and Households: A Seemingly Unrelated Regression Model with Spatial Dependences. Forthcoming in *Journal of Transport Geography*.

Zhou, B. and Kockelman, K. M. (2008). Neighborhood Impacts on Land Use Change: A Multinomial Logit Model of Spatial Relationships. *Annals of Regional Science* 42 (2), 321-340.

Appendix A

Table A.1 Crosswalk between the composite land use/land cover database developed in this study and EPS2 surrogates.

Composite Database Category Code	Composite Database Description	EPS2 Surrogate	EPS2 Description
1	Single Family Residence	4	Urban
2	Large-lot Single Family Residence	4	Urban
3	Mobile Homes	4	Urban
4	Multi-family Residence	4	Urban
11	Commercial	4	Urban
12	Industrial	4	Urban
13	Office	4	Urban
14	Commercial/Industrial/Transportation	4	Urban
15	Transportation	4	Urban
16	Streets and Roads	4	Urban
21	Unknown	4	Urban
22	Utilities	4	Urban
23	Civic	4	Urban
24	Vacant	4	Urban
25	Urban/Recreational Grasses	4	Urban
26	Undeveloped	4	Urban
27	Mining	11, 15	Barren, Rural
31	Bare Rock/Sand/Clay	11, 15	Barren, Rural
32	Quarries/Strip Mines/Gravel Pits	11, 15	Barren, Rural
33	Transitional	11, 15	Barren, Rural
34	Deciduous Forest	7, 15	Deciduous Forest, Rural
35	Evergreen Forest	8, 15	Coniferous Forest, Rural
36	Mixed Forest	9, 15	Mixed Forest, Rural

37	Shrubland	6, 13, 15	Range, Mixed Agricultural and Range, Rural Agriculture,
38	Orchards/Vineyards/Other	5, 13, 15	Mixed Agricultural and Range, Rural Range, Mixed
39	Grasslands/Herbaceous	6, 13, 15	Agricultural and Range, Rural Agriculture,
40	Pasture/Hay	5, 6, 13, 15	Range, Mixed Agricultural and Range, Rural Agriculture,
41	Row Crops	5, 6, 13, 15	Range, Mixed Agricultural and Range, Rural Agriculture,
42	Small Grains	5, 6, 13, 15	Range, Mixed Agricultural and Range, Rural
44	Woody Wetlands	12	Non-forested wetlands
45	Emergent Herbaceous Wetlands	12	Non-forested wetlands
51	Water	10, 15	Water, Rural

Appendix B

B.1 Biogenic Emissions

Isoprene emissions for the Base Case ranged from 1.5 to 3 Mmoles day⁻¹ across the episode with an average of 2 Mmoles day⁻¹ as shown in Table B.1. Differences in land use/land cover led to 2 to 6% reductions in daily biogenic emissions across the 5-county Austin MSA. If the percentage change in biogenic emissions is restricted to grid cells that experienced land cover changes, the percentage reductions are larger, ranging from 5 to 11%, as shown in Table B.2. ECT A, which assumes a typical urban sprawl pattern with the largest consumption of vegetative cover, shows the largest reductions in isoprene emissions. The reductions occur primarily in Travis and Williamson Counties where much of the transition from mixed agricultural and rangeland or mixed forest to developed land occurs.

Table B.1 Percent decrease in biogenic isoprene emissions compared to Base Case emissions

		Date in September, 1999									
		Units	13	14	15	16	17	18	19	20	Avg.
Base Case ISOP	Emissions	Mmoles day ⁻¹	1.5	2.1	1.8	1.5	1.9	2.2	3.0	1.9	2.0
	ECT A	%	5.43	5.50	5.36	5.30	5.35	5.39	5.45	5.20	5.37
	ECT B	%	2.61	2.64	2.58	2.55	2.57	2.59	2.62	2.50	2.58
	ECT C	%	2.61	2.66	2.60	2.58	2.60	2.61	2.64	2.54	2.61
	ECT D	%	1.55	1.59	1.53	1.50	1.33	1.54	1.56	1.46	1.51

Table B.2 Percent decrease in biogenic isoprene emissions in cells that have land use/land cover changes compared to Base Case emissions

		Date in September, 1999									
		Units	13	14	15	16	17	18	19	20	Avg.
	ECT A	%	10.4	10.2	10.3	10.1	10.4	10.7	10.8	10.8	10.5
	ECT B	%	4.5	4.4	4.8	4.1	4.5	4.6	4.7	4.7	4.5
	ECT C	%	6.4	6.0	6.4	5.7	6.0	6.1	5.9	6.2	6.1
	ECT D	%	7.2	7.8	8.4	7.5	7.4	7.3	7.7	7.6	7.6

Differences in spatially allocated biogenic isoprene emissions for each ECT scenario relative to the Base Case are shown in Figure B.1 for one episode day (September 19 at 1400).

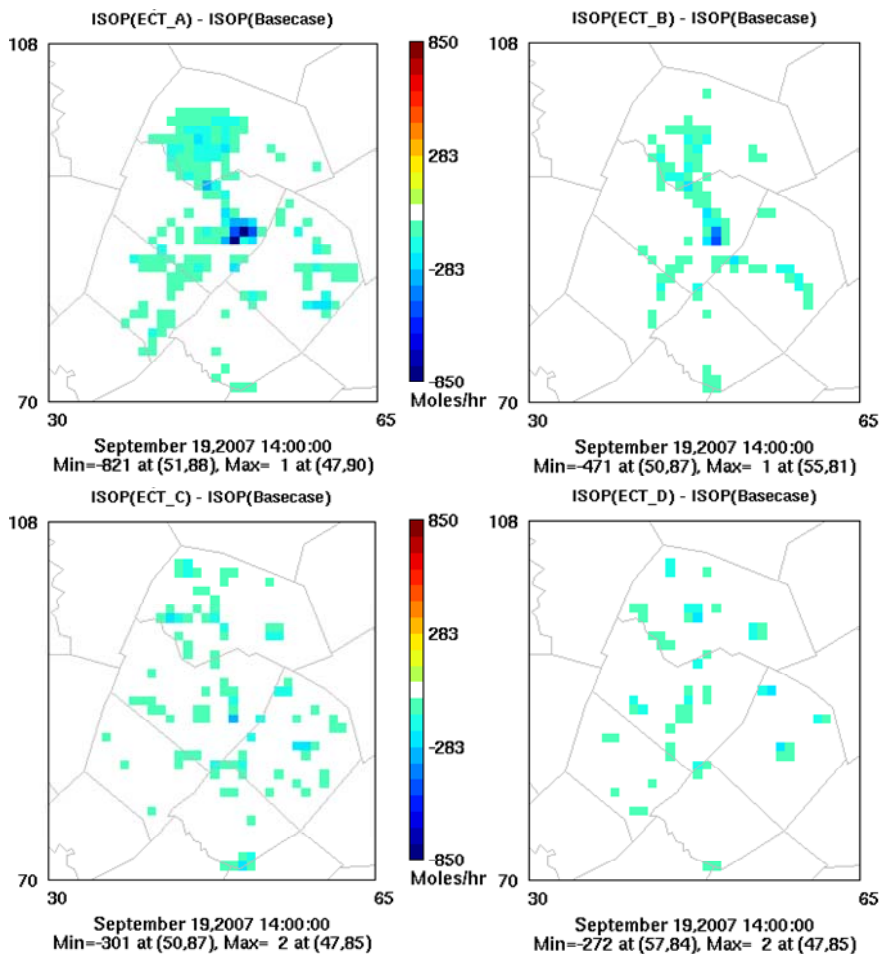


Figure B.1 Differences in biogenic isoprene emissions between ECT scenarios and the Base Case

B.2 On-road Mobile Source Emissions

For the Base Case, on-road mobile source VOC emissions for the five-county Austin area are nearly all attributed to light-duty gasoline vehicles (95%) as shown in Table B.3.

NOx emissions originate from light-duty gasoline vehicles (77%) followed by heavy-duty diesel vehicles (16%). For the ECT scenarios, VOC and NOx emissions are reduced due to more stringent federal motor vehicle emission control programs including the EPA's Tier 2 and heavy-duty 2007 rules. VOC emissions for the ECT scenarios are still primarily from light-duty gasoline vehicles (93%), while NOx emissions are also primarily attributed to light-duty gasoline vehicles (92%).

Table B.3 Weekday on-road mobile source VMT and emissions (tpd) of VOC and NOx for the 2007 Base Case and four ECT Scenarios

Categories	2007 Base Case VMT = 44.5*		ECT A VMT = 82.4*		ECT B VMT = 72.2*		ECT C VMT = 69.5*		ECT D VMT = 65.9*	
	VOC	NOx	VOC	NOx	VOC	NOx	VOC	NOx	VOC	NOx
Light-duty gasoline vehicles	32.1	47.9	20.5	16.9	17.9	14.7	17.5	14.3	15.9	13.2
Heavy-duty gasoline vehicles	1.1	3.3	0.2	0.2	0.2	0.2	0.2	0.2	0.1	0.1
Light-duty diesel vehicles	0.1	0.9	0.0	0.0	0.0	0.0	0.0	0.0	0.0	0.0
Heavy-duty diesel vehicles	0.5	10.0	1.3	1.3	1.1	1.1	1.1	1.1	1.0	1.0
Total	33.8	62.1	22.0	18.4	19.2	16.0	18.8	15.6	17.0	14.3

Note: ECT scenario emissions are calculated for a future year of 2030.

*VMT is given in units of 10^6 miles per day in the 5-county Austin area.

Differences in spatially allocated on-road mobile source NO_x and VOC emissions are shown in Figure B.2 for one episode day (September 20 at 1400). These figures compare emissions from ECT A to the Base Case which represent changes due to the doubling of population with a continuation of current development patterns, and they also compare emissions from ECT D to ECT A, which represent the two most extreme development scenarios.

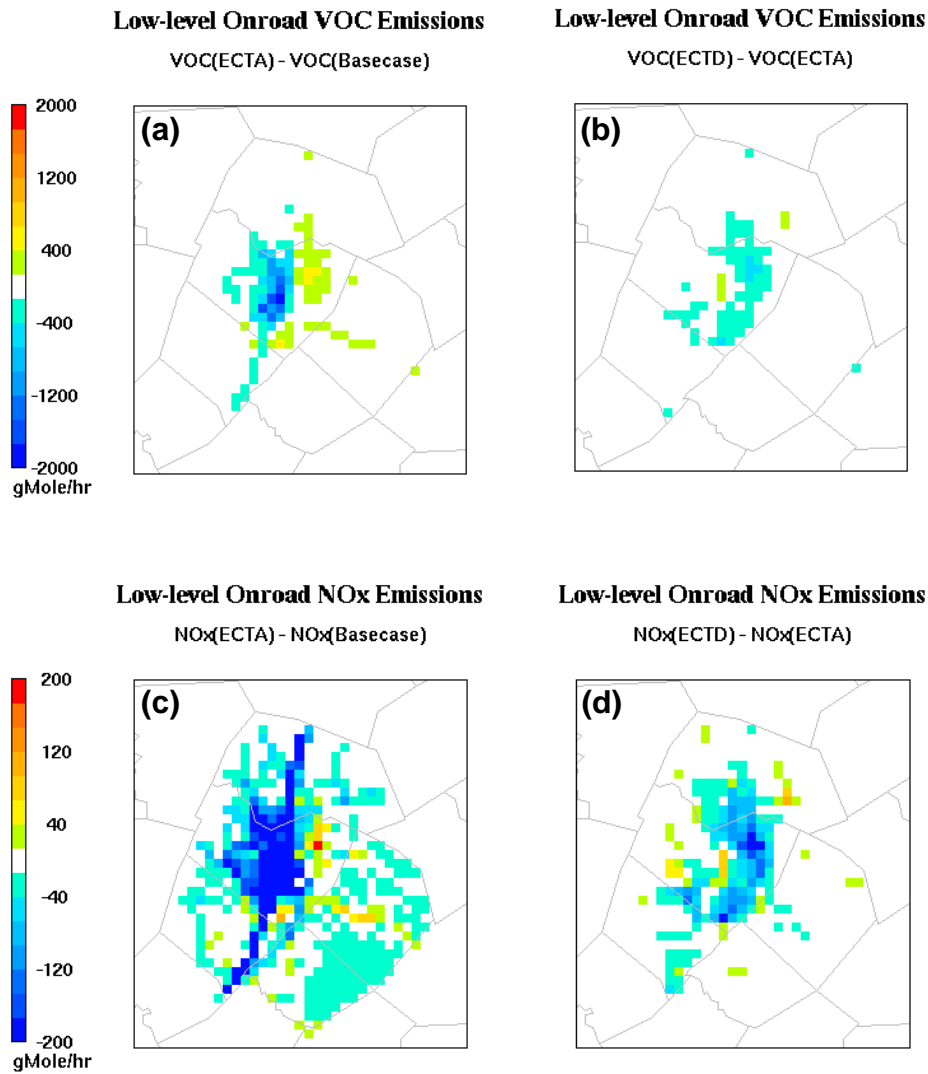


Figure B.2 Differences in on-road mobile source VOC emissions between (a) ECT A and the Base Case, and (b) ECT D and ECT A. Differences in on-road mobile source NO_x emissions between (c) ECT A and the Base Case and (d) ECT D and ECT A.

B.3 Non-road Mobile Source Emissions

For the Base Case, 61% of non-road mobile source VOC emissions for the five-county Austin area are attributed to emissions from lawn and garden equipment, followed by recreational equipment (12%) as shown in Table B.4. NOx emissions are attributed to emissions from construction and mining equipment (55%), followed by railway (14%). For the ECT scenarios, emissions from lawn and garden equipment (71-77%) play a larger role in the total VOC emission inventory; whereas NOx emissions are not dominated by a single category. Emissions from most non-road mobile source categories, with the exception of those from lawn and garden equipment, are less for the ECT scenarios than for the Base Case due to new emission standards, especially for categories associated with industrial and construction/mining equipment affected by the EPA's Tier 4 engine standards. However, VOC and NOx emissions from lawn and garden equipment increased, primarily because emissions from gas cans, included in this category, were projected based on growth in the number of households. In addition, the NONROAD model does not incorporate new emission controls between 2007 and 2030 for most 2-stroke and some 4-stroke lawn and garden equipment.

Table B.4 Weekday non-road mobile source emissions (tpd) of VOC and NOx for the 2007 Base Case and four ECT Scenarios

Categories	2007 Base Case		ECT A		ECT B		ECT C		ECT D	
	VOC	NOx	VOC	NOx	VOC	NOx	VOC	NOx	VOC	NOx
Agricultural	0.1	0.0	0.0	0.0	0.0	0.0	0.0	0.0	0.0	0.0
Commercial	2.1	0.5	2.4	0.5	2.5	0.5	2.5	0.5	2.4	0.5
Construction and Mining	1.8	11.9	1.1	2.4	1.1	2.4	1.1	2.4	1.1	2.4
Industrial	0.8	2.4	0.1	0.4	0.1	0.4	0.1	0.4	0.1	0.4
Lawn and Garden	13.4	1.4	16.6	1.5	18.4	1.7	18.4	1.7	16.6	1.5
Railway	0.2	3.1	0.2	2.3	0.2	2.2	0.2	2.3	0.2	2.3
Recreational	2.7	0.1	1.7	0.1	0.6	0.1	0.6	0.1	1.7	0.1
Airport	0.8	1.1	0.8	1.1	0.8	1.1	0.8	1.0	0.8	1.1
Military	0.3	1.2	0.3	1.2	0.3	1.2	0.3	1.2	0.3	1.2
Total	22.2	21.7	23.2	9.5	24.0	9.6	24.0	9.6	23.2	9.5

Note: ECT scenario emissions are calculated for a future year of 2030.

Differences in spatially allocated non-road mobile source NO_x and VOC emissions are shown in Figure B.3 for one episode day (September 20 at 1400).

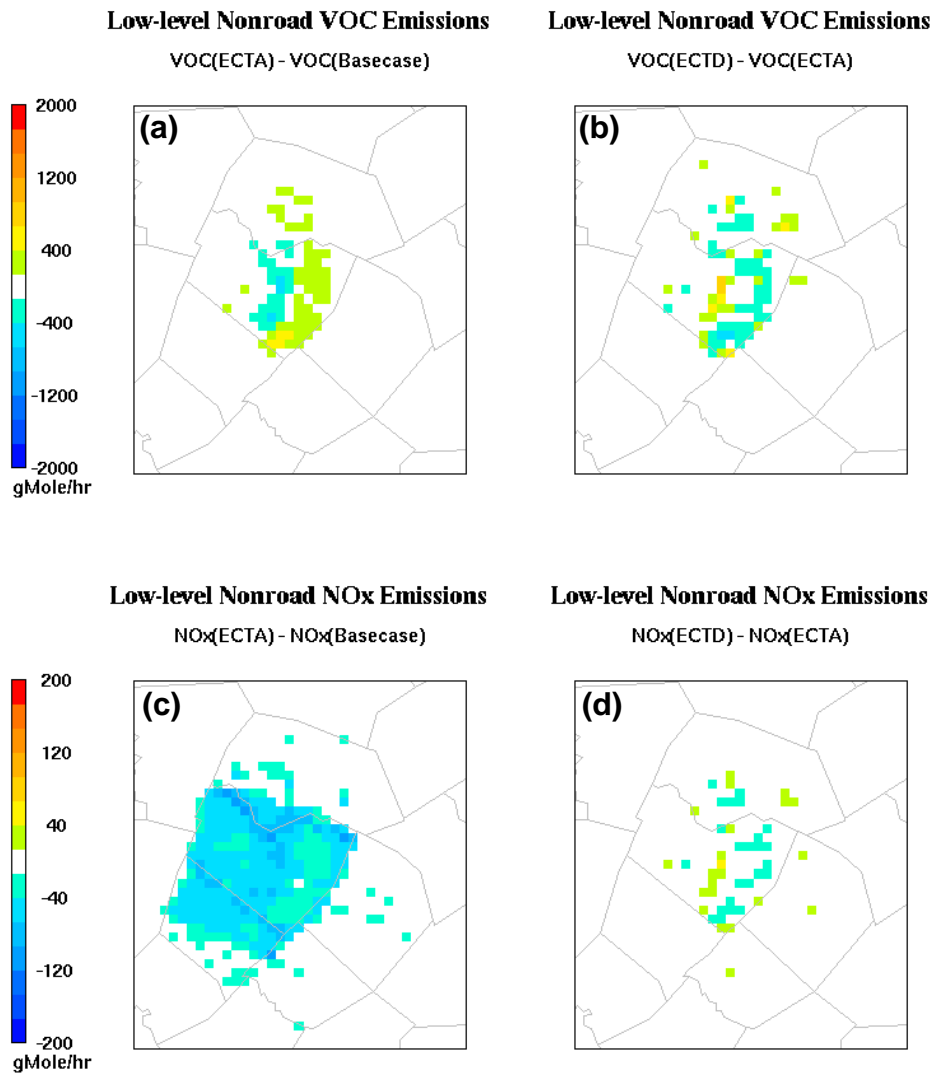


Figure B.3 Differences in non-road mobile source VOC emissions between (a) ECT A and the Base Case, and (b) ECT D and ECT A. Differences in non-road mobile source NO_x emissions between (c) ECT A and the Base Case and (d) ECT D and ECT A.

B.4 Area Source Emissions

For the Base Case, VOC emissions from area sources across the five-county Austin area are attributed to solvent utilization (44%) and service stations (19%); while NO_x emissions are attributed to agricultural production (51%) and stationary source fuel combustion (43%) as shown in Table B.5. About half of the total area source emissions originate from Travis County that includes the City of Austin. Because area source emissions for the ECT scenarios were projected using human population, they approximately double estimates for the Base Case. However, the scenarios were each based on a different spatial development pattern with a different fraction of population for each county (e.g., 57% and 45% of the total population live in Travis County for ECT Scenarios A and C, respectively). Because ECT C had a slightly larger total population than the other scenarios, the largest differences in emissions relative to the Base Case were observed for ECT Scenario C. For ECT Scenario C, VOC emissions are attributed to solvent utilization (34%), followed by industrial processes (29%); while NO_x emissions are attributed to agricultural production (58%), and stationary source fuel combustion (33%). Due to differences in the distribution of the population across each county, other ECT scenarios do not always follow the same trends as ECT Scenario C.

Table B.5 Weekday area source emissions (tpd) of VOC and NO_x for the 2007 Base Case and four ECT Scenarios

Categories	2007 Base Case		ECT A		ECT B		ECT C		ECT D	
	VOC	NO _x	VOC	NO _x	VOC	NO _x	VOC	NO _x	VOC	NO _x
Agriculture Production	5.6	5.1	12.2	11.1	13.8	12.3	15.6	13.8	13.9	12.4
Fuel Storage and Transport	6.9	0.0	13.4	0.0	13.9	0.0	14.3	0.0	13.8	0.0
Industrial Processes	15.5	0.2	33.3	0.4	54.8	0.6	76.7	0.7	54.7	0.6
Miscellaneous Area Sources	2.1	0.4	4.4	0.8	5.0	0.9	5.6	0.9	5.0	0.9
Service Stations	20.8	0	40.2	0	40.8	0	41.6	0	40.5	0
Solvent Utilization	48.8	0	91.2	0	90.5	0	89.7	0	89.6	0
Stationary Source Fuel Combustion	0.2	4.4	0.3	8.1	0.3	8.0	0.3	7.9	0.3	7.9
Storage and Transport	0.9	0	1.8	0	1.8	0	1.9	0	1.9	0

Waste Disposal, Treatment, and Recovery	9.9	0.1	17.5	0.2	16.8	0.3	15.9	0.3	16.5	0.3
Total	110.7	10.2	214.3	20.6	237.7	22.1	261.6	23.6	236.2	22.1

Note: ECT scenario emissions are calculated for a future year of 2030.

Differences in spatially allocated area source NO_x and VOC emissions are shown in Figure B.4 for one episode day (September 20 at 1400).

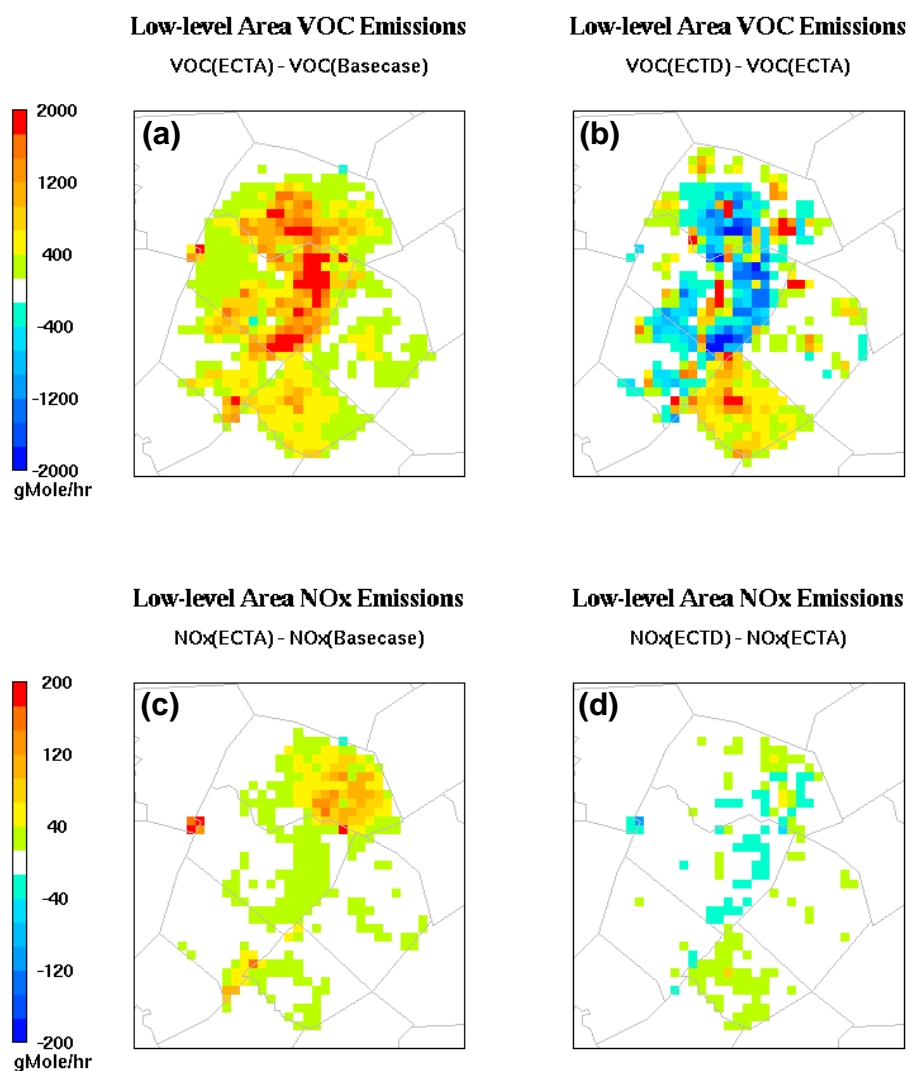


Figure B.4 Differences in area source VOC emissions between (a) ECT A and the Base Case, and (b) ECT D and ECT A. Differences in area source NO_x emissions between (c) ECT A and the Base Case and (d) ECT D and ECT A.

Appendix C. Travel Demand Model

Smart Mobility's TDM Documentation

Much of the material covered here is given in *Envision Central Texas Transportation Model: Technical Documentation*. Thus, we will refer to the technical documentation often. This document is intended to provide an overview of how this model works since the technical documentation does not provide all of the details.

Overview

The model consists of 6 sub-models (auto availability, trip generation, walk/bike trips, trip distribution, mode choice, and assignment), 3 of which require feedback in the form of iterations (the last three).

The model requires several inputs. First, household counts by type (6 types) for each zone are needed where household type is specified by presence of children in the household (yes or no) and the number of workers in the household (0, 1, or 2+). Second, employment counts (the number of workers) by type for each zone are needed where the types include basic (BAS), retail (RET), service (SER), K-12 education (ED1), post-secondary/college education (ED2), and airport (AIR). Last, several urban form variables are needed for each zone. These include household and employment densities, the balance between housing and employment, intersection density, and transit stop density. It is important to note that in working with the SM model, we have never fully understood how the intersection density and transit stop density were computed. We do know that it is not computed using the ECT network files. For our work, we have simply used the ECT values, or interpolated values since the given values are only for years 1997 (the base year) and 2025. In addition, the model makes assumptions regarding network link free-flow speeds that vary by the area type of the zone (rural, suburban, or urban/CBD).

Auto Availability

Multinomial logit models were used for auto availability. The alternatives considered in the models are 0, 1, and 2+ autos. Explanatory variables include the presence of children, housing density, intersection density, and transit stop density, and the models are fully segmented by the number of household workers (thus, there are 3 models).

Based on the models, the number of households are forecast by type. When the model is applied, probabilities (of 0, 1, and 2+ autos) are computed for each household type (6 types) and for each zone. Given these probabilities, it is possible to further disaggregate households by a third dimension (on top of the presence of children and number of workers). In essence, model application gives us the number of households by type where there are now $6 \times 3 = 18$ types (e.g., no children (NC)/0 workers (W0)/0 autos(A0), NC/W0/1 auto (A1), etc.).

Trip Generation

Trip generation consists of trip productions and trip attractions. Trip productions are modeled for 10 trip types based on cross-classification models where each type of household (of the 18 types discussed above) produces a fixed number of trips of a given type. No zonal specific characteristics are used in the models (e.g., household density, etc.) other than the number of households by type. The 10 trip types include home-based work direct (HBWD), home-based work complex (HBWC), home-based work strategic (HBWS), home-based non-work retail (HNWR), home-based non-work other (HNWO), non-home-based work (NHBW), non-home-based other (NHBO), K-12 education (ED1), post-secondary/college education (ED2), and airport (AIR). It should be noted that even the non-home-based trips are modeled by the number of households in the zone even though, by definition, they are not based at the household.

Trip attractions are based on attractions rates estimated for the aggregate number of households and employment by type for each zone. As standard procedure, trip productions and attractions are balanced holding the trip productions fixed (in order that productions equal attractions).

Walk/Bike Trips

Smart Mobility suggests that the Austin zones are too large for walk and bike trips to be handled sufficiently through the regular mode choice model. Therefore, they estimated a separated walk/bike model that removes some of the trips generated from previous model. These trips are not thrown out altogether, though they are not modeled in trip distribution or any of the subsequent models. Separate models were estimated for HBWD, HNWR, HNWO, ED1, ED2, NHBW, and NHBO trips. HBWS and HBWC trips by definition cannot be by the walk/bike mode. In addition, there were not any airport trips in the survey by these modes.

Trip Distribution

For trip distribution, gravity models were estimated for each trip type. Each of the models uses a doubly constrained structure where row and column totals of the distribution matrix must equal the trip productions and attractions estimated in the previous models. Hence, an iterative process is used to find these distributions.

Mode Choice

For mode choice, a nested logit structure is used. In the top level of the nest, there is the choice of auto versus transit, and in the bottom level of transit mode, there is the choice of walk access versus drive access. The models consider in-vehicle time, out-of-vehicle time (for transit), cost, number of household vehicles, housing density, and intersection density. The operating cost for the auto mode was assumed to be \$0.0922/mile. In model application, this is NOT adjusted for vehicle occupancy, though it probably should be for consistency. Due to unreasonably low VOTTs implied in model estimation, VOTT was assumed to be \$9/hr for work trip and \$4.50 for non-work trips. In model application, cost is simply converted to generalized time and added to in-vehicle time. A total of six models were estimated: a home-based work model (includes trip types HBWD, HBWS, HBWC, and AIR), an ED1 model, an ED2 model, a HNWR model, a HNWO model, and a non-home-based model (includes NHBW and NHBO).

Traffic Assignment

At this stage in the model, we have found person trip production-attraction tables. These are converted to vehicle trip origin-destination tables using simple factors as is rather standard in 4-step TDMs. For home-based trips (which includes HBWD, HBWS, HBWC, HNWR, HNWO, ED1, and ED2), factors were computed using trip survey data to convert aggregate trip production-attractions to time-of-day (TOD) specific origin-destinations. For instance, we begin with some number of production-attractions from zone A to zone B. Those are converted into origin-destinations from zone A to zone B and zone B to zone A for each of 4 TODs (AM peak [AM], midday [MID], off-peak [OP], and PM peak [PM]) using factors calibrated from the survey data. In addition, the person trips are divided by the average vehicle occupancy to find vehicle trips. All of the factors are trip type specific (i.e., they are different for each trip type). For NHBW, NHBO, and AIR trips, similar factors are used, but half of all trips produced in zone A and attracted to zone B are assumed to originate in zone A, destined for zone B while the other half are assumed to originate in zone B, destined for zone A. It is important to recognize that this is an INCORRECT way to do this. Non-home-based trips are, by definition, in origin-destination form to begin with. Thus, there is no reason to have factors to convert the trips into origin-destination form. This problem is corrected in the modified code. Like the other trips, average vehicle occupancies are used to convert person trips to vehicle trips. (Note that in the modified code, vehicle occupancy factors were recalibrated, and it seemed that most [if not all] were greater than those used in the SM code [i.e., more persons per vehicle]. It is unclear how SM calibrated their factors)

Once person trip production-attraction tables are converted to TOD specific vehicle trip origin-destination tables, the traffic assignment module is executed. The SM code uses a rather simplistic traffic assignment routine. It does not use generalized time/cost, but instead only considers travel times, while travel costs are ignored (this is modified in the new code). The BPR link performance functions are used with alpha of 0.83 and beta of 5.5 (note that these are typical values), and the routine is performed for each of the 4 TODs. After performing traffic assignment, we now have link travel times for each of the 4 TODs.

Model Feedback

There are a couple of key considerations for the model feedback. First, we have new travel times given from the output of traffic assignment, but it is bad practice to simply input the new travel times directly upstream in the trip distribution model (convergence cannot be insured if this is done). Second, the trip distribution and mode choice sub-models are not specific to TODs, but are instead aggregate totals for the average day. Thus, we must convert the TOD specific travel times to a single travel time, and we must somehow average travel times from iteration to iteration.

First, the TOD specific travel times are converted to a single travel time using TOD specific factors for each trip type. The factors were again calibrated from the trip survey data. The best way to convey how it works is with example. Say we have travel times for the 4 TODs, and say that in the survey data for HBWD trips, 30% of trips are from production (P) zone to attraction (A) zone in AM, 1% are from A zone to P zone in AM, 10% are from P to A in MID, 10% are

from A to P in MID, 6% are from P to A in OP, 5% are from A to P in OP, 8% are from P to A in PM, and 30% are from A to P in PM. Then a weighted sum of the travel time tables is used for the HBWD travel times for this iteration. Say AM travel times are denoted AM_TT and the transpose of AM travel times is denoted AM_TTT, then the HBWD travel times = $0.3*AM_TT + 0.01*AM_TTT + 0.1*MID_TT + 0.1 *MID_TTT + 0.06*OP_TT + 0.05*OP_TTT + 0.08*PM_TT + 0.3*PM_TTT$. This same sort of procedure is executed for each of the trip types and results in a travel time table specific to each.

Second, an averaging across iterations is done to find the input travel times for the subsequent iteration. The method of successive averages is used to do this. For example, if we are currently in the 1st iteration, no averaging is performed (free-flow travel times are used as inputs in the 1st iteration). If we are currently in the 2nd iteration, we take $0.5*1^{st}$ iteration times + $0.5*2^{nd}$ iteration times. If we are in the 3rd iteration, we take $(1/3)*1^{st}$ iteration times + $(1/3)*2^{nd}$ iteration times + $(1/3)*3^{rd}$ iteration times, and so on. It is important to note that this is not the standard procedure for MSA in TDMs. Boyce *et al.* (1994) suggests that feedback should be introduced by performing 2 operations. First, the trip tables are averaged prior to traffic assignment. For example, in the 2nd iteration, traffic assignment is performed on MSA trip table where the MSA trip table is $0.5*1^{st}$ iteration trip table + $0.5*2^{nd}$ iteration trip table. Second, after traffic assignment, MSA is again performed on the link travel times before finding the zone to zone travel times. There is then NO modification needed for zone to zone travel times found using shortest path. However, the method used by SM should yield reasonable results when the network is not overall congested.

Documentation of Changes to Smart Mobility TDM

The reason for modifying the Smart Mobility (SM) TDM was mostly because the SM model does not account for travel cost, except in the mode choice module. Thus the changes made to the model lie in incorporating travel cost sensitivity into the entire model. Therefore, the main changes to the Smart Mobility TDM occur in the trip distribution and traffic assignment modules of the code. These modules were based solely on travel time (as a cost measure) in the original SM TDM. Other changes were considered, but since we were rather familiar with how the SM code worked (and had already performed some runs with the model) and the inputs required to run it, we felt it was best to use as much of the SM TDM as possible while allowing for travel cost sensitivity in a reasonable way.

Trip Distribution

The trip distribution module of the SM model used gravity type models for each trip type based on travel time from zone to zone and number of productions and attractions as modeled in the trip generation phase. The new model instead employs destination choice models for each trip type. Instead of explicitly using employment numbers for each destination zone to model the attractiveness of the zone, the SM trip attractions models were used to compute the total number of attractions for each destination zone, and those values were used as explanatory values in the destination choice model estimation procedure. In addition, a generalized cost term was generated for each alternative and consisted of a weighted sum of zone to zone travel time and cost where the weight on cost was 1.0, and the weight on travel time equaled the value of travel

time (VOTT) for the trip type. For model estimation, the chosen zone alternative was considered along with 50 randomly generated other zone alternatives.

Assumptions for the trip distribution include many things. For work trips and airport trips, VOTT was assumed to be \$9/hr (\$0.15/min), and for non-work trips, VOTT was assumed to be \$4.50/hr (\$0.075/min), both consistent with assumptions of VOTT in SM's mode choice models. Also consistent with SM was the assumption of \$0.0922/mile operating cost. The operating cost was divided by the average vehicle occupancy for the particular trip type to generate zone to zone costs (this also applies in model application). Travel time and mileage data for zone to zone come from CAMPO estimates, which consist of both peak and off-peak travel skims. Factors were developed for each trip type for average departure TOD and average return TOD. These factors were then applied to the travel time skims in generating zone to zone travel times/costs for each alternative. In application, 4 TODs exist, and thus, factors were developed for each of the 4 TODs even though only peak and off-peak base travel times/costs were available from CAMPO. For non-home-based trips, return factors are always zero since the trip productions/attractions are equivalent to origins/destinations.

Traffic Assignment

In the TDM code, the traffic assignment module had to be changed since the simple traffic assignment module used by TransCAD only considers travel time. Instead, the multi-modal, multi-user-class assignment (MMA) module was used to allow for flexibility if needed in the future, and to allow for variation in passenger car equivalents (PCEs) and VOTTs. However, because the MMA assignment takes a long time to perform and because MMA does not allow for the congestion pricing mechanism to be entered properly (given the way congestion pricing is considered in the code), only one user class is considered in assignment, with all of the vehicle trips added together. The inconsistency with congestion pricing occurs in the way the code inputs congestion pricing. Since the congestion charge is a function of volume and varies in the same function form as travel time (the BPR function), congestion charges are recognized by elevating the normal Alpha parameter of 0.83 to $5.395 = \text{Alpha} * (\text{Beta} + 1) = 0.83 * (5.5 + 1)$. Thus, the assignment operation allows for a consistent representation of what the congestion charge is. However, since TransCAD does not recognize that part of this is travel time and part is monetary cost, VOTT's cannot be applied consistently for work and non-work trips. Thus, only one user group is considered with passenger car equivalent (PCE) of 1.0, and VOTT of \$0.1125/min (\$6.75/hr), which is the average of work and non-work VOTTs. Based on the travel survey, about 45% of trips were work and 55% non-work, but after recognizing truck and external trips (which are both assumed to have work VOTT), it was felt that a straight average was reasonable.

Tables

Table C.1. Time-of-Day & Departure/Return Factors by Trip Type using CAMPO’s Expansion Factors

Trip Type		Time-of-Day			
		AM	MID	OP	PM
Home-Based Work (Direct)	Depart	0.2864	0.1062	0.0719	0.0330
	Return	0.0065	0.1206	0.0407	0.3347
Home-Based Work (Strategic)	Depart	0.4685	0.0524	0.0262	0.0014
	Return	0.0016	0.1187	0.0078	0.3234
Home-Based Work (Complex)	Depart	0.4572	0.1201	0.0662	0.0231
	Return	0.0021	0.0817	0.0426	0.2069
Home-Based Non-Work Retail	Depart	0.0385	0.1920	0.0198	0.1276
	Return	0.0092	0.3345	0.0470	0.2313
Home-Based Non-Work Other	Depart	0.1017	0.2024	0.0304	0.1701
	Return	0.0335	0.2086	0.1034	0.1499
Non-Home-Based Work	Depart	0.0753	0.6410	0.0097	0.2739
	Return	0.0000	0.0000	0.0000	0.0000
Non-Home-Based Other	Depart	0.0774	0.5409	0.0597	0.3219
	Return	0.0000	0.0000	0.0000	0.0000
Home-Based Education1 (K-12)	Depart	0.5255	0.0193	0.0068	0.0035
	Return	0.0017	0.1093	0.0000	0.3338
Home-Based Education2 (Post-Secondary/College)	Depart	0.2016	0.2753	0.0000	0.0401
	Return	0.0192	0.2205	0.0564	0.1868
Airport	Depart	0.0820	0.2897	0.0900	0.0465
	Return	0.0752	0.2141	0.0776	0.1251

Table C.2. Average Vehicle Occupancy by Trip Type using CAMPO's Expansion Factors

Trip Type	Average Vehicle Occupancy
Home-Based Work (Direct)	1.1247
Home-Based Work (Strategic)	1.4426
Home-Based Work (Complex)	1.1828
Home-Based Non-Work Retail	1.6391
Home-Based Non-Work Other	1.9571
Non-Home-Based Work	1.3141
Non-Home-Based Other	1.9774
Home-Based Education1 (K-12)	2.7258
Home-Based Education2 (Post-Secondary/College)	1.2719
Airport	1.9675

Table C.3. Destination Choice Model Estimation Results by Trip Type (Work trip types)

		Home-Based Work (Direct)	Home-Based Work (Strategic)	Home-Based Work (Complex)	Non-Home-Based Work
Generalized Cost Variable	Coefficient	-0.3753	-0.2806	-0.3071	-0.6597
	t-stat	-37.69	-12.73	-17.23	-38.95
Number of Destination Zone Attractions	Coefficient	0.000198	0.000212	0.000228	0.000166
	t-stat	39.34	18.02	24.91	24.50
Number of Observations		2,226	359	609	1,800
Log Likelihood at Convergence		-6,644.4	-1,114.8	-1,806.2	-4,885.7
Likelihood Ratio		4,215.7	593.5	1,176.6	4,383.1
Pseudo R-Squared		0.241	0.210	0.246	0.310

Table C.4. Destination Choice Model Estimation Results by Trip Type (Non-Work trip types)

		Home-Based Non-Work Retail	Home-Based Non-Work Other	Non-Home- Based Other	Home- Based Education1 (K-12)	Home-Based Education2 (Post- Secondary/College)
Generalized Cost Variable	Coefficient	-1.6284	-1.2572	-1.4140	-1.7223	-0.7130
	t-stat	-42.16	-67.63	-53.00	-37.77	-9.65
Number of Destination Zone Attractions	Coefficient	0.000119	0.000264	0.000141	0.000181	0.000222
	t-stat	29.06	32.25	31.99	20.27	17.80
Number of Observations		1,543	4,307	2,762	1,052	260
Log Likelihood at Convergence		-3,322.1	-11,417.7	-6,937.7	-2,232.8	-451.8
Likelihood Ratio		5,489.4	11,033.4	7,843.9	3,807.1	1,140.9
Pseudo R-Squared		0.452	0.326	0.361	0.460	0.558

Appendix D. Additional Details in the Travel Demand Model

In personal trip generation, trip production is determined by the number of households by type, including vehicle availability. The cross-tabulation of six household types (categorized by number of workers and presence of children) and three levels of vehicle availability (0, 1 and 2+ autos) results in eighteen types of household, with each assumed to generate, on average, a fixed number of trips of a given type¹⁸. In contrast, commercial travel production is determined by many zonal characteristics: the total number of households, basic jobs, retail jobs, service jobs, education (ED1 and ED2) jobs in a TAZ and the TAZ’s area type (determined by the square root of intersections per square mile). Table D.1 gives the trip production rates for truck flows.

Table D.1. Commercial Trip Generation Rates

	Total Households	Basic Employment	Retail Employment	Service Employment	ED1 Employment	ED2 Employment
Rural	0.253	0.554	0.361	0.398	0.399	0.166
Suburban	0.253	0.471	0.344	0.416	0.399	0.166
Urban	0.225	0.271	0.328	0.198	0.399	0.166

Attraction rates for personal trips are determined by the numbers of households and employment by type for each zone. In contrast, commercial trip attraction is assumed to equal commercial trip production in each zone. A gravity model was then applied to distribute the truck flows, and the trip distribution was later added to the trip matrix in assignment.

As compared to trucks, transit vehicles (or buses) are not loaded in assignment. Evidently, Smart Mobility’s TDM considers the impacts of buses on network congestion to be negligible.

¹⁸ The TDM considers ten trip types: home-based work direct (HBWD), home-based work complex (HBWC), home-based work strategic (HBWS), home-based non-work retail (HNWR), home-based non-work other (HNWO), non-home-based work (NHBW), non-home-based other (NHBO), K-12 education (ED1), post-secondary/college education (ED2), and airport (AIR).

Appendix E. G-LUM Documentation: Model Formulation, Calibration and Application

Household Allocation (RESLOC)

$$N_{i,t}^n = \eta^n \sum_j Q_{j,t}^n B_{j,t-1}^n W_{i,t-1}^n c_{i,j,t-1}^{\alpha^n} \exp(\beta^n c_{i,j,t-1}) + (1 - \eta^n) N_{i,t-1}^n \quad (\text{E.1})$$

where

$$Q_{j,t}^n = \sum_k a_{k,n} \frac{E_{j,t}^k}{1 - u_k} \quad (\text{E.2})$$

$$B_{j,t-1}^n = \left[\sum_i W_{i,t-1}^n c_{i,j,t-1}^{\alpha^n} \exp(\beta^n c_{i,j,t-1}) \right]^{-1} \quad (\text{E.3})$$

$$W_{i,t-1}^n = (L_{i,t-1}^v)^{q^n} (1 + x_{i,t-1})^{r^n} (L_{i,t-1}^r)^{s^n} \prod_{n'} \left[\left(1 + \frac{N_{i,t-1}^{n'}}{\sum_n N_{i,t-1}^n} \right)^{b_{n'}^n} \right] \quad (\text{E.4})$$

and where $N_{i,t}^n$ is the number of households of type n residing in zone i at time t ; $c_{i,j,t-1}$ is impedance (travel time and/or cost) between zones i and j at time $t-1$; $a_{k,n}$ is the number of type n households per type k employee in the study region; $E_{j,t}^k$ is employment (number of jobs) of type k in zone j at time t ; u_k is the unemployment rate for job type k ; $L_{i,t-1}^v$ is vacant developable land in zone i at time $t-1$; $x_{i,t-1}$ is the proportion of developable land already developed in zone i at time $t-1$; $L_{i,t-1}^r$ is residential land in zone i at time $t-1$; and $\eta^n, \alpha^n, \beta^n, q^n, r^n, s^n$ and b_n^n are parameters estimated in model calibration. $Q_{j,t}^n$ converts employment to households, $B_{j,t-1}^n$ is a balancing factor, and $W_{i,t-1}^n$ represents the attractiveness of zone i for household type n at time $t-1$.

Employment Allocation (EMPLOC)

$$E_{j,t}^k = \lambda^k \sum_i N_{T,i,t-1} A_{i,t-1}^k M_{j,t-1}^k c_{i,j,t-1}^{\omega^k} \exp(\rho^k c_{i,j,t-1}) + (1 - \lambda^k) E_{j,t-1}^k \quad (\text{E.5})$$

where

$$A_{i,t-1}^k = \left[\sum_j (E_{j,t-1}^k)^{a^k} (L_j)^{b^k} c_{i,j,t-1}^{\omega^k} \exp(\rho^k c_{i,j,t-1}) \right]^{-1} \quad (\text{E.6})$$

$$M_{j,t-1}^k = (E_{j,t-1}^k)^{a^k} (L_j)^{b^k} \quad (\text{E.7})$$

and $N_{T,i,t-1}$ is total households in zone i at time $t-1$; L_j is the total area of zone j ; and $\lambda^k, \omega^k, \rho^k, a^k$ and b^k are estimated during model calibration. $A_{i,t-1}^k$ is a balancing factor, and $M_{j,t-1}^k$ represents the attractiveness of zone j for employment type k at time $t-1$.

Land Consumption Rates (LU DENSITY)

$$\frac{L_{r,i,t}}{N_{T,i,t}} = k_0 L_{D,i,t-1}^{k_1} \left(\frac{L_{d,i,t-1}}{L_{D,i,t-1}} \right)^{k_2} \left(\frac{L_{b,i,t-1}}{L_{D,i,t-1}} \right)^{k_3} \left(\frac{L_{c,i,t-1}}{L_{D,i,t-1}} \right)^{k_4} * \left(\frac{N_{1,i,t}}{N_{T,i,t}} \right)^{k_5} \left(\frac{N_{2,i,t}}{N_{T,i,t}} \right)^{k_6} \left(\frac{N_{3,i,t}}{N_{T,i,t}} \right)^{k_7} \left(\frac{N_{4,i,t}}{N_{T,i,t}} \right)^{k_8} \left(\frac{N_{5,i,t}}{N_{T,i,t}} \right)^{k_9} \left(\frac{N_{6,i,t}}{N_{T,i,t}} \right)^{k_{10}} \quad (\text{E.8})$$

Error! Bookmark not defined.
$$\frac{L_{b,i,t}}{E_{b,i,t}} = g_0 L_{D,i,t-1}^{g_1} \left(\frac{L_{d,i,t-1}}{L_{D,i,t-1}} \right)^{g_2} \left(\frac{E_{b,i,t}}{E_{T,i,t}} \right)^{g_3} \left(\frac{L_{b,i,t-1}}{L_{D,i,t-1}} \right)^{g_4} \left(\frac{L_{r,i,t-1}}{L_{D,i,t-1}} \right)^{g_5} \quad (\text{E.9})$$

$$\frac{L_{c,i,t}}{E_{c,i,t}} = p_0 L_{D,i,t}^{p_1} \left(\frac{L_{d,i,t}}{L_{D,i,t}} \right)^{p_2} \left(\frac{E_{c,i,t}}{E_{T,i,t}} \right)^{p_3} \left(\frac{L_{c,i,t}}{L_{D,i,t}} \right)^{p_4} \left(\frac{L_{r,i,t}}{L_{D,i,t}} \right)^{p_5} \quad (\text{E.10})$$

where L stands for area of land in each use (r = residential, D = developable, d = developed, b = basic, c = commercial; E stands for employment (b =basic, c =commercial, including retail and service jobs); and the k 's, g 's and p 's are estimated parameters.

Table E.1. Calibration Results for the RESLOC

	η		α		β		q		r		s	
	Coef.	t-stat.	Coef.	t-stat.	Coef.	t-stat.	Coef.	t-stat.	Coef.	t-stat.	Coef.	t-stat.
Type I Households	0.0317	2.94	-2.07	-4.32	-0.0232	-0.55	1.20	1.97	4.82	0.83	0.566	5.18
Type II Households	0.0665	12.34	-1.19	-3.07	-0.0396	-1.81	0.530	4.45	0.371	0.42	0.0342	1.10
Type III Households	0.0747	11.33	-0.772	-1.55	-0.0509	-1.93	0.622	4.87	1.54	1.78	0.0103	0.25
Type IV Households	0.0264	5.83	2.73	1.08	-0.2281	-1.89	0.954	2.10	0.631	0.14	0.312	2.55
Type V Households	0.0467	11.16	51.14	1.20	-7.92	-1.19	0.724	2.67	2.43	1.10	0.0227	0.57
Type VI Households	0.0615	10.27	-1.14	-2.13	-0.0640	-2.02	0.611	3.39	-0.882	-0.64	0.157	1.71
	b_1^n		b_2^n		b_3^n		b_4^n		b_5^n		b_6^n	
	Coef.	t-stat.	Coef.	t-stat.	Coef.	t-stat.	Coef.	t-stat.	Coef.	t-stat.	Coef.	t-stat.
Type I Households	80.02	1.89	-1.69	-0.05	-11.92	-0.48	0.234	0.01	-8.18	-0.27	0.0233	0.00
Type II Households	6.29	1.18	6.41	1.16	9.45	1.67	0.345	0.07	4.32	0.75	0.962	0.19
Type III Households	4.13	0.60	-3.13	-0.44	8.98	1.02	-2.10	-0.26	0.0218	0.00	-2.15	-0.29
Type IV Households	40.09	1.21	-1.31	-0.03	-11.08	-0.34	6.32	0.15	-9.87	-0.26	-0.317	-0.01
Type V Households	2.12	0.21	-1.08	-0.15	-2.33	-0.28	-9.49	-1.37	2.35	0.24	-3.68	-0.44
Type VI Households	20.20	1.51	-11.16	-1.84	-4.76	-0.73	-9.30	-1.52	-7.24	-1.08	-3.59	-0.48

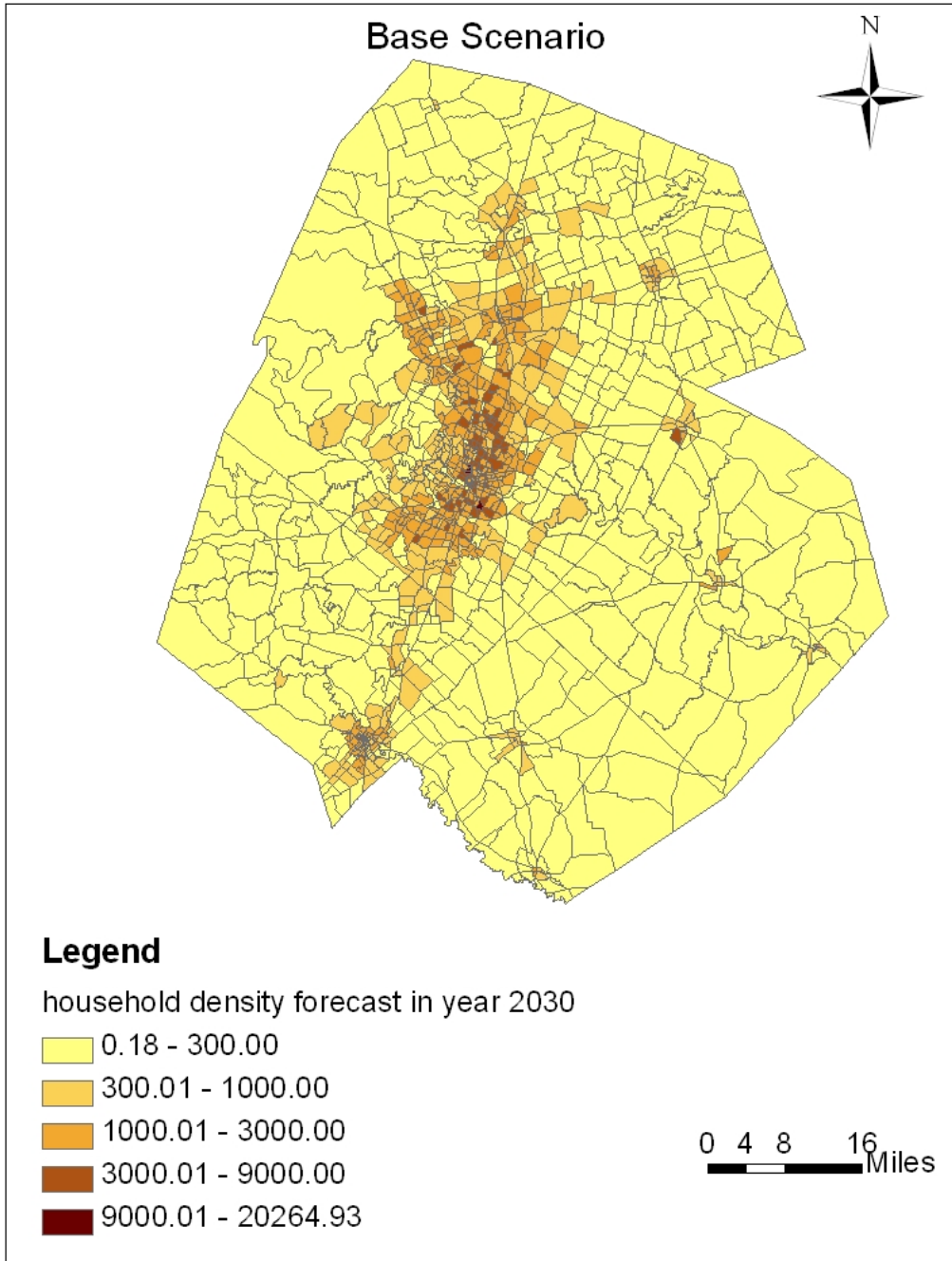
Table E.2. Calibration Results for the EMPLOC

	λ		ω		ρ		a		b	
	Coef.	t-stat.	Coef.	t-stat.	Coef.	t-stat.	Coef.	t-stat.	Coef.	t-stat.
Basic Employment	0.00713	4.13	-5.34	0.00	0.876	0.01	10.56	0.05	-16.76	-0.05
Retail Employment	0.0836	7.72	0.517	0.15	-0.253	-0.79	0.126	0.81	0.611	3.15
Service Employment	0.361	3.68	2.33	1.89	-0.126	-3.81	0.600	7.39	-0.0322	-0.33

Table E.3. Calibration Results for the LUDENSITY

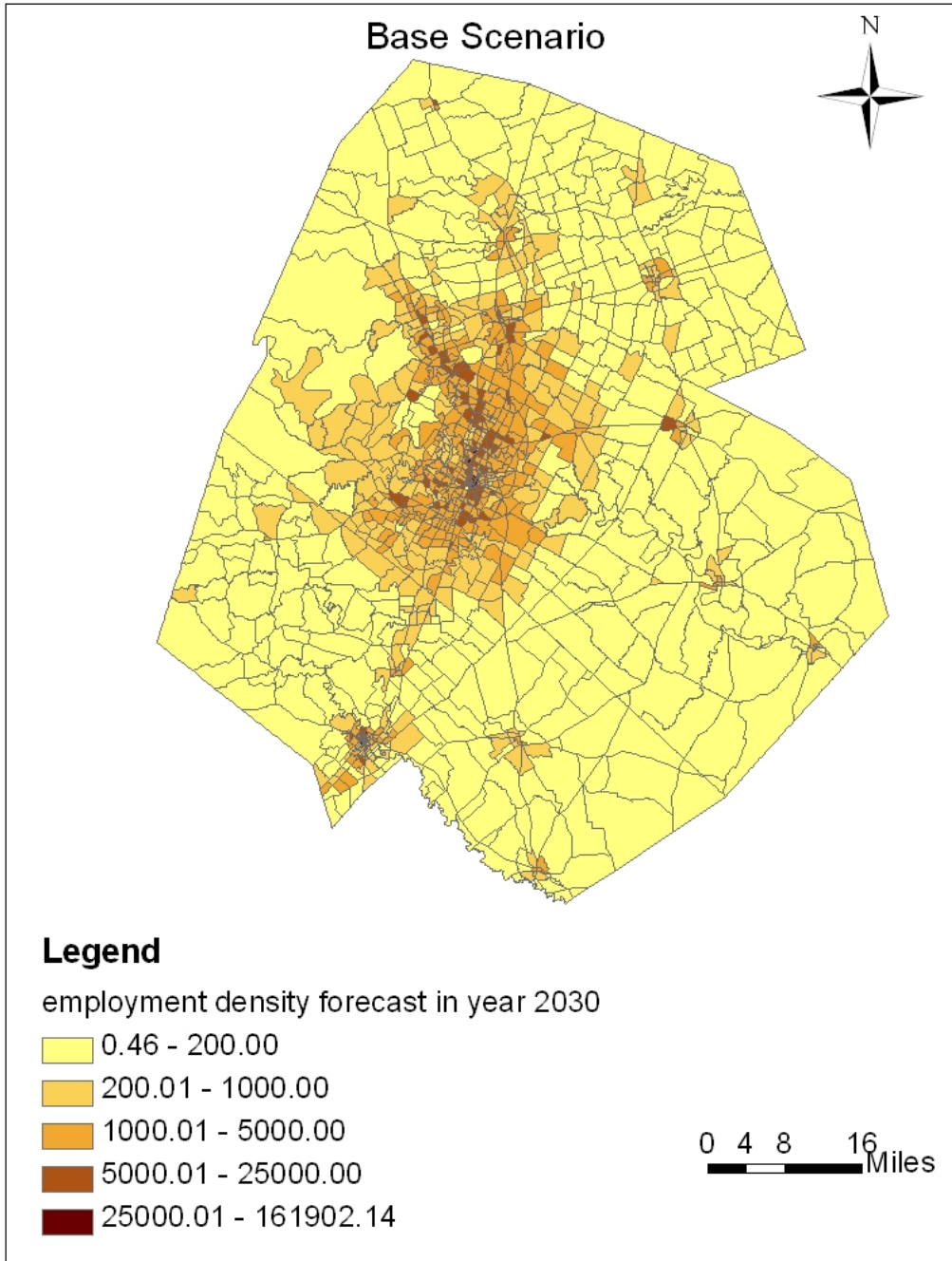
Residential	k ₀		k ₁		k ₂		k ₃		k ₄			
	Coef.	t-stat.										
	1.34	0.31	0.930	14.57	0.279	2.41	-0.0111	-1.45	-0.0481	-2.63		
	k ₅		k ₆		k ₇		k ₈		k ₉		k ₀₀	
	Coef.	t-stat.	Coef.	t-stat.								
0.423	1.46	0.00287	0.01	1.43	2.85	0.00388	0.01	0.218	0.49	3.27	3.87	
Basic Uses	g ₀		g ₁		g ₂		g ₃		g ₄		g ₅	
	Coef.	t-stat.	Coef.	t-stat.								
	0.000249	3.32	3.04	20.67	-1.06	-3.35	-2.38	-5.35	2.82	20.50	-0.00771	-0.86
Commercial Uses	p ₀		p ₁		p ₂		p ₃		p ₄		p ₅	
	Coef.	t-stat.	Coef.	t-stat.								
	0.000580	3.51	1.95	18.29	-1.07	-4.52	-1.05	-7.17	1.75	11.06	-0.0244	-1.01

Figure E.1. Distribution of Total Households for the Base Scenario



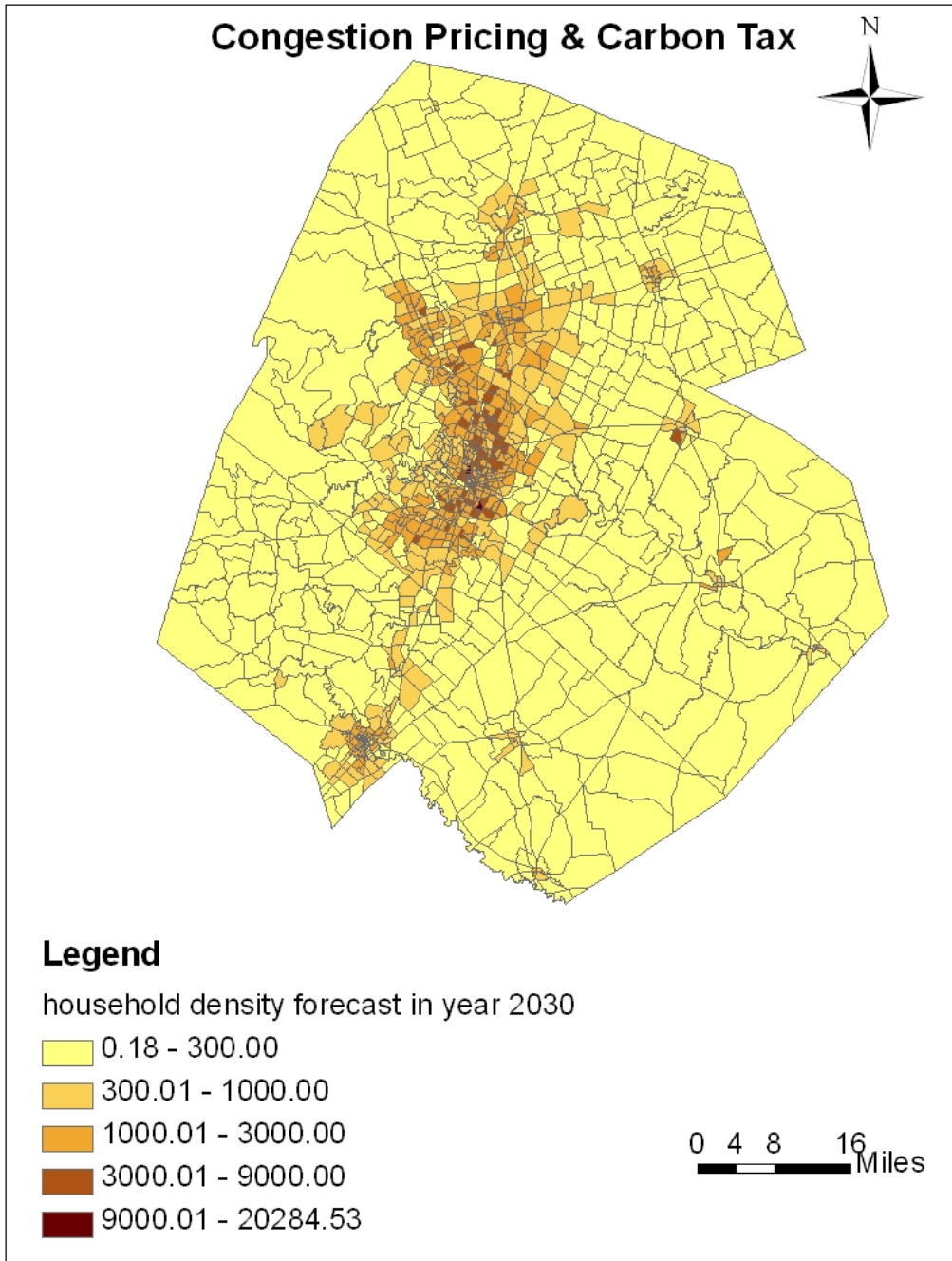
Note: unit is households/square mile

Figure E.2. Distribution of Total Employment for the Base Scenario



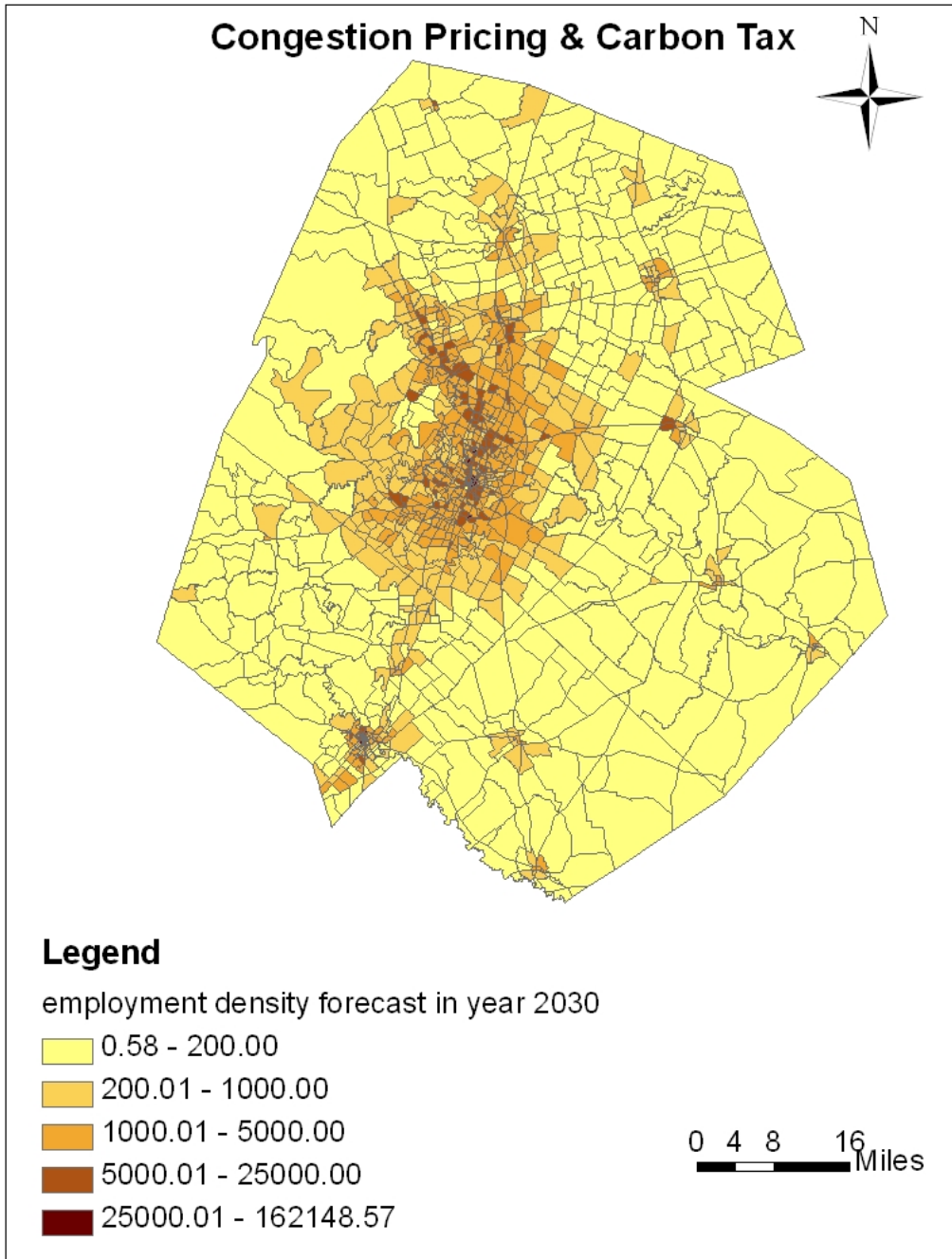
Note: unit is jobs/square mile

Figure E.3. Distribution of Total Households for the Congestion Pricing and Carbon Tax Scenario



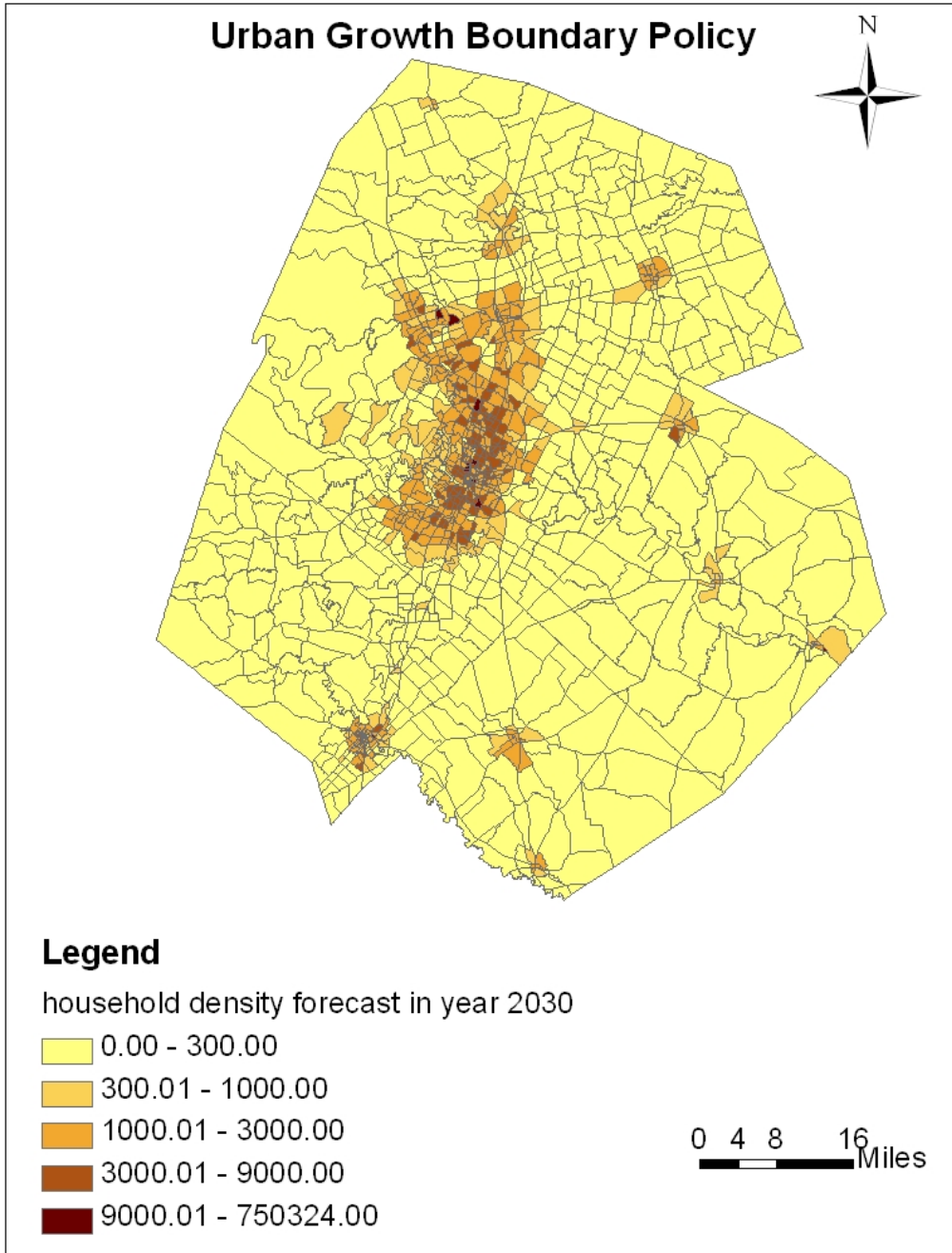
Note: unit is households/square mile

Figure E.4. Distribution of Total Employment for the Congestion Pricing and Carbon Tax Scenario



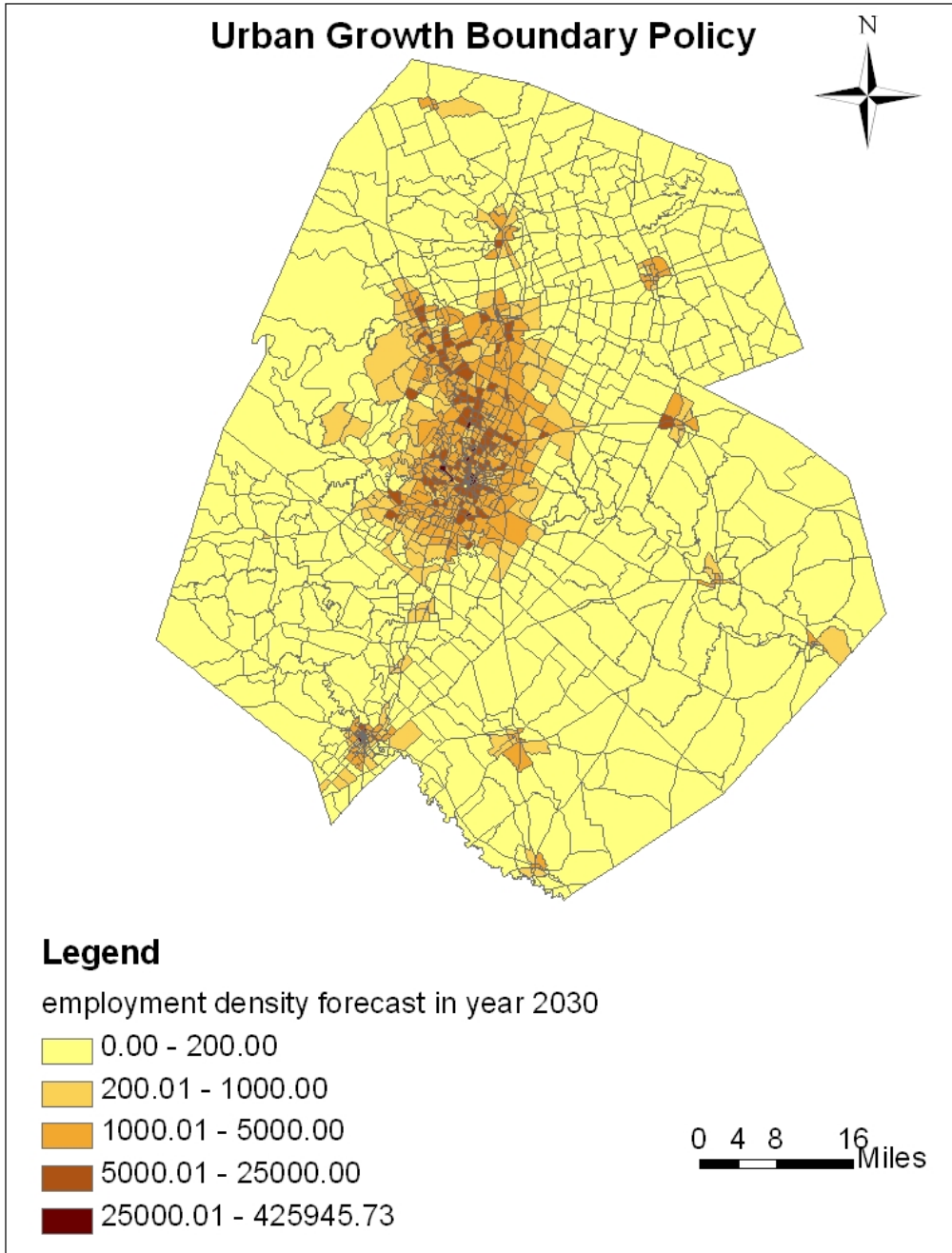
Note: unit is jobs/square mile

Figure E.5. Distribution of Total Households for the Urban Growth Boundary Policy Scenario



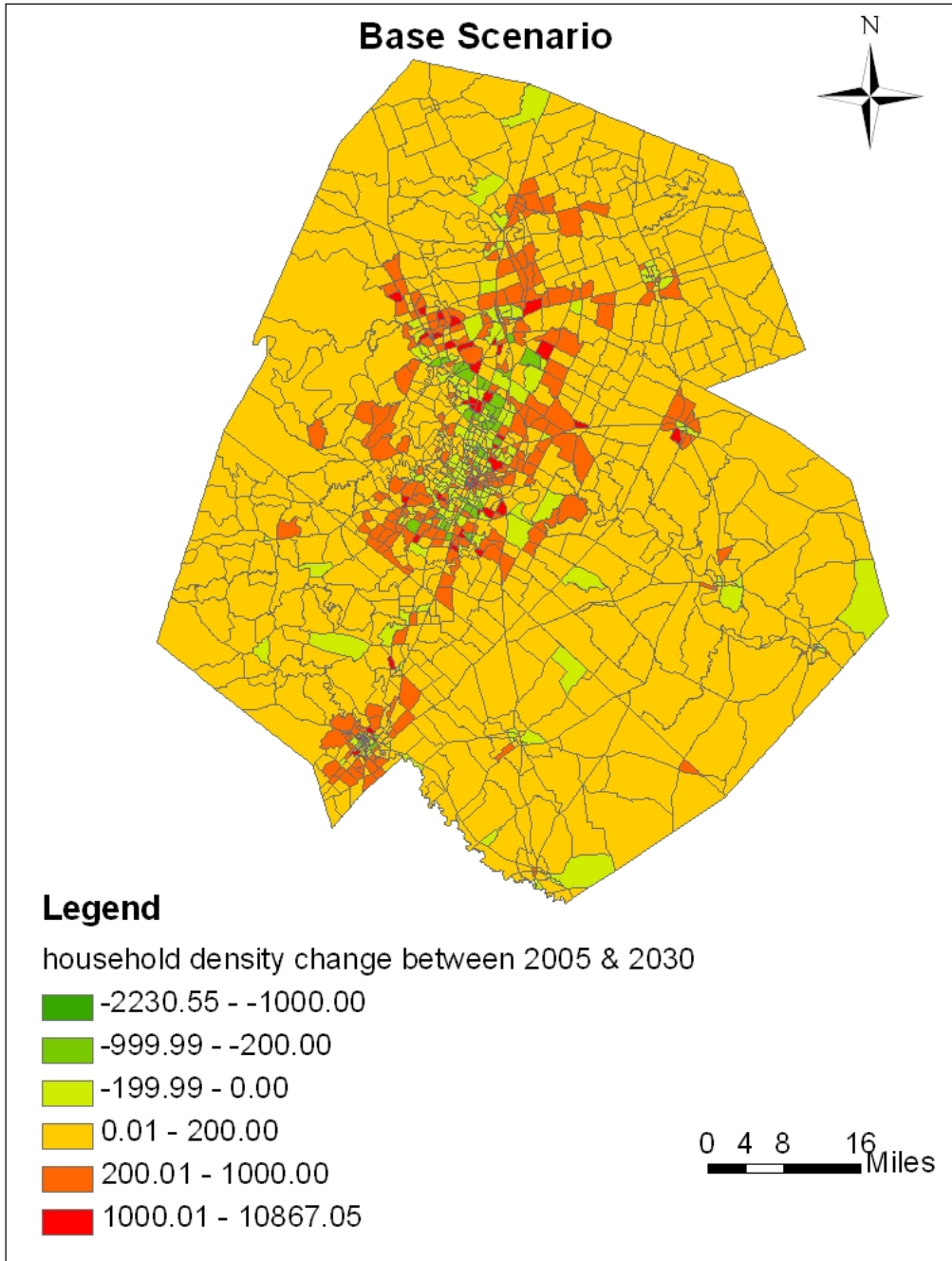
Note: unit is households/square mile

Figure E.6. Distribution of Total Employment for the Urban Growth Boundary Policy Scenario



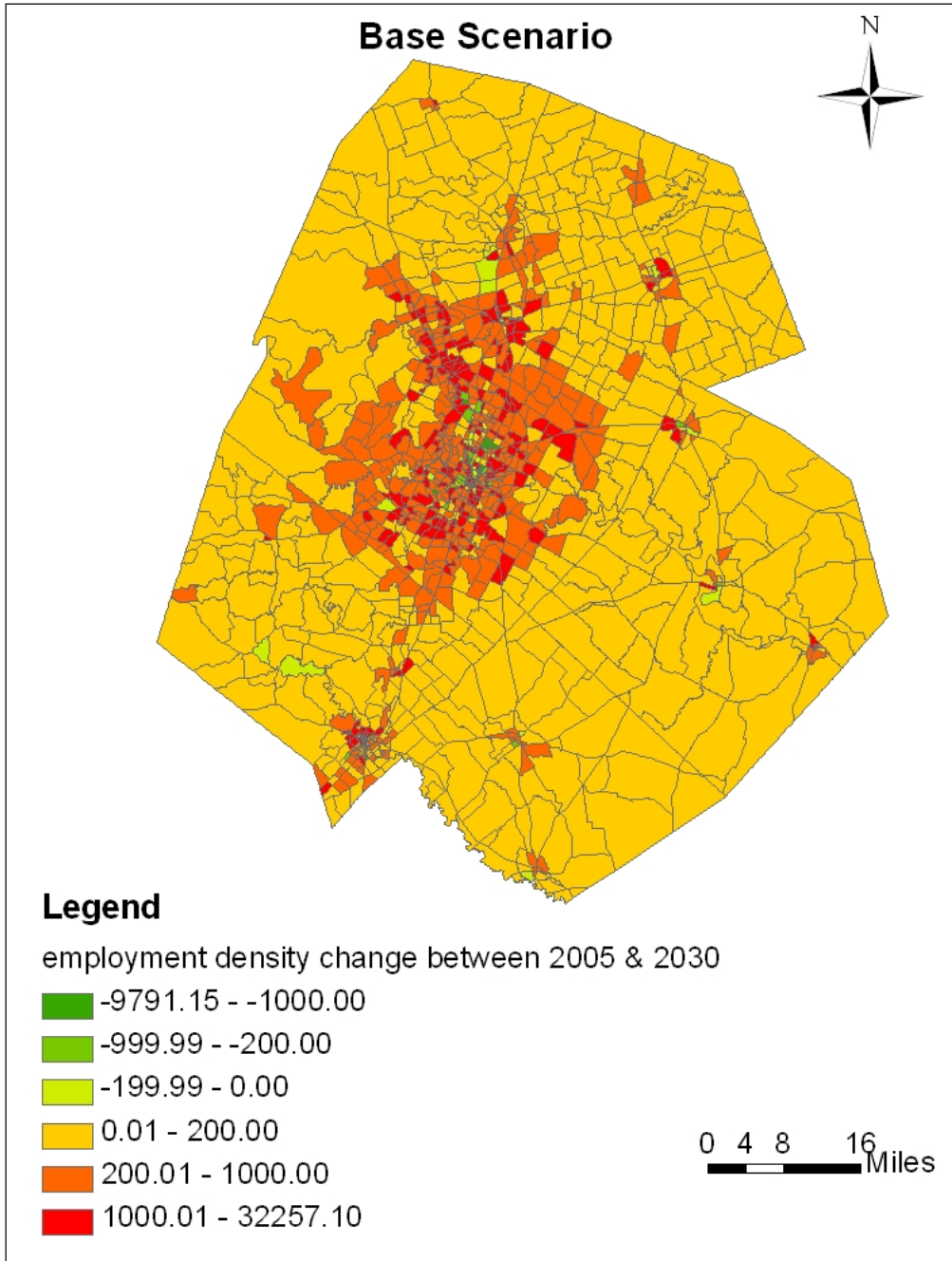
Note: unit is jobs/square mile

Figure E.7. Changes in Household Density across Zones for the Base Scenario



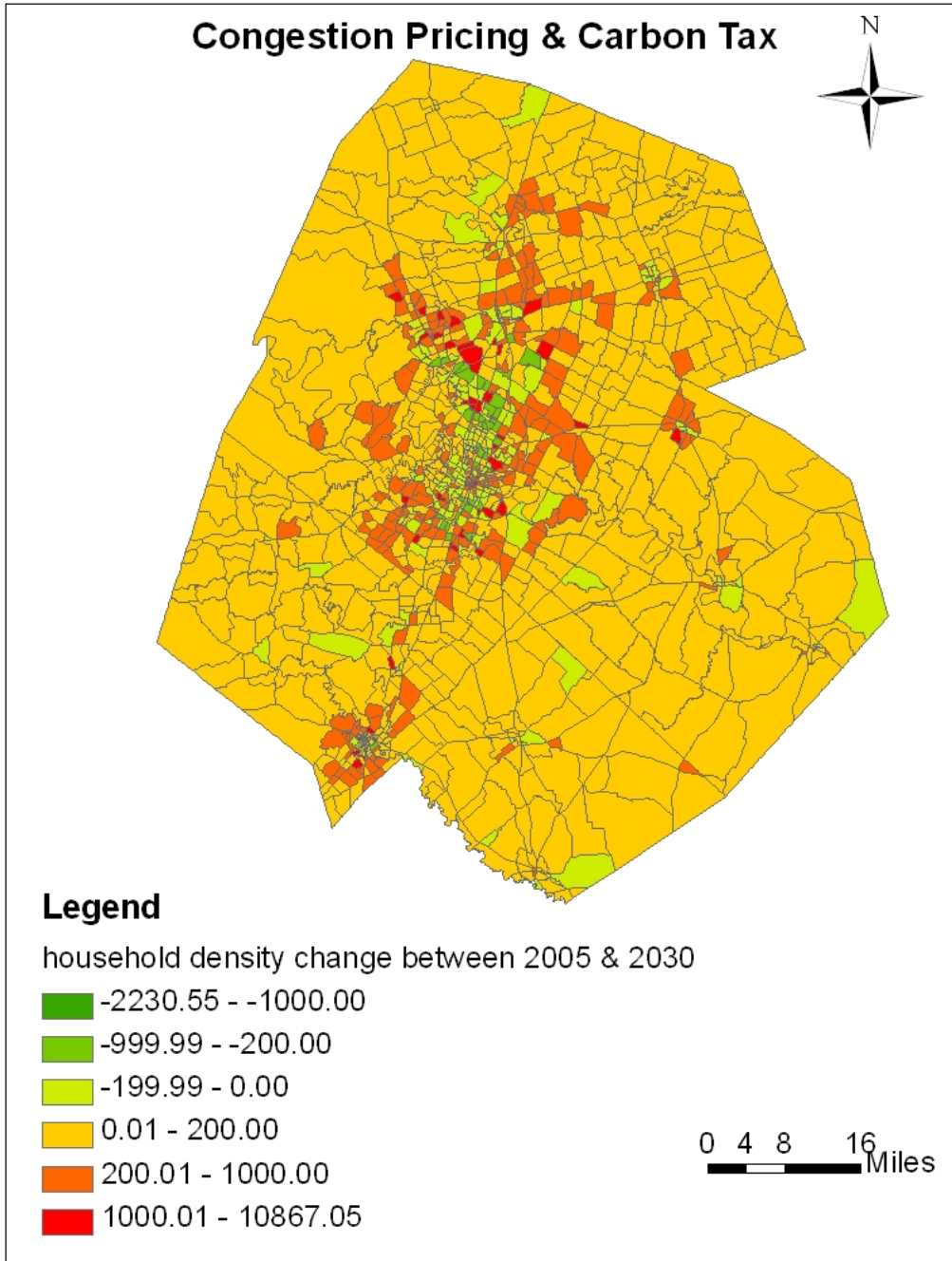
Note: unit is households/square mile

Figure E.8. Changes in Employment Density across Zones for the Base Scenario



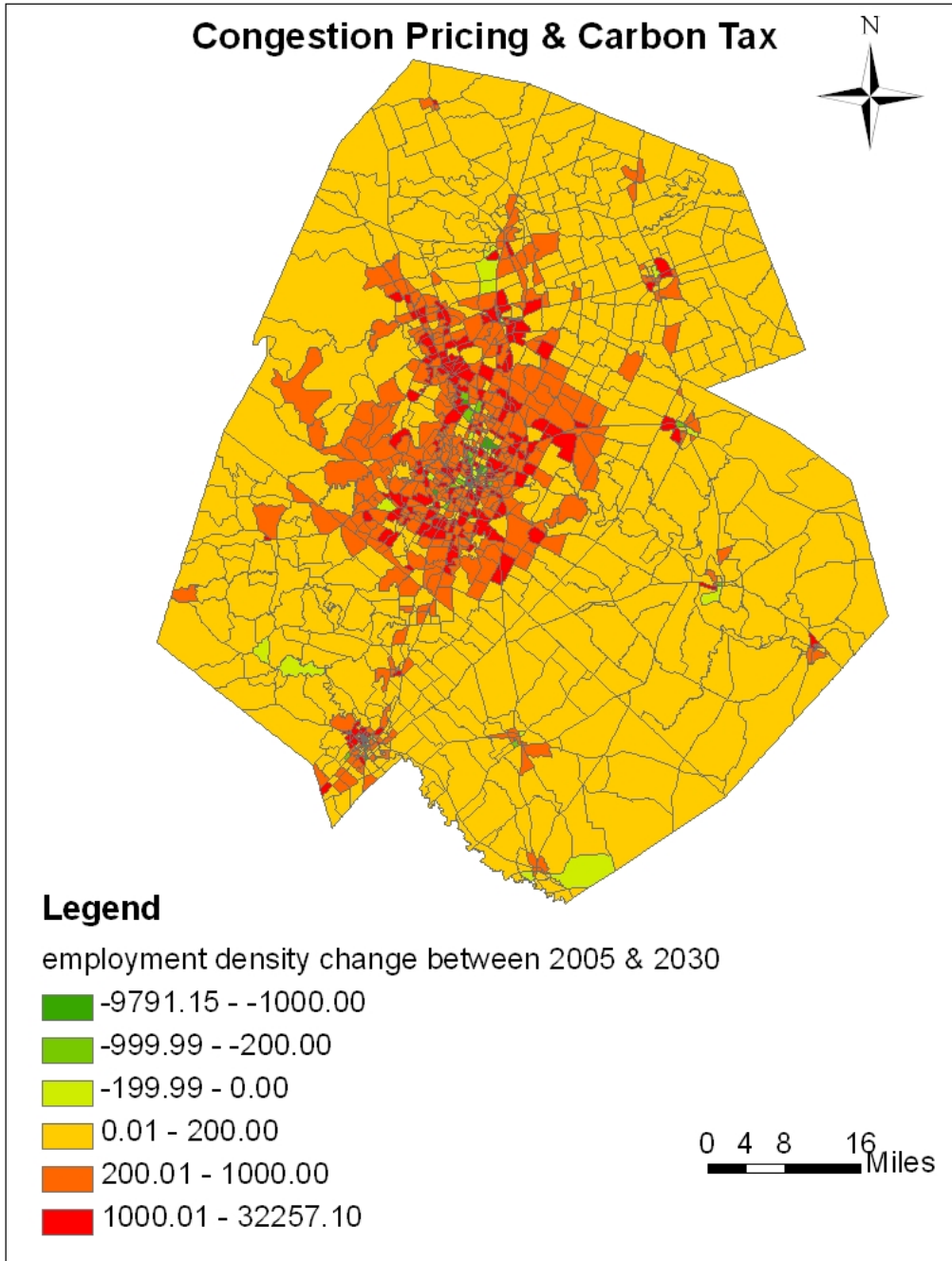
Note: unit is jobs/square mile

Figure E.9. Changes in Household Density across Zones for the Road Pricing Scenario



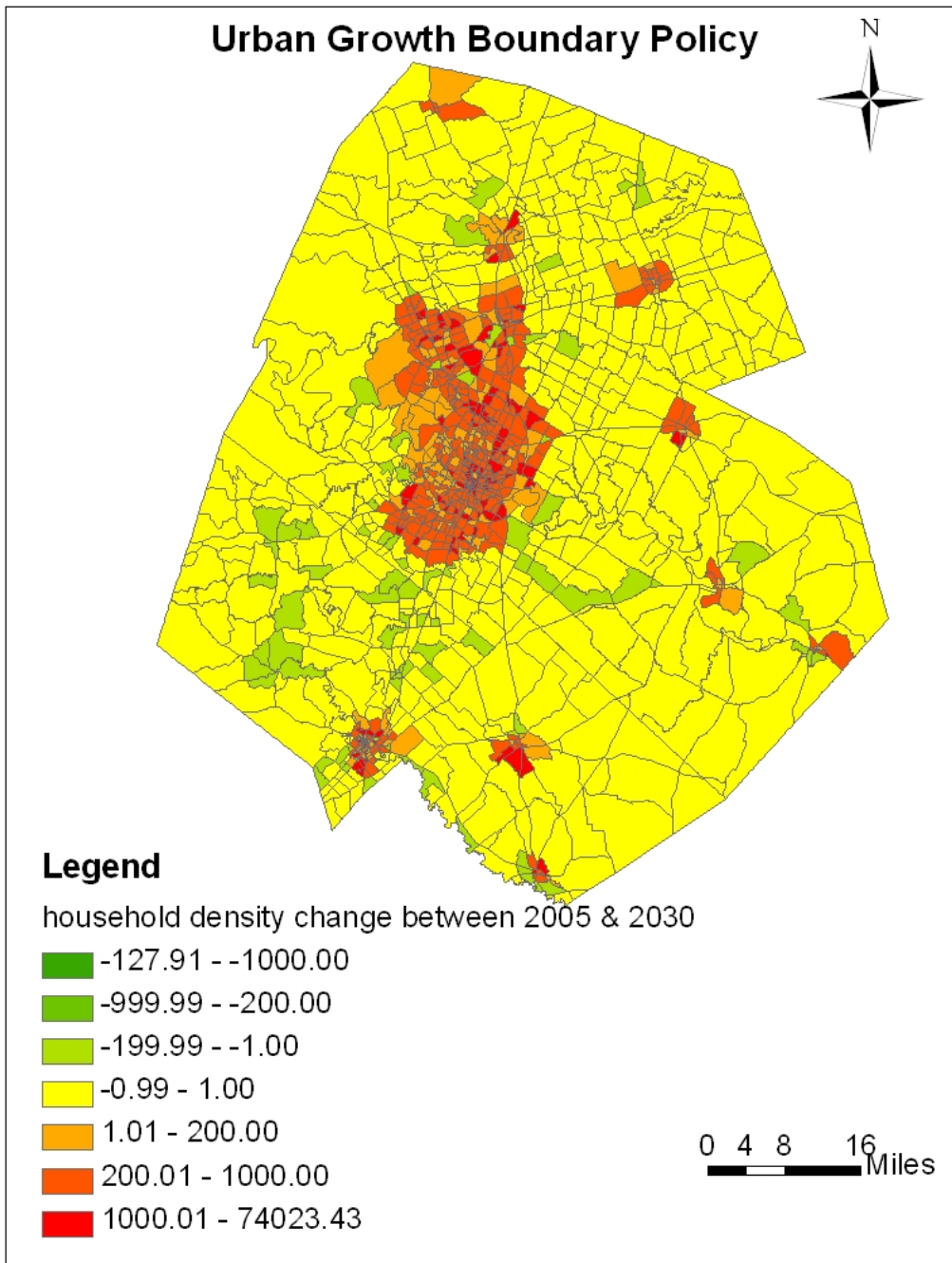
Note: unit is households/square mile

Figure E.10. Changes in Employment Density across Zones for the Road Pricing Scenario



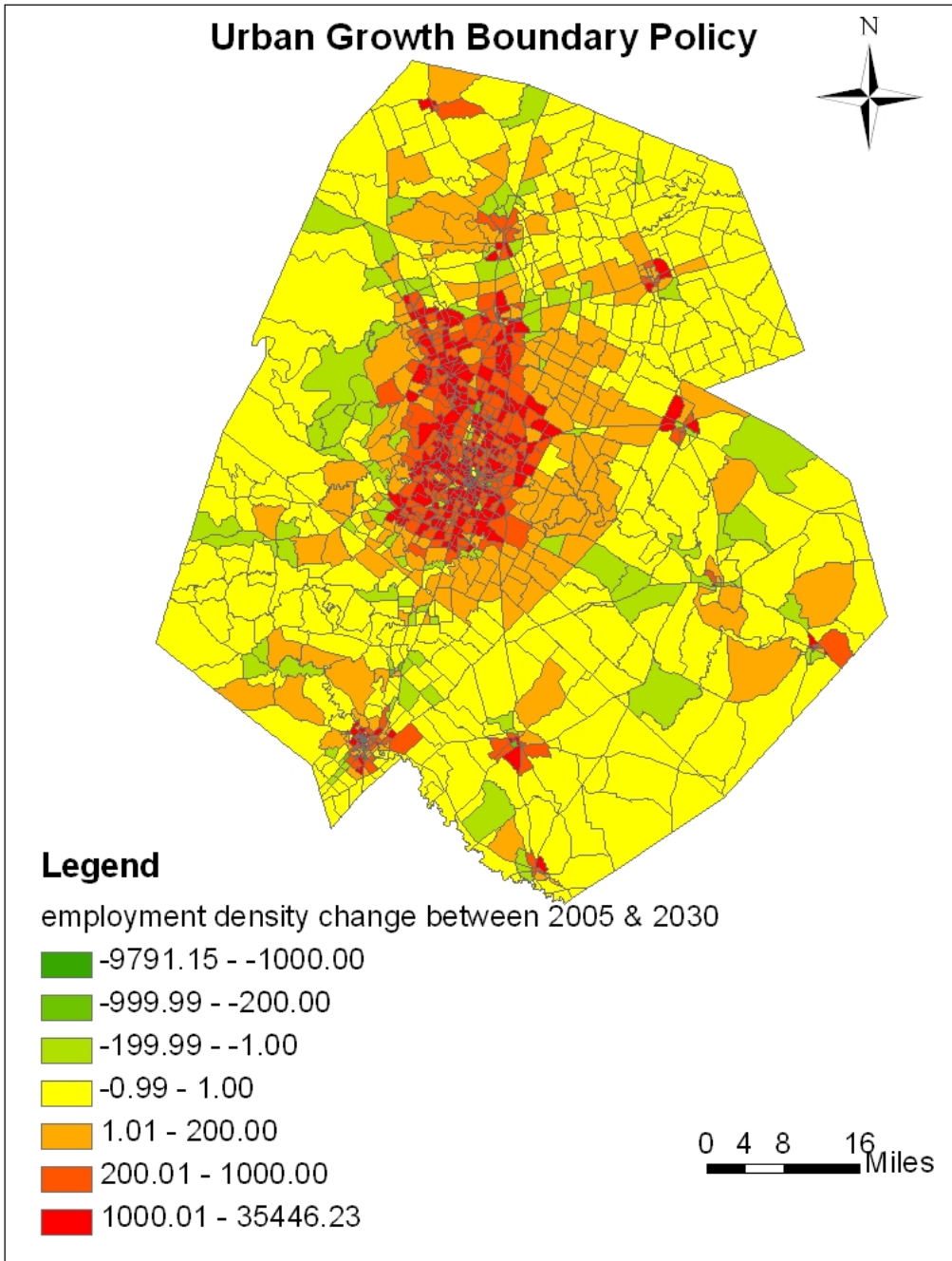
Note: unit is jobs/square mile

Figure E.11. Changes in Household Density across Zones for the Urban Growth Boundary Scenario



Note: unit is households/square mile

Figure E.12. Changes in Employment Density across Zones for the Urban Growth Boundary Scenario



Note: unit is jobs/square mile

Appendix F. LUC-LUI Model System Details: Model Calibration and Application

Table F.1. Description of Dependent Variables in the Subdivision Model

Variables	Description	Minimum	Maximum	Mean	Std. Deviation
Size	Parcel size (miles ²)	0.0000636	1.47	0.00393	0.0278
Ratio	Perimeter/area (miles/miles ²)	3.62	2294	195	94.4
Slope	Average parcel slope (%)	0	23.1	2.67	2.60
TT to CBD	Travel time to CBD under peak-hour conditions (minutes)	0.230	32.6	12.0	7.14
Dist to FWY	Euclidean distance to the nearest freeway (miles)	0	1.22	0.212	0.227
Undev1.0	Total area of undeveloped use within 1.0 mile of the parcel centroid (mile ²)	0.0165	3.04	0.912	0.540

Table F.2. Results of the Binomial Logistic Subdivision Model

Explanatory Variables	Coefficient	t-statistics
Constants	-0.256	-0.860
Size	10.8	6.23
Ratio	-166	-11.8
Slope	-0.0838	-2.11
TT to CBD	0.0730	3.98
Dist to FWY	-1.43	-2.40
Undev1.0	-1.70	-7.45
Log Likelihoods	-510.2	
LRI	0.391	
Number of observations	12,015	

Note: y=1 if parcel subdivides and 0 otherwise.

Table F.3. Description of Dependent Variables in the Parcel Size Model

Variables	Description	Minimum	Maximum	Mean	Std. Deviation
OrigSize	Size of the original, un-divided parcel (capped at 0.35 miles ²);	0.000465	0.350	0.188	0.141
Ratio	Perimeter/area (miles/ miles ²)	3.62	234	24.1	23.6
Accessibility	Regional accessibility under peak-hour conditions	1.11	4.70	3.21	0.735
Dist to FWY	Euclidean distance to the nearest freeway (capped at 1.2 miles)	0.00758	1.20	0.347	0.217
Indus0.5	Total area of industrial land use within 0.5 mile of the parcel centroid (mile ²)	0	0.359	0.0139	0.0425
Indus0.5-1.0	Total area of industrial use within 0.5 to 1.0 mile of the parcel centroid (mile ²)	0	0.775	0.0527	0.114
Civic0.5	Total area of civic land use within 0.5 mile of the parcel centroid (mile ²)	0	0.374	0.0138	0.0265
Civic0.5-1.0	Total area of civic use within 0.5 to 1.0 mile of the parcel centroid (mile ²)	0	0.560	0.0602	0.0727
Undev0.5	Total area of undeveloped land use within 0.5 mile of the parcel centroid (mile ²)	0.00448	0.783	0.424	0.207

Table F.4. Results of the Parcel Size Model

Explanatory Variables	Coefficient	t-statistics
Constants	-5.49	-23.4
OrigSize	7.77	6.37
OrigSize ²	-18.4	-6.52
Ratio	-51.1	-5.63
Accessibility	-0.274	-5.03
Dist to FWY	-6.73	-14.9
Dist to FWY ²	6.79	13.5
Indus0.5	3.93	3.82
Indus0.5-1.0	1.01	2.56
Civic0.5	-6.74	-4.98
Civic0.5-1.0	2.00	3.85
Undev0.5	0.656	3.13
R ²	0.225	
Number of observations	2,388	

Note: $y = \ln(\text{size of new parcels})$.

Table F.5. Description of Dependent Variables in Land Use Change Model

Variables	Description	Minimum	Maximum	Mean	Std. Deviation
Size	Parcel size (mile ²)	0.0000719	0.939	0.00219	0.0124
TT to CBD	Travel time to CBD under peak-hour conditions (minutes)	0.150	25.1	11.8	5.74
Dist to FWY	Euclidean distance to the nearest freeway (miles)	0	4.68	1.15	0.852
Transit Stops	Transit Stops within 0.5 mile of the parcel centroid	0	1825	28.7	62.8
Slope	Average parcel slope (%)	0	69.3	7.52	7.48
Entropy0.5	Land use balance within 0.5 mile of the parcel centroid	0	0.773	0.341	0.139
LLSF0.5	Total area of large lot single-family land use within 0.5 mile of the parcel centroid (mile ²)	0	0.321	0.0144	0.0335
LLSF0.5-1.0	Total area of large lot single-family use within 0.5 to 1.0 mile of the parcel centroid (mile ²)	0	0.652	0.0541	0.103
SF0.5	Total area of single-family land use within 0.5 mile of the parcel centroid (mile ²)	0	0.562	0.199	0.113
SF0.5-1.0	Total area of single-family use within 0.5 to 1.0 mile of the parcel centroid (mile ²)	0.000533	1.28	0.527	0.278
SF1.0-1.5	Total area of single-family land use within 1.0 to 1.5 miles of the parcel centroid (mile ²)	0.00445	1.86	0.806	0.406
MF0.5	Total area of multi-family land use within 0.5 mile of the parcel centroid (mile ²)	0	0.368	0.0178	0.0352
Commercial/Office0.5	Total area of commercial or office land use within 0.5 mile of the parcel centroid (mile ²)	0	0.353	0.0240	0.0401
Indus0.5	Total area of industrial land use within 0.5 mile of the parcel centroid (mile ²)	0	0.475	0.0235	0.0536
Indus0.5-1.0	Total area of industrial use within 0.5 to 1.0 mile of the parcel centroid (mile ²)	0	1.22	0.0915	0.150
Indus1.0-1.5	Total area of industrial land use within 1.0 to 1.5 miles of the parcel centroid (mile ²)	0	1.53	0.188	0.257
Civic0.5	Total area of civic land use within 0.5 mile of the parcel centroid (mile ²)	0	0.456	0.0252	0.0384
Civic0.5-1.0	Total area of civic use within 0.5 to 1.0 mile of the parcel centroid (mile ²)	0	0.862	0.0852	0.102
Excluded0.5	Total area of excluded land use within 0.5 mile of the parcel centroid (mile ²)	0	0.627	0.132	0.114
Excluded0.5-1.0	Total area of excluded use within 0.5 to 1.0 mile of the parcel centroid (mile ²)	0.00533	1.77	0.512	0.356

Excluded1.0-1.5	Total area of excluded land use within 1.0 to 1.5 miles of the parcel centroid (mile ²)	0.06333	2.58	0.835	0.462
Undev0.5	Total area of undeveloped land use within 0.5 mile of the parcel centroid (mile ²)	0.00168	0.737	0.226	0.128
Undev0.5-1.0	Total area of undeveloped use within 0.5 to 1.0 mile of the parcel centroid (mile ²)	0.00930	2.07	0.609	0.318
Undev1.0-1.5	Total area of undeveloped land use within 1.0 to 1.5 miles of the parcel centroid (mile ²)	0.0190	2.62	1.05	0.497

Table F.6. Results of Land Use Change Model

	LLSF	SF	MF	Commercial or Office	Industrial	Civic
Constants	-20.8	0.593	-4.63	-2.09	0.175	-4.26
Size	10.8	-341.1	12.6	9.98	14.1	11.9
TT to CBD	0.227	0.117	0.0766	0.0688		
Dist to HWY	-1.11	-0.524	-0.904	-0.762		-0.413
Transit Stops		-0.00719				
Slope		-0.0380		-0.110	-0.369	-0.0714
Entropy0.5	7.03	-1.38			3.08	
LLSF0.5		5.88	-19.50	-11.70	9.31	
LLSF1.0		-3.54				
SF0.5	12.6	1.63		-8.51	-11.9	2.00
SF1.0		-1.94		2.84		
SF1.5		1.06				
MF0.5			11.37			
Commercial/Office0.5		-3.94		5.01		
Indus0.5	13.9	-3.03	-8.27	-1.91	-2.59	
Indus1.0		-3.50				
Indus1.5		-0.386				
Civic0.5				-7.49	-11.6	
Civic1.0					-2.78	
Excluded0.5	18.3	0.836		-8.71	-4.77	
Excluded1.0		-0.465		2.75		
Excluded1.5		0.272				
Undev0.5	20.1	1.95		-7.18	-5.79	
Undev1.0		-1.94		2.79		
Undev1.5		0.993		-0.685		
Pseudo R ²	0.254					
Number of observations	15,359					

Note: Undeveloped land use type is the base for all variables.

Table F.7. Description of Dependent Variables in Land Use Intensity Model

Variables	Description	Minimum	Maximum	Mean	Std. Deviation
SF Change	Single family land change (mile ²)	-0.0000403	1.81	0.0620	0.142
MF Change	Multi-family land change (mile ²)	-0.0000045	0.150	0.00200	0.00828
Commercial/Office Change	Commercial or office land change (mile ²)	-0.0000340	0.969	0.0183	0.0617
Indus Change	Industrial land change (mile ²)	-0.0000114	0.785	0.00659	0.0374
Civic Change	Civic land change (mile ²)	-0.00000493	2.02	0.0302	0.132
HH	Household count in prior year	0	3984	382.1	562.6
BAS	Base job count in prior year	0	11000	161.6	568.7
RET	Retail job count in prior year	0	2759	93.2	219.0
SERV	Service job count in prior year	0	7881	237.3	634.2
Undev	Undeveloped land in prior year (mile ²)	0	42.3	2.43	4.81
Entropy	Land use balance in prior year	0	0.769	0.269	0.170
Accessibility	Regional accessibility under peak-hour conditions	-2.41	4.81	2.56	1.41

Note: Definitions of Entropy and Accessibility variables are the same as those used in the LUC model.

Table F.8. Results of Land Use Intensity Model

	HH Change		Basic Job Change		Retail Job Change		Service Job Change	
	parameter	t-statistics	parameter	t-statistics	parameter	t-statistics	parameter	t-statistics
Constants	13.6	0.809	-6.20	-0.220	-1.63	-0.386	-34.9	-0.795
SF Change	541	14.9						
MF Change	8179	15.4	2724	1.86	2020	3.67		
Commercial/Office Change	228	3.13			649	8.64		
Indus Change			1868	5.68				
Civic Change	-75.2	-2.06			-83.1	-2.57	136	1.59
HH	0.0465	4.83					0.0470	2.07
BAS	-0.0235	-3.00	-0.385	-12.8	0.0169	2.09	0.128	5.30
RET			0.202	3.21	-0.098	-4.81	0.125	1.99
SERV					0.0203	2.85	-0.218	-6.42
Undev	-3.20	-2.52						
Entropy	-157	-4.34						
Accessibility	8.50	1.66					24.3	1.60
Spatial Lag	0.116	1.78	-0.871	-5.00	0.414	3.58	-0.978	-2.38
Spatial Error	0.146		0.569		-0.368		0.531	
R ² (individual equations)	0.349		0.426		0.182		0.284	
R ²	0.320							
Number of Observation	1245							

Figure F.1 (a). Land Use Predictions in 2010 on Previously Undeveloped Parcels (BAU Scenario)

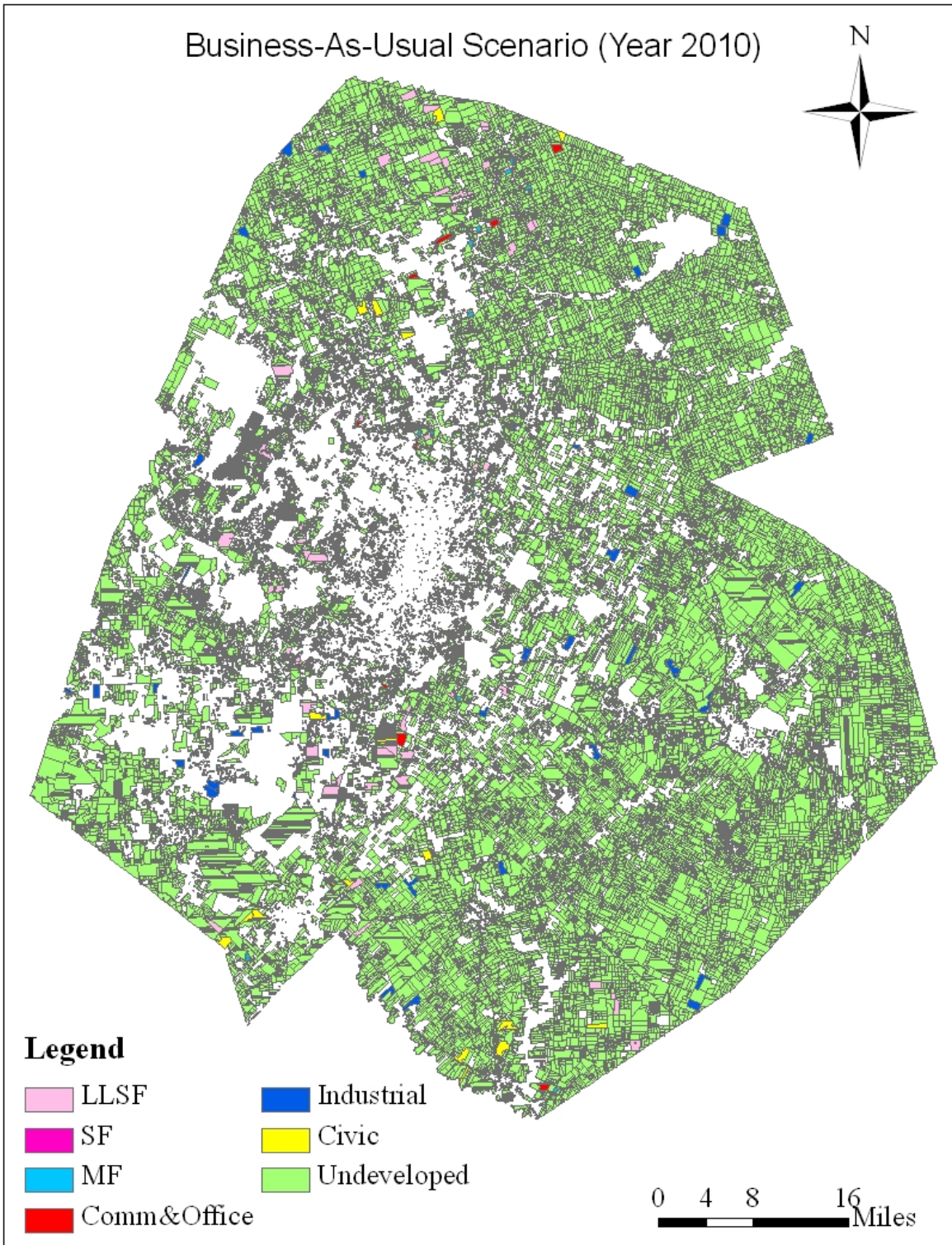


Figure F.1 (b). Land Use Predictions in 2015 on Previously Undeveloped Parcels (BAU Scenario)

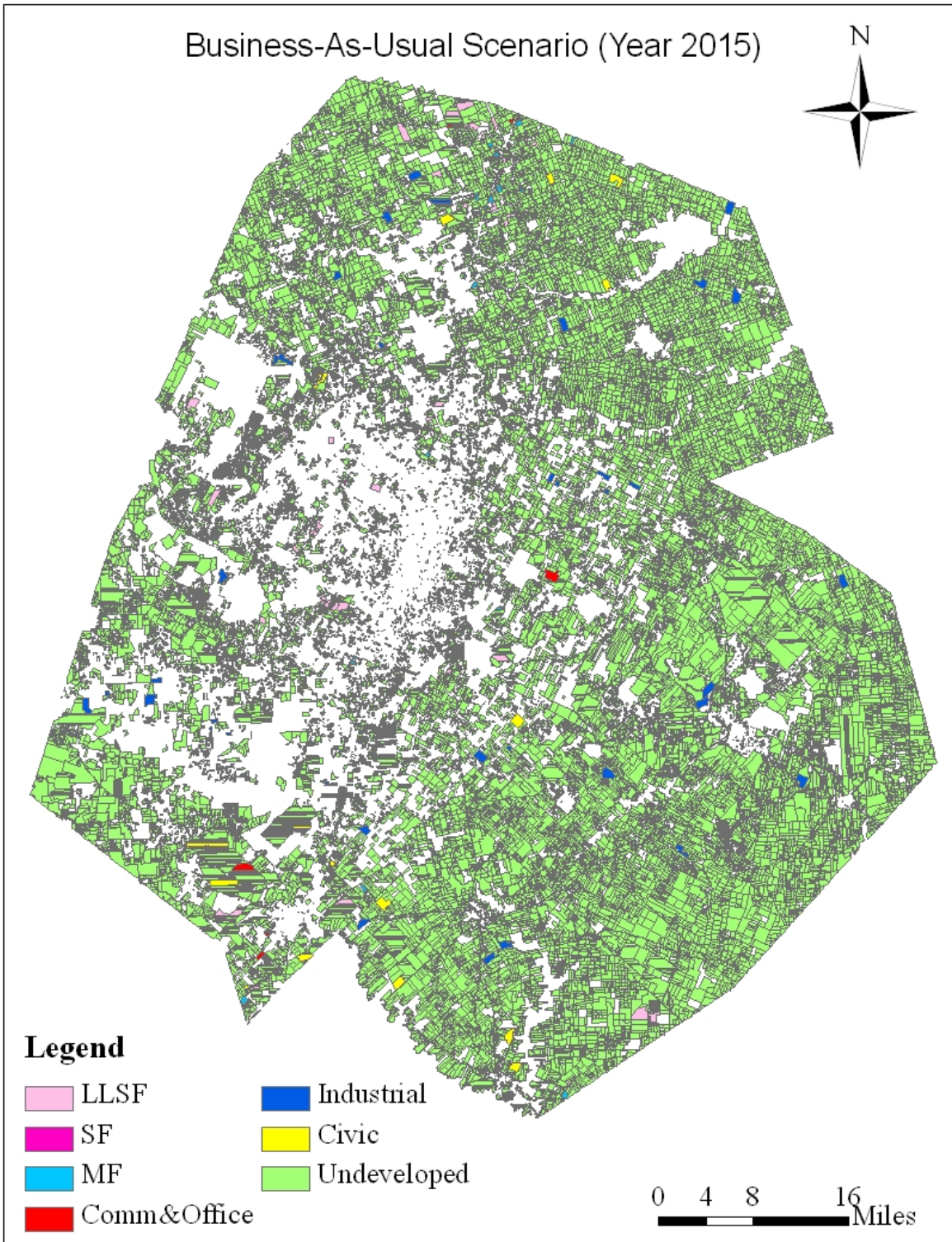


Figure F.1 (c). Land Use Predictions in 2020 on Previously Undeveloped Parcels (BAU Scenario)

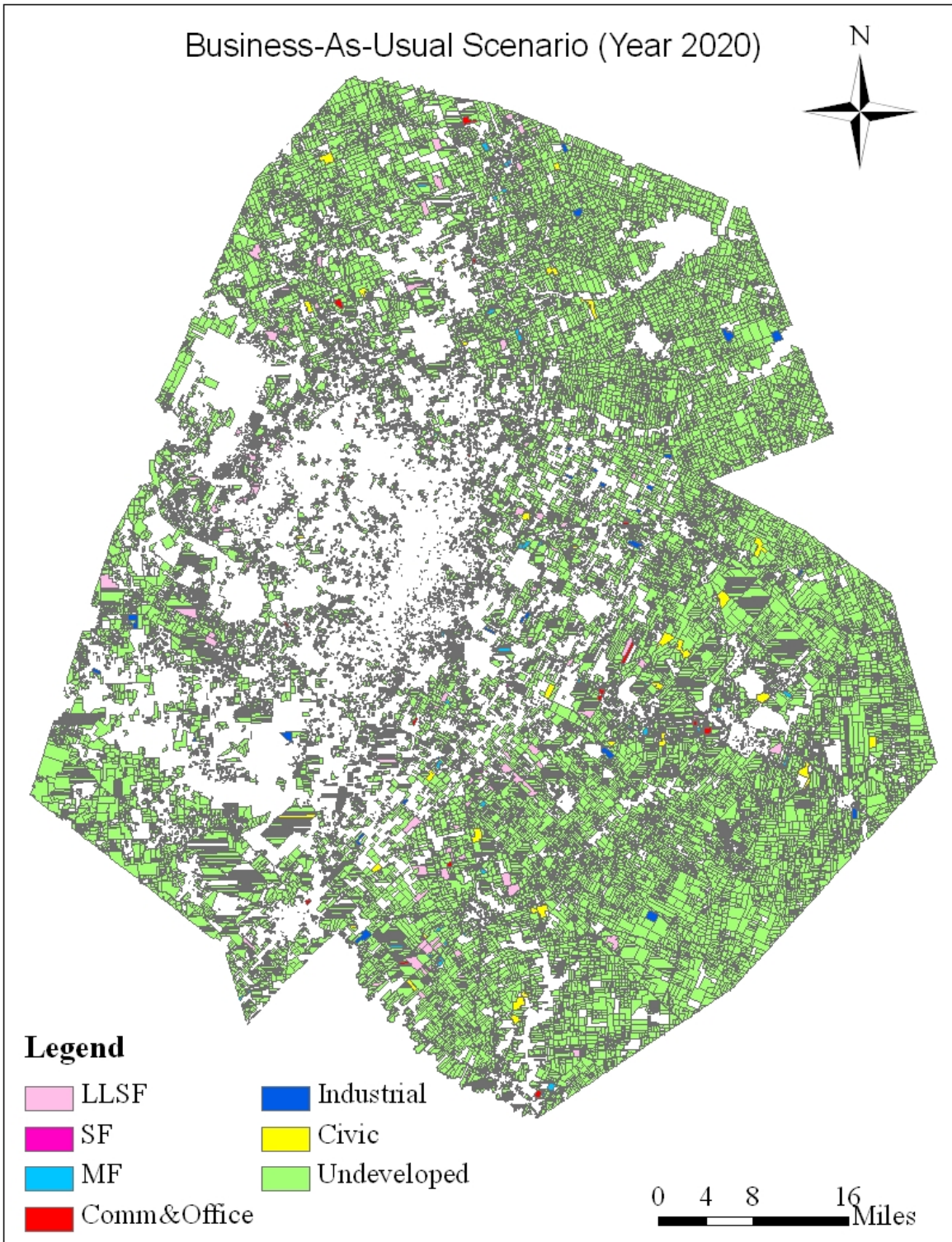


Figure F.1 (d). Land Use Predictions in 2025 on Previously Undeveloped Parcels (BAU Scenario)

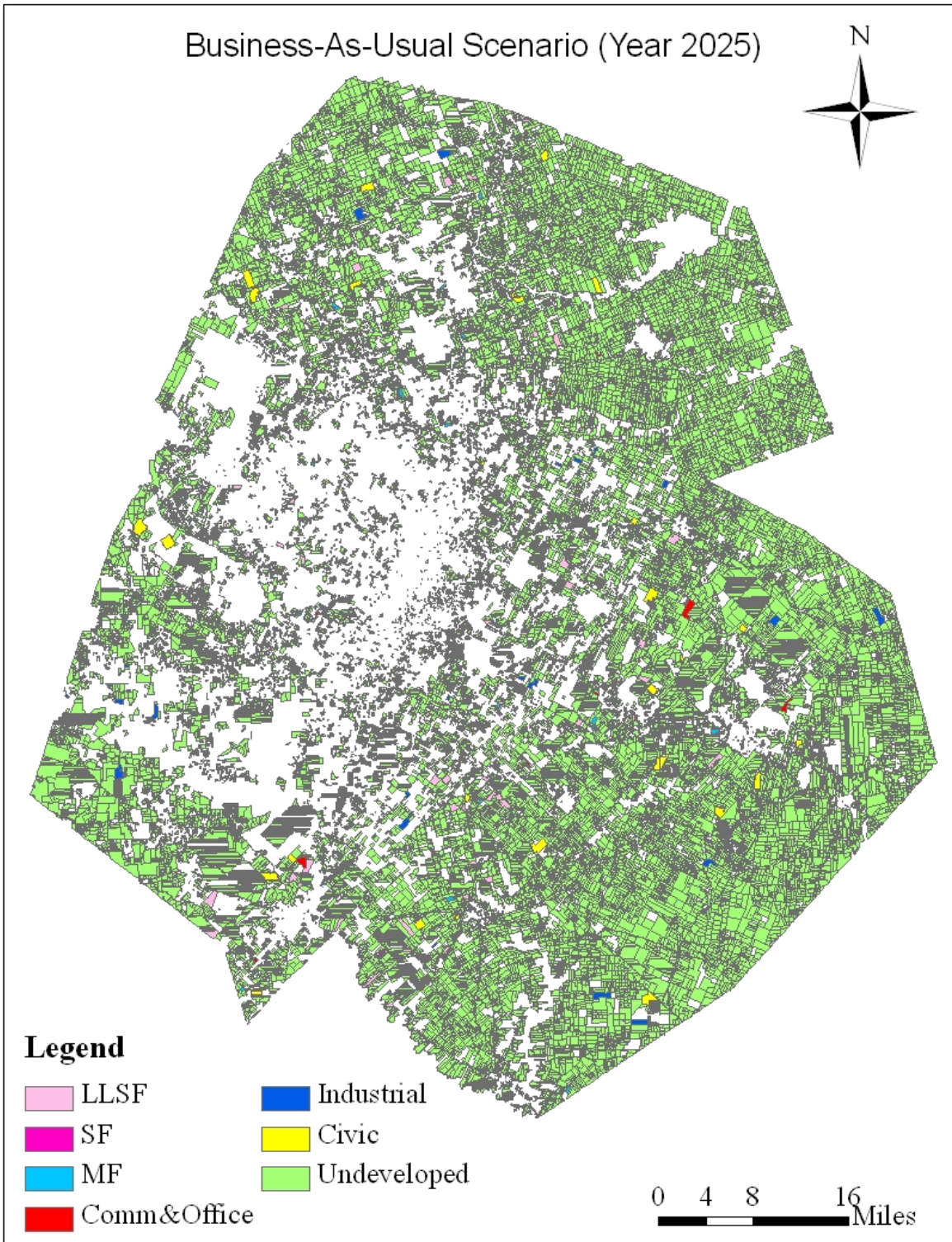


Figure F.1 (e). Land Use Predictions in 2030 on Previously Undeveloped Parcels (BAU Scenario)

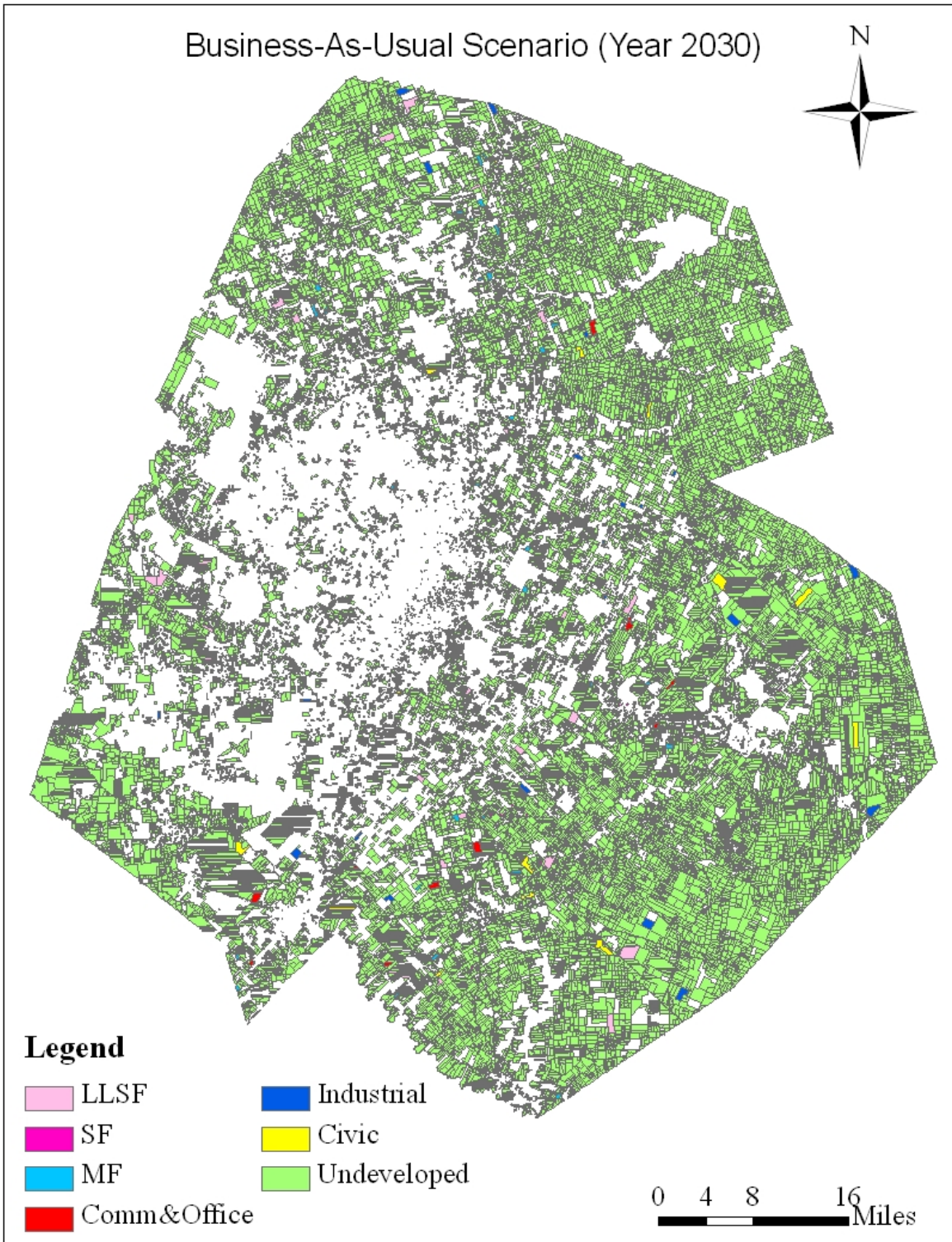


Figure F.2 (a). Land Use Predictions in 2020 on Previously Undeveloped Parcels (Pricing Scenario)

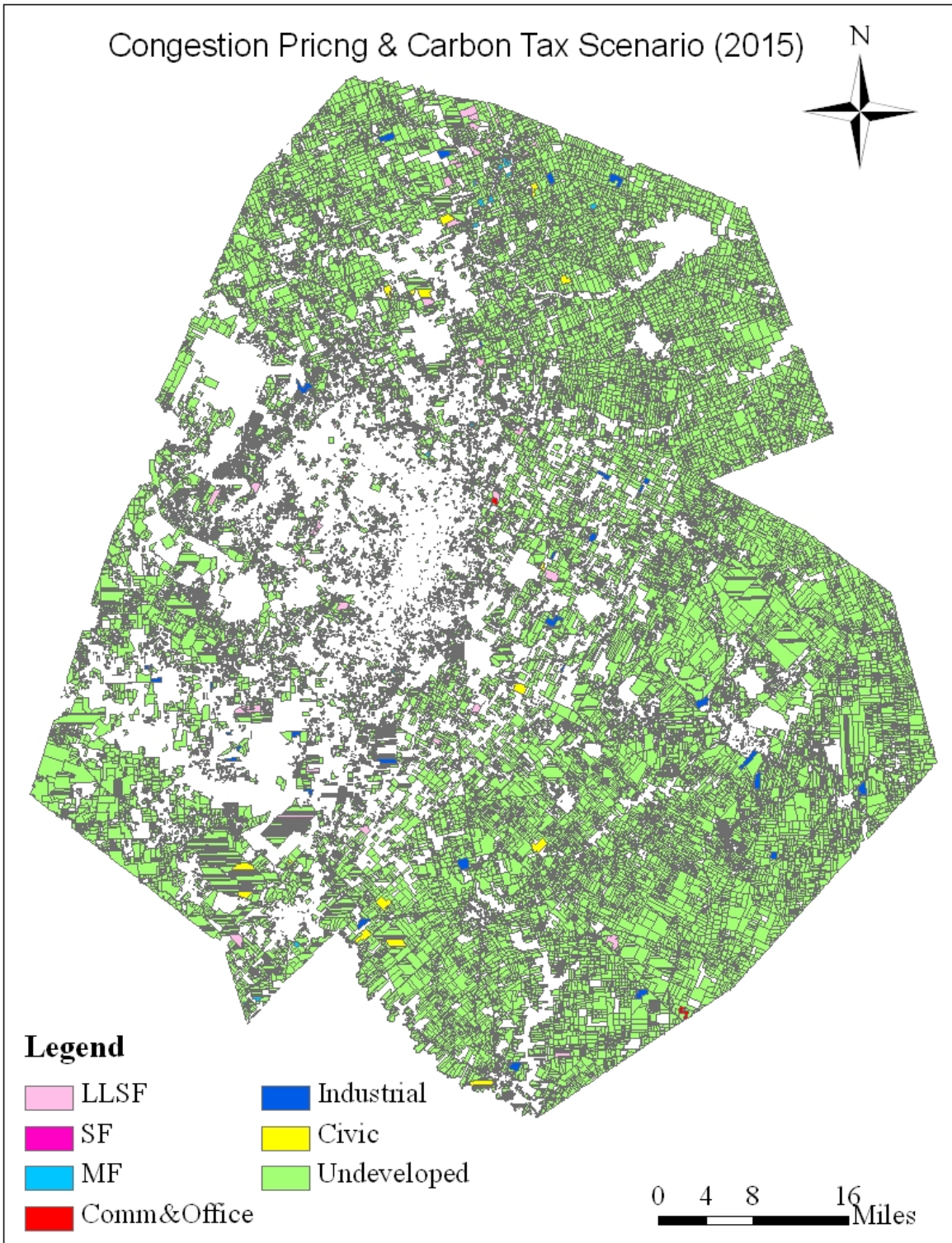


Figure F.2 (b). Land Use Predictions in 2025 on Previously Undeveloped Parcels (Pricing Scenario)

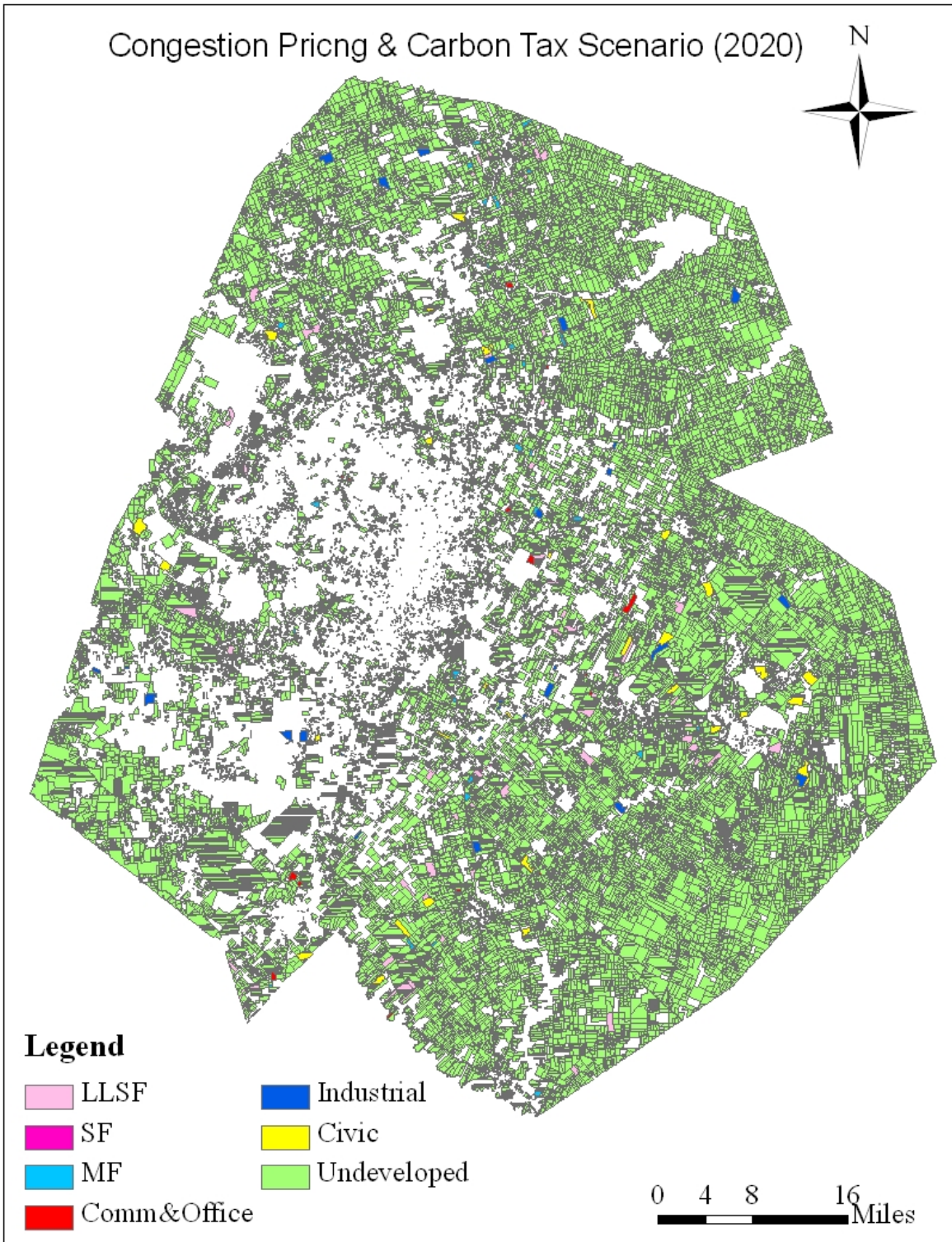


Figure F.2 (c). Land Use Predictions in 2025 on Previously Undeveloped Parcels (Pricing Scenario)

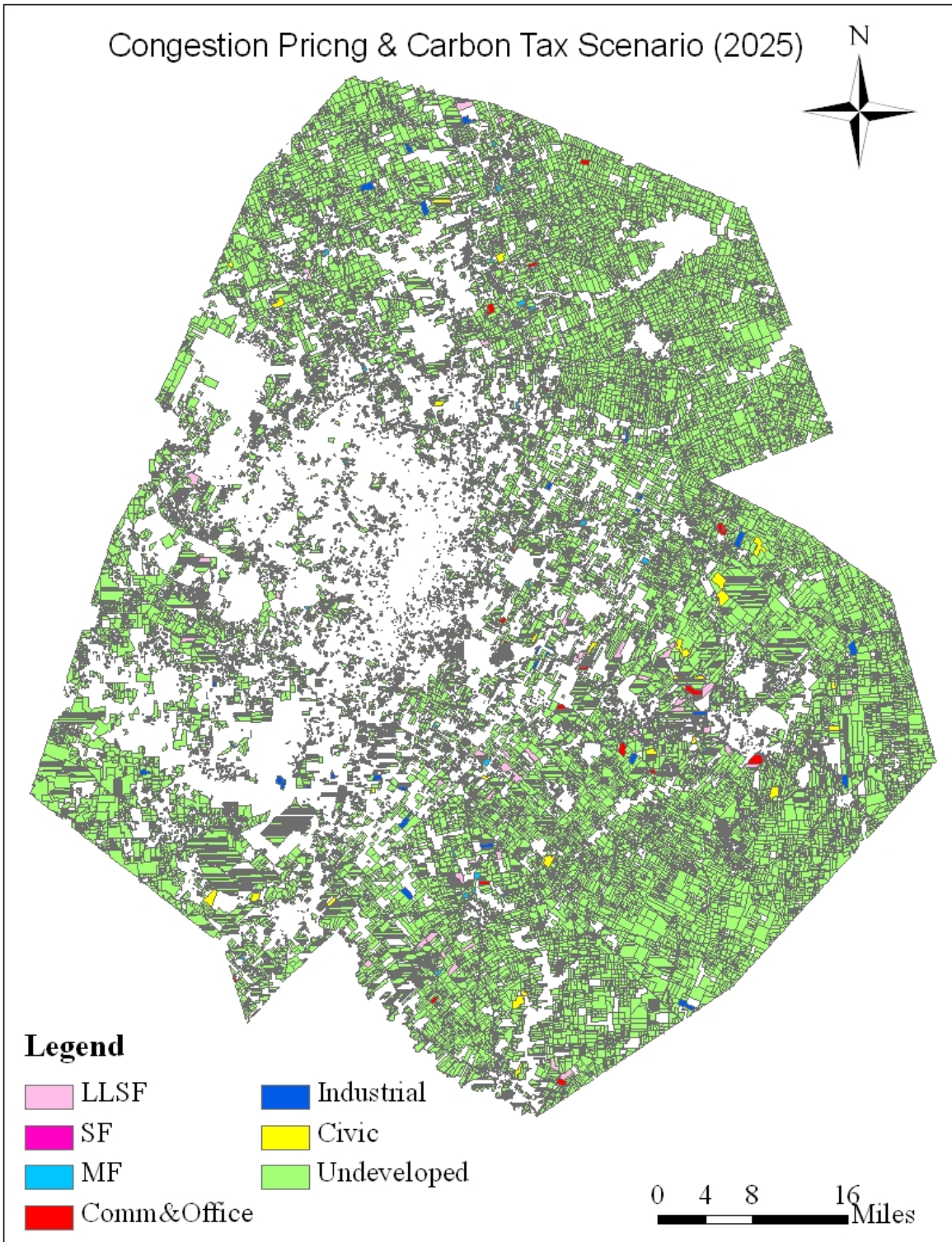


Figure F.2 (d). Land Use Predictions in 2030 on Previously Undeveloped Parcels (Pricing Scenario)

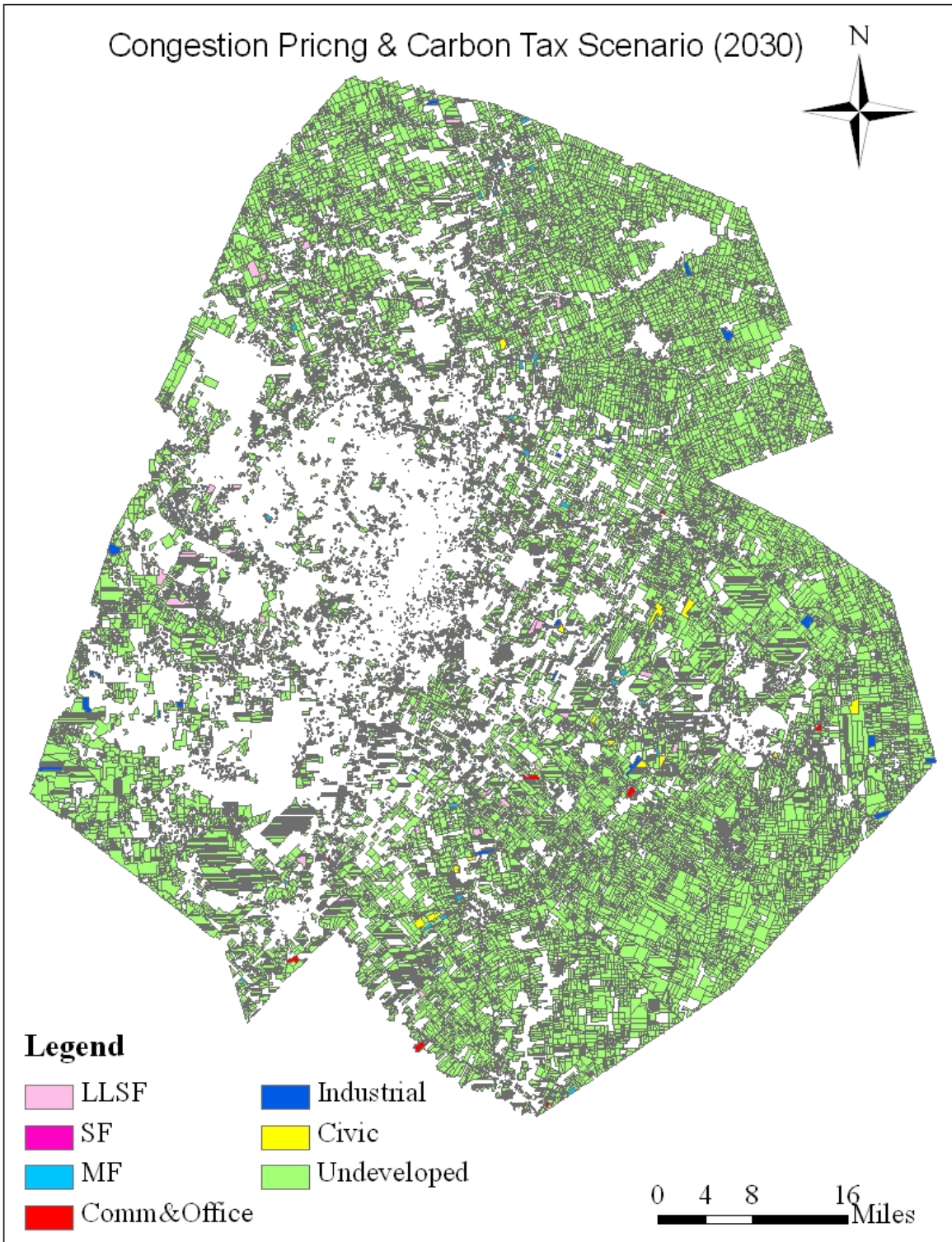


Figure F.3. Household Density in Year 2030 (BAU Scenario
2D & 3D Views)

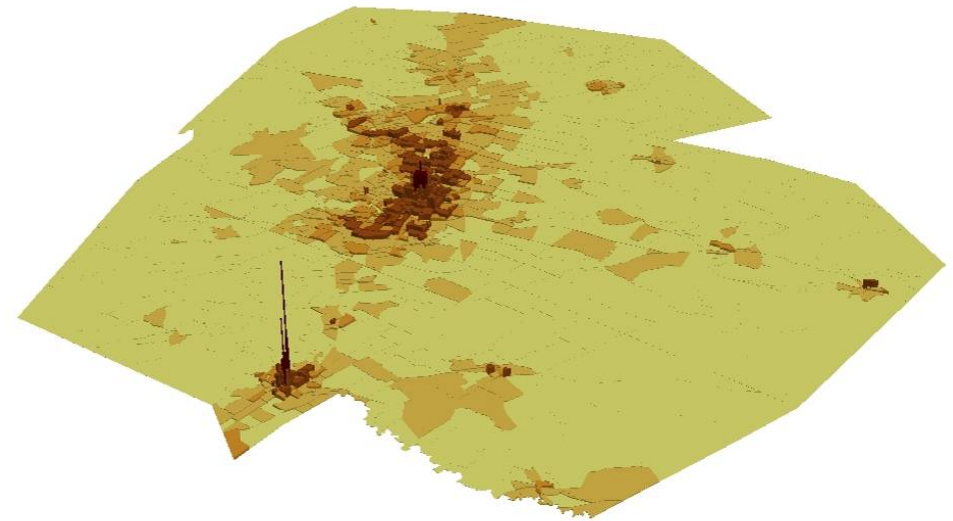
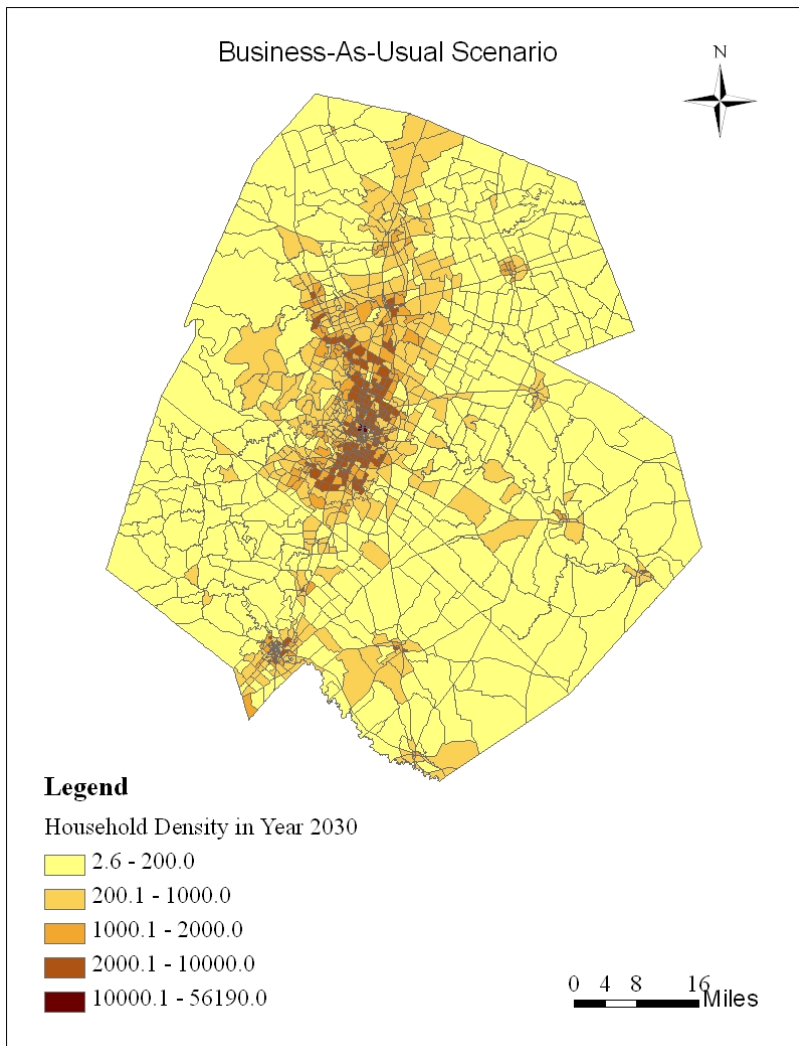


Figure F.4. Employment Density in Year 2030 (BAU Scenario2D & 3D Views)

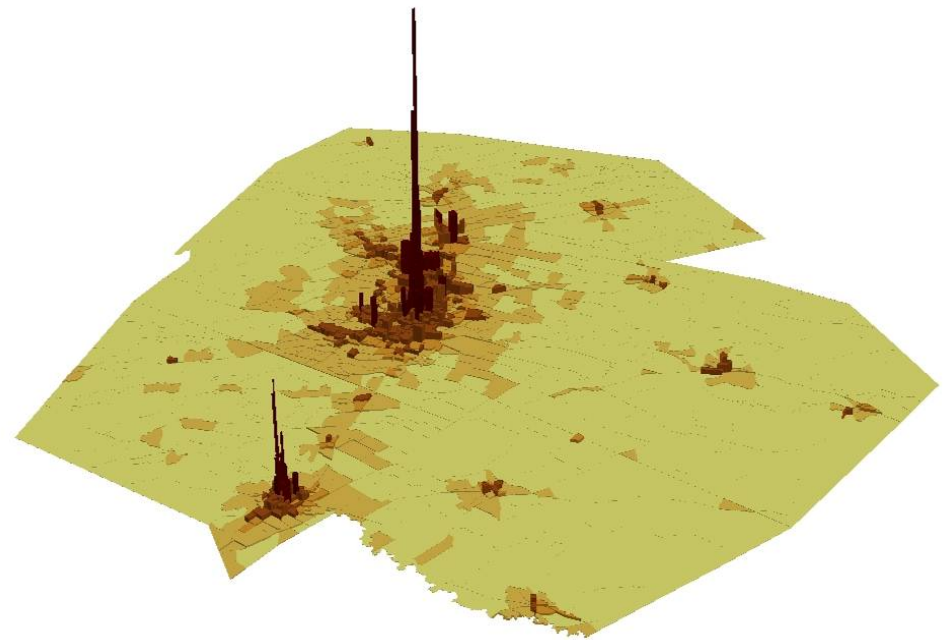
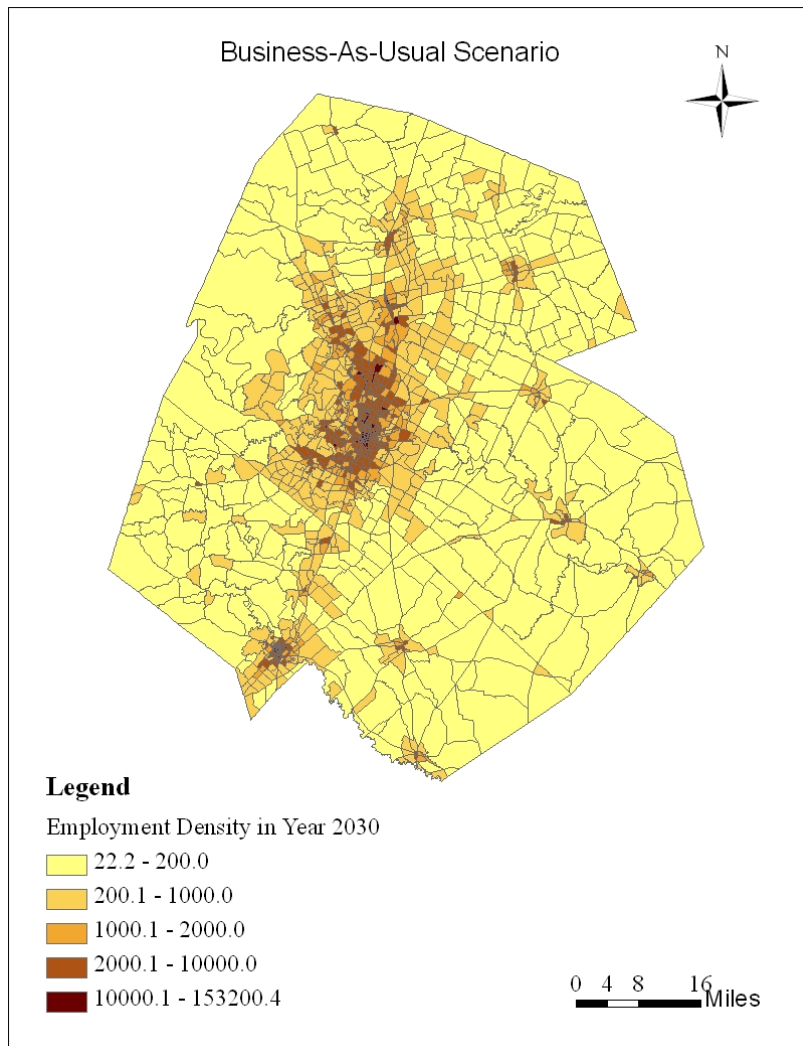


Figure F.5. Household Density in Year 2030 (Pricing Scenario 2D & 3D Views)

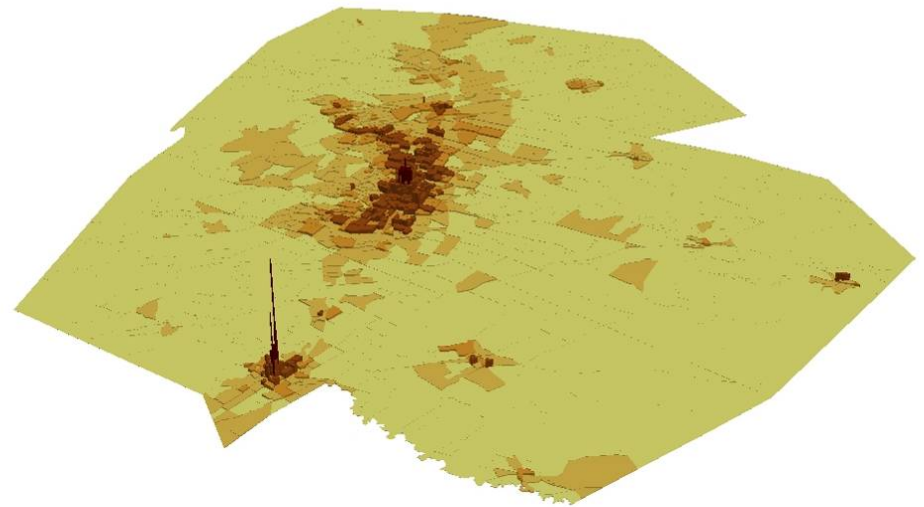
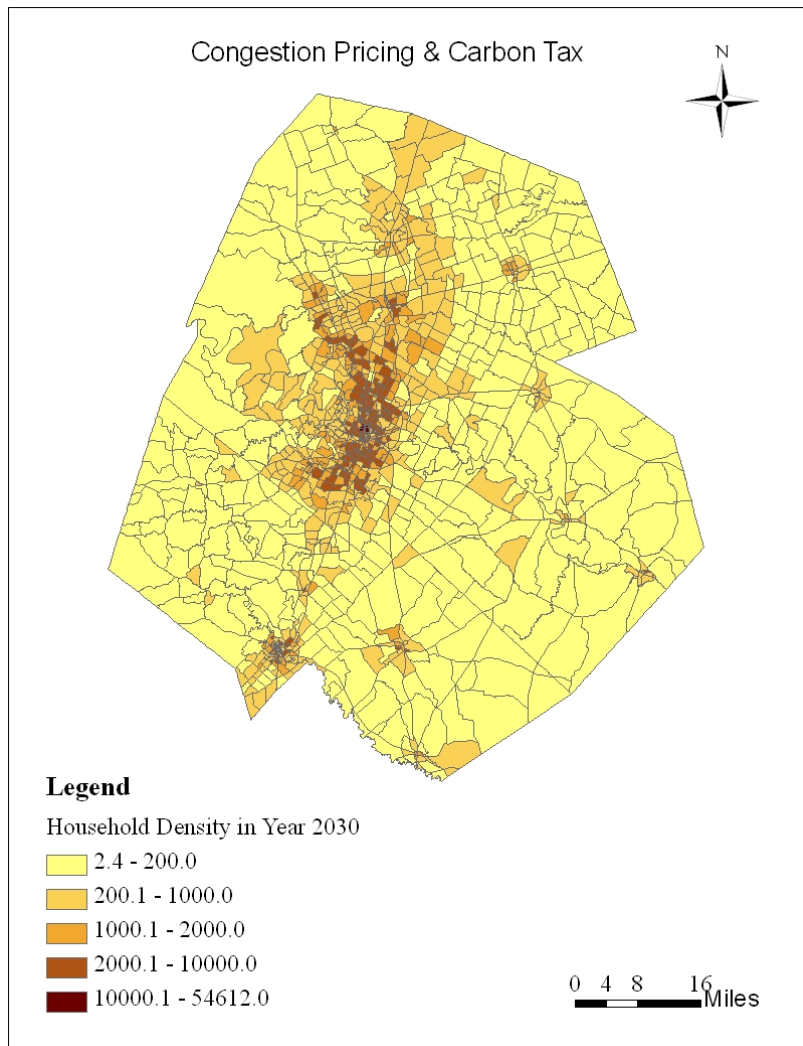
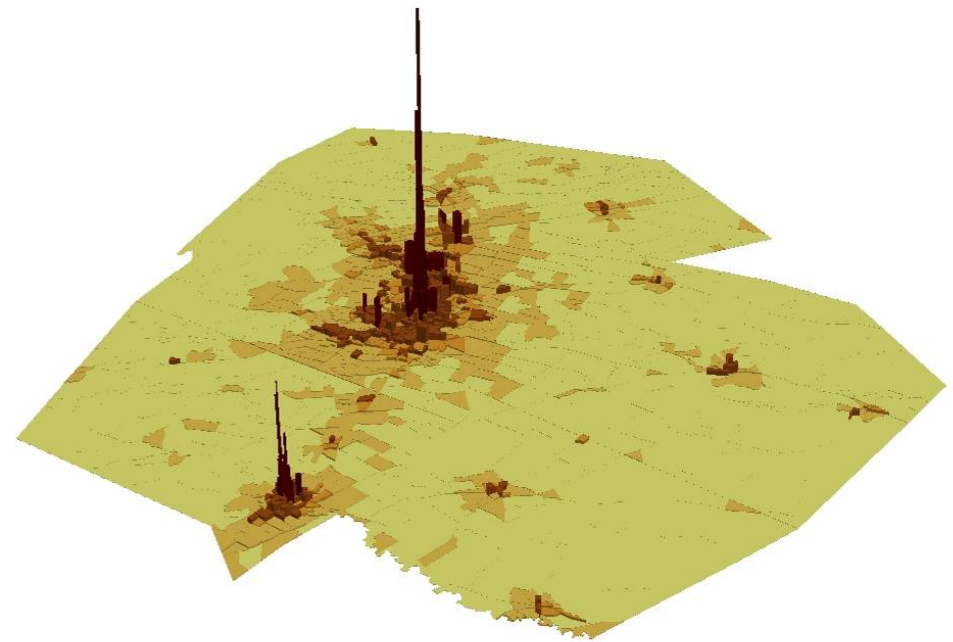
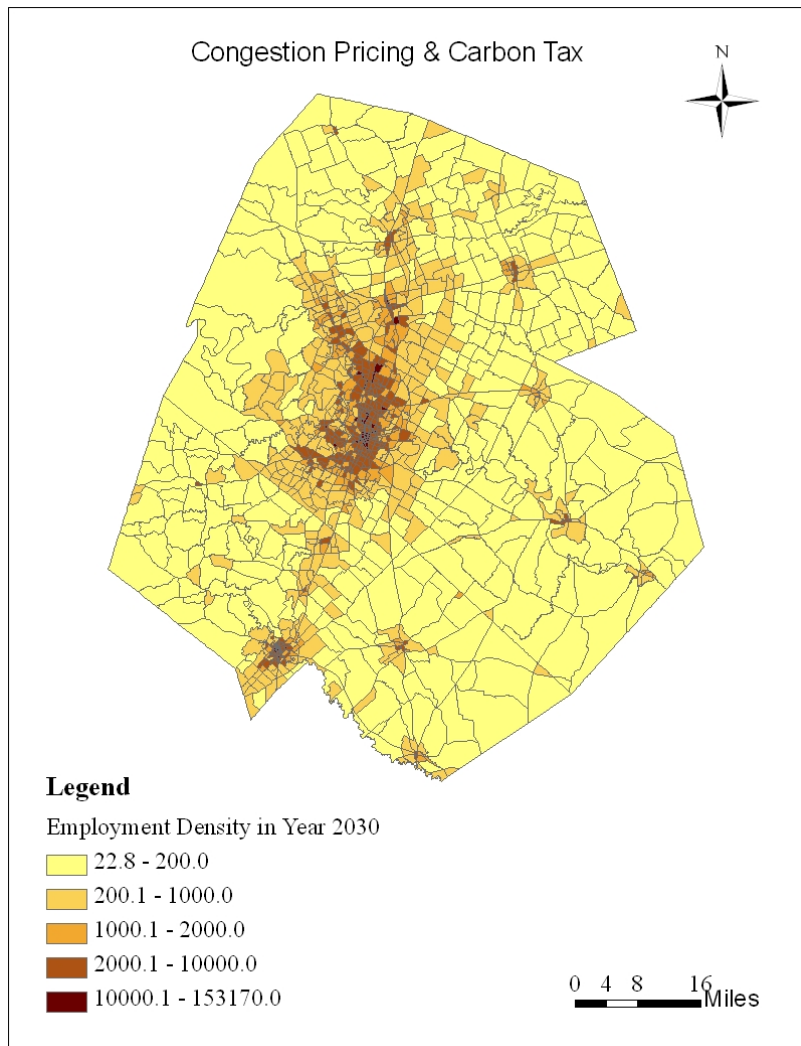


Figure F.6. Employment Density in Year 2030 (Pricing Scenario 2D & 3D Views)



Appendix G

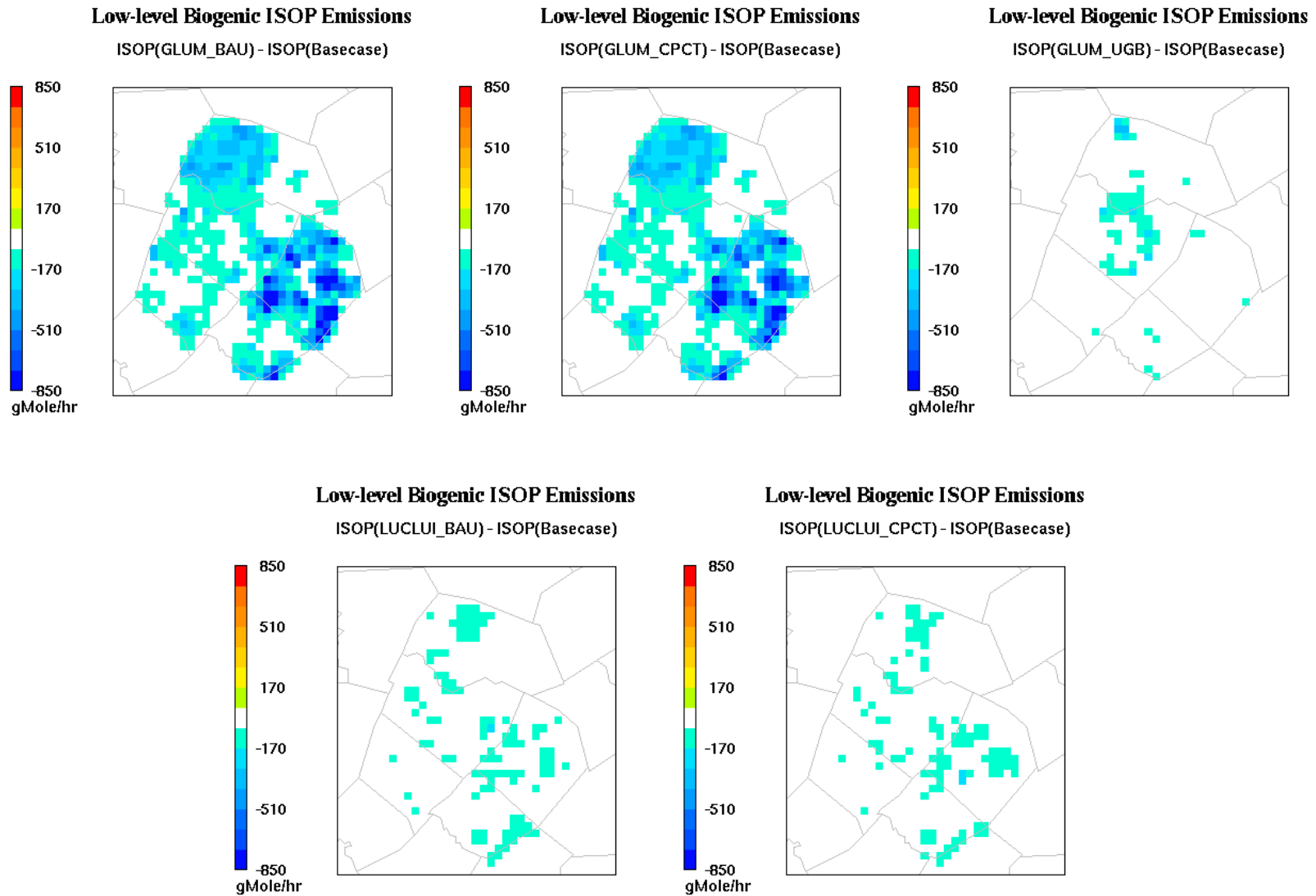


Figure G.1 Differences in biogenic isoprene emissions between ITLUM scenarios and the Base Case for September 19 at 1400

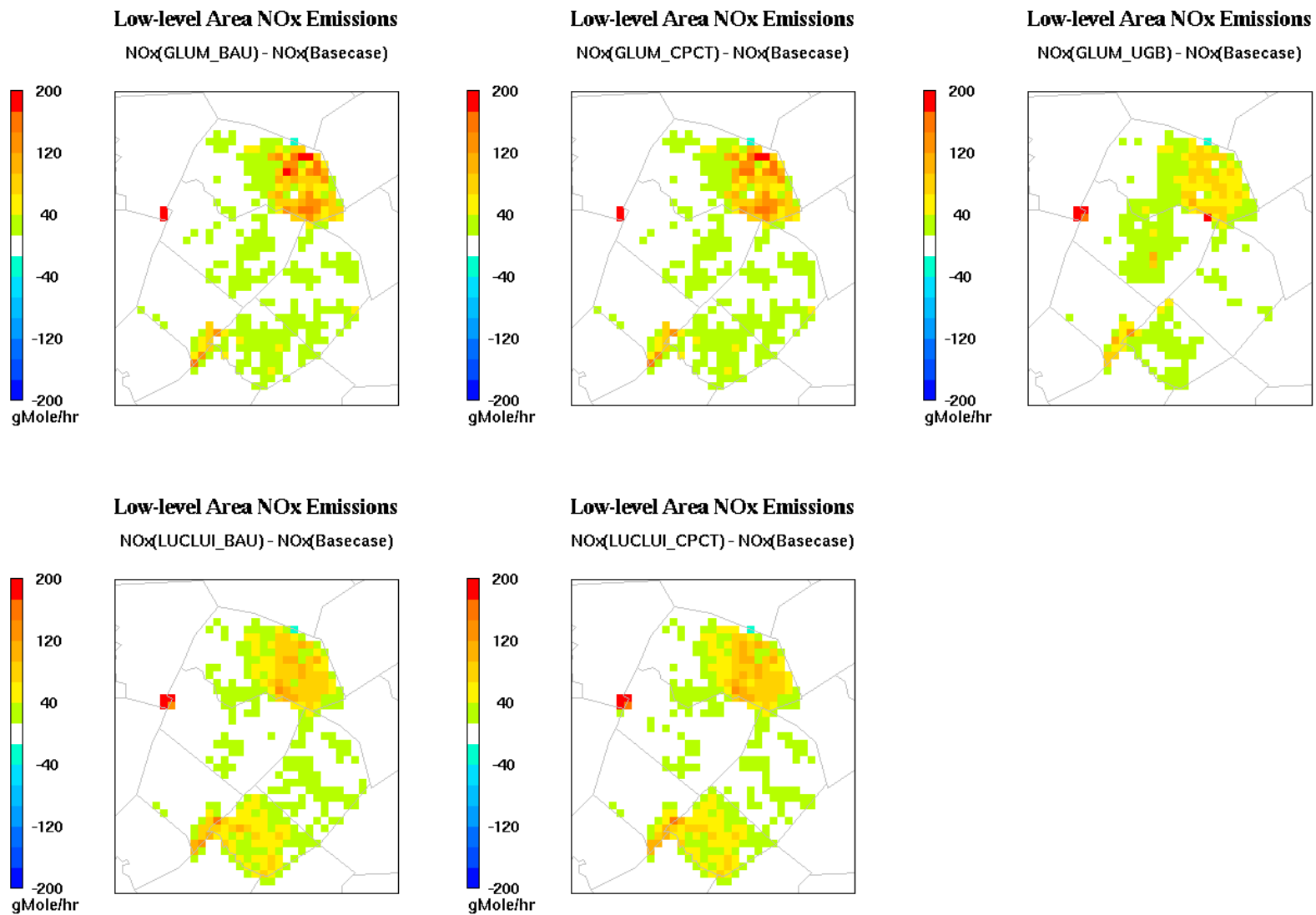


Figure G.2 Differences in area source NO_x emissions between ITLUM scenarios and the Base Case for September 20 at 1400

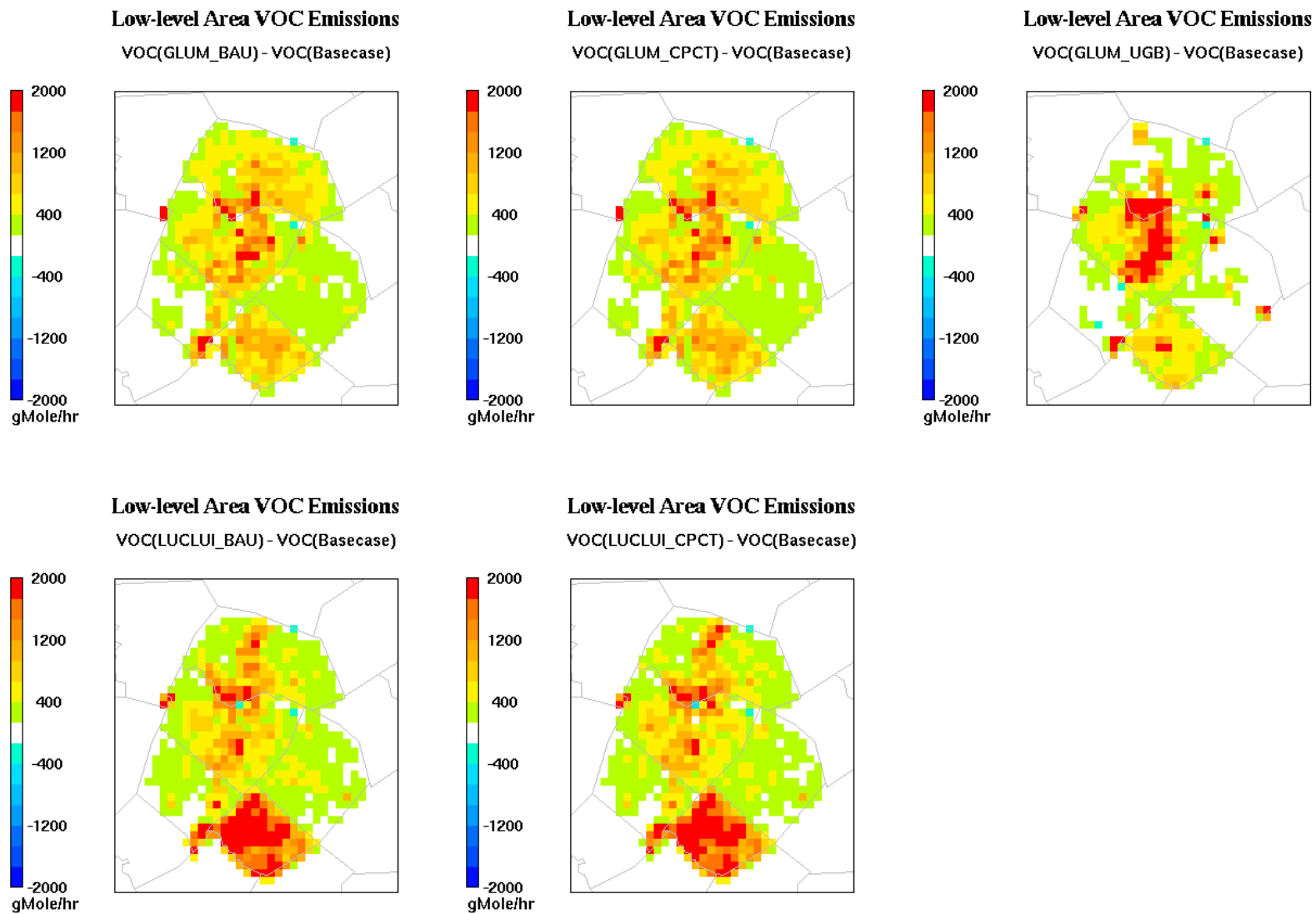


Figure G.3 Differences in area source VOC emissions between ITLUM scenarios and the Base Case for September 20 at 1400

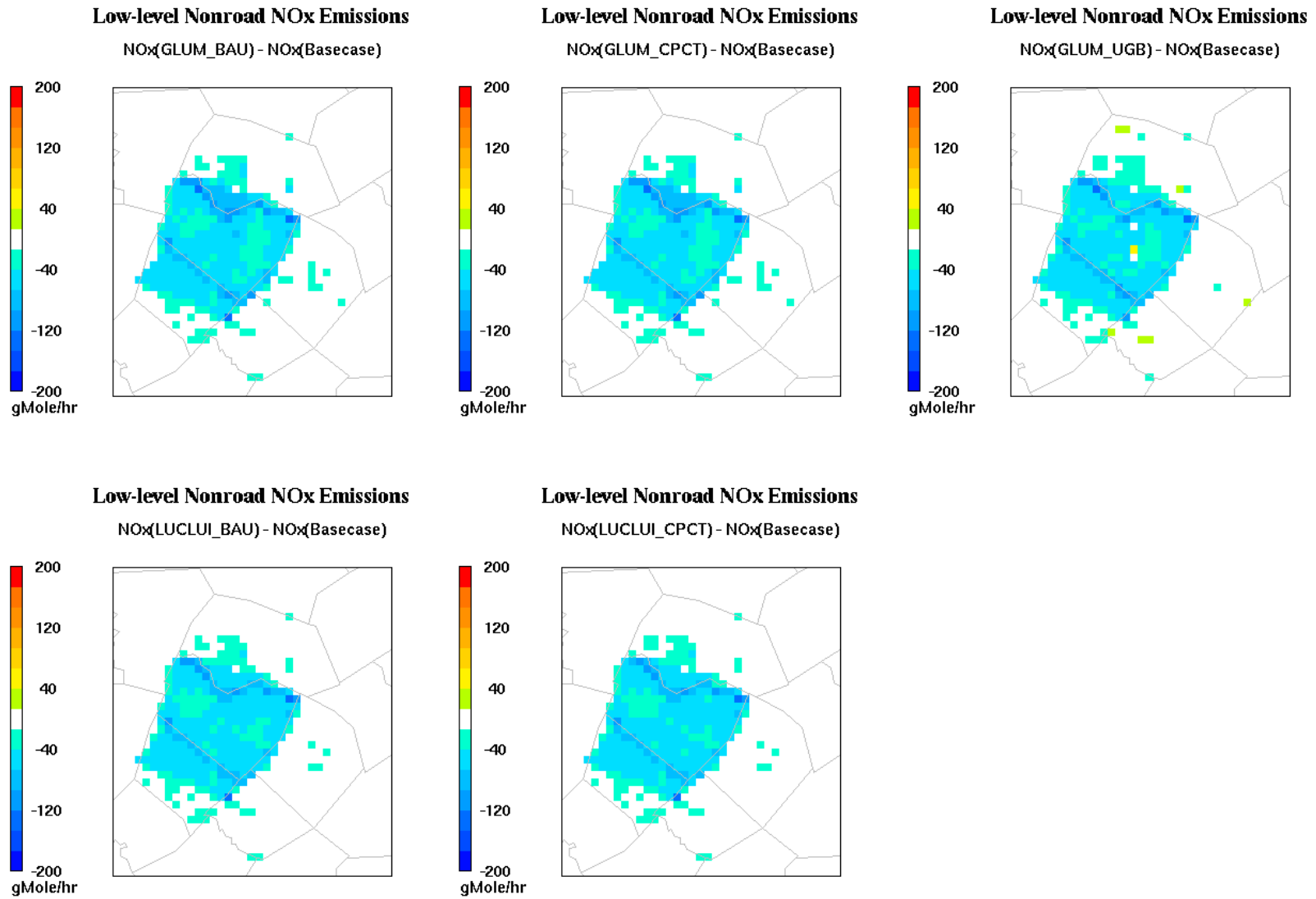


Figure G.4 Differences in non-road source NOx emissions between ITLUM scenarios and the Base Case for September 20 at 1400

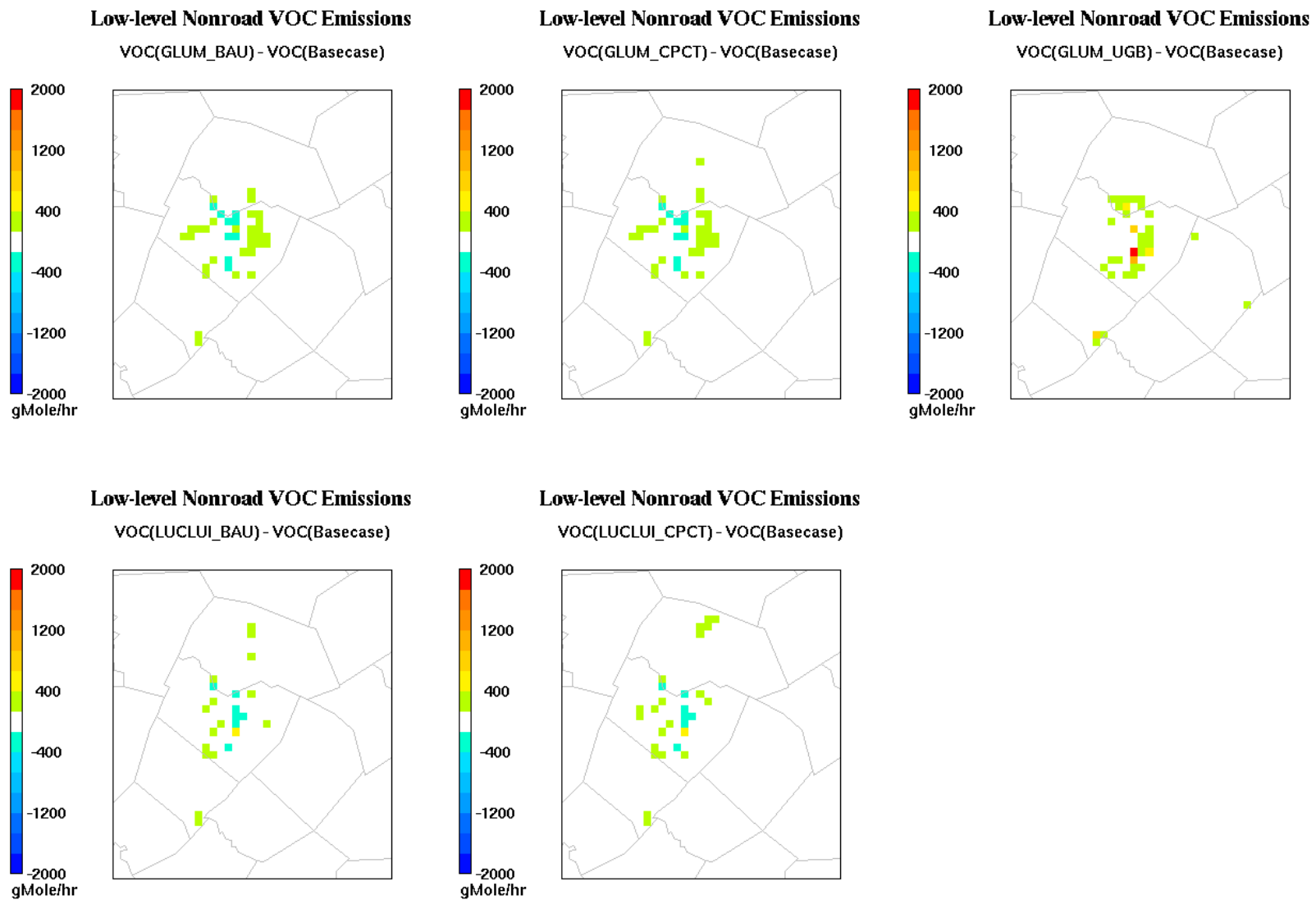


Figure G.5 Differences in non-road source VOC emissions between ITLUM scenarios and the Base Case for September 20 at 1400

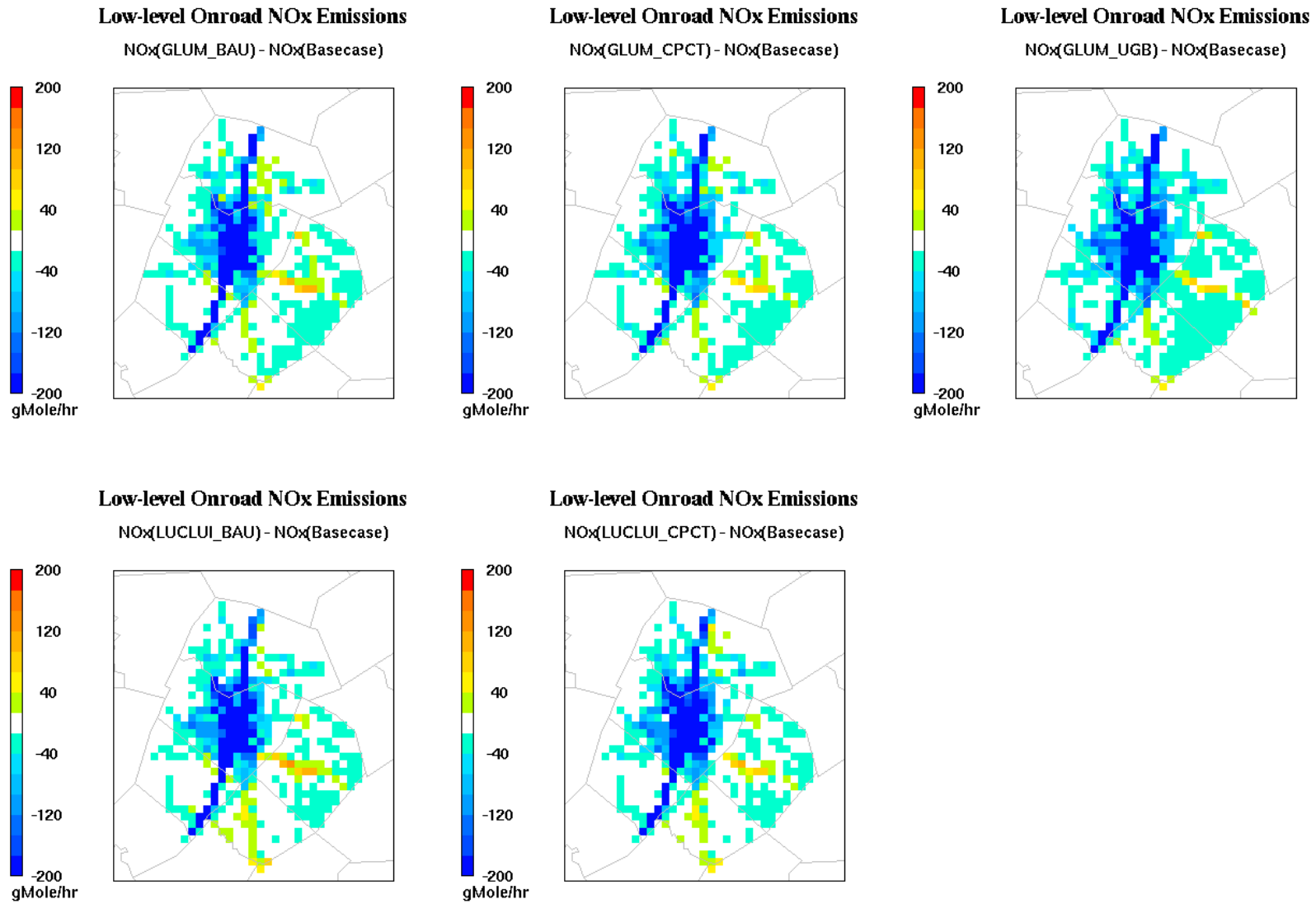


Figure G.6 Differences in on-road source NOx emissions between ITLUM scenarios and the Base Case for September 20 at 1400

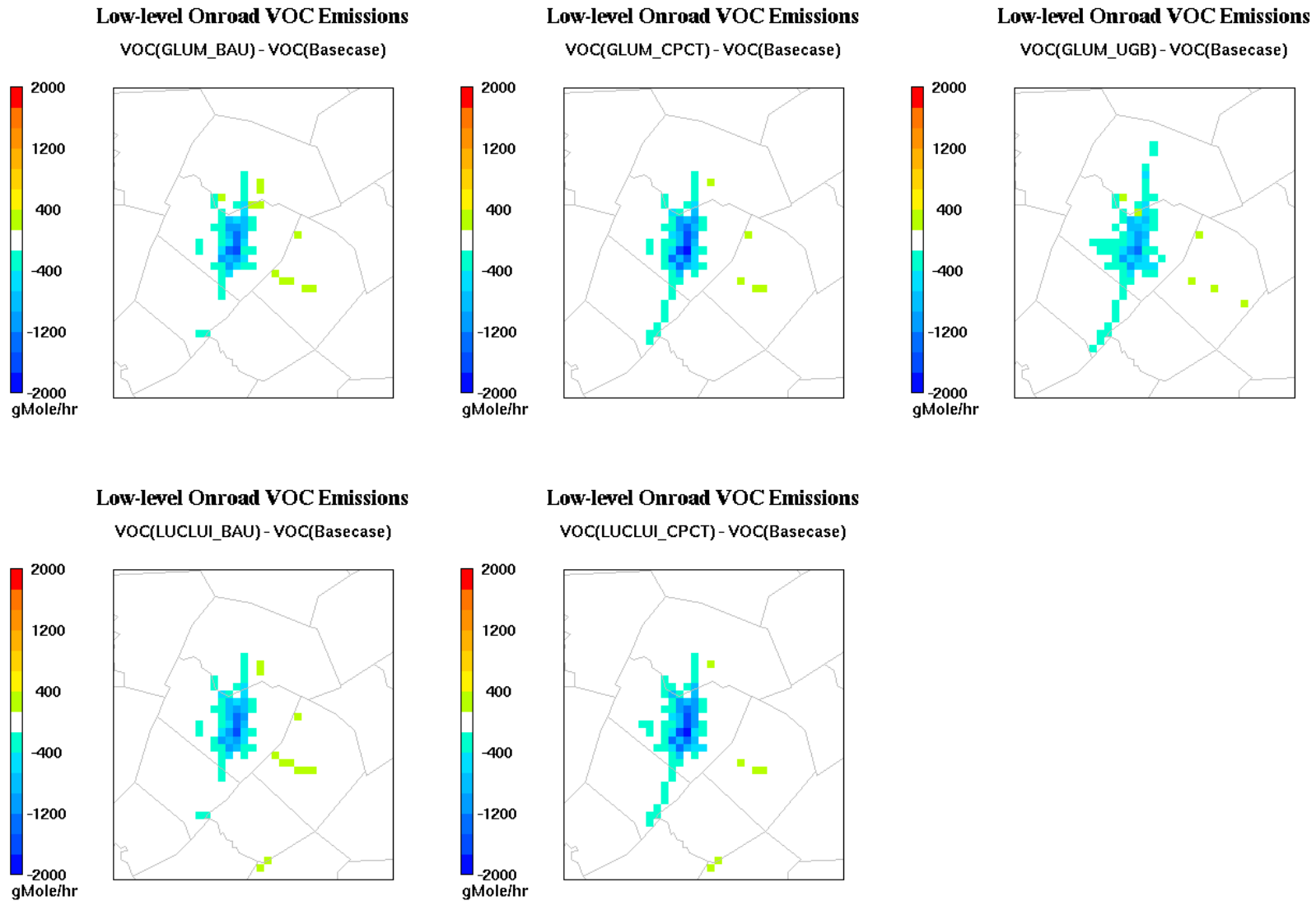


Figure G.7 Differences in on-road source VOC emissions between ITLUM scenarios and the Base Case for September 20 at 140

Appendix H. Vehicle Ownership Model Details

Vehicle ownership has an important effect on vehicle emissions, fuel consumption, highway capacity, congestion and traffic safety. To great extent, this impact depends on the characters of the fleet and households. This appendix chapter provides descriptive analysis of Austin vehicle holdings, including models of vehicle ownership levels, vehicle make and model choices and vehicle transactions under three different scenarios: business as usual (BAU), implementation of an urban growth boundary (UGB), and implementation of gas taxes and tolling. Data for the analysis comes from the 2006 Austin Travel Survey Data and the 1998 Toronto Area Car Ownership Study (TACOS).

H.1 Review of Earlier Work

Various dimensions of vehicle ownership – including the number of vehicles owned (by the household), types of vehicles owned (including general category e.g. SUV versus passenger car), number of miles traveled by each vehicle, age of vehicle, fuel types of each vehicle – have been modeled, mainly using discrete choice models. This review is by no means comprehensive, but aims to highlight key models and methods used in this area. One of the first disaggregate studies is by Lave and Train (1979), who used a multinomial logit model structure for vehicle type choice. Their model controlled for several household attributes, vehicle characteristics, gasoline prices and taxes on larger vehicles. They found that increases in income increase one's likelihood of purchasing expensive vehicle and younger individuals tend to prefer high - performance cars. Berkovec (1985) developed a simulation model to combine a disaggregate model of auto choice with an econometric model for forecasts of automobile sales, stocks¹⁹ and retirement²⁰. Manski and Sherman (1976) developed separate multinomial logit models for the number of vehicles and vehicle types owned by households with one or two vehicles. Choo and Mokatarian (2004) modeled the most driven vehicle in a household's fleet. They find that travel attitudes, lifestyle, and mobility factors are useful predictors of vehicle types owned. Others have looked at two or more dimensions of vehicle ownership. For example, Mohammadian and Miller (2003a) studied the purchase and retirement of vehicles and the type of vehicles via a nested logit structure. Mannering and Winston (1985) employed a dynamic utilization framework using panel data from either side of the 1979 oil shock. They modeled number, type and use of vehicles via discrete choice and linear regression techniques. Other studies in this category include joint choice of vehicle ownership levels and vehicle body types (Hensher and Plastrier, 1985) and the number of vehicles owned and their usage (Golob and Wissen, 1989).

One of the major issues in modeling vehicle choice using discrete choice models is the formulation of choice sets. The rising number of makes and models available in the market makes it²¹ almost impossible to estimate a model that allows for all of them, as most statistical limit the number of alternatives that can be included. Two different procedures have been adopted to counteract this problem. The first is to use a random sampling procedure for the choice set coded in the likelihood function, as suggested by McFadden (1978). In this approach,

¹⁹ stocks: number of vehicles manufactured

²⁰ retirement: selling or giving up a vehicle

a computationally feasible number of alternatives (25 to 30, for example) , including the chosen alternative is taken from the entire pool of available makes and models. The second approach is to consider simply general categories of vehicles type as the choice set. This could be the body type (such as sedan, coupe, pickup truck, sports utility vehicle or van. – as done in Train (1979), Kitamura *et al.*, (2000), and Choo and Mokhtarian, (2004)) or fuel type (Hensher and Greene, 2001), acquisition type Mannerling *et al.*, 2002) and/or vintage (Mohammadian and Miller, 2003b). With large or random choice sets, analysts typically cannot include many or any person- or household-specific attributes in the set of explanatory factors (except, e.g., when interacted with another, generic variable – like household income times fuel economy divided by the price of gas). The models developed and applied here emphasize vehicle body types as alternatives, and thus more easily permit the inclusion of non-generic attributes (like household income and size, interacted with alternative-specific constants).

H.2 Data Description

The number and type of vehicles owned by a household were modeled using the 2006 Austin (Texas) Travel Survey data. Year 2007 purchase prices and engine sizes (in liters) were obtained for each make/model from *Ward's Automotive Yearbook* (2007). After excluding zero-vehicle households and records with missing information, the final sample set included 2346 vehicles across 1342 households. Vehicles have been classified into nine broad classes: (1) luxury cars, (2) large cars, (3) mid-size cars, (4) sub-compacts cars (5) compact cars, (6) pickup trucks, (7) sports utility vehicles (SUVs), (8) cross-over utility vehicles (CUVs), and (9) Vans (mini vans cargo vans).

In order to analyze vehicle buy and sell decisions (transactions), Toronto Area Car Ownership Study (TACOS) dataset was used. TACOS is a retrospective survey conducted by the University of Toronto (Roorda *et. al.* 2000) and contains information on household vehicle transactions over nine years (from 1990 to 1998). Miller et al (2003) used a mixed logit model to analyze vehicle transactions in the TACOS data at the level of “decision making unit”²². However, models of vehicle transactions reported here, are at the household level.

H.2.1 Descriptive Statistics

Table H.1. provides a summary of household attributes from the ATS and TACOS data along with Census 2000 statistics for Austin region. The average household income is slightly higher than the Census estimated income (\$47,212). Household size, employment and number of children are approximately the same as the Census estimates.

²² Miller et al. (2003) defined the decision making unit as any set of persons within a household that make vehicle ownership decisions cooperatively.

Table H.1. Summary of Household Characteristics

S No	Attribute	ATS (2006)	TACOS
1	No of people in household	2.78	2.74
2	No of employees in household	1.18	1.28
3	Pre-school going children(Age 0-5)	0.29	0.23
4	Pre-driving children (Age 6-16)	0.45	0.43
5	No of vehicles in household	1.91	1.28
6	Income of household (\$)	\$53,667	\$52,649

The average number of vehicles per household is 1.91, which is slightly lower than the national average of 2.06 (NHTS 2001). Figure H.1. gives the distribution of number of vehicles per household in the sample. Nearly 50% of the households have two vehicles, and 19% have three or more.

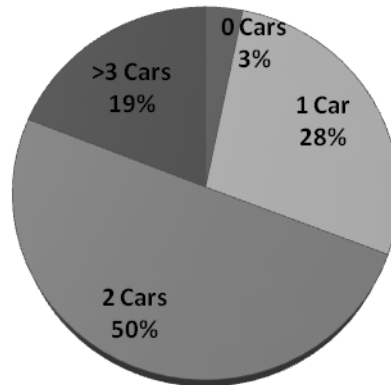


Figure H.1: Number of Vehicles in Household

Almost 3% of Austin area households do not own a vehicle. Figure H.1. provides vehicle-type frequencies in the 2006 ATS data set. 26% of all ATS vehicles are trucks, which is significantly higher than the national share of 18% in 2001 (NHTS 2001). Passenger cars (luxury, large, mid-size, small) constitute about 44% of Austin’s household fleet, whereas other light-duty trucks (i.e., vans, SUVs, and CUVs) constitute the remainder. Among one-vehicle households, pickups constituted only 17% of such vehicles, similar to the cases of SUVs and vans. Thus, household are more likely to own a light-duty truck as a second vehicle. Among two-vehicle households with at least one pickup, the second vehicle was most likely to be some type of SUV (accounting for 26% of such households) and, next, a mid-size car (15% of such households). The share of small cars is nearly 20% in this segment of households (higher than the overall share of 14%).

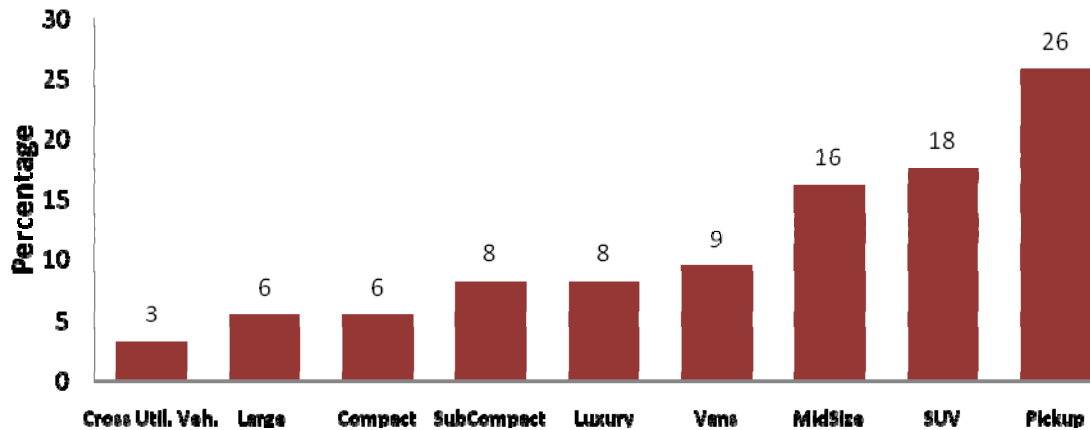


Figure H.2. Vehicle Class Shares in ATS 2006

Table H.2. presents average characteristics for the different vehicle classes, from Wards Automotive Yearbook (2007). As one may expect, pickups have the lowest fuel economy and the largest area, and luxury cars tend to be the most expensive. Small cars enjoy a relatively high fuel economy but lower engine displacement and horsepower. SUVs tend to cost quite a bit more than passenger cars (with the exception of luxury cars), exhibit lower fuel economy, and have larger footprints.

Table H.2. Summary of Vehicle Characteristics (Source: Wards Automobile Yearbook 2007)

SNo	Class	Fuel eco. (mpg)	Price (\$)	Area(ft ²)	GHG score	Weight (lbs)	Engdisp. (lit/cu in)	HP (rpm)
1	Luxury Car	18.61	\$48,004	94.01	5.50	8130.76	3.655	274.35
2	Large Car	17.57	\$30,734	105.11	5.51	8415.66	4.075	248.63
3	Mid-size Cars	19.00	\$25,614	95.65	6.00	7515.2	3.500	215.00
4	Compact	20.65	\$29,576	84.12	6.31	7012.28	2.240	216.41
5	Sub-compact	26.60	\$16,726	82.94	7.70	5807.34	1.930	140.42
6	Pickup	14.67	\$26,825	115.13	3.83	10430.86	4.430	257.17
7	SUV	15.10	\$35,221	104.65	4.04	10166.42	4.710	278.48
8	Minivan	15.18	\$27,411	110.55	4.64	9989.1	4.115	231.46
9	CrossUtilVeh.	18.08	\$26,932	92.04	5.63	8440.3	3.015	204.92

As noted above, the TACOS data set provides vehicle purchase and retirement data over 9 years (from 1990 to 1998), resulting in 4096 household-years. 79% of these observations were ‘do-nothing’ decisions (neither buy nor sell a vehicle), 11% of such data points both gave up/lost and gained at least one vehicle in a given year, and 8% simply added a vehicle, while the remaining 2% of data points (in household years) lost or gave up a vehicle.

H.3. Model Specifications and Results

Table H.3. gives the results of the vehicle-ownership-level model, where the response variable is the number of vehicles in an Austin household (for estimating vehicles owned in the simulations 2005 base year). Four levels of vehicle ownership were modeled here: 0, 1, 2, 3+ vehicles (per household) using an ordered probit model. The central idea here is that the ordered variable of interest is dependent on an unobserved latent index a normally distributed random term (Refer to Greene (2003) for model specifications). Household size and number of workers have a positive effect on ownership levels, as expected. The numbers of pre-driving age children were estimated to have a negative effect, as compared to an additional adult, which is again intuitive. In addition to household income, median neighborhood income was found to have a positive and statistically significant effect, which suggests some kind of location and status effect. Other land use variables that were found to be statistically significant are zonal type (rural vs. non-rural) and distance to the region's CBD, both with positive effect. This may be due to the higher number of transit facilities available in locations closer to CBD and in urban and suburban zones

Table H.3. Ordered Probit Model for Number of Vehicles owned by Austin Travel Survey Households in

Variable	Coef.	t-statistic
Household Size	0.952	13.2
Workers	0.278	5.75
Pre-school Children (<5 yrs)	-1.07	-11.0
Other Pre-driving Age Children (6-16)	-0.897	-10.2
Driving Age Children (16-18 years)	-0.523	-3.61
Rural Zone	0.152	1.48
Income (x 10 ⁻⁵)	0.727	7.33
Median Household Income in Zone(x 10 ⁻⁵)	0.805	4.38
Distance to CBD (miles)	9.15E-03	2.15
Log Likelihood	-1130.25	
Adjusted R ²	0.25	

A multinomial logit model was estimated for vehicle types owned. The pickup truck class was used as the base alternative, and all alternative specific constants were estimated to be negative and statistically significant – except for those on vans and mid-size cars. In other words, vans and midsize cars appear to offer the same base utility as pickups – ceteris paribus.

The ratio of vehicle price to household income has a negative coefficient, as expected (and consistent with previous findings). However, the ratio of fuel cost (in dollars per mile) to household incomes was estimated to be more significant statistically, than the vehicle price. Various household demographics also were significant, ceteris paribus. Larger households exhibit a preference for vans and utility vehicles, no doubt due to the larger seating and luggage capacities of these vehicles. Female drivers (quantified as the female drivers in the household) apparently have a preference for smaller cars, which may be due to ease of driving and maneuverability, as compared to other vehicle types.

Table H.4. Multinomial Logit Model for Vehicles Class Types in a Household

Variable	Coeff.	t-statistic
<i>Alternate Specific Constants</i>		
Cross Utility Vehicle	-1.5946	-8.22
Large Car	-2.3716	-5.67
Luxury Car	-0.5883	-2.96
Mid-size Car	-0.0724	-0.41
Compact Car	-1.1639	-4.89
Sub Compact Car	-1.0868	-4.89
Sports Utility Vehicle	0.3791	2.08
Minivan	-0.2187	-1.15
<i>Price Variables</i>		
Fuel Price/Income * 10 ⁴	-0.6025	-2.46
Price of vehicle/Income	-0.1041	-1.78
<i>Demographic Variables</i>		
HH Size * (Compact, Sub Compact, Mid-Size)	-0.2204	-5.72
HH Size * (Large Car , Luxury Cars)	-0.1783	-4.70
# Workers in HH* Mid-size car	0.1219	1.99
High Income(>75k) * Luxury Car	0.2906	1.70
Age of House Head * Large Car	0.0240	3.88
Female * Sub-Compact	0.3066	3.83
# Preschool Children * Van	-0.4629	-3.07
<i>Land Use Variables</i>		
iRural * Pickup	0.1777	1.58
iSuburban * Large Cars	0.2002	1.39
Density of HH in zone *Small Car * 10 ⁻³	0.0085	1.71
Density of HH in zone *SUV *10 ⁻³	-0.1032	-1.53
Retail firms within 5 miles * SUV *10 ⁻⁴	-0.1250	-2.06
Retail firms within 5 miles * Van *10 ⁻⁴	-0.0932	-1.53
Apartment* Small Car	0.2599	1.35
Apartment* Pickup	-0.4790	-3.05
<i>Vehicle use</i>		
Number of trips by HH * Small car 1	-0.0227	-1.75
Number of trips by HH * Small car 2	-0.0440	-2.74
Log Likelihood	-4649.22	
Adjusted R²	0.0981	

The number of workers in a household has statistically significant effect on the utility of mid-size vehicles, relative to other types, which is surprising. One possible reason for this may be

because workers commute daily, thus prefer comfortable vehicles (mid-size vehicles tend to have larger leg room, head room) for daily commutes. The age of a household's head also was found to have a positive effect on the systematic utility of large cars.

As evident in Table H.4. values, neighborhood land use patterns also were found to have some effect on vehicle choices, and this study modeled the residential location choices of individual households, over the 25-year period. A few interesting results emerge here: First, a neighborhood's household density reduces the utility of SUV ownership while increasing the utility of small cars. This may be due to tighter parking conditions, narrower streets, shorter driving distances, more environmentally conscious households, and any number of other features. Those living in rural areas are more likely to acquire pickup trucks, whereas those in suburban zones appear to be most attracted to large cars *ceteris paribus*. High local retail firms' density was estimated to have a negative effect on the utility of SUVs and vans. The last two variables in Table H.4.'s land use category are for apartment dwellers, who were found to be more likely to own small cars and less likely to own pickups, as expected (due to the relatively commercial or urban nature of most apartment locations).

Table H.5. MNL Model Estimates for Vehicle Transactions by a Household in a Given Year

Variable	Coef.	t-stat
Acquire 1 vehicle	-3.468	-10.26
Dispose 1 vehicle	-4.774	-9.12
Trade (Acquire and Dispose 1 vehicle)	-3.584	-11.1
Acquired* # Preschool Children	0.294	1.87
Acquired* # Retired People	0.367	1.65
Acquired* # Drivers	0.286	2.1
Acquired* # Full time Employees	0.322	1.89
Acquired* Max. Age of Vehicle in HH	-0.066	-1.81
Disposed* Max. Age of Vehicle in HH	0.129	3.16
Trade* # Persons	0.437	1.74
Trade* New Drivers in HH	-0.565	-1.75
Trade* Income $\times (10^{-5})$	1.140	2.56
Trade* Max Age of Vehicle in HH	0.151	6.73
Number of Observations	4096	
Pseudo R ² (LRI)	0.53	

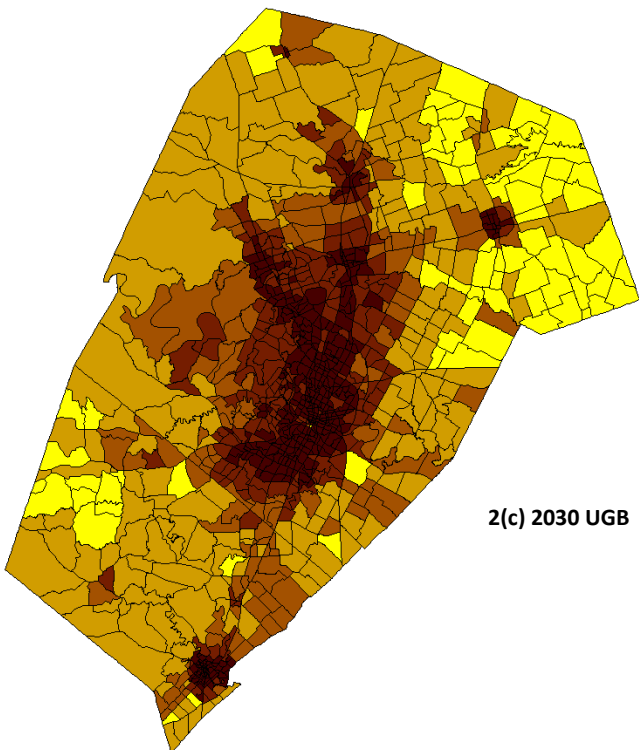
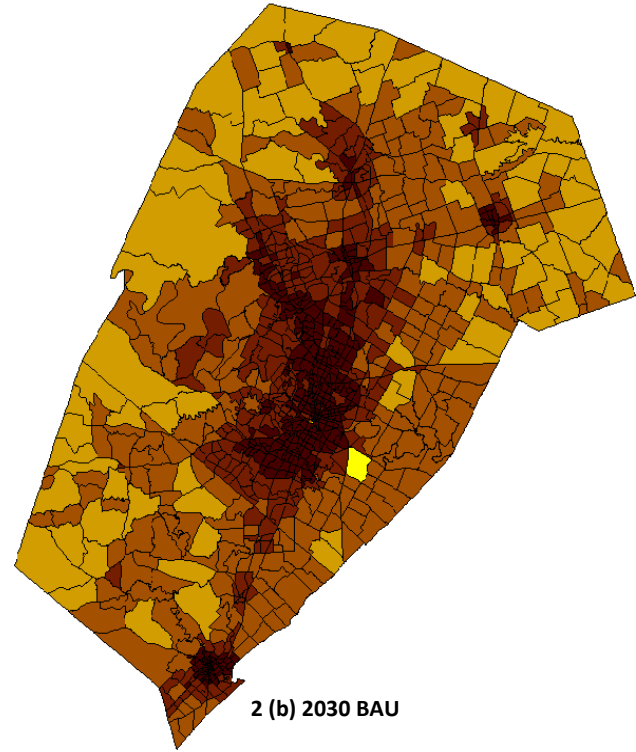
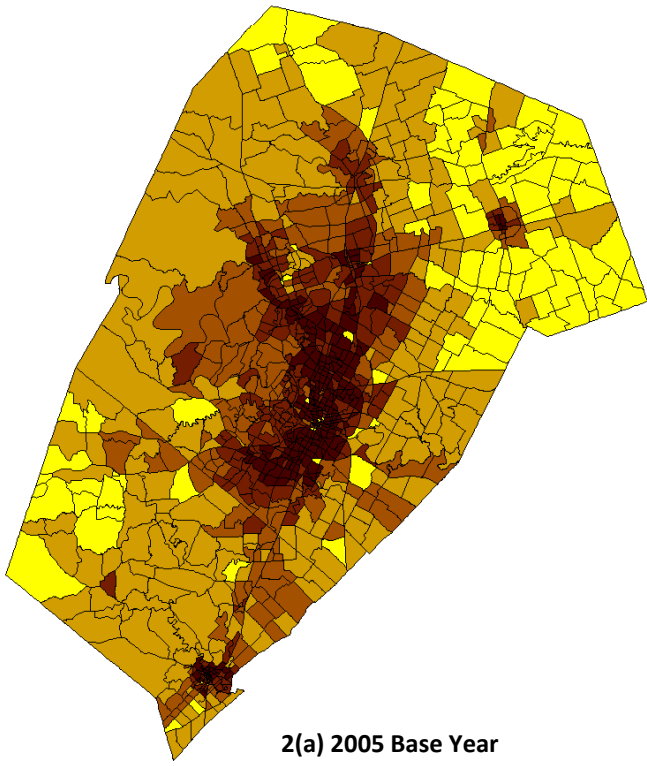
As household and vehicle characteristics change over time, the composition of a household's vehicle fleet also changes. To capture these dynamics over a period of years, a MNL model was estimated with the decision of the household with respect to vehicle fleet. The choices available are buy a vehicle (acquire), sell a vehicle (dispose), sell a vehicle and buy a new vehicle (trade) or "do nothing". Table H.5. presents model estimates. When acquired, new vehicles are selected

based on an MNL model for ownership patterns, as described earlier. The “do-nothing option” (neither buying nor selling/releasing a vehicle in a given year) is taken as the base or reference alternative in this model. All the other alternate-specific constants are estimated to be negative in sign (indicating that they are less common than the do-nothing option). The addition of preschool children, drivers and workers tends to trigger acquisition decisions, which is intuitive.

Using the models described above, year-2030 vehicle ownership patterns were predicted for Austin under a couple of different land use scenarios, using a synthetic population of individual households (as detailed in Kumar (2007) and Tirumalachetty *et. al.* (2008)). Figure H.3. shows the predicted land use patterns for year 2030 across the three-county region. As expected, the models predict greater household densities in centrally located zones when an urban growth boundary (UGB) policy was implemented, as compared to the trend or “business as usual” (BAU) scenario. Table H.6 shows vehicle holdings by class for 2030 under the three scenarios. The base area had 4 million trips generating over 112 million VMT. The effect of the \$3-per-gallon gas tax is somewhat apparent in the composition of year-2030 vehicles, as slight reductions in the shares of large cars and pickups allow for a higher percentage of small cars (compact and subcompact) and SUVs. The share of pickups is predicted to decline just slightly between 2005 and 2030, while small and mid-size cars are predicted to increase marginally over the same period. In the business as usual case, VMT is predicted to double. Implementation of UGB restricts the rise in VMT to 74%, and the pricing scenario restricts it further (to a predicted 60% increase in VMT by 2030). The results presented here are preliminary vehicle usage and emissions are likely to depend on fuel economy improvements, gas price changes, new vehicles technologies introduced into the market.

H.4. Summary

This appendix section has presented models for decisions in different stages of the passenger vehicle cycle of ownership and use. The system of models captures the capturing effects of household demographics and location on vehicle evolution cycle. Demographic characteristics were the key explanatory variables for number of vehicle in a household, while class of vehicle had several explanatory variables including land use characteristics. In the end, implementation of UGB restricts the rise in VMT to 74%, and the pricing scenario restricts it further to a 60% increase, while VMT is estimated to double in BAU scenario. Evolving rising gasoline prices, emerging vehicle technologies, and changes in fuel-economy policy are anticipated to result in a variety of behavioral changes, leading to changes in ownership patterns, use and air quality emissions. Vehicle class is an important input to models of fuel use, emissions, and crash outcomes. Changing attitudes and lifestyle patterns bring constant shifts in household preferences the vehicle fleet of household and it would be useful to capture them, to evaluate emissions accurately.



HH density - # per square mile

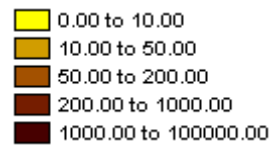


Figure H.3. Household Density: (a) Base year (2005) (b) 2030 BAU and (c) 2030 UGB

Table H.6. Composition of Vehicle Fleet (%)

	2005	2030		
	BAU	BAU	UGB	Pricing *
Vehicle Miles Traveled	112 million	223 million	195 million	180 million
Fleet Composition (%)				
Small Cars**	8.09	8.53	8.94	8.83
Mid-Size Cars	17.24	17.27	17.66	17.68
Large Cars	7.42	6.86	6.97	6.77
Luxury Cars	13.62	12.78	12.91	12.90
Pickups	19.79	18.28	17.62	17.86
Passenger Vans	15.96	17.56	17.86	17.56
SUV/CUV	17.97	18.14	17.99	

*Gas Tax of 3\$ and a fixed toll of 10cents/mile

** Sub-compact and compact cars

Appendix H References

Choo, S. and Mokhtarian, P.L. (2004). What Type of Vehicle do People Drive? The Role of Attitude and Lifestyle in influencing Vehicle Type Choice, *Transportation Research Part A*, 38(3): 201–222

Greene, W. H. (2003) *Econometric Analysis*, 5th edn. New York: Prentice Hall.

Hensher, D.A. and Plastrier, V.L. (1985). Towards a Dynamic Discrete-Choice Model of Household Automobile Fleet Size and Composition, *Transportation Research Part B*, 19(6): 481-495

Hocherman, I., Prashker, J.N. and Ben-Akiva, M. (1983). Estimation and Use of Dynamic Transaction Models of Automobile Ownership. *Transportation Research Record* 944:134-141.

Kitamura, R., Golob, T.F., Yamamoto, T., Wu, G. (2000). Accessibility and Auto Use in a Motorized Metropolis, *Paper presented at the 79th Transportation Research Board Annual Meeting*, Washington, DC.

Kumar, S., 2007. Microsimulation of Household and Firm Behaviors: Coupled Models of Land Use and Travel Demand in Austin, Texas. Master’s Thesis. Department of Civil, Architectural and Environmental Engineering, University of Texas at Austin.

Lave, C.A. and Train, K. (1979). A Disaggregate Model of Auto-type Choice *Transportation Research Part A*, 13(1): 1–9.

Mannering, F., and C. Winston. (1985). Dynamic Empirical Analysis of Household Vehicle Ownership and Utilization. *The RAND Journal of Economics* 16(2): 215-236.

Mannering, F., Winston, C., and Starkey, W. (2002). An Exploratory Analysis of Automobile Leasing by US households, *Journal of Urban Economics*, 52(1)154–176

Manski, C.F. and Sherman, L. (1980). An Empirical Analysis of Household Choice Among Motor vehicles, *Transportation Research Part A*, 14(6)349–366.

McFadden, D. (1978). Modeling the Choice of Residential Location. *Transportation Research Record No 673*: 72-77.

Mohammadian, A., and Miller, E.J. (2003a). Dynamic Modeling of Household Automobile Transactions, in the *Journal of the Transportation Research Record*, 1831: 98-105.

Mohammadian, A., and Miller, E.J. (2003b). Empirical Investigation of Household Vehicle Type Choice Decisions, *Journal of the Transportation Research Record*, No. 1854: 99-106.

Tirumalachetty, S., Kockelman, K., M. and Kumar, S., (2008). Micro-Simulation Models of Urban Regions: Anticipating Greenhouse Gas Emissions from Transport and Housing in Austin, Texas. *Proceedings of the 88th Annual Meeting of the Transportation Research Board and under review for publication in Transportation Research Record*.

Train, K.(1980). The Potential Demand for Non-Gasoline-Powered Automobiles, *Transportation Research Part A*, 14: 405-414.

Ward's Automotive Yearbook 2007 (2007). Ward's Communications, Detroit, MI.